

REGULATION OF THE RAS SIGNALING NETWORK IN *C. ELEGANS*
DEVELOPMENT

A Dissertation

by

HANNA SHIN

Submitted to the Office of Graduate and Professional Studies of
Texas A&M University
in partial fulfillment of the requirements for the degree of

DOCTOR OF PHILOSOPHY

Chair of Committee,	David J. Reiner
Committee Members,	Peter Davies
	Yubin Zhou
	Swathi Arur
	Jeffrey A. Frost
Head of Program,	Warren Zimmer

December 2018

Major Subject: Medical Sciences

Copyright 2018 Hanna Shin

ABSTRACT

An EGF gradient induces the equipotent *C. elegans* vulval precursor cells (VPCs) to assume the 3°-3°-2°-1°-2°-3° pattern of cell fates. EGF triggers the LET-60/Ras-LIN-45/Raf-MEK-2/MEK-MPK-1/ERK canonical MAP kinase cascade to induce 1° fate and synthesis of DSL ligands for the lateral Notch signal. In turn, LIN-12/Notch induces neighboring cells to become 2°. In response to lower dose of EGF signal, LET-60/Ras switches effectors to use the RGL-1/RalGEF-RAL-1/Ral modulatory signaling cascade to promote 2° fate in support of LIN-12. The goals of this research are to define principles by which signaling networks function and to identify an effector cascade downstream of RAL-1. RAL-1 signals through EXOC-8/Exo84, an established Ral binding partner, GCK-2, a CNH domain-containing MAP4 Kinase, and PMK-1/p38 MAP kinase to promote 2° fate. We also show that RGL-1 plays opposing and genetically separable roles in VPC fate patterning. RGL-1 promotes 2° fate via canonical GEF-dependent activation of RAL-1 and 1° fate via a non-canonical GEF-independent activity. Our genetic epistasis experiments are consistent with RGL-1 functioning in the modulatory 1°-promoting AGE-1/PI3-Kinase-PDK-1/PDK-AKT-1/Akt cascade. Animals without RGL-1 experience 15-fold higher rates of VPC patterning errors compared to the wild type. Yet VPC patterning in RGL-1 deletion mutants is not more sensitive to environmental perturbations. We propose that RGL-1 functions as a “Balanced Switch” that orchestrates opposing 1°- and 2°-promoting modulatory cascades to

decrease developmental stochasticity. To investigate how LET-60/Ras switches effectors to promote different cell fates, we used CRISPR to tag endogenous LIN-45/Raf and RGL-1/RalGEF proteins. We found that they are recruited to different subcellular compartments during VPC induction. LIN-45 is recruited to the basolateral membrane in presumptive 1° cells. RGL-1 is recruited to the apical membrane in presumptive 2° cells, and this localization depends on functional LET-60. We hypothesize that RGL-1 apical localization in the VPCs is mediated by phosphorylation or scaffold proteins. Our studies delineate a novel Ral-dependent developmental signaling cascade, bifunctional RGL-1 as a “Balanced Switch”, and LET-60 effector segregation mechanism *in vivo*, thus providing critical insights for understanding Ras biology in cancer and development.

ACKNOWLEDGEMENTS

I would like to thank God leading me to this moment, letting me have warm and lovely people around me, and answering all my prayers.

I would like to thank my mentor, Dr. Dave Reiner, who took care of me during my time in the lab. He gently trained me in the art of presenting my research, learning scientific writing, and how to plan and conduct research. He has made all my days of graduate school, very happy. He helped me every time I had hard time with my research, was sick or had problem in my life. He always supported and encouraged me, which helped me to have confidence in myself. He has taught and showed me how to become a happy scientist. He always showed his passion for his research and training people with optimism and sense of humor. I am so grateful to have has him as my PI during my graduate studies.

I also would like to thank my committee members. Dr. Swathi Arur guided me in our meetings to become an accurate and honest scientist. I learned from her how to develop a research project and how to think logically. She is a friendly mentor, but also is a professional scientist. Dr. Yubin Zhou has passion for his research and taking care of trainees. It was a great experience doing research in his lab as a first-year rotation student. He always has brilliant ideas that encourage curiosity and interest in those around him. Dr. Peter Davies always has a benevolent smile for the students. When I was a rotation student in his lab, he taught me how to think deeply about my research project and helped me as I

started my graduate program. Dr. Jeff Frost is a great lecturer. I met him in the cell biology class as a first-year graduate student. He showed kindness as he taught his students in the classroom. He also showed interest in my research project and guided me during committee meetings.

I also appreciate all those who helped me a lot as I started my graduate program in the United States. It was first time for me to live alone outside of my country. So sometimes, I was overwhelmed and struggled with environment or situations I faced. My friends, Dr. Davies and Dr. Stephan lab members, and Dr. Zhou lab members helped me a lot.

I would like to thank my friends; Can, Sheila, Ana Maria, Chuntang, and Yi who shared in the difficulties of graduate student life and also came together to celebrate or for just fun times. I also would like to thank my friends who helped me when I faced difficulties in my research through discussions and sharing of reagents.

I would like to thank Cindy and Denelle who helped me. Cindy always kindly helps each student with her warm heart. Denelle was like my mom. She helped and took care of me when I was sick or had problems in my life.

I would like to thank my labmates, Sefakor, Afaq, Neal, Tam, Razan, and Qi. It was grateful to have such a lovely labmates like them. They helped me with my research, when I was having hard time and celebrated with me when I passed my qualifying exam, published my research paper, and on my birthday.

I would like to thank Korean Hanbit Church young adult group. They prayed for me when I had important exams or had a hard time in my research. We shared our difficulties and worries in life as international students with each other. We also prayed for each other. I was glad to make many pleasant memories with the Hanbit Church members.

I would like to thank my parents. They always supported and encouraged me with their endless love. And, they were praying for me every moment. I could not imagine I would be where I am today without them.

I would like to also thank to the many others who prayed for me and helped me during graduate journey.

CONTRIBUTORS AND FUNDING SOURCES

This work was supervised by a committee chair, Dr. David J. Reiner (Institute of biosciences and technology, IBT), and committee members, Dr. Peter Davies (IBT), Dr. Yubin Zhou (IBT), Dr. Swathi Arur (MD Anderson Cancer Center), and Dr. Jeffrey Frost (MD Anderson Cancer Center, UTHealth).

The work for Chapter II was contributed to by Hanna Shin, Rebecca E.W. Kaplan, Tam Doung, and Razan Fakieh. Hanna Shin conducted the main body of research and wrote the manuscript with preliminary results being provided by Rebecca E.W. Kaplan. Tam Duong generated *ral-1(re160gf[mKate2^{3xFlag}::ral-1(G26V)])* and Razan Fakieh performed *mig-15(RNAi)* experiments. The work for Chapter III was equally contributed to by Hanna Shin, Christian Braendle, Rebecca E.W. Kaplan, and Kimberly B. Monahan. Tanya P. Zand, Francisca Sefakor Mote, and Eldon Peters generated strains and conducted preliminary experiments. The work for Chapter IV was completed by Hanna Shin. Tam Duong generated *let-23(re202[let-23::mKate2^{3xFlag}])* and Neal Rasmussen generated *lin-45(re208[mNG^{3xFlag}::lin-45])*. This work was supported by funds from the IBT graduate program in the first year, from IBT startup package to Dr. Reiner in the second to fourth years, and from NIGMS R01GM121625 to P.I. Dr. Reiner in the fifth year.

NOMENCLATURE

AC	Anchor Cell
AID	Auxin-Inducible Degradation
CAAX	Cys-Aliphatic-Aliphatic-Any amino acid
Ce	<i>C. elegans</i>
<i>C. elegans</i>	<i>Caenorhabditis elegans</i>
CFP	Cyan Fluorescent Protein
CNH	Citron N-terminal Homology
CPD	Cdc4 PhosphoDegron
CRIB	Cdc42/Rac Interactive Binding
CRISPR	Clustered Regularly Interspaced Short Palindromic Repeats
DIC	Differential Interference Contrast
Dm	<i>D. melanogaster</i>
DRal	<i>Drosophila</i> Ral
DSL	Delta/Serrate/Lag-2
DTCs	Distal Tip Cells
EGF	Epidermal Growth Factor
EGFR	EGF Receptor
FGF	Fibroblast Growth Factor
FP	Fluorescent Protein

GAP	GTPase-activating proteins
GCK	Germinal Center Kinases
GDP	Guanosine Diphosphate
GEF	Guanine nucleotide Exchange Factors
gf	gain-of-function
GFP	Green Fluorescent Protein
GTP	Guanosine Triphosphate
Hppy	Happyhour
Hs	Homo sapiens
HVR	Hyper-Variable Region
ICD	Intracellular Domain
IPTG	Isopropyl-Beta-D-Thiogalactoside
JIP	JNK Interacting Protein
KD	Kinase Dead
L1	First larva stage
L2	Second larva stage
L3	Third larva stage
L4	Fourth larva stage
LBS	Lag Binding Sequence
lf	loss-of-function
LRR	Leucine-rich repeats

MAPK	Mitogen-activated protein kinase/MAP kinase
MAP2K	Mitogen-activated protein kinase kinase
MAP3K	Mitogen-activated protein kinase kinase kinase
MAP4K	Mitogen-activated protein kinase kinase kinase kinase
mK2	mKate2
MKP	Guanine nucleotide Exchange Factors
mNG	mNeonGreen
MMP	Million Mutation Project
Msn	Misshapen
Muv	Multivulva
NGM	Nematode Growth Medium
PTB	Phospho-Tyrosine Binding domain
RA	Ras Association
Ral	Ras like
RalBP1	Ral Binding Protein 1
RalGAP	Ral GTPase Activating Protein
RalGDS	Ral Guanine nucleotide Dissociation Stimulator
RBD	Ras Binding Domain
REM	Ras Exchanger Motif
SEC	Self-Excising Cassette
SEM	Standard Error of the Mean

smFISH	Single molecule fluorescent in situ hybridization
ssODN	Single-stranded oligonucleotides
Su(H)	Suppressor of Hairy
synMuv	synthetic Multivulva
VPCs	Vulval Precursor Cells
Vul	Vulvaless

TABLE OF CONTENTS

	Page
ABSTRACT.....	ii
ACKNOWLEDGEMENTS.....	iv
CONTRIBUTORS AND FUNDING SOURCES.....	vii
NOMENCLATURE.....	viii
TABLE OF CONTENTS.....	xii
LIST OF FIGURES.....	xiv
LIST OF TABLES.....	xvii
CHAPTER I INTRODUCTION AND LITERATURE REVIEW.....	1
<i>C. elegans</i> vulval development.....	1
VPC fate patterning.....	3
Trafficking-dependent Regulation of Receptor Localization and Function.....	16
Upstream and downstream transcriptional regulators in VPC fate patterning.....	23
Transcriptional reprogramming of the VPC signaling network.....	29
Environmental and genetic regulators and variability.....	34
Conclusions.....	35
CHAPTER II RAL SIGNALS THROUGH A MAP4 KINASE-P38 MAP KINASE CASCADE IN <i>C. ELEGANS</i> CELL FATE PATTERNING.....	37
Introduction.....	37
Results.....	46
Discussion.....	76
Materials and Methods.....	84
CHAPTER III DEVELOPMENTAL FIDELITY IS IMPOSED BY GENETICALLY SEPARABLE RALGEF ACTIVITIES THAT MEDIATE OPPOSING SIGNALS.....	105

	Page
Introduction.....	105
Results.....	114
Discussion.....	142
Materials and Methods.....	150
CHAPTER IV RAS EFFECTOR SWITCHING MECHANISM.....	165
Introduction.....	165
Results.....	171
Discussion.....	182
Materials and Methods.....	194
CHAPTER V CONCLUSIONS AND REMARKS.....	200
REFERENCES.....	205

LIST OF FIGURES

	Page
Figure 1. 1 The <i>C. elegans</i> vulva in L4 stage and young adult stage animal.....	2
Figure 1. 2 Overview of the <i>C. elegans</i> VPC fate patterning.....	4
Figure 1. 3 The Morphogen Gradient Model.....	6
Figure 1. 4 The Sequential Induction Model.....	8
Figure 1. 5 Mutual Antagonism.....	12
Figure 1. 6 Reconciling the Sequential Induction and Morphogen Gradient models.....	15
Figure 1. 7 Expression pattern of transcription of either 2°-promoting and 1°-antagonizing or 1°-promoting genes in VPCs.....	31
Figure 2. 1 A model of Ral effector use in VPC fate patterning and MAP4K families and sensitized backgrounds.....	39
Figure 2. 2 <i>C. elegans</i> CNH-domain organization MAP4Ks and VPC fate patterning.....	42
Figure 2. 3 EXOC-8 functions in VPC fate patterning.....	48
Figure 2. 4 EXOC-8 but not SEC-5 or RLBP-1 functions in VPC fate patterning.....	49
Figure 2. 5 Loss of GCK-2 but not MIG-15 confers the same phenotype as loss of RAL-1.....	51
Figure 2. 6 Loss of GCK-2 but not MIG-15 conferred defects consistent with a RAL-1 effector.....	53
Figure 2. 7 RAL-1 and GCK-2 are sufficient to drive 2° fate induction.....	55

	Page
Figure 2. 8 Design and validation of endogenous GCK-2 mid-deletion and GCK-2 mid-deletion transgenics.....	57
Figure 2. 9 GCK-2 functions downstream of LIN-3/EGF and RAL-1 cell autonomously.....	59
Figure 2. 10 GCK-2 functions cell autonomously downstream of Ral.....	61
Figure 2. 11 Endogenously tagged GCK-2 and RAL-1 are expressed in VPCs.....	64
Figure 2. 12 CRISPR knock-in strategies, western blot validations, and localization of endogenously tagged GCK-2, RAL-1(G26V), and RAL-1.....	65
Figure 2. 13 PMK-1/p38 functions downstream of RAL-1.....	72
Figure 2. 14 PMK-1 expression and localization.....	73
Figure 3. 1 Schematics of VPC fate patterning and its signaling network..	106
Figure 3. 2 Signaling network comparisons between humans and <i>C. elegans</i>	111
Figure 3. 3 RGL-1 and RAL-1 are functionally non-equivalent in VPC patterning.....	117
Figure 3. 4 RGL-1 controls cell fate decision.....	120
Figure 3. 5 VPC expression pattern of the rgl-1 transcriptional GFP fusion over time.....	123
Figure 3. 6 N-terminal CRISPR tagging of endogenously expressed RGL-1 protein.....	125
Figure 3. 7 RGL-1 encodes genetically separable functions.....	127
Figure 3. 8 Genetically separable functions of RGL-1.....	130
Figure 3. 9 RGL-1 may function in the 1°-promoting PI3K-PDK-Akt cascade.....	133

	Page
Figure 3. 10 RGL-1 interacts genetically with the 1°-promoting AGE-1/ PI3K-PDK-1-AKT-1 cascade.....	135
Figure 3. 11 Deletion of RGL-1 increases patterning errors but not susceptibility to environmental stress.....	141
Figure 3. 12 PCR detection of <i>rgl-1(ok1921)</i>	151
Figure 3. 13 PCR detection of <i>rgl-1(tm2255)</i>	152
Figure 4. 1 Subcellular localization of LIN-45::mNG in VPCs at different stages.....	172
Figure 4. 2 Subcellular localization of mNG::RGL-1 in VPCs at different stages.....	175
Figure 4. 3 mNG::RGL-1 is localized to the apical membrane in 2° cells, but not in 1° cell at late L3 stage.....	177
Figure 4. 4 The validation of mNG::RGL-1 apical localization system by using LET-60 null mutant.....	178
Figure 4. 5 mNG::RGL-1 co-localizes with LET-23::mK2 at the plasma membrane.....	179
Figure 4. 6 mNG::RGL-1 is localized to the apical membrane in VPCs in <i>let-23 (sy1)</i> background.....	181
Figure 4. 7 Three axes of Ras effectors recruitment to the membrane.....	188
Figure 4. 8 RGL-1/RaGEF RA domain is conserved between species.....	190

LIST OF TABLES

	Page
Table 2. 1 Strains for GCK-2 study.....	93
Table 2. 2 Primers for GCK-2 study.....	96
Table 2. 3 Plasmids for GCK-2 study.....	102
Table 2. 4 sgRNA sequences and PAMs.....	104
Table 2. 5 Repair ssODN.....	104
Table 3. 1 <i>rgl-1</i> and <i>ral-1</i> alleles and mutant phenotypes.....	159
Table 3. 2 Strains for RGL-1 study.....	160
Table 3. 3 Primers for RGL-1 study.....	163
Table 4. 1 Strains for effector switching mechanism study.....	197
Table 4. 2 Primers for effector switching mechanism study.....	197

CHAPTER I

INTRODUCTION AND LITERATURE REVIEW

***C. elegans* vulval development**

The *C. elegans* vulva is a textbook system for the study of developmental biology and signal transduction. The completed vulva is an epithelial tube that connects the uterus to the outside of the hermaphrodite: the vulva mediates egg-laying and mating with males. Importantly from the perspective of a developmental geneticist, the vulva is dispensable for viability. In vulvaless hermaphrodites, self-fertilized eggs hatch within the mother to produce live progeny. Consequently, this system is amenable to genetic manipulation, with genetic perturbations resulting in visible phenotypes such as Multivulva (Muv) and Vulvaless (Vul) (Horvitz and Sulston, 1980).

During early larval development, the six vulval precursor cells (VPCs; also known as the Pn.p cells, P3.p-P8.p) are generated to form the vulval equivalence group. These cells are roughly equipotent, with any VPC capable of assuming any of the three potential VPC fates, 1°, 2°, or 3° (called primary, secondary, or tertiary). The VPCs are induced during the third larval (L3) stage. After initial patterning, the 22 daughter cells (eight cells from P6.p and seven cells from each P5.p and P7.p) form the vulva (Sternberg, 2005). The final positioning of the vulva is at the

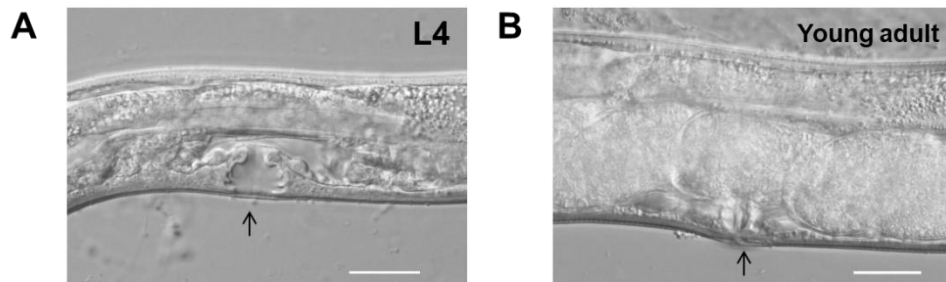


Figure 1. 1 The *C. elegans* vulva in L4 stage and young adult stage animal. The DIC images are captured by Dr. Rasmussen from Dr. Reiner lab. (white scale bar = 10 μ m in the DIC images) **A.** The black arrow indicates a vulva in the L4 stage animal. **B.** The black arrow indicates a vulva in young adult stage animal.

anteroposterior mid-point, between the nose and tail of the hermaphrodite, at the ventral midline (Figure 1. 1).

In this review I focus on the signaling network that governs developmental patterning of VPCs fates. Other important features of vulval development are outside the scope of this review, and are covered elsewhere (Sternberg, 2005). For example, generation of the VPCs and establishment of competency occur before the events are not described in this chapter. The timing of vulva development is controlled by the well-studied heterochronic system (Euling and Ambros, 1996). Generation of VPC lineages is relatively under-studied, beyond a sketch of a transcriptional gene regulatory network (Inoue et al., 2002; Inoue et al., 2005; Ririe et al., 2008). Polarity of 2° vulval lineages is controlled by overlapping Wnt systems (Inoue et al., 2004; Kidd et al., 2015; Minor et al., 2013).

Vulval morphogenesis is also relatively under-studied, though an interesting start has been made (Farooqui et al., 2012; Mok et al., 2015; Pellegrino et al., 2011).

VPC fate patterning

Pattern formation of the *C. elegans* vulval cell fates has proved to be an excellent model for the study of cell-cell communication. A confluence of research in the *C. elegans* VPCs, the *Drosophila* R7 photoreceptor, and mammalian cell culture and biochemistry led to the first consensus description of an intercellular signal, from ligand to nucleus. This signal is EGF (Epidermal Growth Factor)-EGFR (EGF Receptor) signaling through the Ras proto-oncogene activation of the Raf-MEK-ERK canonical MAP kinase cascade, which is the main 1°-promoting signal in VPC patterning. Also of great impact was the characterization of the Notch receptor signaling system, which is the main 2°-promoting signal in VPC fate patterning. Thus, VPC patterning holds a central place in the history of cell-cell signaling research in both development and cancer (Egan et al., 1993; Greenwald and Rubin, 1992). Here I discuss an undated view of the signaling network that patterns VPC fate.

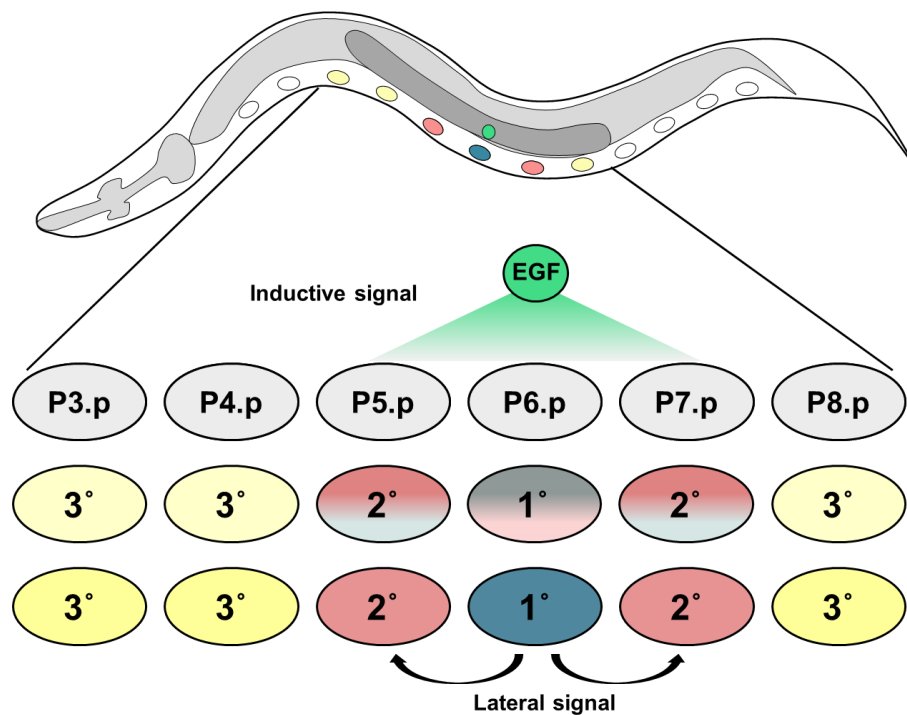


Figure 1. 2 Overview of the *C. elegans* VPC fate patterning. The six naïve VPCs are numbered P3.p through P8.p. P6.p receives high level of inductive signal because of its closest distance from the anchor cell. P5.p and P7.p receives low level of inductive signal and lateral signal from the P6.p. P5.p, p6.P, and P7.p adopt vulval fate and develop vulva after three time of cell division. P3.p, P4.p, and P8.p receive insufficient inductive and lateral signal and adopt nonvulval fate fused with surrounding hpy7 hypodermis.

The vulval equivalence group consists of six equipotent VPCs, arranged anteriorly-to-posteriorly along the ventral midline. These specialized cells are part of the epithelium (termed the “hypodermis” in *C. elegans*). During the L3 stage, the final pattern of fates emerges: 3°-3°-2°-1°-2°-3°. The 1° and 2° cells are induced vulval fates: these VPCs go on to form the vulva after characteristic cell division

lineages. The 3° cells are the “uninduced” or “ground” cell fate: they divide once and then fuse with the surrounding syncytial epithelium (Figure 1. 2; Sulston and Horvitz, 1977). This pattern occurs with 99.8% accuracy and the resulting cell lineages are invariant (Braendle and Felix, 2008). This pattern is induced by a signal from the Anchor Cell (AC), part of the somatic gonad, plus signals amongst the VPCs (Kimble, 1981; Sulston and White, 1980). Ablation of gonad during L1 stage, or the AC before the L3 stage, caused all VPCs to adopt 3° fate and fail to develop the vulva. The first detectable event of AC induction is positioning of the VPCs relative to the AC. P6.p, the presumptive 1° cell, becomes centered next to the AC (Grimbert et al., 2016). Classical developmental biology experiments followed by decades of molecular genetics analysis has led to three non-exclusionary mechanistic models that describe VPC fate patterning. Here I discuss the signaling network that generates the pattern of VPC fate.

The Morphogen Gradient Model.

Combining cell lineage analysis with ablation of selected cells with a laser microbeam revealed the presence of cell-cell signaling events between the AC and VPCs and among VPCs (Horvitz and Sulston, 1980; Kimble, 1981; Sternberg and Horvitz, 1986; Sulston and Horvitz, 1981; Sulston and White, 1980).

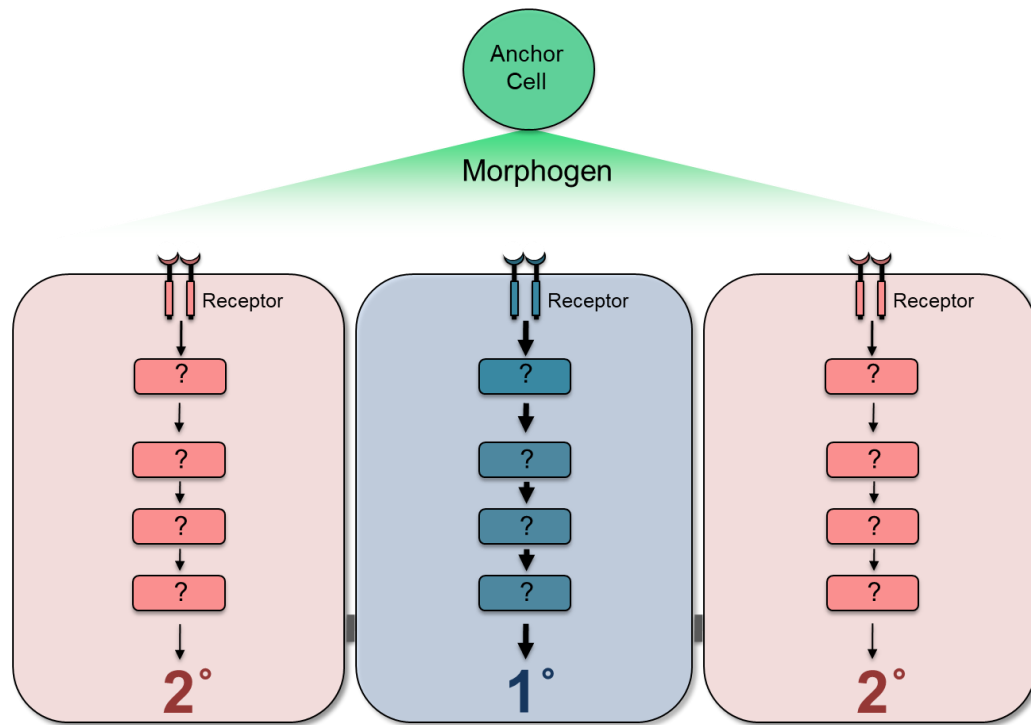


Figure 1. 3 The Morphogen Gradient Model. The equipotent VPCs are patterned by graded morphogen, LIN-3/EGF from the anchor cell (AC) through the activation of the receptor, LET-23/EGFR.

Additionally, an extensive collection of mutations was generated that perturbed patterning in distinctive ways (Ferguson and Horvitz, 1985; Ferguson et al., 1987; Greenwald et al., 1983). From an elegant combination of these approaches arose the Morphogen Gradient Model (Figure 1. 3).

The AC induces equipotent VPCs to assume their fate. P6.p, the VPC closest to the AC, nearly always becomes 1° (Sulston and Horvitz, 1977; Sulston and White, 1980). Isolated VPCs (generated by ablation of other VPCs with a laser

microbeam) assume 1° or 2° fate based on distance from the source of signal: VPCs close to the AC become 1°, while those distal from the AC become 2° (Sternberg and Horvitz, 1986). This observation led to the model that it is dose of a “morphogen” signal that dictates VPC fate. Yet this model does not preclude cell-cell signaling among VPCs.

lin-3 and *let-23* are essential for 1° fate, and encode proteins similar to EGF and EGFR, respectively (Aroian et al., 1990; Hill and Sternberg, 1992). LIN-3 is expressed in the AC during the induction of VPCs at L2 to L4 stages and is required in the AC for VPC induction (Gonzalez-Serricchio and Sternberg, 2006; Hill and Sternberg, 1992; Liu et al., 1999). Ectopic expression of LIN-3 is sufficient to induce VPCs in the absence of gonad, indicating that LIN-3 is also sufficient to induce 1° fate (Hill and Sternberg, 1992). Again in isolated VPCs, 1° or 2° fate was induced by LIN-3 and LET-23 signaling dose, manipulated by genetic or transgenic means (Katz et al., 1995; Katz et al., 1996). The presence of a gradient was later validated visually using a transgenic molecular marker. The *egl-17::gfp* transcriptional fusion is a 1° fate marker that expresses GFP in induced 1° cells (Berset et al., 2001; Burdine et al., 1998). A more sensitive *P_{egl-17}::cfp::lacZ* transcriptional reporter revealed a transient flash of CFP in induced 2° cells. This weaker signal is sustained in the 2° lineages when negative regulators of 1° signaling are perturbed (Yoo et al., 2004; Yoo and Greenwald, 2005).

Taken together, these results indicate that a spatially graded signal is detected by VPCs: this “Morphogen Gradient” contributes to the 3°-3°-2°-1°-2°-3°

VPC fate pattern, the morphogen is the EGF ortholog LIN-3, and its receptor is the EGFR ortholog LET-23 (Kenyon, 1995). Yet these results were difficult to reconcile with the subsequent flood of molecular identification of genes identified in mutant screens for Vul and Muv mutants (Ferguson and Horvitz, 1985; Ferguson et al., 1987; Horvitz and Sulston, 1980).

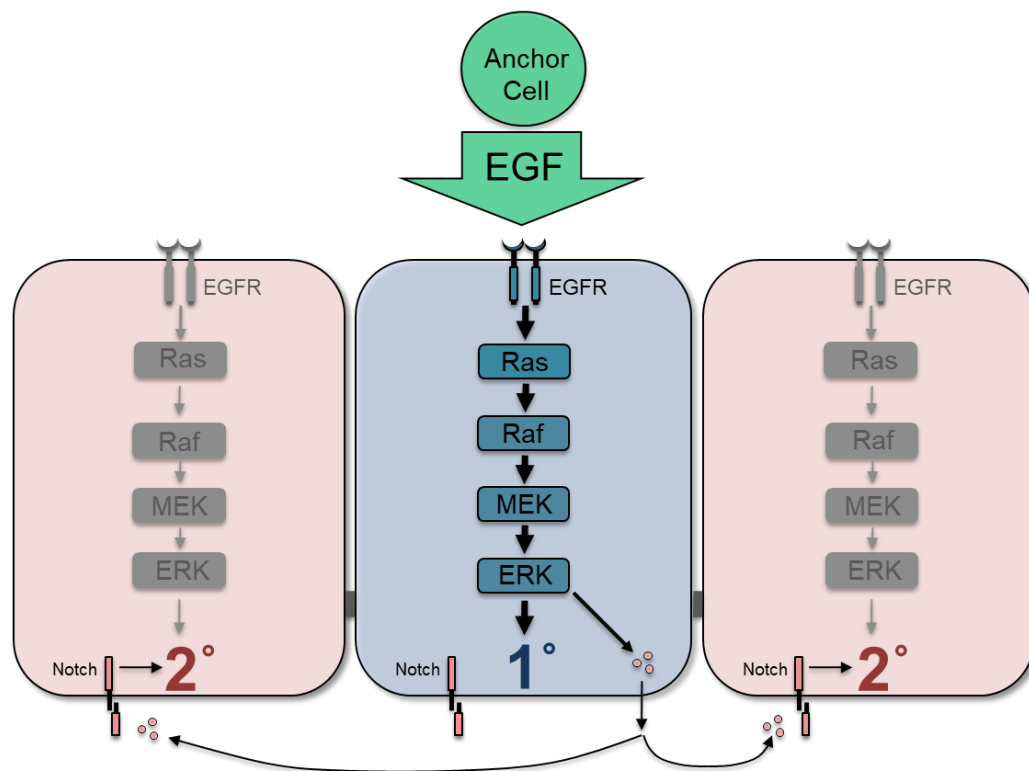


Figure 1. 4 The Sequential Induction Model. In the response to the LIN-3/EGF, LET-23/EGFR activates LET-60/Ras-LIN-45/Raf-MEK-2/MEK-MPK-1/ERK signaling cascade to promote 1° fate. LET-23-mediated inductive signal induces DSL/Notch ligands transcription in the presumptive 1° cell. The DSL induces LIN-12/Notch activation in the neighboring presumptive 2° cells.

The Sequential induction Model.

Molecular genetic characterization of core signaling components necessary for VPC patterning argued that patterning occurred 1° first, then 2°. This model is called the Sequential Induction Model (Simske and Kim, 1995; Figure 1. 4). Extensive mutant screens identified genes that are necessary and sufficient for 1° and 2° fate (Ferguson and Horvitz, 1985; Ferguson et al., 1987; Greenwald et al., 1983). Molecular cloning and analysis of these genes, plus epistatic ordering of genes into pathways, identified a major (necessary and sufficient) cascade for inducing primary 1° fate. Via the SEM-5/Grb adaptor and SOS-1/Sos Ras exchange factor, LET-23 activates the LET-60/Ras-LIN-45/Raf-MEK-2/MEK-MPK-1/ERK canonical MAP kinase cascade to induce 1° fate (Beitel et al., 1990; Chang et al., 2000; Clark et al., 1992; Han et al., 1990; Han et al., 1993; Kornfeld et al., 1995a; Lackner et al., 1994; Wu et al., 1995). Screens for suppression of the Muv phenotype caused by activated LET-60/Ras discovered proteins now accepted as components of Ras-Raf-MEK-ERK signaling: SOC-2/SUR-8 is thought to function as a scaffold for LET-60/Ras-LIN-45/Raf (Selfors et al., 1998; Sieburth et al., 1998) and KSR-1 is thought to function as a scaffold for LIN-45/Raf-MEK-2/MEK-MPK-1/ERK (Kornfeld et al., 1995b; Sundaram and Han, 1995). Thus, this highly conserved cascade is necessary and sufficient to induce 1° fate. Subsequent studies in humans have connected human RASopathies,

spectrums of congenital defects, with causative molecular etiologies that serve to weakly activate the Ras-Raf-MEK-ERK cascade (Bustelo et al., 2018).

Critical for the induction of 2° fate is the Notch ortholog, LIN-12 (Greenwald et al., 1983), which mediates the lateral signal from presumptive 1° cell to presumptive 2° cells (Sternberg, 1988; Sternberg and Horvitz, 1989). Three DSL Notch ligands, LAG-2, APX-1 and DSL-1, are synthesized in the presumptive 1° cell in response to inductive signal. These ligands are redundantly required to laterally signal the neighboring P5.p or P7.p to become 2° cells (Chen and Greenwald, 2004; Zhang and Greenwald, 2011).

Genetic mosaic experiments showed expression of *let-23(+)* in P6.p, but not in P5.p and P7.p, supports normal vulva induction (Koga and Ohshima, 1995; Simske and Kim, 1995). Strikingly, genetic mosaic analyses indicated that LET-23 function is required to induce 1° but not 2° fate (Koga and Ohshima, 1995; Simske and Kim, 1995). Coupled with the synthesis of DSL ligands for LIN-12 in presumptive 1° cells, these results are consistent with a different model for VPC fate patterning. The Sequential Induction Model proposes that the VPC that receives the strongest LIN-3 dose because 1°, then signals its neighbors to become 2°. This stepwise signaling – first 1°, then 2° – was considered to be inconsistent with the Morphogen Gradient Model.

Mutual antagonism.

A key mechanism by which the VPCs are accurately patterned is what we term “Mutual Antagonism”. Though they start as equipotent, initially specified VPCs alter their signaling network to exclude signals that promote the opposing fate. This feature of the signaling network likely reduces conflicting signals, and thus the rate of VPCs committing to inappropriate or ambiguous cell fates. In turn, by decreasing formation of aberrantly patterned vulvae, this network feature likely increases the reproductive fitness of the animal.

Multiple lines of evidence point to an antagonistic tension between presumptive 1° and 2° cells (illustrated in Figure 1. 5). Prior to induction in L2 and early L3 stages, all six VPCs express LIN-12 (Levitan and Greenwald, 1998; Wilkinson and Greenwald, 1995). Upon induction, in the developing 1° cell LIN-12 is internalized and degraded (Deng and Greenwald, 2016a; Levitan and Greenwald, 1998; Shaye and Greenwald, 2002, 2005). The mechanism of LIN-12 down-regulation is as yet unknown, but it depends on the MPK-1/ERK 1°-promoting target, SUR-2 of the Mediator complex (see below).

In addition, the 1°-promoting LET-23-LET-60-LIN-45-MEK-2-MPK-1 canonical MAP kinase cascade is inhibited in specified 2° cells, P5.p and P7.p. After induction, transcription of the ERK phosphatase, LIP-1, is induced by LIN-12/Notch signaling in these cells (Berset et al., 2001). The *egl-17* gene is a transcriptional target of 1°-promoting MPK-1 inhibition of the LIN-1/Ets



Figure 1. 5 Mutual Antagonism. There are antagonistic mechanisms that prevent a specific VPC from adopting a wrong cell fate. In the presumptive 1° cell, LIN-12/Notch, a 2°-promoting signal, is blocked by LET-23/EGFR-mediated signal through internalization and degradation of the Notch receptor. In the presumptive 2° cells, the Notch target gene, *lip-1*, is transcribed upon LIN-12 activation. The 1°-promoting MPK-1/ERK is inhibited through dephosphorylation by the ERK phosphatase LIP-1/MPK.

transcription factor (Burdine et al., 1998; Tiensuu et al., 2005). In wild-type VPCs, a transient pulse of *egl-17* transcriptional reporter can be observed in presumptive 2° cells (Yoo et al., 2004). In the absence of LIP-1 and other LIN-12 transcriptional client genes, the *lst* genes, *dpy-23* and *ark-1* (see below), the signal from the *egl-*

17 reporter persists (Berset et al., 2001; Yoo et al., 2004). In addition to LIP-1, the DEP-1 receptor tyrosine phosphatase, predicted to inhibit LET-23 activity, is expressed in 2° cells after induction to antagonize the 1°-promoting signal (Berset et al., 2005).

An additional mechanism that may fit conceptually into the Mutual Antagonism category is the concept of “Balanced Switches” (Chapter 3; Shin *et al.*, submitted). We found that RGL-1 harbors genetically separable and antagonistic functions. As demonstrated in mammalian cells (Feig, 2003) and validated in *C. elegans*, the canonical GEF function of RalGEF is activated by Ras and stimulates activation of Ral; in VPCs this is a modulatory 2°-promoting activity. Of signaling cascades defined in VPC fate patterning, an AGE-1/PI3K-PDK-1/PDK signal, with the DAF-18/PTEN lipid phosphatase as a negative regulator, has been shown to promote 1° fate in a modulatory capacity (Nakdimon et al., 2012). We showed that AKT-1/Akt likely also functions in this cascade (Shin *et al.*, submitted), thus constituting a classic PI3K-Akt signaling cascade. Our genetic epistasis data are consistent with RGL-1 performing a GEF-independent function as a scaffold of PDK-1 and AKT-1. Such a function was originally described in mammalian cells for the RalGEF, RalGDS (Hao et al., 2008; Tian et al., 2002). RGL-1 appears to participate in antagonistic 1°-promoting and 2°-promoting activities. We term this phenomenon the “Balanced Switch”. By deleting RGL-1, we appear to abolish the activity of both modulatory cascades, with no net change in the balance of 1° and 2° signals. But animals without RGL-1 display a 15-fold

higher error rate in VPC patterning. The “Balanced Switch”, exemplified by RGL-1, may define a novel category of Mutual Antagonism (Shin *et al.*, submitted; Chapter 3).

Thus, in response to signaling cascades necessary for 1° and 2° fate, each cell type enacts programs to exclude promotion of the competing cell fate. A series of orphan 1° - and 2° - antagonizing “modifier genes” have been identified, but not placed functionally in the VPC patterning network (Greenwald, 2005; Sundaram, 2005). These gene products could provide yet additional layers of Mutual Antagonism mechanisms. Perturbation of multiple antagonistic mechanisms confers patterning errors, suggesting that, collectively, these Mutual Antagonism mechanisms are critical for accurate VPC fate patterning.

Reconciling the Sequential Induction and Morphogen Gradient models.

The “Sequential Induction” model does not explain how graded EGF signal promotes 2° fate or varying levels of LIN-3 and LET-23 signaling dose result in different signaling outcomes. This contradiction remained in the field for 16 years (Kenyon, 1995). However, work from our lab reconciled these two models by showing that graded LIN-3-LET-23 signaling promotes 2° fate through a LET-60 switching effectors. In contrast to the LET-60-LIN-45-MEK-2-MPK-1 cascade that is necessary and sufficient to induce 1° fate, the LET-60-RGL-1/RalGEF-RAL-1/

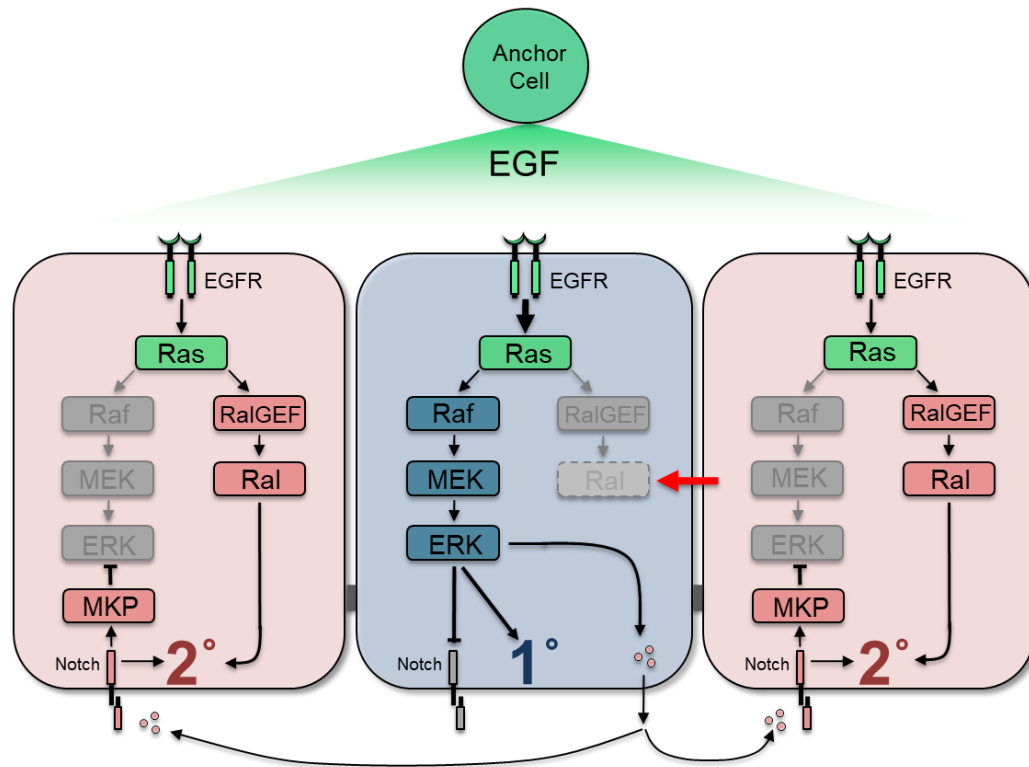


Figure 1. 6 Reconciling the Sequential Induction and Morphogen Gradient models. The Morphogen Gradient Model and Sequential Induction Model were reconciled by the study done by Zand et al., 2011. The LET-23/EGFR-LET-60/Ras-LIN-45/Raf-MEK-2/MEK-MPK-1/ERK promotes 1° fate. In the response to the graded LIN-3/EGF, LET-23 activates LET-60/Ras-RGL-1/RalGEF-RAL-1/Ral to induce 2° fate in support of LIN-12/Notch.

Ral signal promotes 2° fate as a positive modulator in support of LIN-12 (Zand et al., 2011; Figure 1. 6). RalGEF-Ral is a proto-oncogenic non-canonical Ras effector in human cells (reviewed in Gentry et al., 2014; Kashatus, 2013). We further investigated downstream of RAL-1 and found that RAL-1 signals through EXOC-8/Exo84-GCK-2/MAP4K-PMK-1/p38 MAPK to promote 2° fate (Chapter 2).

Yet while LET-60 effector switches from LIN-45/Raf to RGL-1/RalGEF, we do not understand the mechanism of effector switching.

Isolated VPCs distal from the AC were originally shown to frequently assume 2° fate (Katz et al., 1995; Katz et al., 1996; Sternberg and Horvitz, 1986). Yet since LIN-12 is theorized to be essential for assuming 2° fate (Greenwald et al., 1983), it was unclear how these isolated VPCs were induced to become 2° cells. A resolution of this contradiction is that a combination of low dose LIN-3 and autocrine signaling by DSL Notch ligands could induce distal and isolated VPCs to assume 2° fates (Hoyos et al., 2011). While it is unclear how this signaling mechanism intersects with sequential induction and morphogen gradient signaling mechanisms, a plausible model is that all three mechanisms collaborate to spatially induce, reinforce, and restrict 2° fate induction, thereby increasing patterning fidelity.

Trafficking-dependent Regulation of Receptor Localization and Function

In addition to the importance of intercellular spatial relationships in VPC fate patterning, intracellular spatial localization of signals within VPCs has been found to have critical importance. After LET-23 was identified to be an ortholog of the EGF receptor (Aroian et al., 1990) and function cell autonomously in the presumptive 1° cell, P6.p (Hoskins et al., 1996; Koga and Ohshima, 1995; Simske and Kim, 1995), over-expressed GFP fusion proteins and antibody staining

suggested that LET-23 is localized to plasma membrane, with particularly strong localization to junctions (Kaeck et al., 1998; Simske et al., 1996; Whitfield et al., 1999). Subsequent analysis with lower copy number transgene *zh/s35[let-23::GFP + unc-119(+)]* suggests that LET-23 expression is dynamically regulated during VPC patterning (Haag et al., 2014). Our results analyzing CRISPR-mediated tag, LET-23::mKate2, supports this observation (H. Shin and T. Duong, personal communication; Chapter 4). These observations, plus many genetic results and our cell biological results (see Chapter 4), argue that subcellular localization of LET-23/EGFR and perhaps LIN-12/Notch provide critical regulatory axes to control the VPC fate patterning signaling network.

LET-23 basolateral localization system.

The *C. elegans* VPCs are polarized epithelial cells that are connected by adherens junctions (Chisholm and Hardin, 2005). Through these junctions, the six VPCs are tightly connected in the ventral midline in a single row. And, the cell junctions generate separated spatial domains of each VPC: the apical and basolateral plasma membranes of each VPC. Lipids and transmembrane proteins are potentially segregated by these adherens junctions, thus creating potentially distinct signaling domains.

Localization of LET-23 to the basolateral plasma membrane of VPCs is necessary for 1° fate induction. A critical genetic tool for this discovery was the

let-23(sy1) mutation, which introduces a premature stop that truncates the last six residues of the receptor. *let-23(sy1)* animals are vulvaless through lack of 1° induction, but are unaffected for other phenotypes regulated by LET-23, like development of the excretory duct cell or fertility (Aroian et al., 1990; Aroian and Sternberg, 1991). The *sy1* mutation causes LET-23 to be mis-localized to the apical membrane of VPCs, suggesting that the 1°-promoting signal occurs at the basolateral surface, closest to the AC (Simske et al., 1996). Mutations in *lin-2*, *lin-7*, and *lin-10* similarly caused a Vul phenotype without impacting other LET-23 dependent developmental events. LIN-2, LIN-7, and LIN-10 encode orthologs of CASK, Veli, and Mint, respectively, and form a protein complex to localize LET-23 to the basolateral membrane of VPCs (Hoskins et al., 1996; Kaech et al., 1998; Kim, 1997; Simske et al., 1996; Whitfield et al., 1999). LIN-2 has a CaM kinase domain, a calmodulin-binding domain, and a PDZ domain, a SH3 domain, and a guanylate kinase domain (Kim, 1997). LIN-7 has a single PDZ domain (Simske et al., 1996). LIN-10 has a two PDZ domains and a phospho-tyrosine binding domain (PTB) (Kaech et al., 1998). Of particular note is LIN-7, whose PDZ domain may recognize the PDZ recognition sequence in the C-terminus of LET-23 that is removed by the *let-23(sy1)* mutation that causes inappropriate apical localization of LET-23. Taken together, these results indicate that the 1°-promoting signal of LET-23 occurs at the basolateral surface, and requires the LIN-2/-7/-10 complex to proper localization.

A genetic screen for identification genes required for proper localization of LET-23::GFP identified ERM-1 (Ezrin/Radixin/Moesin). ERM-1 may function to keep LET-23::GFP sequestered in basolateral compartments, thus influencing trafficking, and ERM-1 is thought to function independently of LIN-2/-7/-10 (Haag et al., 2014). Thus, multiple axes of spatial regulation likely impact LET-23 signaling.

Negative regulators of LET-23 function through endocytosis, trafficking, and degradation.

A series of negative regulators of the LET-23 1°-promoting signal may control endocytosis and intracellular trafficking of LET-23. Reduced function alleles of *unc-101* were discovered as suppressors of the *let-23(sy1)* vulvaless phenotype (Lee et al., 1994). UNC-101 encodes a medium chain of the clathrin-associated complex AP-1. In a computational screen for genes with LAG-1 binding sites that are putative LIN-12 transcriptional targets, DPY-23 was found to antagonize the 1°-promoting signal (Yoo et al., 2004). DPY-23 has also been implicated in endocytosis of other signaling cascades, including Wnt (Pan et al., 2008). In mammalian cells, the ortholog of DPY-23, which is a subunit of the clathrin Adaptor Protein Complex 2 (AP-2), functions in the degradation of EGFR (Letunic et al., 2002; Rapoport et al., 1997).

C. elegans AGEF-1 is homologous to mammalian BIG1 and BIG2 ArfGEFs (guanine nucleotide exchange factors for the Arf family of small GTPases), which are involved in secretory trafficking between *trans*-Golgi, endosomes and plasma membrane through AP-1 recruitment (Casanova, 2007; Ishizaki et al., 2008; Manolea et al., 2008; Morinaga et al., 1996; Skorobogata et al., 2014). Mutant *C. elegans* AGEF-1 suppressed the vulvaless phenotype of *let-23(sy1)* and *lin-2(e1309)*, suggesting that AGEF-1 functions as a negative regulator of LET-23 signaling; ARF-1.2 and ARF-3, potential GTPase substrates of AGEF-1, are also implicated as negative regulators of LET-23 (Skorobogata et al., 2014). The basolateral localization of LET-23 in LIN-2 mutant is partially restored by AGEF-1 mutant. This result suggests that AGEF-1 represses LET-23 basolateral localization in VPCs.

Mutations in SLI-1 (Suppressor of Lineage defect) were identified as suppressors of the vulvaless phenotype of *let-23(sy1)* (Jongeward et al., 1995; Yoon et al., 1995). SLI-1 is the *C. elegans* ortholog of *Drosophila* D-Cbl and the mammalian proto-oncogene, c-Cbl (Yoon et al., 1995), and its paralogous relatives Cbl-b and Cbl-c. Like other Cbl family members, SLI-1 has four-helix bundle (4H), EF hand, SH2 domain, RING finger domain, SH3 motifs, and two YXN motifs (Yoon et al., 2000; Yoon et al., 1995). Mammalian c-Cbl functions as an E3 ubiquitin ligase. c-Cbl interacts with a broad set of signaling proteins harboring a phospho-tyrosine consensus sequence, mostly EGF Receptor Tyrosine Kinase (Mohapatra et al., 2013; Thien and Langdon, 2001). c-Cbl can

function to trigger proteasome-dependent degradation of EGFR via polyubiquitylation, or endosomal trafficking and recycling via monoubiquitylation (Joazeiro et al., 1999; Levkowitz et al., 1999). A plausible target site by which SLI-1 inhibits LET-23 is through binding to putative phospho-tyrosine site 2 (out of 8 in the LET-23 cytoplasmic region), which has been shown to be a negative regulatory site (Lesa and Sternberg, 1997). Whether this negative regulation is via degradation or subcellular trafficking is unknown.

Mammalian Rab5 and Rab7, Rab family small GTPases, regulate early endosome and late endosome, respectively (Ceresa, 2006). Rab5 promotes EGFR internalization, while Rab7 regulates EGFR trafficking from late endosomes to lysosomes (Barbieri et al., 2000; Dinneen and Ceresa, 2004; Lanzetti et al., 2000; Martinu et al., 2002; Tall et al., 2001). The ortholog of mammalian Rab7, *C. elegans* RAB-7 was shown to be a negative regulator of LET-23: the *rab-7* mutant suppressed the vulvaless phenotype of *let-23(sy1)* and *lin-2(e1309)* (Skorobogata and Rocheleau, 2012). In the RAB-7 mutant, LET-23::GFP is localized at both the apical membrane and the basolateral membrane in P6.p. And, the LET-23::GFP is accumulated in the endocytic vesicles suggesting that RAB-7 regulates LET-23 trafficking.

ARK-1 encodes the Ack-related cytoplasmic tyrosine kinase containing SH3 and CRIB (Cdc42/Rac interactive binding) domains (Hopper et al., 2000). The ARK-1 mutant suppresses vulvaless phenotype in *let-23(sy1)*, *lin-2*, *lin-7*, and *lin-10* mutants and confers a synthetic Muv phenotype in double mutant

combinations with mutations in *sli-1* or *unc-101*, suggesting that ARK-1 redundantly inhibits LET-23 (Hopper et al., 2000). The *ark-1* gene was identified as a potential transcriptional target of LIN-12 (Yoo et al., 2004), suggesting that ARK-1 antagonizes LET-23 specifically in 2° cells, perhaps to prevent inappropriate 1°-promoting signal in 2° cells.

Negative and spatial regulation of LIN-12.

At L2 through early L3 stage before inductive signal starts, LIN-12 protein was shown to be equally expressed in VPCs. Specifically, LIN-12 was shown to be localized to the apical plasma membrane (Levitan and Greenwald, 1998; Shaye and Greenwald, 2002). However, the LIN-12 expressed only in 2° cells and their daughter cells after the VPC fate specification (Levitan and Greenwald, 1998; Shaye and Greenwald, 2002). This suggests that LIN-12 is down-regulated by inductive signal in presumptive 1° cell. LIN-12 may be negatively regulated by internalization and degradation mechanisms. SEL-2 has been shown to be a negative regulator of LIN-12 in 1° cell (de Souza et al., 2007). In SEL-2 mutant, LIN-12 was localized at the basolateral membrane in VPCs, indicating that SEL-2 regulates endocytic trafficking of LIN-12 (de Souza et al., 2007).

Upstream and downstream transcriptional regulators in VPC fate patterning

Changes in transcriptional regulation is central to most developmental processes. In VPC induction, controlled expression of the LIN-3 ligand in the AC patterns the VPCs, which have themselves undergone a prolonged developmental program that includes migrations and competency (Sternberg, 2005). Downstream of inductive signaling lie transcriptional events that execute initial 1°- and 2°-specific fate programs. Here I briefly review known transcriptional programs upstream and downstream of the VPC signaling network.

Upstream: repression of LIN-3 expression by the synMuv genes.

The synthetic multivulva (synMuv) phenotype was discovered by accident in screens for defective vulval formation: two genes are required to be mutated in order to have Muv phenotype, while neither single gene mutant shows normal vulva induction (Ferguson and Horvitz, 1985). Initial examples discovered by accident were the *lin-8*; *lin-9* and *lin-15A/B* double mutants, each of which were shown to comprise mutations in two distinct genes. The synMuv classes A and B were subsequently populated by further screens for the synMuv phenotype in non-Muv single mutants (Ceol and Horvitz, 2004; Ceol et al., 2006; Ferguson and Horvitz, 1989). Subsequent analyses found many more synMuv genes, and argued that even double mutants among the class B mutants confer the synMuv

phenotype at high temperature (Andersen et al., 2008). Some synMuv genes may fall into a third class, Class C (Ceol and Horvitz, 2004).

SynMuv genes are thought to antagonize LIN-3/EGF-LET-23/EGFR signaling. The synMuv mutant combination conferred a Muv phenotype that was suppressed by reduction of *let-23* function (Ferguson et al., 1987). Early genetic mosaic experiments suggest that the synMuv *lin-15A/B* genes function in the hypodermal/epithelial cells surrounding the VPCs, leading to the model that the collection of synMuv genes defined a third pathway that inhibited vulval induction (Herman and Hedgecock, 1990). Consistent with these results, mosaic analysis and use of heterologous promoters indicated that the *lin-35* synMuv gene functions in hypodermis to repress vulval induction (Myers and Greenwald, 2005). Critically, depletion of *lin-3* by RNAi demonstrated that the phenotype caused by mutation of synMuv genes requires LIN-3. Mutation of synMuv genes increases LIN-3 expression in hypodermal cells, and ectopic expression of LIN-3 from hypodermal cells was sufficient to confer a Muv phenotype (Cui et al., 2006). Of critical importance was the identification of a dominant synMuv A mutation, *lin-3(n4441)*, in the promoter of *lin-3*. smFISH experiments indicated that transcription of *lin-3* is tightly regulated spatially, but in synMuv mutants is derepressed show expression in the surrounding hypodermal cells (Saffer et al., 2011). Consequently, a consensus model has emerged that the synMuv genes function collectively to repress the promoter of the *lin-3* gene, thus spatially

restricting LIN-3 expression to the AC and robustly limiting the inductive signal to a precise point source.

Accordingly, many synMuv genes encode transcriptional and/or epigenetic regulators (reviewed in (Fay and Yochem, 2007)). For example, some of synMuv A group genes encode proteins that contain a zinc-finger-like THAP domain (Clark et al., 1994; Davison et al., 2011; Huang et al., 1994). The synMuv B group genes have homology with mammalian proteins that are involved in chromatin remodeling, transcription repression, and histone modification (Andersen and Horvitz, 2007; Ceol and Horvitz, 2001; Couteau et al., 2002; Lu and Horvitz, 1998; Poulin et al., 2005; Solari and Ahringer, 2000; Unhavaithaya et al., 2002). A combination of direct transcriptional repression and gene epigenetic repression is thought to impose strict spatial restriction of the LIN-3 inductive signal. Less well understood is the role of four LIN-3 splice variants/isoforms and the potential role of the ROM-1/Rhomboid protease in propagation of the inductive signal (Dutt et al., 2004; Pu et al., 2017; Van Buskirk and Sternberg, 2007).

Downstream: 1°- and 2°-promoting transcriptional complexes.

Screens for mutants conferring a Muv defect identified the genes *lin-1* and *lin-31*. By genetic epistasis both were found to function downstream in the 1° induction signaling cascade (Beitel et al., 1995; Ferguson et al., 1987; Miller et al., 1993). LIN-1 is an ETS/ELK-1-like transcription factor, which is frequently found

as a downstream ERK target in mammalian cells (Hart et al., 2000). Strong *lin-1* alleles confer an excess 1° phenotype that is insensitive to upstream pathway activity, leading to the model that MPK-1/ERK represses LIN-1 activity, which in turn represses 1° fate. This model was validated by gain-of-function mutations in *lin-1* that confer a vulvaless phenotype, and which identify C-terminal repressive MPK-1/ERK phosphorylation sites (Fantz et al., 2001; Jacobs et al., 1998). The transcriptional targets of 1°-promoting signaling are *egl-17* and LIN-12/Notch ligands, DSL ligands encoded by *lag-2*, *apx-1*, and *dsl-1* (Burdine et al., 1998; Chen and Greenwald, 2004).

LIN-31 is a winged helix transcription factor orthologous to mammalian HNF-1 and *Drosophila* Forkhead (Miller et al., 1993); in modern nomenclature, FoxB. Similar to LIN-1, LIN-31 is also phosphorylated by MPK-1/ERK, and a putative LIN-31-LIN-1 heterodimer is disrupted by this phosphorylation. Over-expression of non-phosphorylatable LIN-31 repressed vulval fates, consistent with this model (Tan et al., 1998). But subsequent CRISPR knock-ins of phosphodeficient and phosphomimetic mutations in the same putative MPK-1 sites failed to alter VPC patterning, so regulation of LIN-31 may be more complex (Dickinson et al., 2013). Yet in contrast to LIN-1, disruption of LIN-31 function confers both Muv and Vul phenotypes: the vulval lineages of *lin-31* mutants could be described as randomized, with any VPC assuming any fate. (Miller et al., 1993; Tan et al., 1998). Consequently, LIN-31 is perceived as a critical determinant of all three potential

VPC fates, but its regulation and interactions with other transcriptional machinery is still not understood.

SUR-2/Med23 and LIN-25/Med24 are important for 1° fate induction and were identified, respectively, based on suppression of activated LET-60/Ras and a Vul phenotype. SUR-2 and its partner LIN-25 are subunits of the multi-subunit transcriptional Mediator complex, and function downstream of or parallel to MPK-1 in VPCs (Nilsson et al., 1998; Nilsson et al., 2000; Singh and Han, 1995; Tiensuu et al., 2005; Tuck and Greenwald, 1995). Through use of diverse cofactors to generate a variety of distinct complex types, the Mediator complex functions to bridge tissue-specific transcription factors and RNA polymerase II, as well as potentially integrating inputs of various transcriptional enhancers and repressors (Allen and Taatjes, 2015). Mammalian Elk1, an ortholog of LIN-1, interacts with the MED23/Sur2 in an ERK-dependent manner (Stevens et al., 2002), validating the model of MPK-1 repression of LIN-1 and the role of SUR-2/LIN-25 and the Mediator complex in VPC induction. SUR-2 and the Hox protein LIN-39, which is required for VPC competence (Guerry et al., 2007; Maloof and Kenyon, 1998; Wagmaister et al., 2006), likely collaborate to promote transcription of the lateral signaling genes *lag-2*, which encodes a DSL ligand for LIN-12/Notch (Zhang and Greenwald, 2011). Genetic analyses suggest that various subtypes of the Mediator complex, particularly the CKM module, function to set activity thresholds and discriminate between MPK-1/ERK 1°- and LIN-12/Notch 2°-promoting signaling activity, thus providing a key integration point between the VPC signaling

network and precise transcriptional execution of VPC fates (Grants et al., 2016; Underwood et al., 2017).

In parallel to these transcriptional mechanisms are EOR-1 and EOR-2 (EGL-1 suppressor, Di-Q uptake defective, Raf enhancer), which also functions together downstream of MPK-1 to positively regulate vulva induction (Howard and Sundaram, 2002). The EOR-1 encodes a BTB and C₂H₂ Zinc finger protein and the EOR-2 is a binding partner of EOR-1 (Howard and Sundaram, 2002; Howell et al., 2010).

Notch receptors are unusual, in that they comprise the entirety of their signal transduction cascade, from the plasma membrane to the nucleus. Specifically, upon ligand binding and activation, a series of proteolytic cleavage events released the intracellular domain (ICD) of Notch receptors, including LIN-12, which then translocates to the nucleus. There, the ICD functions as a transcriptional co-activator (Struhl et al., 1993); reviewed in (Greenwald, 2005; Greenwald and Kovall, 2013).

A critical advance in *C. elegans* Notch biology was the discovery that the two nematode Notch receptors, GLP-1 and LIN-12, share functional redundancy in certain processes. The double mutant conferred a distinctive first stage (L1) larval arrest dubbed the LAG phenotype (LIN-12 and GLP-1; Lambie and Kimble, 1991). Screens for this phenotype identified two additional genes in the Notch system, LAG-1 and LAG-3 (LAG-2 encodes a shared LIN-12 and GLP-1 DSL ligand; Tax et al., 1997). LAG-1 encodes the nematode ortholog of *Drosophila* Suppressor of

Hairy (Su(H)) and mammalian CBF1, established DNA-binding proteins. Like Su(H)/CBF1, LAG-1 binds a conserved consensus target sequence, RTGGGAA (Christensen et al., 1996). LAG-1 binds the ICD, and together they can activate transcription (Roehl et al., 1996). LAG-3 (*a.k.a.* SEL-8) is a Glutamine-rich protein similar to *Drosophila* mastermind that forms a complex with LAG-1 (Doyle et al., 2000; Petcherski and Kimble, 2000). Together, these proteins and the ICD likely form a ternary complex that regulates transcription of tissue-specific client genes.

Using a more refined consensus binding sequence from other systems (YRTGTGAA; “Lag binding sequence (LBS)”) potential target genes of Notch signaling were identified computationally. Candidates were validated by RNAi depletion and promoter::GFP transcriptional fusions. Thus, the Notch target genes such as *dpy-23*, *lst-1*, 2, 3, and 4, *mir-61*, were identified. Collectively, these genes appear to function to antagonize 1°-promoting signals, contributing to the Mutual Antagonism Model. Target genes that promote 2° fate have not yet been identified, suggesting that they share redundant functions (Yoo et al., 2004; Yoo and Greenwald, 2005).

Transcriptional reprogramming of the VPC signaling network

Prior to induction of naïve VPCs, expression of promoter::GFP fusions is typically uniform. Soon after induction, however, expression levels of many promoters, particularly of modulatory genes, is dynamically regulated. This

reprogramming contributes to key mechanisms of VPC fate patterning, such as mutual antagonism (see above), and thus represents plasticity of the signaling network that accompanies initial specification of fates. Furthermore, we posit that reprogramming of the expression of modulatory signals helps reinforce initial patterning, so VPCs can commit to their fate decisions while mitigating conflicting signals, or “noise”, can could introduce developmental error.

Mostly, transcriptionally reprogrammed genes have been identified as negative regulators of 1°-promoting signal, or computationally discovered as transcriptional targets of the LIN-12/Notch lateral signal. Whether the latter are 2°-promoting or anti-1° is difficult to determine by existing genetic assays, since the two signals are mutually antagonistic. The restriction of gene expression to specific VPC lineages reinforces the final commitment and fidelity during VPC fate patterning. Here I describe the examples of transcriptional reprogramming in VPC fate patterning.

Reporters for LIN-12/Notch target genes are expressed consistently in VPCs at the early L3 stage, before VPC fate patterning has happened. However, at late L3 stage, typically before the first cell division, expression from reporters is excluded from the 1° but not the 2° cell/lineage. Reporters are expressed strongly in 2° cells after VPC fate patterning (Figure 1. 7A). For example, the 2°-promoting *ral-1* gene, LIN-12/Notch target genes *dpy-23*, *lst-1*, 2, 3, and 4, and 1°-antagonizing genes *lip-1* and *dep-1* all showed this transcriptional expression pattern in VPCs (Berset et al., 2001; Berset et al., 2005; Yoo et al., 2004; Zand et

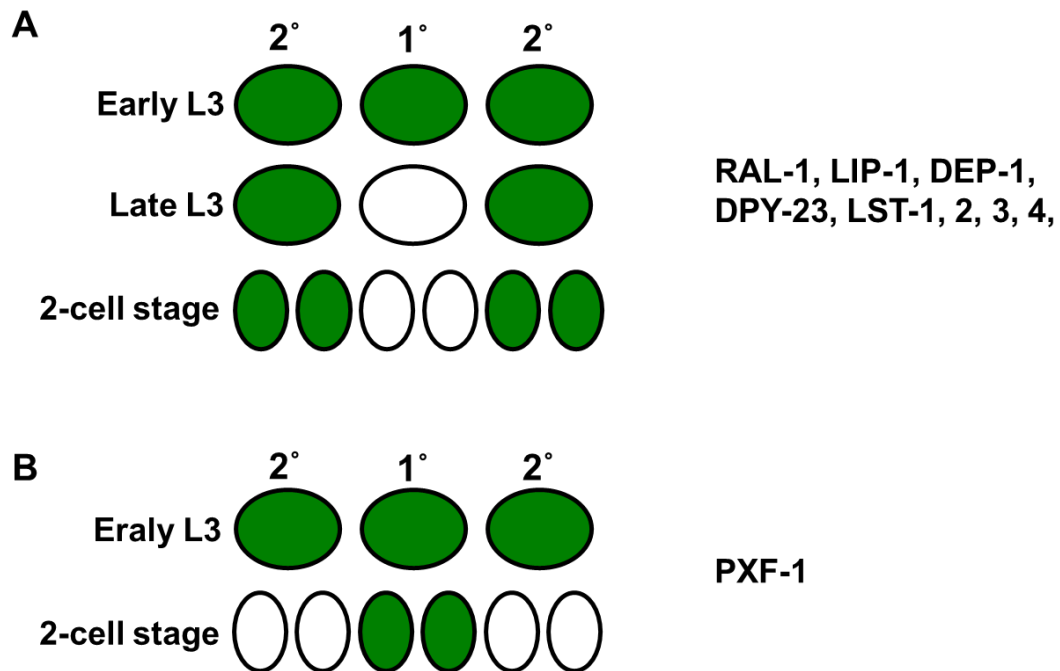


Figure 1. 7 Expression pattern of transcription of either 2°-promoting and 1°-antagonizing or 1°-promoting genes in VPCs. Transcriptional reprogramming is shown by promoter GFP fusion in VPCs. **A.** 2°-promoting RAL-1 and 1°-antagonizing LIP-1, DEP-1, DPY-23, LST-1, -2, -3, and -4 are transcribed in both 1° and 2° cells at early L3/before induction. However, they are transcriptionally down-regulated in 1° cells, but still expressed in 2° cells and their daughters at late L3 and 2-cell stage. **B.** 1°-promoting PXF-1 is transcribed in 1° and 2° cells at early L3 stage. The transcription of PXF-1 persists in the daughters of 1° cell at 2 cell stage. However, PXF-1 transcription is negatively regulated in the daughters of 2° cells at 2-cell stage.

al., 2011). Strikingly, after induction, expression from these reporters was excluded from the presumptive 1° cell, but persisted strongly in presumptive 2° cells. We speculate that such transcriptional reprogramming of these genes reinforces 1°-antagonizing and/or 2°-promoting function, thereby better demarcating cell fate signaling and increasing developmental fidelity in the system.

An exception to this observation is highlighted by the ligands for the lateral 2°-promoting signal mediated by LIN-12/Notch: transcriptional reporters for *apx-1*, *dsl-1*, and *lag-2* are expressed in the presumptive 1° cell in response to inductive signal and repressed in non-1° cells (Chen and Greenwald, 2004; Zhang and Greenwald, 2011). That their reporter expression reflects that otherwise expected for 1°-promoting genes is consistent with their cell non-autonomous role as the ligands for the LIN-12/Notch lateral signal. This observation is an important validation of the Sequential Induction Model, and may be the exception that proves the rule for transcriptional reprogramming.

Transcriptional reporters for 1°-promoting genes also reveal initially consistent expression that dynamically changes after induction. But in this case the induction reflects reprogramming consistent with initial specification to promote 1° fate (Figure 1. 7B). A different modulatory signaling axis, that of PXF-1/RapGEF signaling to the very close LET-60/Ras sibling, RAP-1/Rap1, promotes 1° fate in parallel to LET-60 (Rasmussen et al., in revision). CRISPR-tagged endogenous RAP-1 is expressed ubiquitously, and GFP expressed from a transgenic promoter fusion of *pxf-1* showed uniform expression in all VPCs at

early L3 stage before VPC fate patterning. However, after induction, *pxf-1* reporter GFP expression was excluded from 2° cells and increased in 1° cells at the Pn.px stage. This result is consistent with transcriptional reprogramming of PXF-1 expression restricting activation of 1°-promoting RAP-1 to the 1° cell while abrogating the activation of RAP-1 in 2° cells. Consequently, we hypothesize that PXF-1-RAP-1 functions as a spatially refined positive feedback loop to promote 1° fate.

Transcriptional reporters for the *egl-17* gene reveal an expression pattern that reflects the putative morphogen gradient: reporter expression is absent prior to induction, then after induction is high in presumptive 1° cells and faint and transient in presumptive 2° cells (Burdine et al., 1998; Yoo et al., 2004). Mutations in *lip-1* and *dep-1*, negative regulators of the 1°-promoting cascade, cause the *egl-17* reporter to persist in 2° cells (Berset et al., 2001; Berset et al., 2005; Yoo et al., 2004). Yet this reporter is likely not a reporter for 1° fate, but rather a direct transcriptional target of LIN-1/ELK1, downstream of MPK-1/ERK (Tiensuu et al., 2005). EGL-17 is an ortholog of mammalian FGF, and its secretion by the presumptive 1° cell helps the migrating SM cells home in on the A-P midpoint of the animal (Burdine et al., 1997).

The regulation of genes at the transcriptional level does not necessarily reflect expression of protein at the translational level. For example, the promoter::GFP transcriptional fusion of *ral-1* showed dynamic changes in levels during VPC induction (Zand et al., 2011). In contrast, the endogenously tagged

RAL-1 by CRISPR appears to be expressed consistently throughout VPC development, and localized to the plasma membrane in all VPCs (Shin et al., 2018). How do we reconcile these differences? One possibility is that transgenic promoter fusions mis-express GFP in a pattern that does not reflect endogenous protein expression. However, transcriptional changes may not dramatically impact stable endogenous protein with low turnover. But transcriptional changes coupled with other layers of post-transcriptional and post-translational changes may still collectively impact signaling outputs, and thus restrict signaling activity to certain cell types and exclude signals from others. We hypothesize that the observed transcriptional reprogramming is functionally significant, and contributes to the fidelity of the VPC patterning system.

Environmental and genetic regulators and variability

Changes in the environment could represent one of the main perturbations to the fidelity of a developmental system. Errors in VPC patterning can result in decreasing progeny. Thus, the result of VPC fate patterning is related to reproductive success and evolutionary fitness. The *C. elegans* VPC fate patterning is precise and robust process. The VPC fate patterning has 99.8% rate of accuracy with variable environmental conditions (Braendle and Felix, 2008). The fidelity of VPC fate patterning is controlled by signaling network, mainly 1°-promoting Ras and 2°-promoting Notch signals. Therefore, perturbation of these

signals can provoke variation of VPC fate patterning with increased error rate (Braendle and Felix, 2008). This system has also been used to assess the impact of heterogeneity in polymorphic wild *C. elegans* isolates (Grimbert and Braendle, 2014; Sterken et al., 2017). Mutual Antagonism and the putative RGL-1-mediated “Balanced Switch” may be key mechanisms that decrease developmental error (see above). An intriguing observation is that deletion of the RGL-1 “Balanced Switch” increases error rate as a result of stochasticity but not environmental perturbation. In contrast, while mutation perturbation of the balance of 1° vs. 2° signaling axes increases sensitivity to environmental perturbations, basal signaling error is not increased (Barkoulas et al., 2013; Braendle et al., 2010; Dubeau and Felix, 2012; Milloz et al., 2008). We conclude that complex mechanisms exist to reduce noise in the signaling network that controls VPC patterning. Also, the consequences of perturbing the “Balanced Switch” is different than the consequences of perturbing the balance of 1° and 2° signals. Perhaps distinct mechanisms have evolved to minimize the consequences of these two different sources of “noise”.

Conclusions

A view is emerging of a sophisticated signaling network that controls the fate patterning of the *C. elegans* VPCs. In response to LIN-3/EGF, VPCs are precisely patterned by two main signaling cascades. The necessary and sufficient EGFR-

and Notch-mediated signals establish the skeleton pattern of initial fate specifications. A signaling gradient, orchestrated modulatory signaling cascades, and transcriptional reprogramming of mutual antagonism induction programs act together to further sculpt these fate decisions both spatially and temporally. Collectively, these and presumably additional, unknown mechanisms collaborate to generate a highly precise and robust pattern prior to terminal differentiation. Most of the signaling molecules described in the VPC patterning network are conserved in mammals as proto-oncogenes or tumor suppressor genes. Thus, study of the VPC patterning system provides insights into our understanding of signaling networks in both development and pathology. With the advent of additional insights into the mechanisms underpinning fidelity and robustness, the VPC patterning system potentially elucidates the role of noise in both defects and oncogenesis.

CHAPTER II

RAL SIGNALS THROUGH A MAP4 KINASE-P38 MAP KINASE CASCADE IN *C. ELEGANS* CELL FATE PATTERNING*

Introduction

Ras is the most mutated oncoprotein. Yet strategies to inhibit oncogenic Ras have failed, so Ras is considered to be mostly “undruggable” (Papke and Der, 2017). Consequently, attention has shifted to oncogenic Ras effectors to identify therapeutic targets. Canonical oncogenic Ras effectors, the Raf-MEK-ERK and PI3K-PDK-Akt cascades, are among the best studied and most targeted signaling cascades (Ryan et al., 2015; Wong et al., 2010). Yet even potent small molecule inhibitors, like the BRAF inhibitor vemurafenib, are subject to multiple bypass mechanisms that permit initially responsive tumors to relapse (Sun et al., 2014). Thus, successful treatment will likely require multi-pronged regimens to simultaneously inhibit multiple Ras effectors.

In addition to the canonical Raf and PI3K cascades, Ras uses RalGEF-Ral to promote tumorigenesis (Feig, 2003). Historically, canonical Ras-Raf and Ras-

Reprinted with permission from. *MAP kinase cascade in *C. elegans* cell fate patterning.” by Hanna Shin[#], Rebecca E.W. Kaplan[#], Tam Duong, Razan Fakieh and David J. Reiner, Cell Reports Vol. 24, Issue 10, P2669-2681.e5, September 04, 2018. Doi: <https://doi.org/10.1016/j.celrep.2018.08.011>, Copyright [2018] by all authors. [#]These authors contributed equally to this work.

PI3K signaling was shown to cause cancer transformation of mouse primary fibroblasts (Khosravi-Far et al., 1996; Kyriakis et al., 1992; White et al., 1995). The emergence of immortalized human epithelial cell culture led to the key finding that Ras-RalGEF-Ral is also a critical player in human oncogenesis (Hamad et al., 2002; Urano et al., 1996; White et al., 1996). RalGEF is an exchange factor that promotes GTP loading of the Ral (Ras like) small GTPase (Feig, 2003). Loss of RalGAP (Ral GTPase activating protein), a putative tumor suppressor, increases tumorigenesis without activated Ras (Oeckinghaus et al., 2014; Saito et al., 2013), further supporting the importance of Ral signaling in cancer.

Three binding partners of Ral have been well validated: RalBP1 (Ral binding protein 1) and Sec5 and Exo84 subunits of the heterooctameric exocyst complex (reviewed in Gentry et al., 2014; Fig. 2. 1A). The exocyst represents an unusual roadblock to biochemical bootstrapping of signaling activities: the exocyst is broadly integral to essential cell biological processes (e.g. exocytosis, PAR/polarity complex; Wu and Guo, 2015) and potentially binds to hundreds of partners, thus mostly precluding identification of downstream signaling partners via binding studies. Consequently, beyond these immediate binding partners, we know little of downstream functions of Ral signaling through the exocyst *in vivo*.

Studies in *Drosophila* provided key hints to the nature of Ral downstream signaling in development. In morphogenetic events, DRal was implicated in antagonizing the JNK MAP kinase (Sawamoto et al., 1999). In bristle apoptosis assays, DRal was found to have negative and positive relationships with JNK and

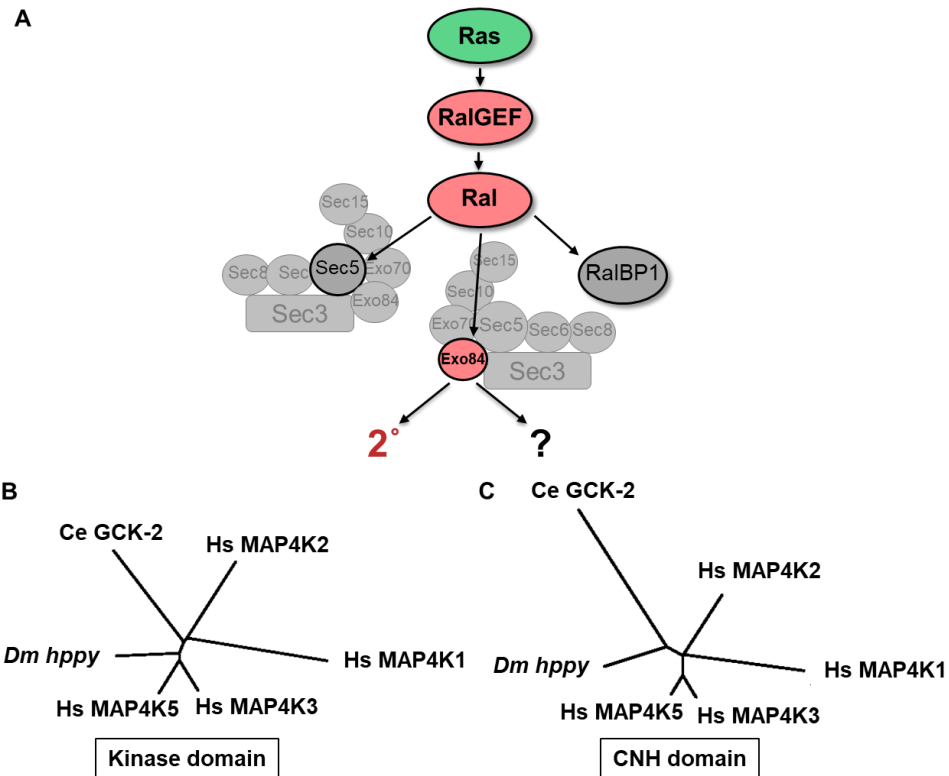


Figure 2. 1 A model of Ral effector use in VPC fate patterning and MAP4K families and sensitized backgrounds. A. Ras signals through RalGEF-Ral in cancer and *C. elegans* 2° fate induction. Mammalian Ral has three known oncogenic binding partners: Exo84, Sec5, and RalBP1. **B-C.** Unrooted dendrograms of GCK-2/GCK-I subfamily (*C. elegans* GCK-2, *Drosophila* Happyhour (Hppy), mammalian MAP4K1/HPK1, MAP4K2/GCK, MAP4K3/GLK, and MAP4K5/GCKR/KHS1) kinase (B) and CNH (C) domains. Between the GCK-2 and *Drosophila* Hppy orthologs, the kinase and CNH domains share 71% and 31% identity, respectively. *Reprinted with permission from Shin et. al, 2018*

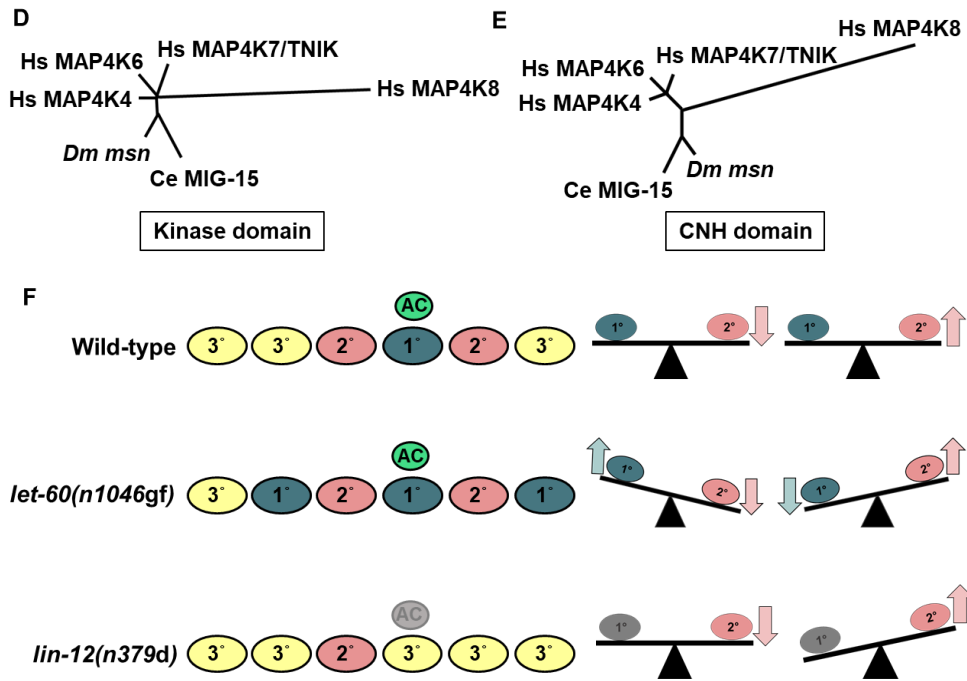


Figure 2.1 Continued. D-E. Unrooted dendrograms of MIG-15/GCK-IV subfamily (*C. elegans* MIG-15, *Drosophila* Misshapen (Msn), vertebrate MAP4K4/NIK/HGK, MAP4K6/MINK, MAP4K7/TNIK, and MAP4K8/NRK/NESK) kinase (D) and CNH (E) domains, calculated by CLUSTALW. Ce: *C. elegans*, Dm: *D. melanogaster*, and Hs: *Homo sapiens*. Between the GCK-2 and MIG-15 paralogs, the kinase domain and CNH domain share 45% and 29% sequence identity, respectively. Between the MIG-15 and *Drosophila* Msn orthologs, the kinase and CNH domains share 83% and 79% identity, respectively. Thus, sequence conservation is greater within a subfamily between species than across subfamilies within a species. **F.** Schematics of genetically sensitized backgrounds and responses to altered degree of modulatory 2° signaling (Zand et al., 2011). Wild-type animals have the 3°-3°-2°-1°-2°-3° pattern of vulval cell fates. In the *let-60(n1046gf)* background with ectopic 1° cells, levels of ectopic 1°s go up when 2°-promoting signal is blocked and go down when 2°-promoting signal is activated. In the *lin-12(n379d)* background without an AC (and hence no LIN-3/EGF) and with occasional ectopic 2° cells, levels of ectopic 2° cells are unaltered when 2°-promoting signal is blocked and increased when 2°-promoting signal is activated. *Reprinted with permission from Shin et. al, 2018*

p38 MAP kinase cascades, respectively (Balakireva et al., 2006). Importantly, this study also established that exocyst component Sec5 binds to HGK/NIK/MAPK4, a CNH domain containing MAP4 kinase. The *Drosophila* ortholog, Msn (Misshapen) was found to function antagonistically to DRal (Balakireva et al., 2006), and is known to function with JNK in *Drosophila* embryonic dorsal closure and other morphogenetic events (Su et al., 1998). Yet these studies relied on ectopic over-expression and dominant-negative reagents, which complicated interpretation. Furthermore, direct genetic epistasis could not be assayed because many of the proteins studied are essential for development in *Drosophila*.

The Ste20 family of mitogen-activated protein kinase kinase kinases (MAP4 Kinases or MAP4Ks) is conserved throughout eukaryotes (Dan et al., 2001; Delpire, 2009). Two paralogous subfamilies of this group, GCK-I and GCK-IV (Germinal Center Kinases), are defined by distinctive domain architecture: an N-terminal S/T kinase domain, a C-terminal CNH domain (for Citron N-terminal Homology), and an unstructured poly-proline linker region (Fig. 2. 2A; Dan et al., 2001). *C. elegans* GCK-2 (ZC404.9) is an 829-residue protein in the GCK-I subfamily (the “GCK-2 group”: *Drosophila* Hppy (Happyhour), mammalian MAP4K1/HPK1, MAP4K2/GCK, MAP4K3/GLK, and MAP4K5/GCKR/KHS1; Figs. 2. 1B-C). *C. elegans* MIG-15 is in the GCK-IV subfamily (the “MIG-15 group”: *Drosophila* Msn, mammalian MAP4K4/NIK/HGK, MAP4K6/MINK, MAP4K7/TNIK, and MAP4K8/NRK/NESK; Figs. 2. 1D-E).

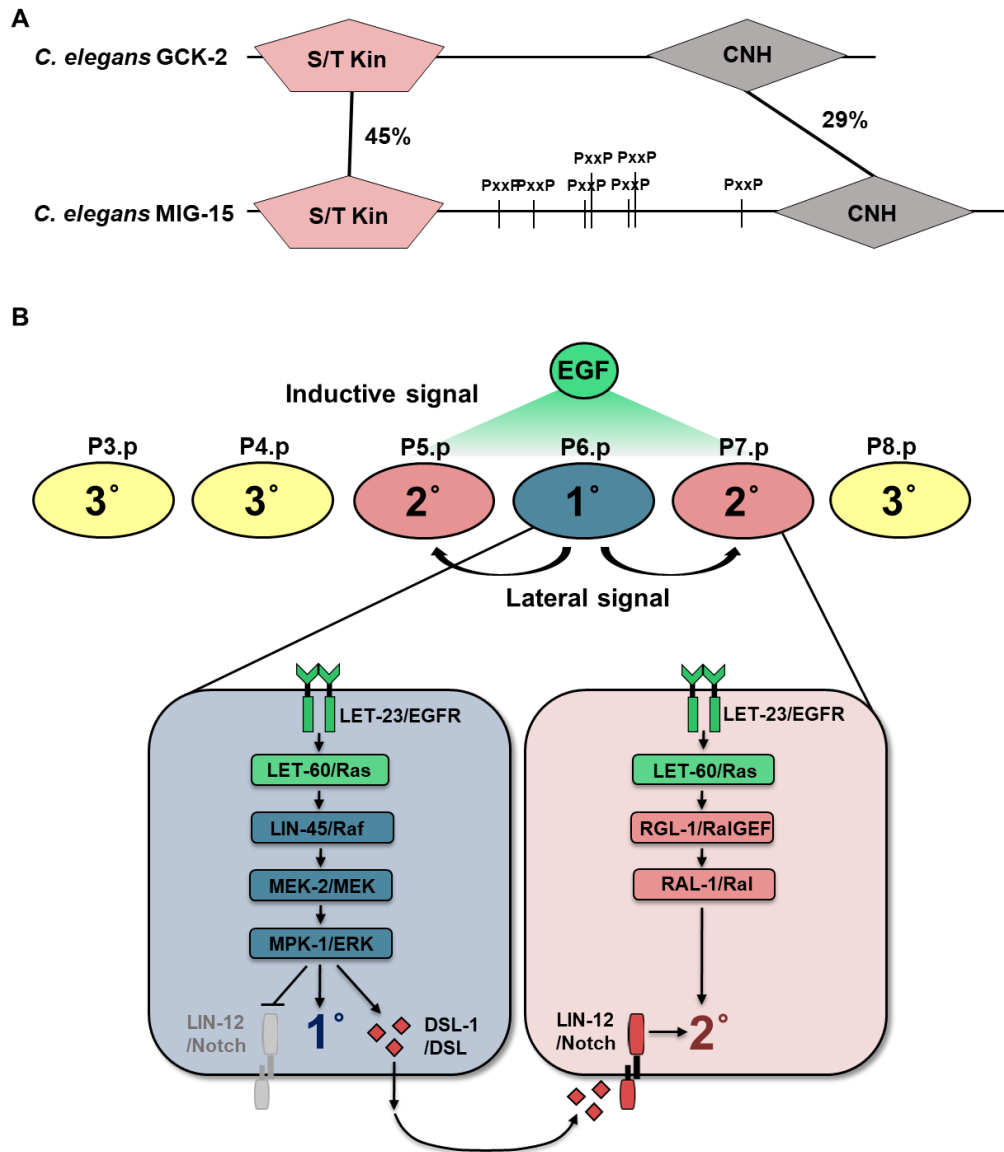


Figure 2. 2 *C. elegans* CNH-domain organization MAP4Ks and VPC fate patterning. **A.** Domain organization and conservation of paralogous *C. elegans* MAP4Ks GCK-2 and MIG-15. **B.** VPCs, P3.p through P8.p, are patterned to assume 3°-3°-2°-1°-2°-3° fate by coordinated graded action of EGF secreted from the anchor cell and Notch lateral signal. LET-60/Ras-LIN-45/Raf-MEK-2/MEK-MPK-1/ERK and LET-60/Ras-RGL-1/RaIGEF-RAL-1/Ral promote 1° fate and 2° induction, respectively. *Reprinted with permission from Shin et. al, 2018*

Critically, *Drosophila* Hppy was as yet undiscovered at the time of Msn investigation relative to DRal (Balakireva et al., 2006). Hppy antagonizes canonical EGFR signaling through ERK MAPK in ethanol response; its relationship to DRal was not studied (Corl et al., 2009). Thus, we turned to *C. elegans* VPC fate patterning to investigate a signaling cascade downstream of Ral relative to these enigmatic MAP4 kinases.

During the L3 stage, EGF produced by the gonadal Anchor Cell (AC) induces six initially equipotent Vulval Precursor Cells (VPCs), P3.p through P8.p, to assume the highly reproducible 3°-3°-2°-1°-2°-3° pattern (Fig. 2. 2B). 1° and 2° cells undergo stereotyped divisions and morphogenesis to form the mature vulva, while uninduced 3° cells divide once and fuse with surrounding cells (Sternberg, 2005). Historically, two competing models, the “Morphogen Gradient Model” and the “Sequential Induction Model”, were posited to describe VPC fate patterning. In the “Morphogen Gradient Model”, graded inductive signal controls fate patterning: the VPC closest to the AC (typically P6.p) receives the highest LIN-3/EGF-LET-23/EGFR signal to induce 1° fate, while neighboring VPCs, P5.p and P7.p, receive lower LIN-3/EGF-LET-23/EGFR signal, and thus become 2° (Katz et al., 1995; Katz et al., 1996; Sternberg and Horvitz, 1986, 1989). Yet identification of key genes in VPC patterning led to the potentially contradictory “Sequential Induction Model”. LET-23/EGFR and LIN-12/Notch are necessary and sufficient for 1° and 2° induction, respectively (Aroian et al., 1990; Greenwald et al., 1983). Activation of LET-23/EGFR triggers a LIN-45/Raf-MEK-2/MEK-MPK-

1/ERK canonical MAP kinase (MAPK) cascade to induce 1° fate (reviewed in Sundaram, 2013). These presumptive 1° cells in turn secrete DSL ligands to induce neighbors to become 2° via the LIN-12/Notch (Chen and Greenwald, 2004). LET-23/EGFR was found to function cell autonomously to induce 1° fate, further supporting the “Sequential Induction Model” (Koga and Ohshima, 1995; Simske and Kim, 1995). The two models long remained unreconciled, and no mechanism was known by which graded LIN-3/EGF-LET-23/EGFR activity promotes 2° fate (Kenyon, 1995).

Overlaid on this system are “Mutual Antagonism” mechanisms by which, after initial induction, presumptive 1° and 2° cells enact programs to exclude potentially contradictory signals. For example, in presumptive 1° cells, LIN-12/Notch receptor is internalized and degraded to prohibit conflicting 2°-promoting signaling (Shaye and Greenwald, 2002, 2005). Conversely, in presumptive 2° cells LIN-12/Notch-dependent transcription of LIP-1/ERK phosphatase impedes conflicting 1°-promoting MPK-1/ERK signaling (Berset et al., 2001; Yoo et al., 2004). Such antagonistic signals are proposed to act collectively to transition from initial patterning specification to commitment (Sternberg, 2005), thereby avoiding inappropriate and/or ambiguous cell fates that can result from inappropriate signals.

Given the importance of Ras-RalGEF-Ral signaling in cancer, we set out to define a role for this signaling module in VPC fate patterning. We found that LET-60/Ras uses the non-canonical RGL-1/RalGEF-RAL-1/Ral effector to promote 2°

fate in support of LIN-12/Notch (Zand et al., 2011). Thus, both the Sequential Induction and Morphogen Gradient models are correct: LET-60/Ras switches effectors to interpret the EGF gradient. This mechanism reconciled the two competing models and established a platform for the *in vivo* study of RAL-1/Ral signaling in VPC fate patterning (Reiner, 2011; Zand et al., 2011; Fig. 2. 2B). Yet the downstream output of the LET-60/Ras-RGL-1/RalGEF-RAL-1/Ral 2°-promoting signal remained unknown.

In this study, we determine that EXOC-8/Exo84, a well-validated Ral-binding protein in mammalian cells, is required to propagate the RAL-1 2°-promoting signal. Significantly, we find that RAL-1 requires the CNH domain-containing GCK-2/MAP4K and PMK-1/p38 MAPK to promote 2° fate. Genetic perturbation of components of this cascade phenocopied perturbation of RAL-1, and these components are necessary for the 2°-promoting activity of mutationally activated RAL-1. 2°-promoting EGF signal requires GCK-2, putative mutationally activated endogenous GCK-2 is sufficient to increase ectopic 2° cell induction, and GCK-2 functions cell autonomously in the VPCs. Using CRISPR/Cas9-dependent genome engineering to tag endogenous gene products with fluorescent protein (FP) and epitope, we observed expression and subcellular localization of endogenous RAL-1, GCK-2, and PMK-1 proteins in VPCs. Our *in vivo* analysis connects Ral to a novel effector cascade in *C. elegans* VPC fate patterning.

Results

Criteria for a RAL-1-dependent 2°-promoting signal.

Since LIN-12/Notch, but not the LET-60/Ras-RGL-1/RalGEF-RAL-1/Ral signal, is necessary for 2° fate induction, we used a combination of parallelism and epistasis to test the genetic relationships among members of the VPC fate-patterning network. Specifically, for this genetic analysis we used two sensitized genetic backgrounds (Fig. 2. 1F). The *let-60(n1046gf)* G13E activating mutation confers excess 1° induction, levels of which are sensitive to perturbation of both 1° - and 2°-promoting signals. The weakly activating *lin-12(n379d)*/Notch mutation both causes ectopic 2° cells and abrogates development of the AC. Consequently, *lin-12(n379d)* provides a simplified signaling milieu in which EGF is not present (Greenwald et al., 1983). This background is sensitive to perturbation of 2° - but not 1°-promoting signals and responds to the EGF-dependent 2°-promoting signal (Zand et al., 2011).

Partly by using these tools, we developed a set of expectations for RAL-1 2°-promoting effectors. (1) Loss of effector function should phenocopy loss of *ral-1* function. (2) Constitutively activated effector should phenocopy constitutively activated RAL-1. (3) Loss of effector function should be epistatic to constitutively activated RAL-1. (4) The effector should function cell autonomously in the VPCs. (5) The effector should be expressed in the VPCs. Using these criteria, we

systematically evaluated a putative RAL-1 signaling cascade in 2° VPC fate induction.

EXOC-8 functions in VPC fate patterning.

We tested whether known Ral binding partners, Sec5 and Exo84 of the exocyst complex and RalBP1/RLIP76 (reviewed in Gentry et al., 2014; Fig. 2. 1A), met our first criterion for a RAL-1 effector: loss of effector function should phenocopy loss of *ral-1* function. The heterooctameric exocyst complex generally consists of eight subunits used in different contexts: Sec3, Sec5, Sec6, Sec8, Sec10, Sec15, Exo70 and Exo84 (Wu and Guo, 2015), all of which have single conserved orthologs in *C. elegans*.

Deletion of *ral-1* leads to defects in cell polarity, apparently by disruption of the exocyst complex (Armenti et al., 2014), consistent with previous observations that mammalian Ral functions as a membrane-tethering member of the exocyst (Issaq et al., 2010; Moskalenko et al., 2002; Moskalenko et al., 2003). We previously found that *ral-1(RNAi)* alone did not confer significant vulval patterning defects, nor did a non-null intronic deletion allele of *ral-1* that conferred sterility (Zand et al., 2011). We characterized the *ral-1(gk628801rf)* R139H mutation, which did not confer visible defects (Shin et al., in preparation). In the *let-60(n1046gf)* background, *gk628801rf* caused increased 1° induction, consistent with as a loss-of-function (lf) but not null allele in *ral-1*. This result validated our

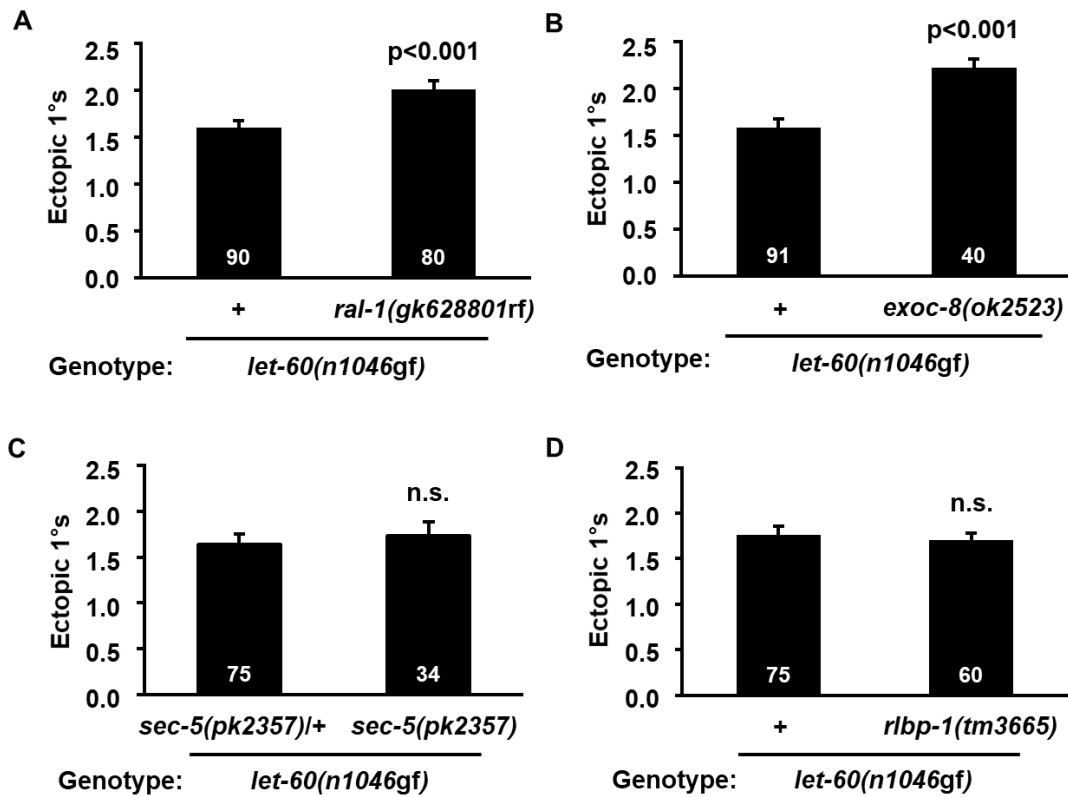


Figure 2. 3 EXOC-8 functions in VPC fate patterning. The Y-axis indicates number of ectopic 1° cells. **A-B.** The *ral-1* (*gk628801rf*) R139H missense (A) and *exoc-8(ok2523)* deletion (B) mutations increased ectopic 1° induction in the *let-60(n1046gf)* background. **C.** The *sec-5(pk2357)* late nonsense allele (Frische et al., 2007) did not alter ectopic 1° induction in the *let-60(n1046gf)* background. **D.** The *rlbp-1* out-of-frame deletion allele, *tm3665*, conferred no change in the *let-60(n1046gf)* background. N indicated in white on columns. P value calculated by *t* test. Error bars = S.E.M. Reprinted with permission from Shin et. al, 2018

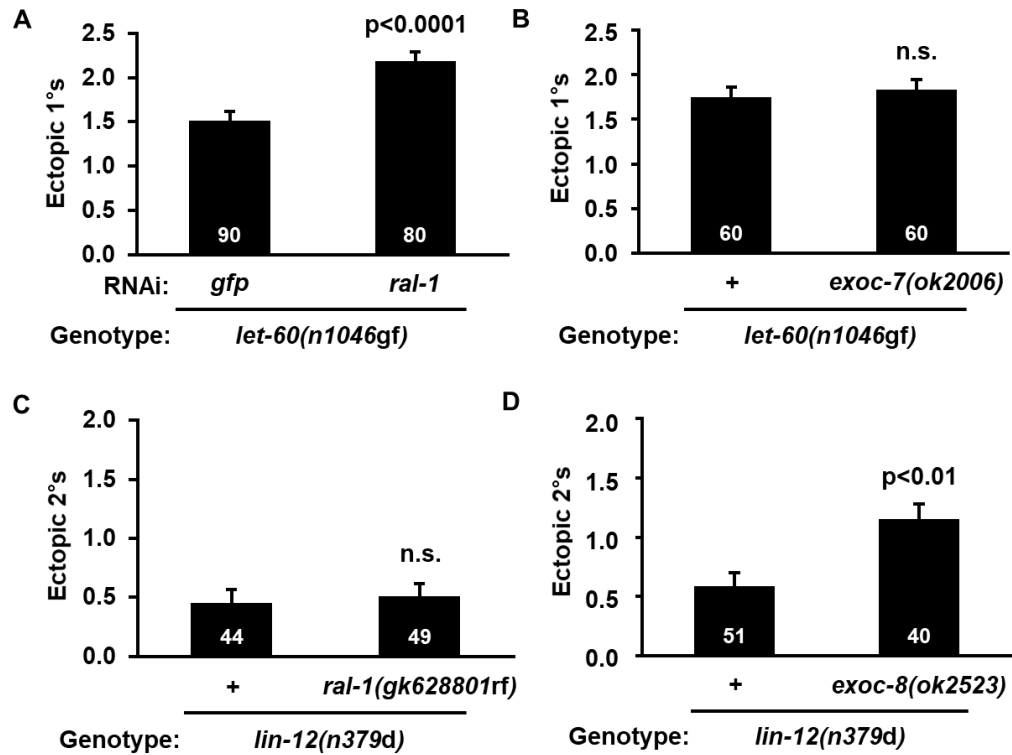


Figure 2. 4 EXOC-8 but not SEC-5 or RLBP-1 functions in VPC fate patterning.

Y axes indicate number of ectopic 1° or 2° cells. **A.** *ral-1(RNAi)* increased ectopic 1° induction in the *let-60(n1046gf)* background. *gfp*-directed RNAi was used for negative control (Zand et al., 2011). **B.** The *exoc-7(ok2006)* deletion did not alter ectopic 1° induction in the *let-60(n1046gf)* background. **C.** As predicted, the *ral-1(gk628801)* R139H missense mutation did not alter ectopic 2° induction in the *lin-12(n379d)* background. **D.** The *exoc-8(ok2523)* deletion conferred increased ectopic 2° induction *lin-12(n379d)*. P values calculated by *t* test. Error bars = S.E.M. Reprinted with permission from Shin et. al, 2018

previous findings that reduced *ral-1* signaling and hence reduced 2° signaling increased 1°-promoting signals (Figs. 2. 3A, 2. 4A).

In the same genetic background, we tested effects of the *sec-5(pk2357)*

strong hypomorph (Frische et al., 2007), *exoc-8(ok2523)*, and *rlbp-1(tm3665)* deletion alleles (*exoc-7(ok2006)* was included as a negative exocyst control). Among these candidate RAL-1 effectors, only *exoc-8(ok2523)*, a deletion allele, phenocopied *ral-1(gk628801rf)* (Figs. 2. 3B-D, 2. 4B). As expected, *ral-1(gk628801rf)* caused no phenotypic changes in the *lin-12(n379d)* background (Fig. 2. 4C). These results are consistent with EXOC-8 mediating RAL-1 2°-promoting signal.

We also tested *exoc-8(ok2523)* in the *lin-12(n379d)* background. We observed increased ectopic 2° induction (Fig. 2. 4D). This result is inconsistent with our expectation of a RAL-1 effector. Thus, EXOC-8 performs multiple functions in VPC fate patterning, one of which could include mediating a RAL-1 2°-promoting signal.

Loss of GCK-2 but not MIG-15 confers the same phenotype as loss of RAL-1.

To further explore our first criterion, we used *C. elegans* genetics to determine relationships among Ral and the paralogous “GCK-2 Group” and “MIG-15 Group” MAP4Ks. *gck-2(ok2867)* is an in-frame 549 bp deletion in exon 5, resulting in deletion of a part of the kinase domain. *gck-2(tm2537)* is an out-of-frame 565 bp deletion in exon 5, resulting in early stop codons (Khan et al., 2012). Most genetics were done using these alleles and *gck-2*-directed bacterially mediated RNAi (clone V-4P08; Fig. 2. 5A). *mig-15(rh148)* is a V168E missense mutation predicted

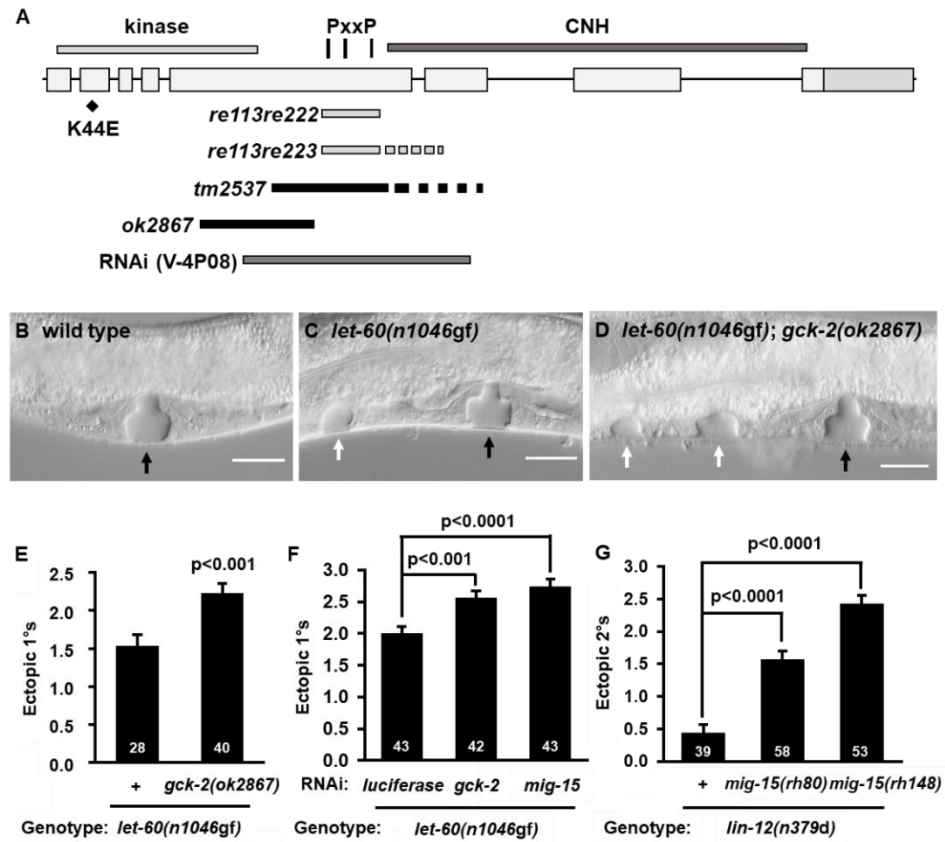


Figure 2. 5 Loss of GCK-2 but not MIG-15 confers the same phenotype as loss of RAL-1. **A.** *gck-2* gene structure, domain location, and genetic tools. Light gray: the *re113re222* (312 bp deletion) in-frame and *re113re223* (312 bp deletion, 35 bp insertion) out-of-frame mid-deletions remove the three PxxP sites. Black: *tm2537* (565 bp out-of-frame deletion) and *ok2867* (549 bp in-frame deletion). Dark gray: RNAi target sequence (Kamath et al., 2003). **B-D.** DIC images of late L4 vulvae and ectopic pseudovulvae. (B) N2 wild type (C) *let-60(n1046gf)*, (D) *let-60(n1046gf); gck-2(ok2867)*. Black arrow indicates normal vulva, white arrow indicates ectopic 1° pseudovulvae. Scale bar = 20 μm. **E.** *gck-2(ok2867)* enhances ectopic 1° induction in the *let-60(n1046gf)* background. **F.** *gck-2(RNAi)* (V-4P08) and *mig-15(RNAi)* (X-5G21) both increase 1° induction in the *let-60(n1046gf)* background. **G.** *mig-15(rh80)* and *mig-15(rh148)* do alter ectopic 2° induction in the *lin-12(n379d)* background. P values calculated by *t* test (E) or ANOVA (F, G). Error bars = S.E.M. Reprinted with permission from Shin et. al, 2018

to abolish kinase function. *mig-15(rh80)* is a W898* late nonsense mutation thought to confer strong loss of function (Chapman et al., 2008). We also used *mig-15*-directed bacterially mediated RNAi (clone X-5G21).

gck-2(ok2867) conferred increased 1° induction in the *let-60(n1046gf)* background (Figs. 2. 5B-E), similar to *ral-1(gk628801rf)* or *exoc-8(ok2523)*. *gck-2(RNAi)* conferred a phenotype similar to that of *ral-1(RNAi)* (Fig. 2. 5F vs. Fig. 2. 4A). Also, *mig-15(RNAi)* conferred increased 1° induction in the *let-60(n1046gf)* background (Fig. 2. 5F). We also tested the *mig-15(rh148)* reduced function allele in the *let-60(n1046gf)* background. However, we observed severe vulval morphogenesis defects: 2° cells/lineages failed to migrate to join the 1° cell/lineage (Fig. 2. 6A). Thus, in double mutant animals we could not discriminate between ectopic 1°s and 2°s that had failed to join the 1° of the normal vulva, which precluded interpretation of VPC induction in these strains (Fig. 2. 6B). Taken together, these results are consistent with both GCK-2 and MIG-15 functioning as either 2°-promoting or 1°-antagonizing signals.

We assessed the roles of MIG-15 and GCK-2 in the *lin-12(n379d)* background (AC/EGF absent, mild ectopic 2° induction). Neither *ral-1(gk628801rf)* nor *gck-2(ok2867)* or *tm2537* altered 2° induction in the *lin-12(n379d)* background (Figs. 2. 4C, 2. 6C, 2. 6D, respectively). In marked contrast, reduction of *mig-15* function robustly elevated 2° induction in the *lin-12(n379d)* background (Figs. 2. 5G, 2. 6E; the strongest *mig-15* allele, *rh326*, was not assayed due to poor viability). This assay was possible with *mig-15* alleles because the isolated 2°s in

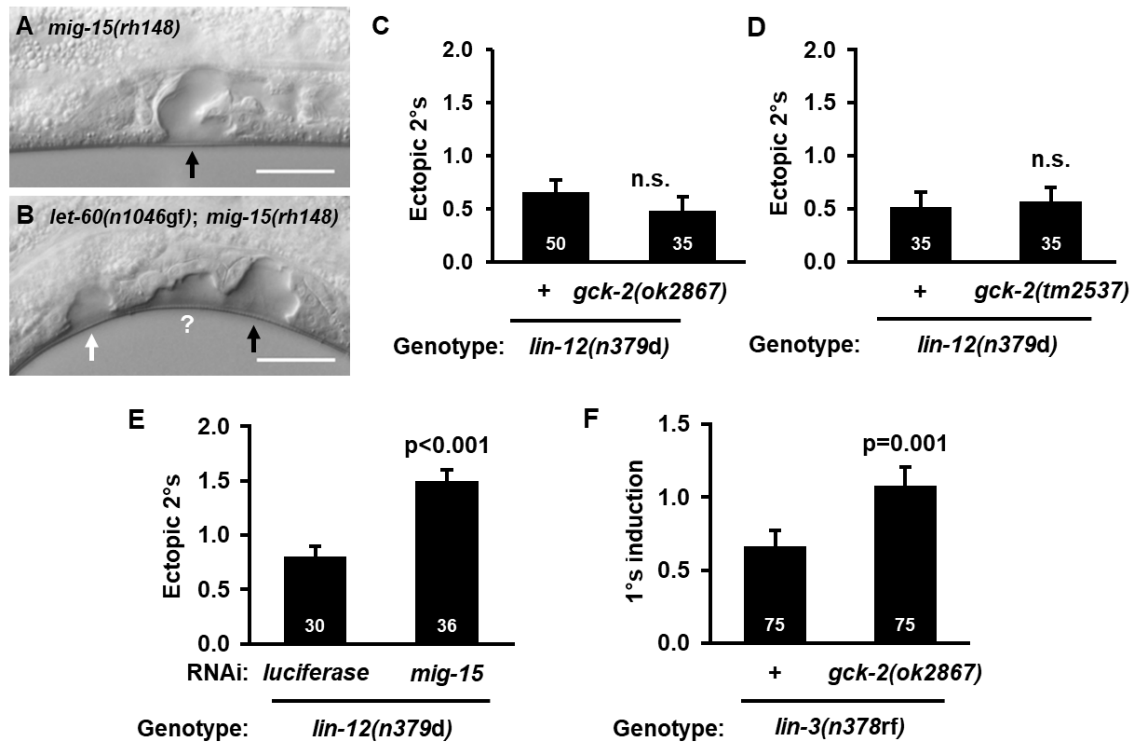


Figure 2. 6 Loss of GCK-2 but not MIG-15 conferred defects consistent with a RAL-1 effector. A-B. Representative vulval morphogenetic defects in *mig-15(rh148)* (A) and *let-60(n1046gf); mig-15(rh148)* (B). Vulval morphogenetic defects of *mig-15(rh148)* animals precluded conventional scoring of 1° induction because 2° lineages fail to join the central 1° lineage (see Fig. 2. 5G). However, this *mig-15* mutant morphogenetic defect does not confound scoring of isolated 2°s in the *lin-12(n379d)* background, because no migration occurs. Black arrows indicate normal vulvae, white arrows indicate ectopic pseudovulvae, the question mark is probably a 2°, but separated from the main vulva due to morphogenetic defects. **C-D.** *gck-2(ok2867)* or *gck-2(tm2537)* does not alter 2° induction. **E.** *mig-15(RNAi)* shows increased ectopic 2° induction in the *lin-12(n379d)* background. **F.** *gck-2(ok2867)* partially suppresses the absent 1° induction phenotype of *lin-3(n378rf)*. P value calculated by *t* test. Error bars = S.E.M. Reprinted with permission from Shin et. al, 2018

the *n379* background could be readily identified, unlike as in the *n1046* background, above.

To test background specificity, we evaluated the impact of *gck-2(ok2867)* in the *lin-3/EGF(n378rf)* hypo-induced rather than the *let-60(n1046gf)* hyper-induced background. *lin-3(n378rf)* supports 20% vulval induction (Hill and Sternberg, 1992). *gck-2(ok2867)* conferred increased vulval induction (Fig. 2. 6F), suggesting that the 2°-promoting signal of GCK-2 is not *let-60(n1046gf)* background dependent.

Collectively, these genetic results are consistent with the hypothesis that GCK-2 functions as an effector of RAL-1 2°-promoting activity. Meeting our first criterion, GCK-2 antagonizes 1° signal and is neutral in the absence of 2°-promoting EGF. This interpretation is supported below by further genetic analysis.

Conversely, MIG-15 is not consistent with a simple criterion of a RAL-1 2°-promoting effector. Unlike RAL-1, MIG-15 antagonizes both 1° and 2° signals, even in the absence of EGF. We cannot exclude MIG-15 as a second RAL-1 effector, perhaps in a negative regulatory relationship, which we will address in the Discussion. Yet we conclude that further analysis of MIG-15 function is outside the scope of this study.

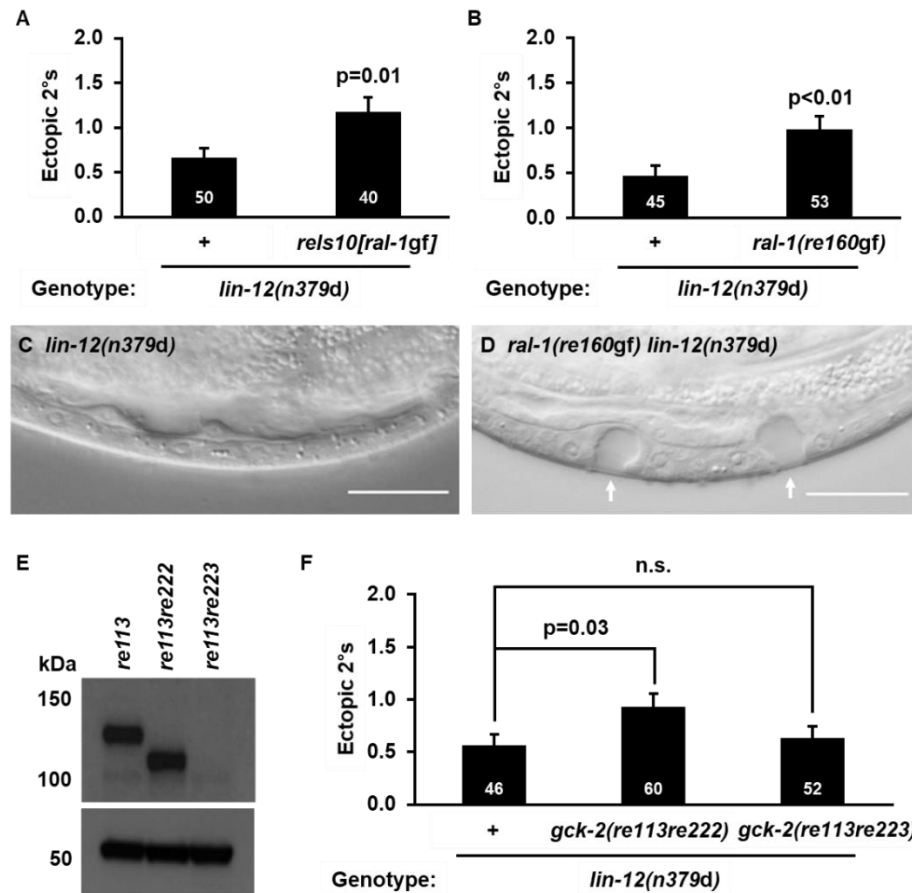


Figure 2. 7 RAL-1 and GCK-2 are sufficient to drive 2° fate induction. A-B. Exogenous (*rels10[P_{lin-31}::ral-1(gf)]*) (A) and endogenous (*ral-1(re160gf[mKate2^Δ3xFlag::ral-1(G26V)])*) (B) activated RAL-1 increase 2° induction in the *lin-12(n379d)* background. Ectopic 2° induction is on the Y axis. **C.** Vulvaless (Vul) late L4 *lin-12(n379d)* animal. **D.** Ectopic 2° pseudovulvae (white arrows) in *ral-1(re160gf) lin-12(n379d)*. Scale bar = 20 μm. **E.** Western blot detection of GCK-2 from lysates from endogenously tagged wild-type (*re113*), in-frame mid-deletion (*re113re222*), and out-of-frame mid-deletion (*re113re223*) animals, detected by anti-Flag antibody (1:2000). The mNG::3xFlag::GCK-2 fusion protein is predicted to be ~124 kDa, the mid deletion ~110 kDa. **F.** The in-frame mid-deletion *gck-2(re113re222)* but not the out-of-frame mid-deletion *gck-2(re113re223)* caused increased 2° induction in the *lin-12(n379d)* background. Ectopic 2° induction is on the Y axis. P value calculated by *t* test or ANOVA. Error bars = S.E.M. *Reprinted with permission from Shin et. al, 2018*

GCK-2 is sufficient to induce 2° fate in support of LIN-12/Notch.

Our second criterion is that activated effector should phenocopy constitutively activated RAL-1. RAL-1 is sufficient to promote 2° fate: transgenic VPC-expressed *ral-1(gf)* significantly increased ectopic 2° induction in the *lin-12(n379d)* background (Zand et al., 2011). This same extrachromosomal array, when integrated as *rels10[ral-1(gf)]* (Shin et al., in preparation), also increased ectopic 2° s in the *lin-12(n379d)* background (Fig. 2. 7A). Using CRISPR/Cas9-mediated genome editing, we generated a gain-of-function mutation (G26V) in the endogenous *ral-1* locus, also including an in-frame 5'-end mKate2^{3x}Flag tag. The resulting *ral-1(re160gf[mKate2^{3x} Flag::ral-1(G26V)])* caused increased 2° fate induction in the *lin-12(n379d)* background (Figs. 2. 7B-D).

To test whether GCK-2 is sufficient to induce 2° fate, we used CRISPR to generate a putative *gck-2(gf)*. Deletion of the proline-rich linker is thought to constitutively activate *Drosophila* Msn ("MIG-15 group"; Su et al., 2000). We deleted the linker in GCK-2 by using the co-CRISPR strategy (Arribere et al., 2014). The *gck-2(re113re222)* mid-Δ was generated in *gck-2(re113[mNG^{3x}Flag::gck-2])*, which we had already engineered (see below and Figs. 2. 7E, 2. 8A). We also generated the *gck-2(re113re223)* out-of-frame mid-Δ, which served as a negative control. We assessed protein expression in these alleles by western blot: the out-of-frame *re113re223* but not the in-frame *re113re222* abolished detectable tagged GCK-2 (Fig. 2. 7E). The in-frame

re113re222 but not the out-of-frame *re113re223* significantly increased ectopic 2° induction in the *lin-12(n379d)* background (Fig. 2. 7F).

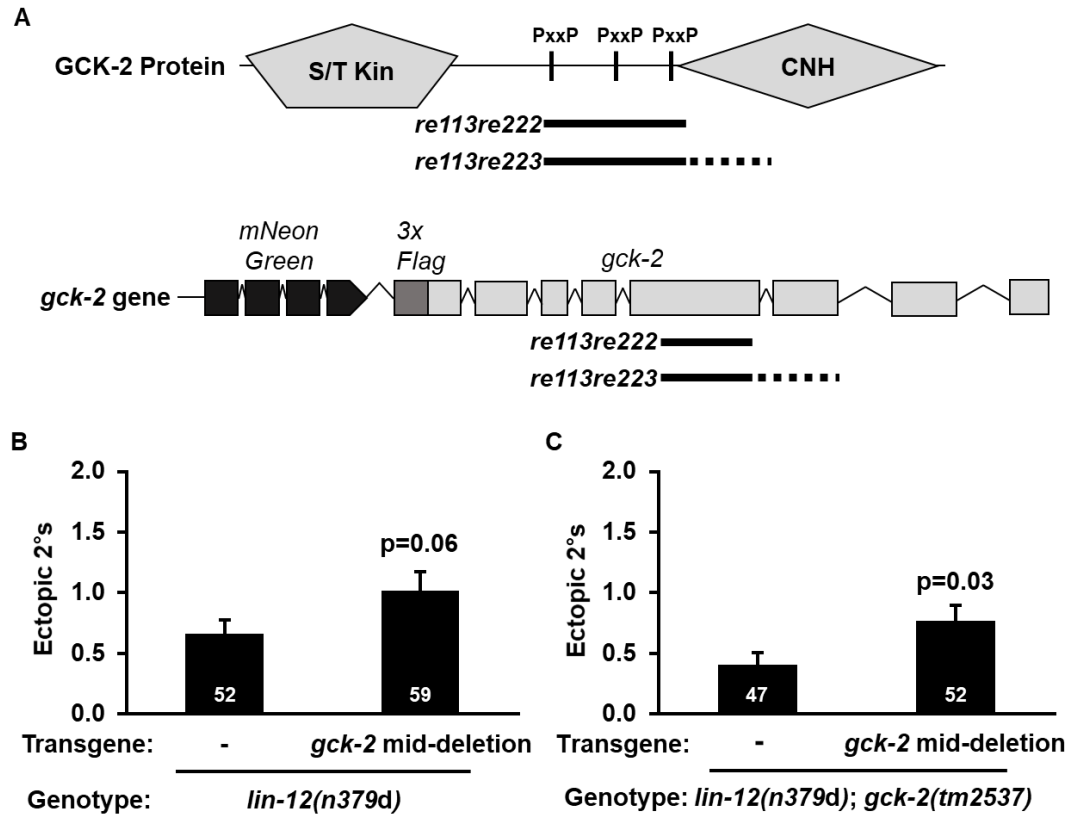


Figure 2. 8 Design and validation of endogenous GCK-2 mid-deletion and GCK-2 mid-deletion transgenics. A. The *gck-2* mid-deletion removes the central proline-rich region from the gene and protein. The solid black line shows the in-frame deletion while the line that becomes dotted represents the out-of-frame deletion. **B.** *reEx143*[*P_{lin-31}::gck-2(mid-deletion)*, *P_{myo-2}::gfp*] extrachromosomal array in the *lin-12(n379d); gck-2(+)* background. **C.** *reEx161*[*P_{lin-31}::gck-2(mid-deletion)*, *P_{myo-2}::gfp*] extrachromosomal array in the *lin-12(n379d); gck-2(tm2537)* background. P value calculated by *t* test. Error bars = S.E.M. Reprinted with permission from Shin et. al, 2018

We also tested GCK-2 cell autonomy by generating transgenes expressing VPC-specific putative activating *gck-2*(mid-Δ) into the *lin-12(n379d)* background, where we observed weakly increased ectopic 2° induction (p = 0.06; Fig. 2. 8B). The same transgene in the *lin-12(n379d); gck-2(tm2537)* background significantly increased ectopic 2° induction (p = 0.03; Fig. 2. 8C). Thus, GCK-2 is sufficient to induce increased 2° induction in support of LIN-12/Notch, consistent with GCK-2 functioning as a 2°-promoting effector of RAL-1.

GCK-2 functions downstream of LIN-3/EGF and RAL-1.

Our third criterion is that loss of effector function should be epistatic to constitutively activated RAL-1. *rels10[ral-1(gf)]* enhanced ectopic 2° induction in the *lin-12(n379d)* background (Fig. 2. 7A) and was blocked by *gck-2(ok2867)* and *gck-2(tm2537)* (Fig. 2. 9A). Thus, GCK-2 meets our third criterion for a RAL-1 effector.

Critically, in light of complex results from *exoc-8(ok2523)* in different backgrounds (Fig. 2. 4D; see above), *rels10[ral-1(gf)]*-dependent ectopic 2° induction was blocked by *exoc-8(ok2523)* (Fig. 2. 9B). That RAL-1 2°-promoting activity depends on EXOC-8 is consistent with EXOC-8 functioning downstream of RAL-1 to transduce the 2°-promoting signal. We therefore speculate that a RAL-1-EXOC-8-GCK-2 cascade transduces a 2°-promoting signal, while acknowledging that EXOC-8 may perform other functions (see Discussion).

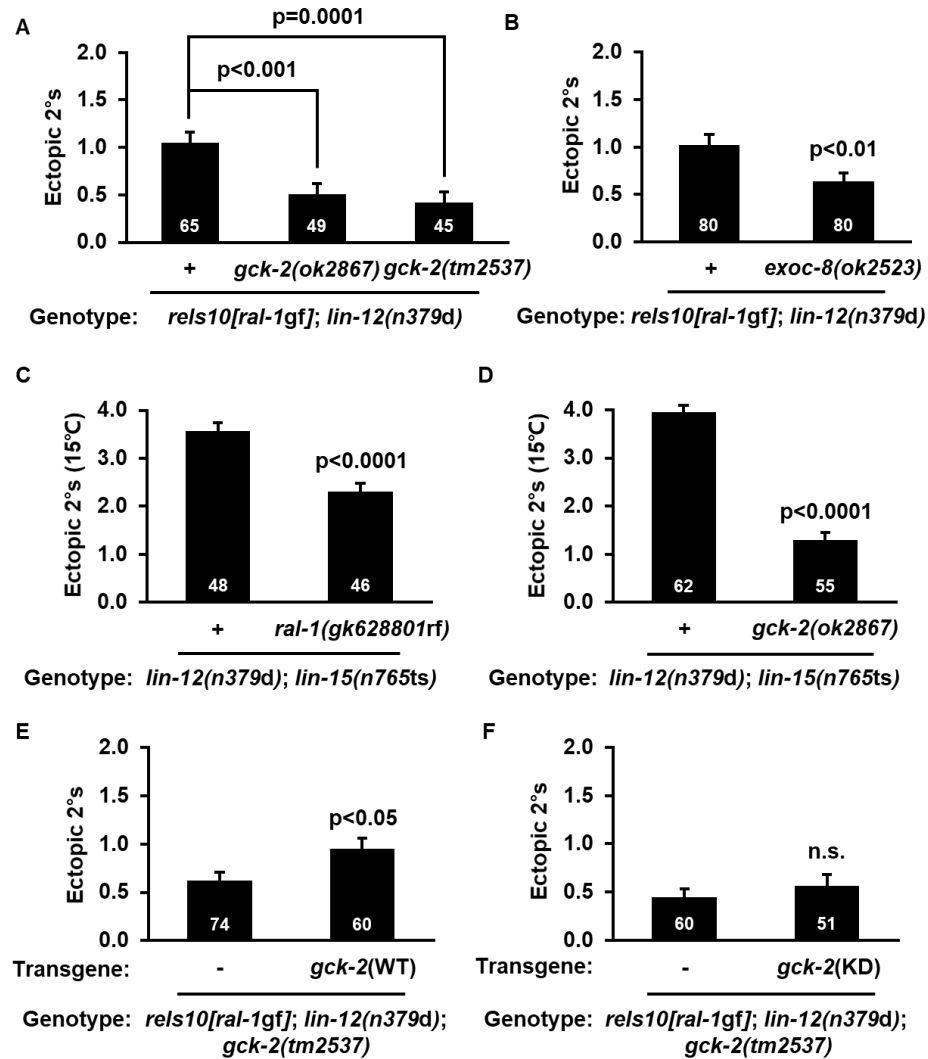


Figure 2. 9 GCK-2 functions downstream of LIN-3/EGF and RAL-1 cell autonomously. A-B. *gck-2(ok2867)* and *gck-2(tm2537)* (A) blocked the 2°-promoting activity of *rels10[P_{lin-31::ral-1(gf)}]* in the *lin-12(n379d)* background, as does *exoc-8(ok2523)* (B). **C-D.** Strong enhancement of *lin-12(n379d)*-dependent 2° induction by *lin-15(n765ts)* at 15° is reduced by *ral-1(gk628801rf)* (C), and *gck-2(ok2867)* (D). **E-F.** Vulva-specific expression of wild-type (*reEx176*) (E) but not K44E putative kinase dead (*reEx181*) GCK-2 (F) rescues the suppression of *rels10[ral-1(gf)]* by *gck-2(tm2537)* in the *lin-12(n379d)* background. Each column pair compares array-bearing vs. non-array-bearing siblings. P value calculated by *t* test or ANOVA. Error bars = S.E.M. Reprinted with permission from Shin et. al, 2018

Multiple lines of evidence indicate that LIN-15 and many other genes in the “synMuv” group cooperate to redundantly restrict LIN-3/EGF expression to the AC (Cui et al., 2006; Fay and Yochem, 2007; Herman and Hedgecock, 1990; Huang et al., 1994; Myers and Greenwald, 2005). We previously exploited this feature of the vulval system to titrate LIN-3/EGF “dose” to induce ectopic 2° but not 1° VPCs in the *lin-12(n379d)* background (Zand et al., 2011), consistent with earlier manipulations of LIN-3/EGF and LET-23/EGFR signals to promote 2° fate, which supported the Morphogen Gradient Model (Katz et al., 1995; Katz et al., 1996). At 15°C, a temperature-sensitive mutation in *lin-15, n765ts*, supports normal vulva induction without inducing ectopic 1° cells. But in the *lin-12(n379d)* background at 15°C, *n765ts* strongly increased ectopic 2° induction. We showed that this 2°-promoting activity depends on LIN-3/EGF, LET-60/Ras, RGL-1/RalGEF, and RAL-1: RNAi depletion of *let-60, rgl-1*, and *ral-1* blocked the increased ectopic 2°s conferred by *lin-12(n379d); lin-15(n765ts)* at 15°C. We further showed that excess expression of LIN-3/EGF and an activating mutation in LET-23/EGFR conferred similar promotion of 2° fate via activation of the LET-60-RGL-1-RAL-1 module (Zand et al., 2011).

As expected, *ral-1(gk628801rf)* decreased ectopic 2° induction in the *lin-12(n379d); lin-15(n765ts)* background at 15°C (Fig. 2. 9C), validating our prior results using *ral-1(RNAi)* (Zand et al., 2011). Similarly, *gck-2(RNAi)* and *gck-2(ok2867)* reduced ectopic 2° induction in the *lin-12(n379d); lin-15(n765ts)* background (Figs. 2. 9D; 2. 10A). Thus, we conclude that the 2°-promoting signal

of EGF is, at least in part, GCK-2-dependent, consistent with RAL-1 signaling though GCK-2.

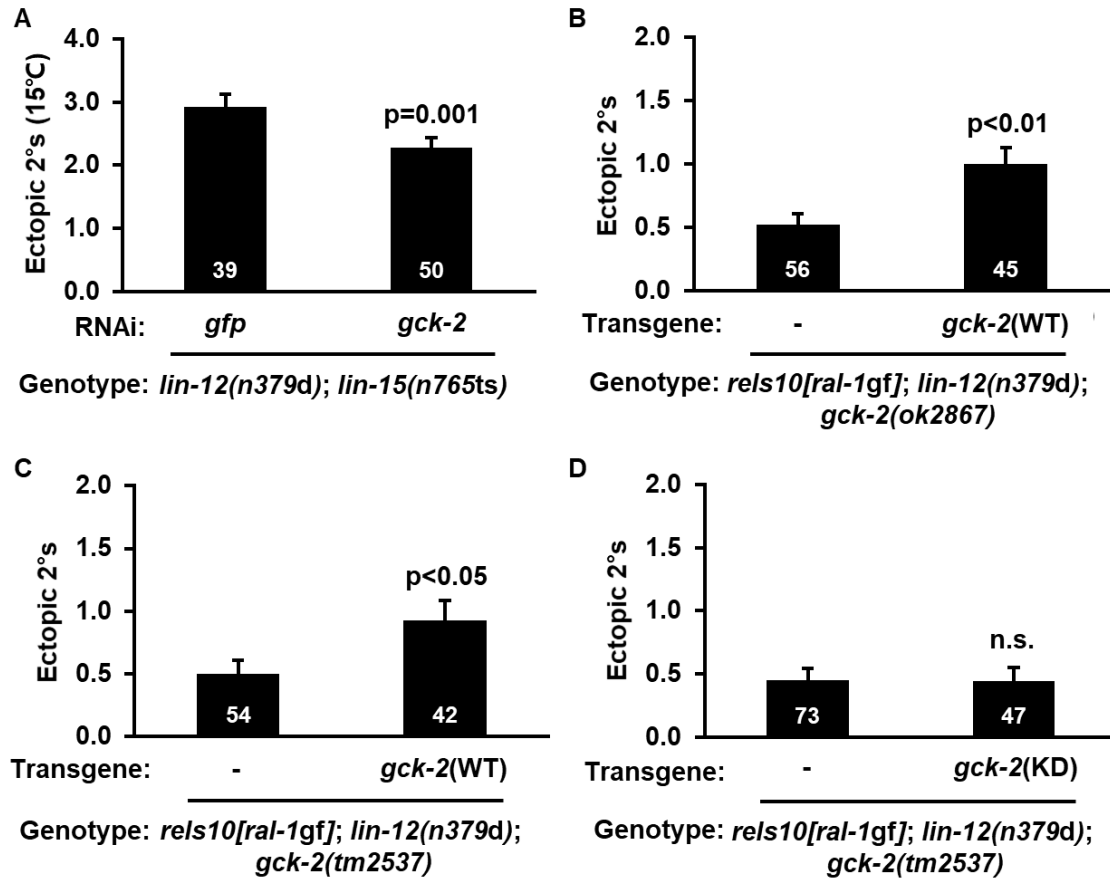


Figure 2. 10 GCK-2 functions cell autonomously downstream of Ral. A. Strong enhancement of *lin-12(n379d)*-dependent 2° induction by *lin-15(n765ts)* at 15° is inhibited by *gck-2(RNAi)*, with *gfp(RNAi)* as a negative control. **B-D.** Additional transgenic arrays to repeat Figs. 2. 9E and 2. 9F (B: *reEx167[P_{lin-31::gck-2(+)}, P_{myo-3::gfp}]*, C: *reEx177[P_{lin-31::gck-2(+)}, P_{myo-3::gfp}]*, and D: *reEx180[P_{lin-31::gck-2(K44E)}, P_{myo-3::gfp}]*). Reprinted with permission from Shin et. al, 2018

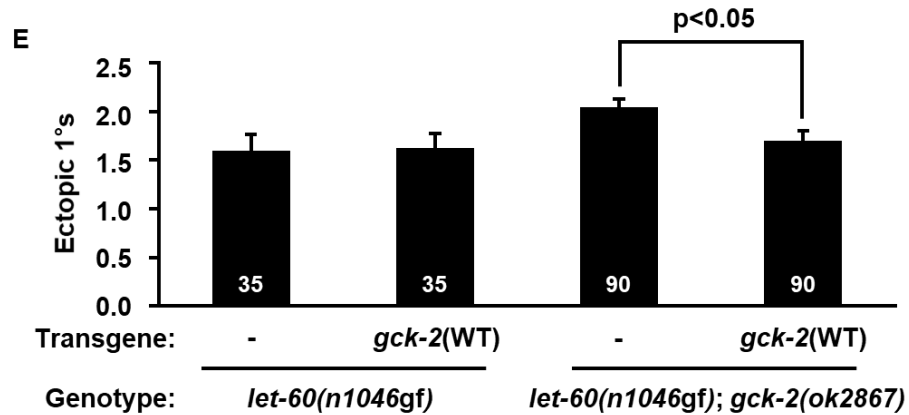


Figure 2. 10 Continued. E. Vulva-specific expression of GCK-2(+) does not alter ectopic 1° induction in the *let-60(n1046gf)* background (first two columns, *let-60(n1046gf); reEx113[P_{lin-31}::gck-2(+), P_{myo-2}::gfp]*), but does rescue the enhancement of ectopic 1° induction by the *gck-2(ok2867)* mutation (second two columns, *let-60(n1046gf); gck-2(ok2867); reEx112[P_{lin-31}::gck-2(+), P_{myo-2}::gfp]*). Each column pair compares array-bearing vs. non-array-bearing siblings. P value calculated by *t* test. Error bars = S.E.M. *Reprinted with permission from Shin et. al, 2018*

Kinase-dependent GCK-2 functions cell autonomously in VPCs.

Our fourth criterion for a RAL-1 effector is that its 2°-promoting activity function cell autonomously. We generated transgenic extrachromosomal arrays expressing VPC-specific GCK-2(+) and assessed rescue of mutant *gck-2* suppression of activated RAL-1. In the *rels10[ral-1(gf)]; lin-12(n379d); gck-2(tm2537)* and *rels10[ral-1(gf)]; lin-12(n379d); gck-2(ok2867)* backgrounds, VPC-specific expression of wild-type GCK-2 restored the increased 2° induction phenotype suppressed by *gck-2* mutations (Figs. 2. 9E; 2. 10B-C). Conversely, in

the same backgrounds VPC-specific expression of putative kinase dead (KD) GCK-2 (for HPK1/MAP4K1, “GCK-2 group”; Kiefer et al., 1996) failed to rescue mutant *gck-2* suppression of *rels10* (Figs. 2. 9F; 2. 10D). Remember that *gck-2(ok2867)* enhanced ectopic 1° induction in the *let-60(n1046gf)* background (see Fig. 2. 5E, above). VPC-specific expression of GCK-2(+) had no effect in the *let-60(n1046gf)* background, controlling for effects of VPC-specific GCK-2(+) overexpression (Fig. 2. 10E). VPC-specific expression of GCK-2(+) restored baseline levels of ectopic 1° induction in the *let-60(n1046gf); gck-2(ok2867)* background (Fig. 2. 10E). Taken together, these results suggest that GCK-2 functions cell autonomously in VPCs, via its kinase activity.

RAL-1 and GCK-2 are expressed in VPCs.

Our fifth criterion is that a RAL-1 effector be expressed in the VPCs. When analyzing the *sEx10525[P_{gck-2}::gfp+dpy-5(+)]* transcriptional reporter transgene (Hunt-Newbury et al., 2007), we observed no GFP expression in VPCs. Therefore, we used CRISPR-Cas9 genome editing to insert mNG::3xFlag into the 5' end of the endogenous *gck-2* gene, generating *gck-2(re113[mNG^3xFlag::gck-2])* (Fig. 2. 12A). We confirmed alleles by western blot (Fig. 2. 12B). We observed cytosolic tagged GCK-2 throughout vulval development (Figs. 2. 11A-B; 2. 12C-F). We observed the expression of GCK-2 in all tissues, including the germline and embryos in the adult hermaphrodite (Figs. 2. 12G-H).

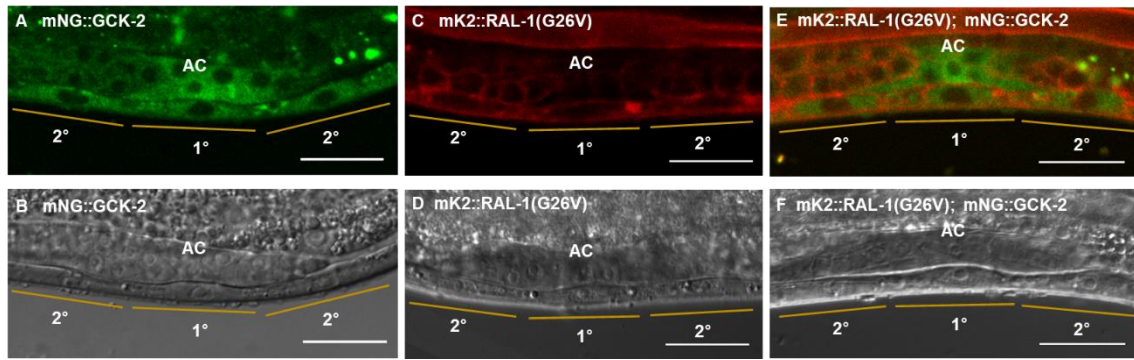


Figure 2.11 Endogenously tagged GCK-2 and RAL-1 are expressed in VPCs. **A-B.** Representative confocal and DIC micrographs of the presumptive 1° (P6.p) and 2° (P5,7.p) VPCs of *gck-2(re113[mNeonGreen^{3xFlag::gck-2}])* animals. **C-D.** Confocal and DIC micrographs of the presumptive 1° (P6.p) and 2° (P5,7.p) VPCs of *ral-1(re160gf[mKate2^{3xFlag::ral-1(G26V)}])* animals. **E-F.** Merged confocal and DIC micrographs of the presumptive 1° and 2° VPCs of the *ral-1(re160gf); gck-2(re113)* double mutant, from a separate animal than the single tags. “AC” label is placed directly above the Anchor Cell. Scale bar = 20 μm. *Reprinted with permission from Shin et. al, 2018*

We also inserted mKate2::3xFlag into the 5' end of the endogenous *ral-1* gene, with and without the activating G26V mutation (Figs. 2. 12I-J, 2. 12Q-R). The observed subcellular localization of RAL-1 and RAL-1(G26V) was similar, suggesting that the activating mutation does not alter localization. We observed tagged RAL-1 and RAL-1(G26V) throughout vulval development (Figs. 2. 11C-D; 2. 12K-N; 2. 12S-X). Tagged RAL-1 and RAL-1(G26V) expression in the animal was ubiquitous, including vulva and germline, and localized primarily to plasma membrane and adherens junctions (Figs. 2. 12O-P, 2. 12Y-Z). To assess co-localization of RAL-1 and GCK-2, we made the *ral-1(re160gf[mKate2^{3xFlag::ral-}*

1(G26V)); *gck-2(re113[mNG^{3xFlag}::gck-2])* strain. We observed strong localization of RAL-1(G26V) to plasma membrane and junctions and GCK-2 to cytosol at Pn.p (1-cell) and Pn.px (2-cell) stages (Figs. 2. 11E-F; 2. 12AA-AB).

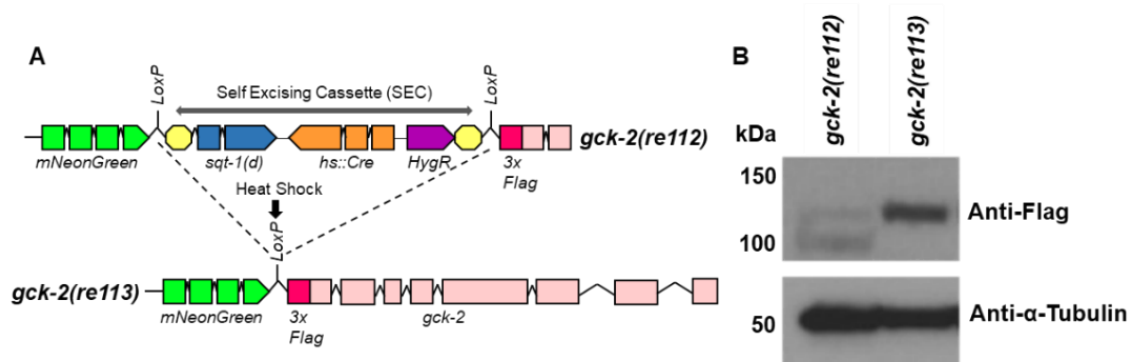


Figure 2. 12 CRISPR knock-in strategies, western blot validations, and localization of endogenously tagged GCK-2, RAL-1(G26V), and RAL-1. A. The Self-Excising Cassette (SEC) has positive selection marker *HygR* (hygromycin resistance), negative selection marker *sqt-1(d)* (confers a dominant Rol phenotype), and heat-shock Cre to excise the cassette (Dickinson et al., 2015). Before heat shock, animals are selected by Rols that survive hygromycin treatment. After heat-shock, the region between the two LoxP sites is excised, and functional endogenously tagged *gck-2* is generated. **B.** CRISPR knock-in results were confirmed by western blot. First lane: *gck-2(re112[mNG^{SEC}3xFlag::gck-2])*, second lane: *gck-2(re113[mNG^{3xFlag}::gck-2])*. Endogenously tagged GCK-2 protein (mNG::3xFlag::GCK-2) is ~124 kDa, and was detected by anti-Flag antibody (1:2000) (Sigma-Aldrich F1804), with loading control Anti- α -Tubulin (1:2000) (Sigma-Aldrich T6199). “mNG” = mNeonGreen (Shaner et al., 2013). *Reprinted with permission from Shin et. al, 2018*

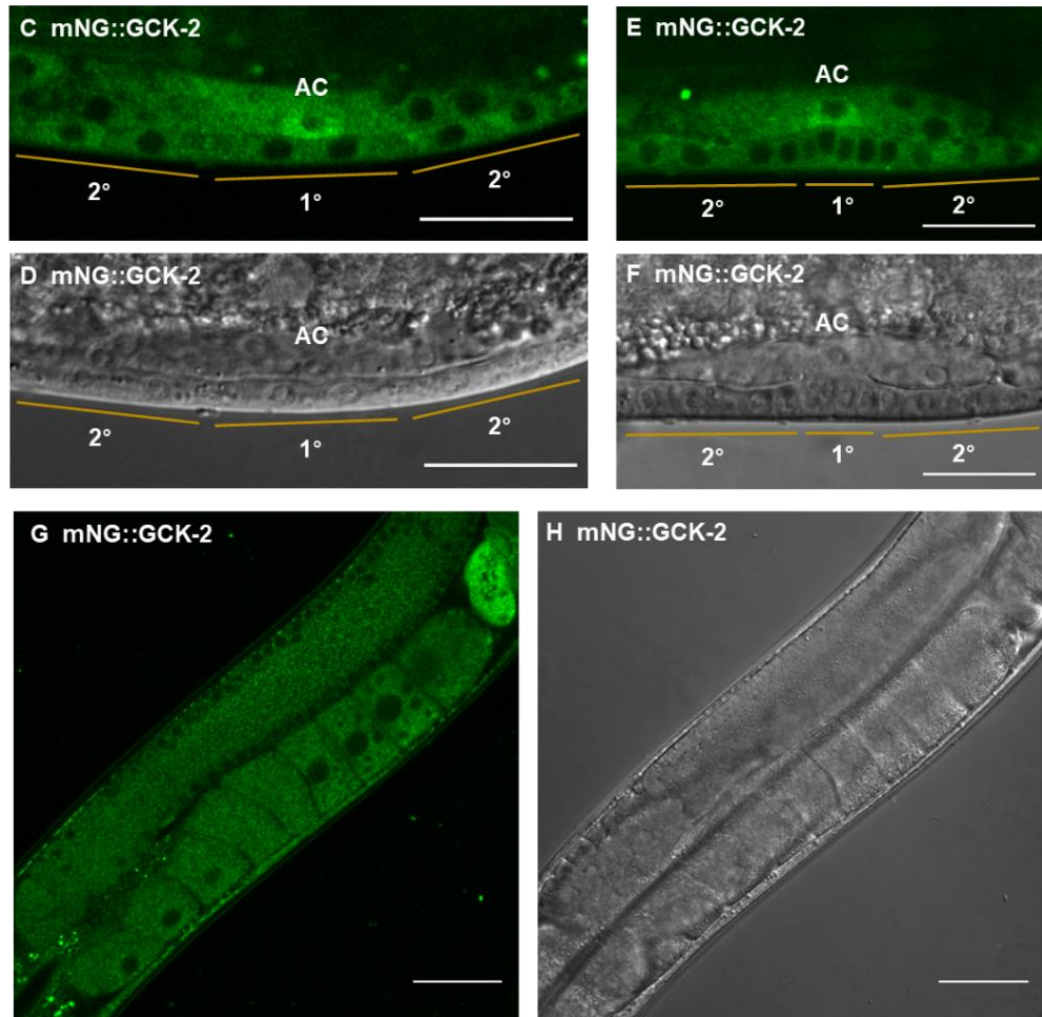


Figure 2. 12 Continued. C-F. Representative confocal and DIC micrographs of the 1° and 2° vulval lineages of *gck-2(re113[mNG^{3xFlag}::gck-2])* animals at the Pn.px (2-cell) and Pn.pxx (4-cell) stages. Tagged GCK-2 is cytosolic in vulval lineages. The Anchor Cell (AC) exhibits strong cytosolic tagged GCK-2. “AC” label is placed directly above the Anchor Cell. **G-H.** Representative confocal and DIC micrographs of adult germlines of *gck-2(re113[mNG^{3xFlag}::gck-2])* animals, exhibiting cytosolic expression. Brighter expression at the right side of the image is the spermatheca. *Reprinted with permission from Shin et. al, 2018*

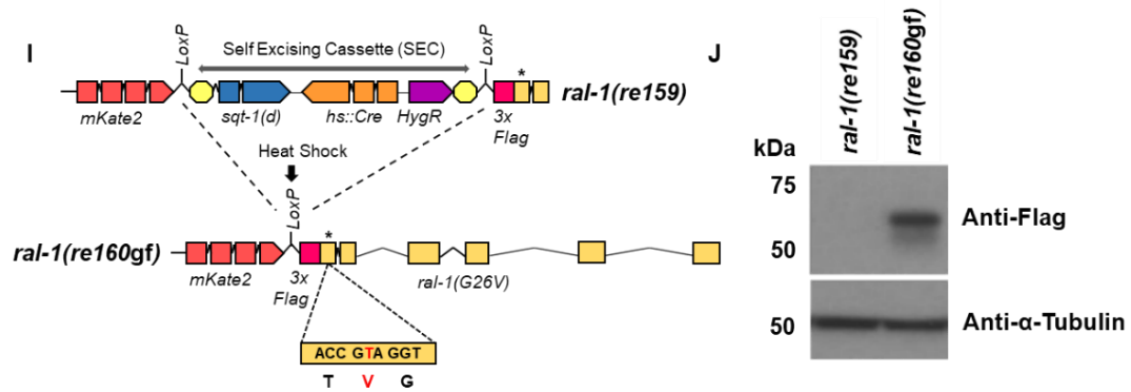


Figure 2. 12 Continued. I. SEC strategy for N-terminal tagging and G26V mutagenesis of endogenous RAL-1 was similar as for N-terminal tagging of GCK-2 (Fig. 2. 12A), except *mKate2* was substituted for *mNeonGreen* and the downstream homology arm sequence contained a missense mutation predicted to confer a G26V change in tagged RAL-1 protein. J. CRISPR knock-in results were confirmed by western blot: First lane: *ral-1(re159[mKate2^SEC^3x Flag::ral-1(G26V)])*, second lane: *ral-1(re160gf[mKate2^3xFlag::ral-1(G26V)])*. Endogenously tagged *mKate2::3xFlag::RAL-1(G26V)* was detected by anti-Flag antibody (1:2000) (Sigma-Aldrich F1804), showing a protein size of ~56 kDa for RAL-1A, with loading control Anti-α-Tubulin (1:2000) (Sigma-Aldrich T6199). “mK2” = *mKate2* (Shcherbo et al., 2009). RNAseq data for *ral-1* in Wormbase predict a potentially longer isoform predicted to run at 61 kD (RAL-1B), but with far less transcript (~13% of total). RAL-1B, if made, would encode an N-terminal extension not found in other species. Since we did not detect an additional band by western blotting, we hypothesize that RAL-1B is simply an extended 5'UTR that is not translated into an alternate isoform. *Reprinted with permission from Shin et. al, 2018*

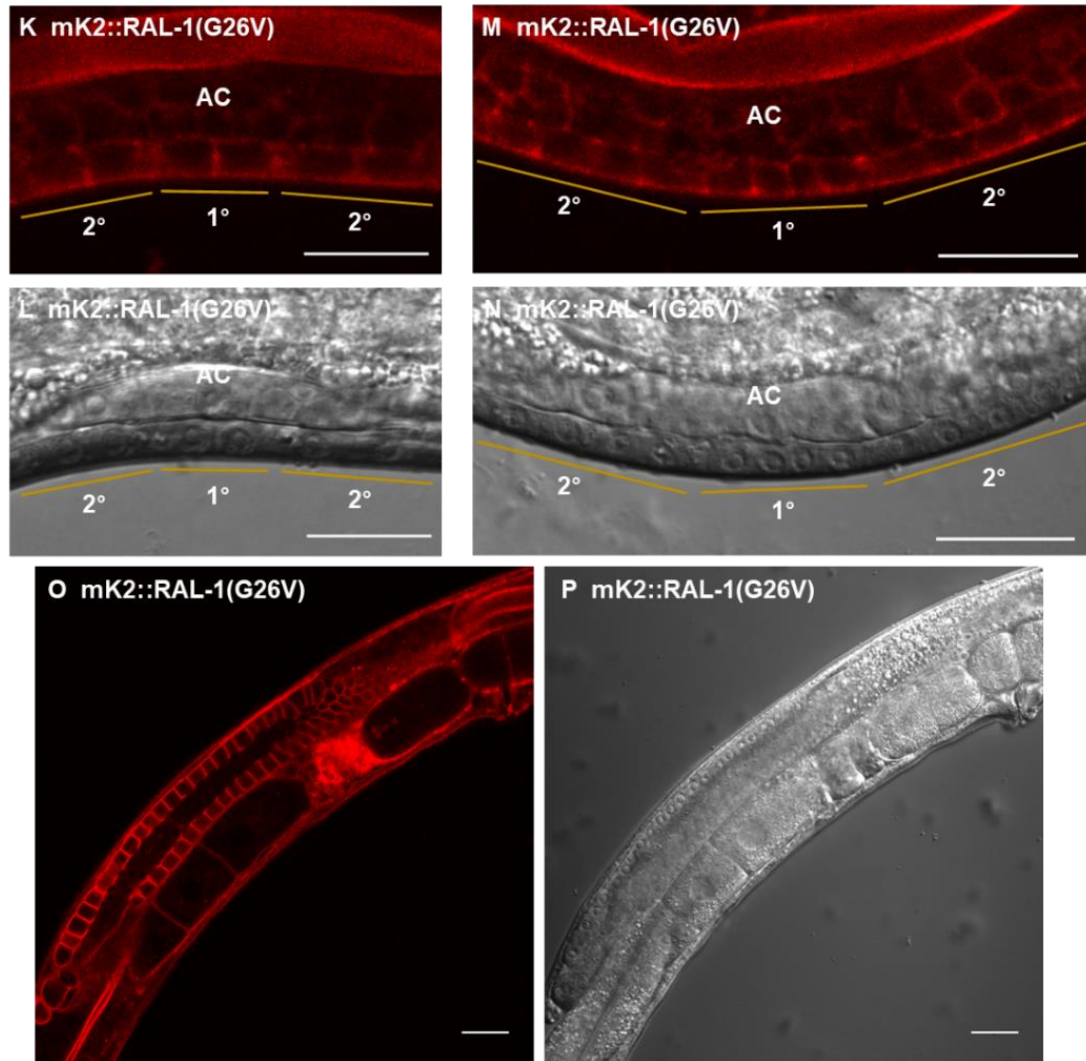


Figure 2. 12 Continued. K-N. Representative confocal and DIC micrographs of the 1° and 2° vulval lineages of *ral-1(re160gf[mKate2^{3xFlag}::ral-1(G26V)])* animals at the Pn.px (2-cell) and Pn.pxx (4-cell) stages show predominantly localization to plasma membrane and adherens junctions. **O-P.** Representative confocal and DIC micrographs of adult germlines of *ral-1(re160gf[mKate2^{3xFlag}::ral-1(G26V)])* animals, showing plasma membrane localization. The lower left corner of (O) shows the double line of the intestinal lumen, where tagged RAL-1(G26V) is strongly localized to adherens junctions. *Reprinted with permission form Shin et. al, 2018*

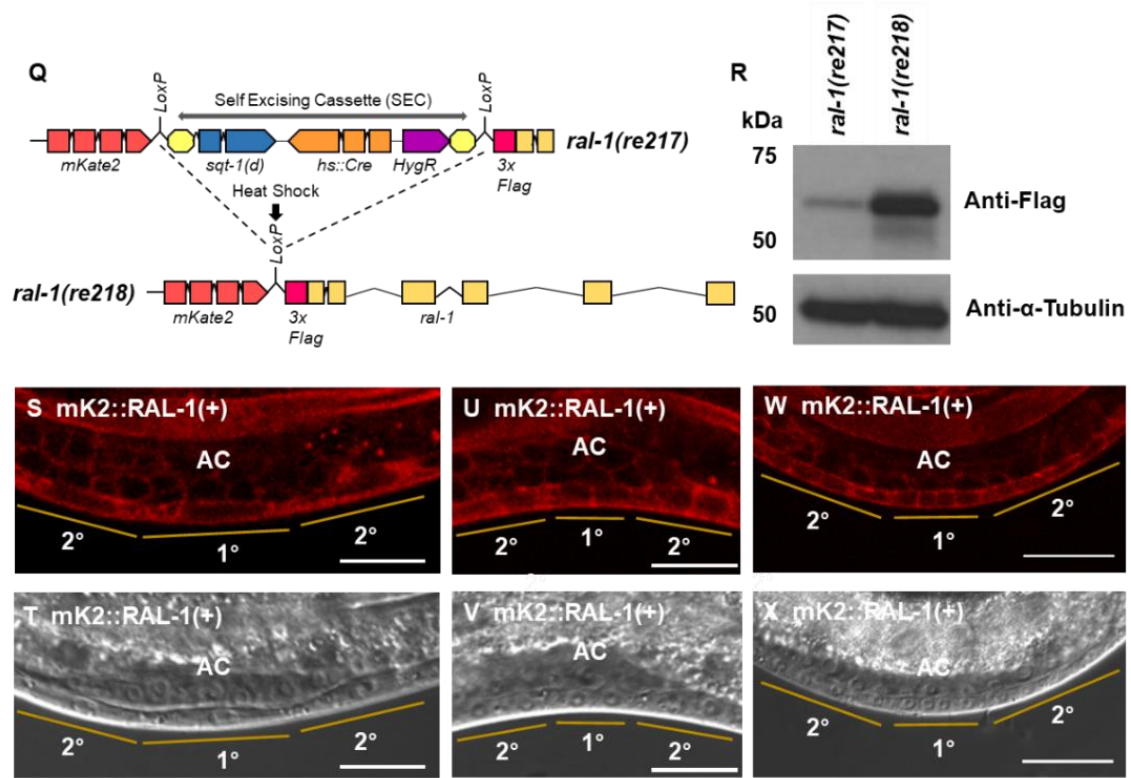


Figure 2. 12 Continued. Q. SEC strategy for N-terminal tagging of endogenous RAL-1(+). **R.** CRISPR knock-in results were confirmed by western blot: First lane: *ral-1(re217)[mKate2^SEC^3xFlag::ral-1(+)]*, second lane: *ral-1([mKate2^3xFlag::ral-1(+)]*). Endogenously tagged *mKate2::3xFlag::RAL-1(+)* was detected by anti-Flag antibody (1:2000) (Sigma-Aldrich F1804), with loading control Anti- α -Tubulin (1:2000) (Sigma-Aldrich T6199). **S-X.** Representative confocal and DIC micrographs of the 1° and 2° vulval lineages of *ral-1(re218)[mKate2^3xFlag::ral-1(+)]* animals at the Pn.p (1-cell), Pn.px (2-cell), and Pn.pxx (4-cell) stages show predominantly localization to plasma membrane and adherens junctions. *Reprinted with permission form Shin et. al, 2018*

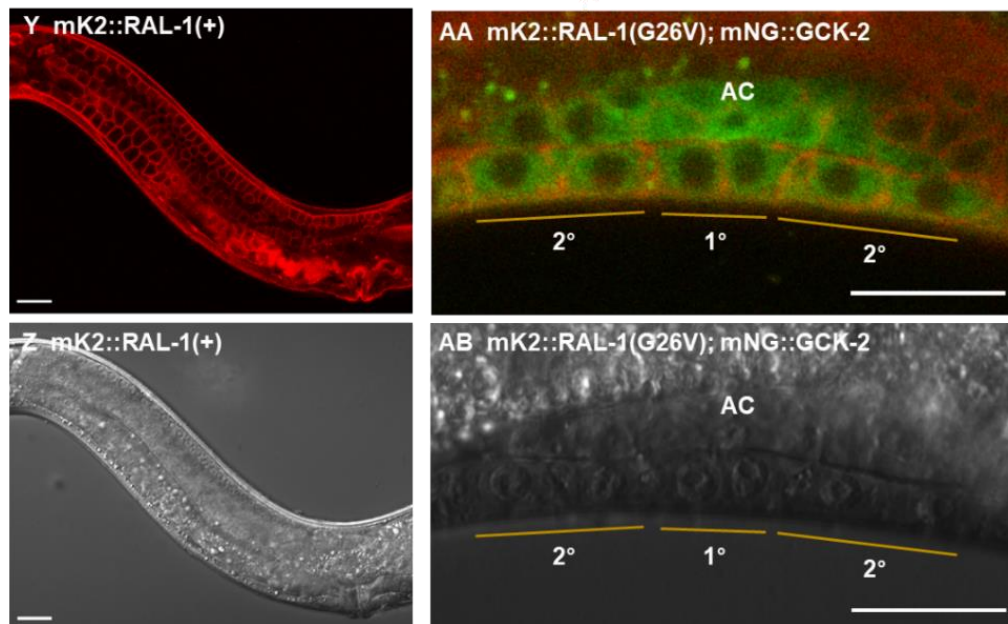


Figure 2. 12 Continued. Y-Z. Representative confocal and DIC micrographs of adult germlines of *ral-1(re160gf[mKate2³xFlag::ral-1(G26V)])* animals, showing plasma membrane localization. **AA-AB.** Merged confocal and DIC micrographs of the presumptive 1° (P6.p) and 2° (P5,7.p) lineages of the *ral-1(re160gf[mKate2³xFlag::ral-1(G26V)]); gck-2(re113[mNG³xFlag::gck-2])* double mutant at the Pn.px (2-cell) stage. Scale bar throughout = 20 μm. *Reprinted with permission from Shin et. al, 2018*

Thus, expression of tagged endogenous RAL-1 (wild-type and G26V) and GCK-2 are expressed in VPCs, one of our criteria for a RAL-1-GCK-2 signaling cascade. However, we did not observe evidence of 2°-specific recruitment of GCK-2 to the plasma membrane by activated RAL-1. We will consider this incongruity further in the Discussion.

The PMK-1/p38 MAP kinase functions downstream of RAL-1 and is expressed in VPCs.

The “GCK-2 group” is part of the Ste20 family of MAP4 kinases and is frequently associated with activation of JNK or p38 MAP kinase cascades (Dan et al., 2001; Delpire, 2009). Based on our model that RAL-1 signals through GCK-2, we investigated components of MAPK cascades as functioning downstream of RAL-1, identifying MLK-1/MAP3K and PMK-1/p38 as putative components of the RAL-1-GCK-2 2°-promoting signaling cascade.

C. elegans encodes orthologs of MAP3Ks and MAP2Ks (Sakaguchi et al., 2004). The *km19* deletion in MLK-1/MLK/MAP3K (Mizuno et al., 2004) enhanced *let-60 (n1046gf)* vs. *n1046gf* alone ($p=0.009$, N of 90 and 60, respectively), consistent with MLK-1/MAP3K acting in this cascade. In contrast, the *ok1382* deletion in MTK-1/MEKK4/ MAP3K failed to enhance *let-60(n1046gf)* vs. *n1046gf* alone ($p=0.4$, N of 50 and 91, respectively). The *km4* deletion in SEK-1/MKK3/6/MAP2K (Tanaka-Hino et al., 2002) and the *ok1545* deletion in MKK-4/MKK4/MAP2K failed to enhance *let-60(n1046gf)* vs. *n1046gf* alone ($p=0.6$ N of 60, 60; and $p=0.2$ N of 90, 90, respectively). Several other MAP2Ks were not tested.

C. elegans encodes three p38/MAPK paralogs in an operon, in order: PMK-2, PMK-3, and PMK-1. Of these, PMK-2 and PMK3 are expressed primarily in intestine, while PMK-1 is expressed more broadly. All three are thought to

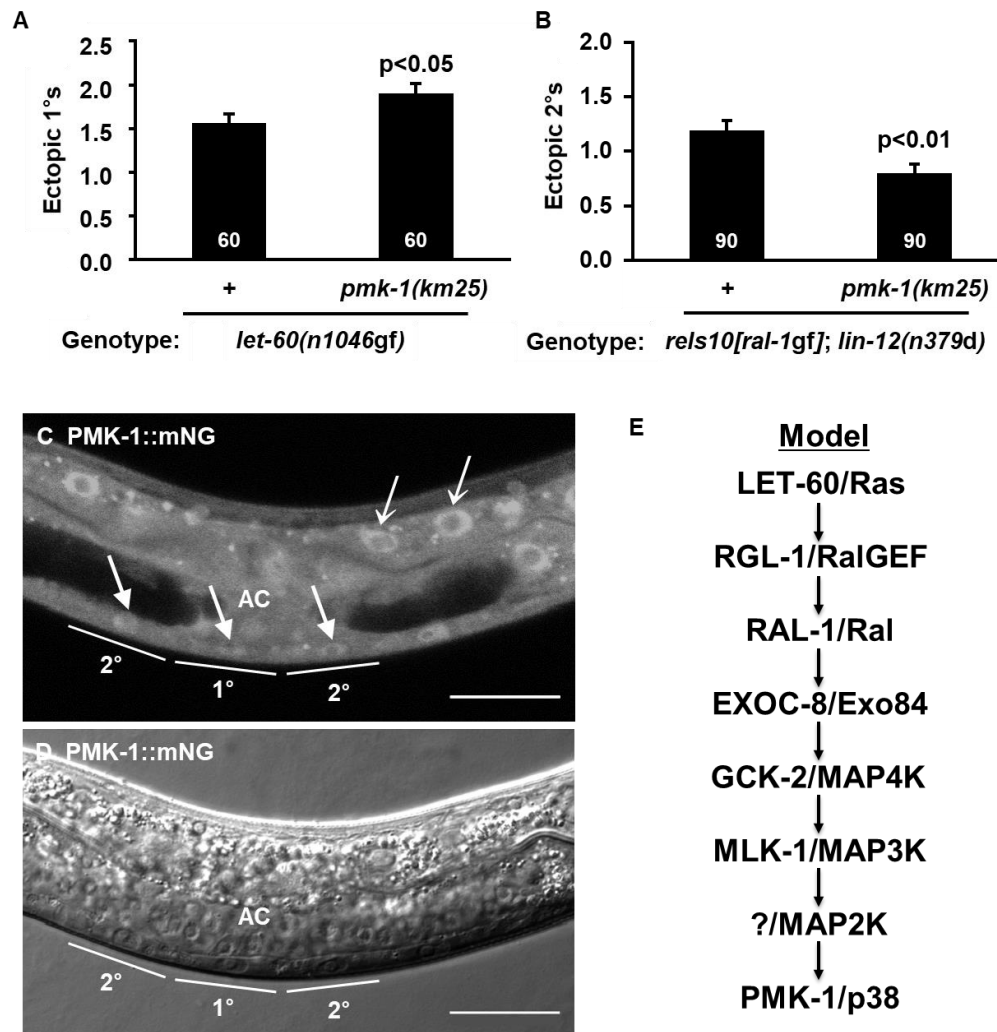


Figure 2. 13 PMK-1/p38 functions downstream of RAL-1. **A.** Putative null, *pmk-1(km25)* confers increased ectopic 1°s in the *let-60(n1046gf)* background. **B.** *pmk-1(km25)* blocks the increased 2°s in the *rels10[P_{lin-31}::ral-1(gf)]; lin-12(n379d)* background. P values calculated by *t* test. Error bars = S.E.M. **C-D.** Representative confocal and DIC micrographs of *pmk-1(re170[pmk-1::mNG^{3xFlag}])*. Endogenously tagged PMK-1 is expressed in VPCs. Solid arrow: VPC nuclei. Open arrow: Gut nuclei. Scale bar = 20 μ m. **E.** A signaling transduction model. A LET-60/Ras-RGL-1/RalGEF-RAL-1/Ral-EXOC-8/Exo84-GCK-2/MAP4K-MLK-1/MAP3K-PMK-1/MAPK cascade promotes 2° fate in *C. elegans* VPC fate patterning. Reprinted with permission from Shin et. al, 2018

contribute to innate immunity and stress response (Mertenskotter et al., 2013). Fitting some of our criteria for a RAL-1 effector, putative null *pmk-1(km25)* (Mizuno et al., 2004) conferred increased ectopic 1° induction with *let-60(n1046gf)* and blocked increased ectopic 2° induction with *ral-1(gf); lin-12(n379d)* (Figs. 2. 13A-B).

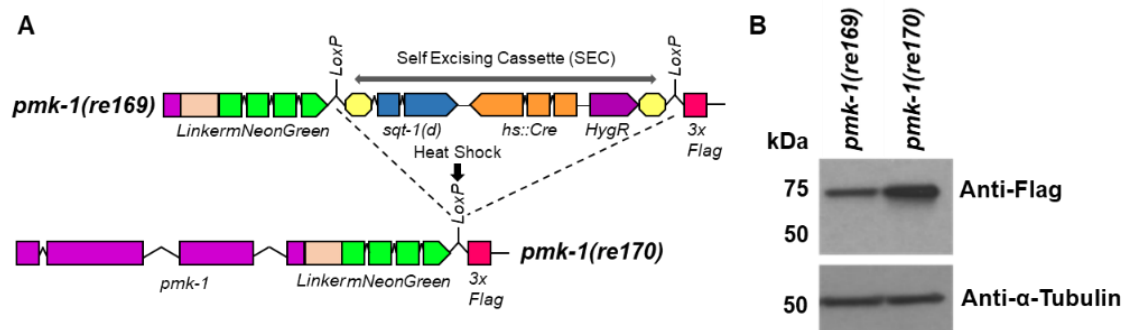


Figure 2. 14 PMK-1 expression and localization. **A.** We used a similar CRISPR knock-in strategy for C-terminal tagging of PMK-1 as for N-terminal tagging of GCK-2 and RAL-1 (Figs. 2. 12A, 2. 12I, 2. 12Q). **B.** CRISPR knock-in results were confirmed by western blot: First lane: *pmk-1(re169)[pmk-1::mNG^SEC^3xFlag]*, second lane: *pmk-1(re170)[pmk-1::mNG^3xFlag]*. Endogenously tagged PMK-1::mNG^3xFlag was detected at ~74 kDa by anti-Flag antibody (1:2000) (Sigma-Aldrich F1804), with loading control Anti-α-Tubulin (1:2000) (Sigma-Aldrich T6199). *Reprinted with permission from Shin et. al, 2018*

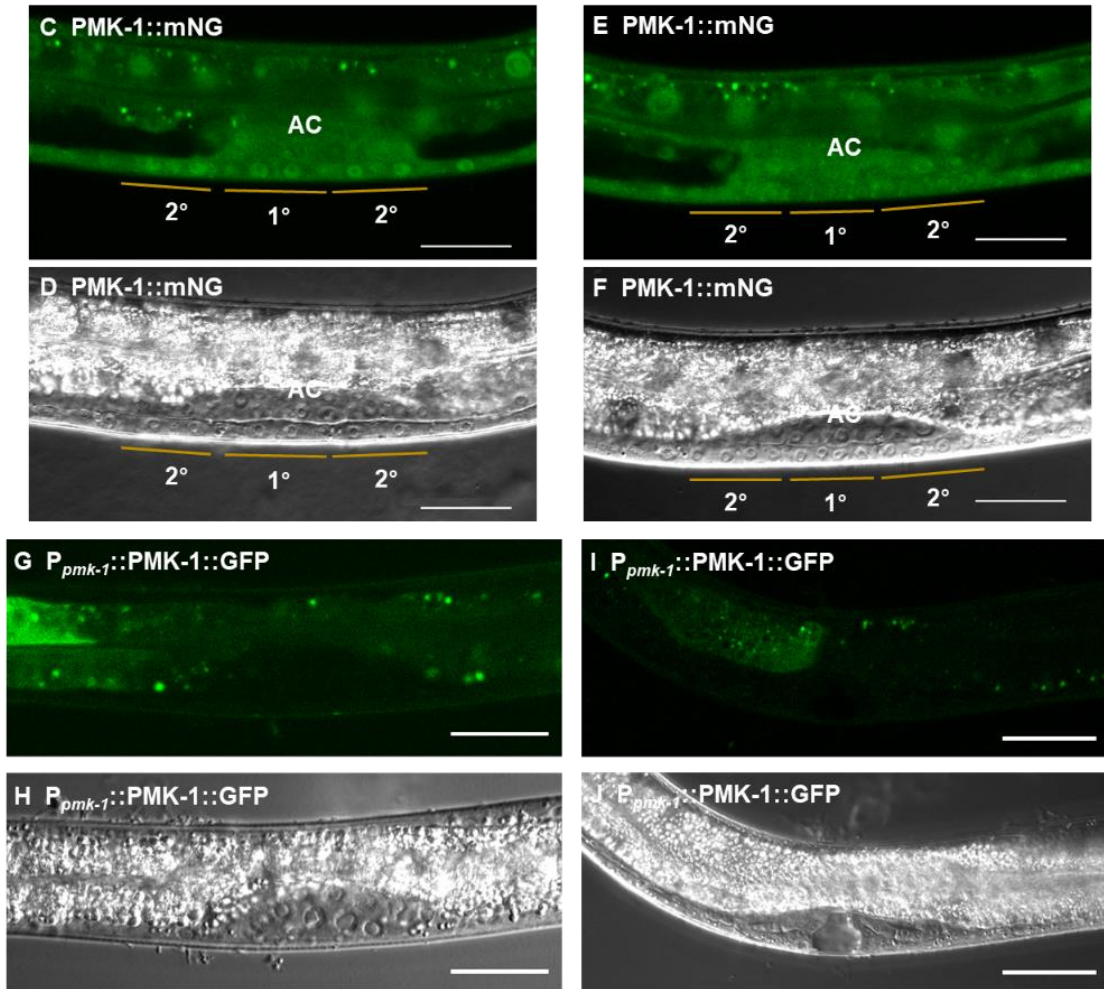


Figure 2. 14 Continued. C-F. Representative confocal and DIC micrographs of the 1° and 2° vulval lineages of *pmk-1(re170[pmk-1::mNG^{3xFlag}])* animals at the Pn.px (2-cell) and Pn.pxx (4-cell) stages show the expression both in nucleus and in cytoplasm of VPCs. G-J. confocal and DIC micrographs of P_{pmk-1}::*pmk-1(+):gfp*, *rol-6 (su1006)* animals showing expression in intestine, but not in VPCs at L3 stage and vulva at L4 stage. Reprinted with permission from Shin et. al, 2018

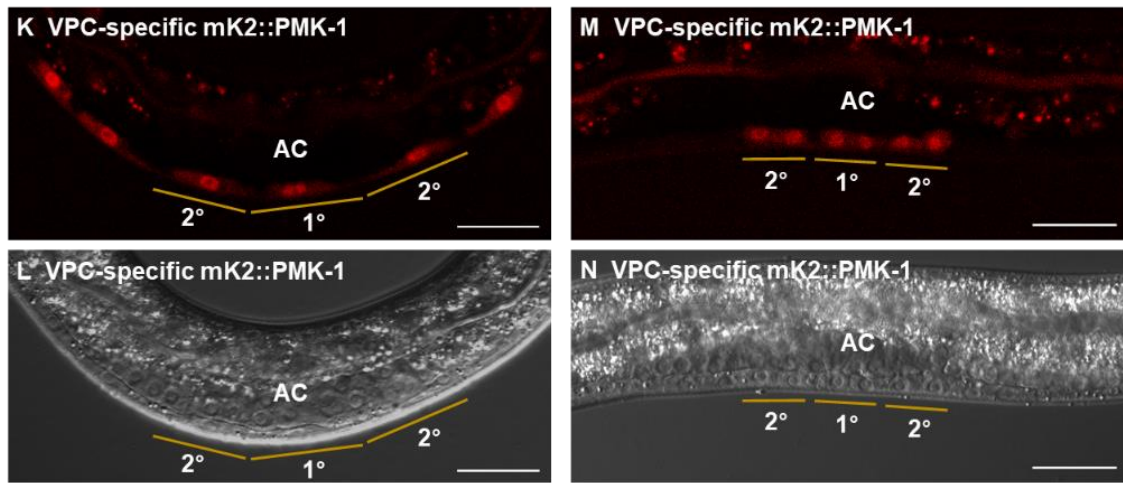


Figure 2. 14 Continued. K-N. Confocal and DIC micrographs of low copy number of *reSi6[P_{lin-31}::mKate2::linker::pmk-1::unc-54 3'UTR]* at the Pn.p (1-cell) and Pn.px (2-cell) stages also shows the expression both in nucleus and in cytoplasm of VPCs. *Reprinted with permission from Shin et. al, 2018*

We tagged the endogenous *pmk-1* gene with mNG::3xFlag at the 3' end (Figs. 2. 14A-B). We observed PMK-1::mNG expression in vulval lineages and throughout the rest of the animal, with the exception of the germline; germline expression appeared to be silenced, an established phenomenon with certain foreign DNA insertions (Figs. 2. 13C-D; 2. 14C-F; Dickinson et al., 2015). Thus, expression of PMK-1 meets the criteria of an effector that functions downstream of RAL-1. Using a transgenic *pmk-1* promoter translational GFP fusion (*P_{pmk-1}::pmk-1::gfp*; Mertenskötter et al., 2013), we observed no vulval signal (Figs. 2.14G-J). However, since *pmk-1* is the last gene in an operon, key regulatory elements may be absent from the construct.

We had hoped to observe activity-dependent cytosol-to-nucleus translocation (Ben-Levy et al., 1998) of PMK-1 as a biomarker for upstream RAL-1 signaling activation. Instead, we observed nuclear and cytosolic localization in all cells, including vulval lineages (Figs. 2. 13C-D; 2. 14C-F). We considered our C-terminal CRISPR tagging scheme may have altered PMK-1 localization, even though we did not observe phenotypic changes conferred in the sensitized background by PMK-1::mNG. Therefore, we N-terminally tagged PMK-1 expressed from *lin-31* promoter in VPCs, using the miniMos system (de la Cova et al., 2017), and with mKate2 rather than mNG. We observed localization to both nuclei and cytosol of VPCs (Figs. 2. 14K-N). Consequently, we propose that our tagging strategies do not disrupt PMK-1 function, but rather that part of the endogenous PMK-1 population is constitutively targeted to the nucleus. We speculate that over-expression from the extrachromosomal array shows mostly cytosolic localization because only a small subset of the total PMK-1 molecules occupy the nucleus, and that the proportion of nuclear PMK-1 to total protein is much higher when looking at endogenous rather than over-expressed protein.

Discussion

We found that EXOC-8/Exo84 contributes to the LET-60/Ras-RGL-1/RalGEF-RAL-1/Ral 2°-promoting signal during patterning of *C. elegans* VPC fate. By our genetic criteria GCK-2, a CNH domain-containing MAP4K

orthologous to *Drosophila* Hppy and mammalian MAP4K1, 2, 3 and 5, is a downstream effector of RAL-1, as are MLK-1/MAP3K and PMK-1/p38 MAPK (Fig. 2. 13E). The LET-60-RGL-1-RAL-1-EXOC-8-GCK-2-MLK-1-PMK-1 cascade is a non-essential 2°-promoting signal in *C. elegans* VPC fate patterning that supports the essential 2°-promoting signal via LIN-12/Notch. We showed that GCK-2 and PMK-1 function downstream of RAL-1 cell autonomously, and that GCK-2 is sufficient to promote 2° fate in support of LIN-12/Notch. We did not observe evidence of ectopic 2° induction by *rels10[ral-1(gf)]* or *ral-1(re160gf)*. Thus, given the modest modulatory role of the RAL-1 2°-promoting cascade, there is no reason to propose that RAL-1 is sufficient to induce 2° fate, though the actual experiment in the absence of *lin-12* is as yet prohibitively difficult (abrogation of LIN-12 function duplicates the anchor cell, and thus results in complex VPC induction; (Greenwald et al., 1983).

Sec5 and Exo84 are subunits of the exocyst complex and known Ral binding partners in mammals (reviewed in (Gentry et al., 2014; Kashatus, 2013). Ral-Exo84 and Ral-Sec5 regulate exocytosis, cancer cell proliferation, and immunity (Chien et al., 2006; Fukai et al., 2003; Issaq et al., 2010; Jin et al., 2005; Moskalenko et al., 2002; Moskalenko et al., 2003; Sugihara et al., 2002). Yet we do not understand how Ral signaling is propagated through the Sec5 and Exo84 exocyst partners. Exo84 and Sec5 also confound biochemical identification of downstream signaling partners, since the exocyst is involved in central cell biological processes and potentially interacts with myriad partners (Tanaka et al.,

2017; Wu and Guo, 2015). There are some exceptions: RalB-Sec5 directly recruits and activates the atypical I κ B kinase family member TBK1 to contribute to human cancer cell survival (Chien et al., 2006), RalB-Exo84 promotes autophagosome assembly under starvation conditions in human epithelial cells (Bodemann et al., 2011), while under replete conditions RalB-Sec5 stimulates mTORC1 activation in pancreatic tumor cells to promote cell invasion and inhibit autophagy (Martin et al., 2014). Yet we lack biomarkers for activated Ral and have limited knowledge of effectors downstream of Sec5 and Exo84. Using developmental patterning of the *C. elegans* VPCs as a simple model system, we defined a potentially new signaling cascade downstream of RAL-1 in development. Additional signaling cascades may function downstream of Ral in different tissues.

The GCK-2 paralog, MIG-15, also contributes to VPC patterning: depletion of *mig-15* derepressed both 2°- and 1°-inducing backgrounds, respectively *lin-12(n379d)* and *let-60(n1046gf)*. A 3°-promoting gene might be predicted to similarly antagonize both 1°- and 2°-promoting signals. However, the connection of MIG-15 to 1°-promoting signals and 2°-promoting signals is unclear, and is complicated by the role of MIG-15 in vulval morphogenesis. In contrast, we clearly delineated GCK-2 genetically as a component of a positive regulatory cascade downstream of RAL-1-EXOC-8.

While mutation of neither RLBP-1/RalBP1 nor SEC-5/Sec5 altered vulval patterning in sensitized backgrounds, mutation of EXOC-8/Exo84 conferred phenotypes consistent with functioning as a signaling intermediary in a RAL-1 2°-

promoting cascade. However, mutation of EXOC-8 also conferred defects consistent with other activities in VPC fate patterning: unlike reduced RAL-1 or GCK-2 function, reduced EXOC-8 function conferred increased 2° induction in the *lin-12(n379d)* 2°-inducing background. We speculate that EXOC-8 performs at least two functions: (1) an intermediary in RAL-1-GCK-2 2°-promoting signaling, and (2) in an anti-2° capacity, perhaps with MIG-15. Thus, the roles of EXOC-8 and MIG-15 in VPC fate patterning are enigmatic, and will be the subject of future genetic and biochemical studies, particularly as we develop better experimental tools via use of CRISPR.

Activation of the p38 and JNK families of MAPKs have variously been associated with activation of the GCK-I (GCK-2) and GCK-IV (MIG-15) subfamilies of CNH domain MAP4Ks (Delpire, 2009). Neither subfamily has been studied systematically. Our ongoing observation of the literature is consistent with the GCK-2 and MIG-15 subfamilies generally being associated with p38 and JNK, activation, respectively. Yet so many of these studies depend on protein over-expression that we hesitate to draw general conclusions. Here we connect GCK-2 with PMK-1/p38 function, while in *Drosophila* dorsal closure of the embryo Msn (MIG-15 subfamily) is associated with JNK function (Su et al., 2000; Su et al., 1998).

Activation of MAP kinases is often associated with cytosol-to-nuclear translocation, initially shown with the canonical ERK MAPK (Gonzalez et al., 1993; Lenormand et al., 1993) but also shown for p38 MAPK (Ben-Levy et al., 1998).

Extrachromosomal transgenic *C. elegans* PMK-1::GFP similarly translocated from cytosol to the nucleus upon stress (Mertenskötter et al., 2013). Yet we found that this PMK-1::GFP fusion was not expressed in the VPCs, perhaps because *pmk-1* is expressed as part of a multi-gene operon, and so the transgene is missing key regulatory sequences. Further, the transgenic PMK-1::GFP is likely to be over-expressed, as is typical for *C. elegans* transgenic arrays, and thus may obscure more nuanced regulatory inputs. Consequently, we generated endogenous PMK-1::mNG via CRISPR and also introduced VPC-specific single-to-low copy mK2::PMK-1 (Fig. 2. 13, Fig. 2. 14). While we observed that endogenous PMK-1::mNG was expressed in VPCs, to our surprise we observed consistent nuclear PMK-1::mNG throughout the animal, including VPCs throughout their fate patterning, and nuclear mK2::PMK-1 in VPCs throughout their patterning. One could speculate that we perturbed PMK-1 function both through C- and N-terminal tagging, yet we showed that PMK-1::mNG function appeared normal in the *let-23(sa62gf)* background. These observations leave us at an impasse. Is the prevailing model for MAP kinase activation flawed? Is PMK-1/p38, a known stress kinase, tonically activated as a consequence of endogenous stressors or culture conditions? Or is translocation a modest part of the activation process that was previously masked by assay conditions? Our observation may lead to important mechanistic considerations of p38 activation and activation of MAP kinases in general, and is worth further investigation.

Many small GTPases, including mammalian RalA and RalB, are membrane-targeted through prenylation. Based on its C-terminal CAAX sequence, RAL-1 is inferred to be geranylgeranylated (Reiner and Lundquist, 2016), and our CRISPR tag of endogenous RAL-1 showed strong localization to the plasma membrane in all cells. The canonical mechanism for effector activation, originally defined for Ras-Raf (Block et al., 1996; Chiu et al., 2002), is recruitment of cytosolic effector to the plasma membrane by activated small GTPase. While our genetic analysis indicates that GCK-2 functions downstream of the 2°-promoting RAL-1 in VPCs, we did not observe co-localization of tagged endogenous RAL-1 and GCK-2, or activity-dependent enrichment of plasma membrane GCK-2, in presumptive 2° cells. This observation could be explained by activated, membrane-tethered RAL-1 recruiting only a small portion of cytosolic GCK-2. Alternatively, perhaps RAL-1 effector activation proceeds through an atypical mechanism, consistent with the non-canonical nature of the exocyst as an effector. The exocyst presents an interesting conundrum in signaling: it is clearly required for much Ral signaling (reviewed in Gentry et al., 2014), yet thwarts conventional biochemical bootstrapping through signaling cascades. Thus, the lack of co-localization of RAL-1 and GCK-2 could also be explained by certain populations of RAL-1 and GCK-2 being constitutively associated, perhaps at the exocyst complex. Though not the same subfamily (GCK-2 vs. MIG-15), this model is consistent with co-immunoprecipitation of mammalian Sec5 and HGK/MAP4K4 (Balakireva et al., 2006). We speculate that the complex of RAL-1/EXOC-8/GCK-2 recruits a co-

activator when RAL-1 is activated. Such a mechanism was implicated in studies of mammalian MAP4K3 (in the GCK-2 subfamily), in which a putative activating phosphorylation event was detected (Yan et al., 2010). While shown to be inhibited by PP2A^{T61E}, the kinase(s) mediating this phosphorylation event remains unknown. Alternatively, perhaps RAL-1 and GCK-2 never physically interact, and thus genetic analysis was required to reveal this cascade.

The advent of CRISPR-based tools permits analysis of endogenous proteins, and hence potentially improved cell biological and biochemical analysis. For example, all known Ral binding partners were discovered by yeast two-hybrid analysis, an approach with a strong record but also ample false negatives, say, in conditions of activity-dependent interactions or metazoan-specific subcellular localization. Thus, we may be able to use biochemical approaches to with tagged endogenous RAL-1 to identify novel interactors. Yet we also recognize the balance of strengths and weaknesses in the model invertebrate system, so mammalian cell-based studies may complement our genetic analysis to elucidate details of molecular mechanisms.

It is as yet unclear whether our findings of a genetic requirement for PMK-1 downstream of the RAL-1 2°-promoting activity herald a similar use of p38 downstream of mammalian Ral isoforms during development or cancer. An alternative possibility is that Ral in various metazoa signals through an array of effectors, only of some of which are relevant to cancer. Genetic and tissue heterogeneity of tumors, coupled with the historic difficulty of assessing Ral

activation levels in tumors, make this question non-trivial to address rigorously. This question is further complicated by the diverging functions of RalA and RalB in cancer, and their mostly poorly defined roles in non-pathogenic development and physiology. Yet this study could lead to surveys of phospho-p38 levels in Ras-positive tumors as a function of RalA or RalB, thus potentially satisfying the great demand for cancer biomarkers of Ral activation. Alternatively, establishment of a viable *in vivo* invertebrate model for RAL-1 function, added to the development of elegant genetic tools, should lead to extensive investigation of RAL-1 in diverse areas of biology, potentially leading us to clinically important biomarkers and “druggable targets” other than p38.

In conclusion, we have demonstrated that the LET-60/Ras-RGL-1/RalGEF-RAL-1/Ral 2°-promoting signal acts through exocyst component EXOC-8/Exo84 to trigger a GCK-2/MAP4K-PMK-1/p38 cascade. From a developmental biology standpoint, the mechanism by which the EGF morphogen gradient promotes 2° VPC fate in support of LIN-12/Notch is of long-standing interest (Kenyon, 1995). From a cancer biology standpoint, this study may also contribute to development of diagnostic biomarkers and small molecule inhibitors for Ras- and Ral-dependent cancers.

Materials and Methods

C. elegans handling and genetics.

All strains were derived from the N2 wild type. Nomenclature was as described (Horvitz et al., 1979). Animals were cultured using standard conditions on OP50 bacteria on NGM agar plates at 20°C (Brenner, 1974) except where noted. Strains used are shown in Table 2. 1.

PCR primers are listed in Table 2. 2. Single animal genotyping PCR reactions used Taq PCR Master Mix (QIAGEN). Deletions in *gck-2* were detected by triplex primers REW88/89/90 (Tm: 58°C, 32 cycles), resulting in 298 bp (wild-type), 478 bp (*ok2867*), and 462 bp (*tm2537*) amplicons. PCR products were sequenced to confirm reported allele perturbations (Khan et al. 2012). The *exoc-8(ok2523)* deletion was detected by triplex primers REW109/110/111 (Tm: 58°C, 32 cycles), resulting in 411 bp (wild-type) and 270 bp (*ok2523*) amplicons. The *pmk-1(km25)* was detected by PCR using triplex primers, REW85/86/87 (Tm: 55.5°C, 32 cycles), resulting in 345 bp and 591 bp (wild-type) and 216 bp (*km25*). *ral-1(gk628801)* was detected by primers DJR778/779 (Tm: 57°C, 32 cycles) to generate a 250 bp amplicon, followed by overnight digestion with HpyCH4IV (NEB) to yield wild-type (121 bp, 51 bp, 48 bp and 30 bp) and *gk628801* (151 bp, 51 bp and 48 bp) bands.

The *sec-5(pk2357)/+* mutation was maintained as a stable heterozygote by GFP-tagged balancer *mln1mls14*, and homozygotes were obtained by scoring non-green progeny.

Vulval induction scoring assay.

To score vulval induction, late L4 animals were mounted on slides with a 3% agar pad in M9 buffer with 5 mM sodium azide. Invaginations of ectopic pseudovulvae were scored under DIC/Nomarski optics (Nikon eclipse Ni). Images were captured using NIS-Elements AR 4.20.00 software. The vulval induction index for ectopic 1° and 2° induction was scored as described elsewhere. Briefly, we counted vulval invaginations, comprising cell lineages of single VPCs undergoing morphogenesis, which were distinct from the composite 2°-1°-2° normal vulva lineages (the “Christmas tree”, which we argue more closely resembles the Stanley Cup). As expected, in the *let-60(n1046gf)* background the normal vulva was oriented on the AC in the center of the gonad. The morphology of ectopic 1° lineages generally conformed with the symmetrical “cap” characteristic of isolated 1° lineages (Katz et al., 1995). In the *lin-12(n379d)* background, the AC and normal vulva were mostly absent, as described (Greenwald et al., 1983). The morphology of ectopic 2° lineages generally conformed with the asymmetric “beret” characteristic of isolated 2° lineages (Green et al., 2008; Katz et al., 1995). When the AC and normal vulva were

present in a *lin-12(n379d)* animal, data from that animal were flagged and excluded from the final count of ectopic 2° cells.

As previously described (Zand et al., 2011), the *let-60(n1046gf)* strain is liable to drift, resulting in increased induction of 1° cells. We established many frozen strains of *n1046* single mutants, and *n1046* outcrossed to N2, and established that the typical baseline is 1.2 to 1.5 ectopic 1° cells. We have also consistently observed that the *n1046* baseline is increased by ~0.2 when grown on bacterially mediated RNAi, including *gfp* or *luciferase* control strains (Zand et al., 2011; this study). Consequently, for all strains harboring an *n1046* mutation, we use a stringent protocol to minimize drift: strains are scored and a parafilm plate established immediately after construction or thawing, strains are refreshed (if necessary) by chunking, and animals are never grown for several generations in culture. Assays in which *n1046* control strains deviate from the expected baseline are discarded. When using this rigorous protocol, we rarely observe significant deviations from expected baselines. Each figure panel with VPC counts is from animals grown together at the same time.

Plasmids, generation of transgenic lines and integrated lines.

Details of plasmid construction are available upon request. Plasmids are listed in Table 2. 3. Transgenic lines were generated by microinjection of pB255-derived plasmids (50 ng/μl) with co-injection marker (20 ng/μl; either pPD118.33

[*P_{myo-2}::gfp*] or pPD93.97 [*P_{myo-3}::gfp*]) into the relevant strain and maintained by selecting for fluorescent animals. *rels10[P_{lin-31}::*ral-1*(Q75L)+ *P_{myo-2}::gfp*]* was generated and mapped to position I+5.1 (Shin, *et al.*, in preparation).

Fluorescent microscopy.

L3 animals were mounted in 5 mM sodium azide/M9 buffer on slides with 3% agar pad. *pmk-1(re170[pmk-1::mNG^{3xFlag}])* animals were grown on *Comamonas sp.* (DA1877) (Avery and Shtonda, 2003) and mounted in 2 mg/mL tetramisole in M9 buffer on slides with 3% agar pad. We hypothesized that stress caused constitutive translocation to the nucleus. However, growth on *Comamonas sp.* bacteria, which are thought to be non-inflammatory (Avery and Shtonda, 2003), did not alter the degree of nuclear translocation. Similarly, mounting animals on tetramisole rather than sodium azide did not abolish nuclear translocation. All images were captured by A1si Confocal Laser Microscope (Nikon) using NIS Elements Advanced Research, Version 4.40 software (Nikon).

CRISPR/Cas9-dependent genome editing.

Repair templates were generated by PCR amplification from genomic DNA of ~500 bp homology by Q5 polymerase (NEB), digesting of the target SEC vector, and Gibson Assembly (NEB) directed by homologous ends. The sgRNA targeting

sequences were inserted into pJW1236, the Cas9+sgRNA (F+E) plasmid (Ward, 2015), by Q5 site-Directed Mutagenesis (NEB). Plasmids, sgRNA sequences including PAM, and repair ssODNs used were listed in Tables 2. 3-2. 5. mNG^{3xFlag}::GCK-2 was generated by microinjection of repair template (20 ng/μl), sgRNA-Cas9 #1 (25 ng/μl), sgRNA-Cas9 #2 (25 ng/μl), and injection marker *P_{myo-2}::mCherry* (2.5 ng/μl) into wild-type (N2) animals. sgRNA targeting sequences are listed (Table 2. 4). mKate2^{3xFlag}::RAL-1(+) and mKate2^{3xFlag}::RAL-1(G26V) were generated by microinjection of repair template (20 ng/μl), sgRNA-Cas9 #1 (25 ng/μl), sgRNA-Cas9 #2 (25 ng/μl), and injection marker *P_{myo-2}::gfp* (10 ng/μl) into N2. The *ral-1*(G26V) mutation was generated by Q5 site-Directed Mutagenesis (NEB) into the homology arm of the repair template used for CRISPR. PMK-1::mNG^{3xFlag} was generated by microinjection of repair template (10 ng/μl), sgRNA-Cas9 #1 (50 ng/μl), sgRNA-Cas9 #2 (50 ng/μl), and injection marker *P_{myo-2}::mCherry* (2.5 ng/μl) into N2. To minimize steric hindrance, the linker sequence N-SAGGSAGGSAGG-C (Komatsu et al., 2011; 5' -TCAGCCGGAGGTAGCGCCGGCGGAAGTGCTGGTGGGA - 3') was inserted between *pmk-1* and mNG coding sequences, while RAL-1 and GCK-2 tagging had shorter linker N-SAGG-C (5' -GGAGCCGGATCT- 3') between FP::epitope and the N-terminus. Animals were handled and treated with 5 mg/ml hygromycin as described (Dickinson et al., 2015). The CRISPR knock-in results were confirmed by genotyping PCR using Taq PCR Master Mix (QIAGEN) and sequencing (Genewiz). Using the previously tagged DV3228 *gck-*

2(re113[mNG^{3xFlag::gck-2}]) as a starting point, the *gck-2(mid-Δ)* was generated by Co-CRISPR using *dpy-10(cn64gf)* as a Co-CRISPR marker (Arribere et al., 2014). sgRNA-Cas9 constructs were prepared by Q5 site-Directed Mutagenesis (NEB) of pJW1236. The repair ssODN, providing 35 bases of flanking homology arms on each side of the repaired break, was synthesized by IDT. We microinjected DV3228 with the two sgRNA-Cas9 constructs (each 25 ng/μl), repair oligo (10 μM), sgRNA for *dpy-10(cn64gf)* (pJA58) (25 ng/μl), ssODN repair donor for *dpy-10(cn64gf)* (600 nM), and injection marker *P_{myo-2}::mCherry* (2.5 ng/μl). Animals were handled and isolated as described (Arribere et al. 2014) by picking Rols and Dpys for PCR genotyping to detect the deletion, followed by sequence analysis of the repaired region and outcrossing to N2.

We assessed CRISPR tagged alleles for possible impacts on function by crossing tagged alleles into the *let-60(n1046gf)* and the *let-23(sa62gf)* sensitized backgrounds and comparing ectopic 1° induction of *n1046* or *sa62* alone vs. *n1046* or *sa62*+tagged allele strains. We observed induction indices of 1.4 vs. 1.4 for *n1046* vs. *n1046; gck-2(re113)*, respectively (P = 0.9), 1.4 vs. 1.2 for *n1046* vs. *n1046; ral-1(re218)*, respectively (P = 0.3), and 1.3 vs. 1.3 for *sa62* vs. *sa62; pmk-1(re170)*, respectively (P = 0.8). The functional impact of CRISPR putative gain-of-function mutations are shown in Fig. 2. 7B (for the *ral-1(re160gf)* G26V allele) and Fig. 2. 7F (for the *gck-2(re113re222)* mid-Δ allele). By visual inspection, none of the CRISPR tags or mutations altered the wild-type development.

Western blotting.

Animals were lysed in 4% SDS loading buffer by boiling at 90°C for 2 minutes. Protein samples were run on 4-15% SDS gel (BIO-RAD). Monoclonal anti-Flag antibody (Sigma-Aldrich F1804) and monoclonal anti- α -tubulin antibody (Sigma-Aldrich T6199) were diluted 1:2000 in blocking solution. Secondary antibody, goat anti-mouse (MilliporeSigma 12-349), diluted in 1:5000 in blocking solution. ECL reaction (Thermo Fisher Scientific) has done for signal generation. Immunoactive proteins were detected by film processor, SRX-101A (Konica Minolta) on X-ray film (Phenix).

Bacterially mediated RNA interference.

RNAi plasmids used were: III-7M13 (*ral-1*), V-4P08 (*gck-2*), X-5G21 (*mig-15*), *gfp* (Zand et al., 2011), and *luciferase*. For an RNAi negative control, a luciferase fragment not having sequence overlap with the *C. elegans* genome was amplified from SRE-luciferase plasmid and cloned into the HindIII- and XhoI-cut sites of L4440/pPD129.36. The host of bacterially-mediated RNAi clones was HT115 (Timmons and Fire, 1998). RNAi experiments were performed at 23°C on NGM agar plates supplemented with 1 mM IPTG and 50 μ g/ml carbenicillin. Plates were seeded with 80 μ l dsRNA-producing bacteria, grown overnight at room temperature, then populated with late L4 animals. Parents were transferred to

another RNAi plate after 1 day, and ectopic pseudovulvae were scored by DIC at the late L4 stage, 2 days later.

MiniMos.

reSi6 [*P_{lin-31}::mKate2::linker::pmk-1::unc-54 3'UTR*] was generated by miniMos (de la Cova et al., 2017; Frokjaer-Jensen et al., 2014). *mKate2::linker*(SAGG) was tagged to the N-terminal of *pmk-1* with *lin-31* promoter and *unc-54* 3'UTR. MiniMos-based plasmid pSH41 was generated by subcloning of *mKate2::linker::pmk-1* into pCC249 (*P_{lin-31}::unc-54 3'UTR*) using Gibson Assembly (NEB). We microinjected N2 wildtype with the *P_{myo-2}::gfp* (20 ng/μl), pGH8 (*P_{rab-3}::mCherry::unc-54 3'UTR*) (10 ng/μl), pCFJ601 (*P_{eft-3}::mos1 transposase::tbb-2 3'UTR*) (65 ng/μl), pMA122 (*P_{hsp16.41}::peel-1::tbb-2 3'UTR*) (10 ng/μl), and pHS41 (*P_{lin-31}::mKate2::linker::pmk-1::unc-54 3'UTR*) (10 ng/μl). The insertion site is unknown. MiniMos results were tracked by observing mKate2 signal in VPCs.

Quantification and statistical analysis.

In every bar graph panel, animals were scored concurrently to avoid variability, using scoring standards described in the Methods. Values represe

nt either ectopic induction (0-3; 1° or 2°), or, in the case of under-induction, total number of VPCs induced (0-3; both 1° and 2°). Each bar represents mean induction of the cell type indicated, with error bars representing S.E. M. N equals the animals scored, and is indicated as a white number on each bar. To avoid bias, N was determined randomly, with all prepared animals scored and statistical tests only performed *post hoc*. General statistical methods are described in each figure legend. Briefly, pairwise tests were performed by t-test, multiple tests by ANOVA. P value is shown in each panel, n.s. = not significant. Significance was defined as >0.05 , but in most cases each relationship was tested via multiple assays. For statistical analyses we used GraphPad Prism 5.

Table 2. 1 Strains for GCK-2 study

Strain	Genotype	Used in Figures
MT2124	<i>let-60(n1046gf)</i> IV	2. 3A, 2. 3B, 2. 3C, 2. 3D, 2. 4A, 2. 4B, 2. 5C, 2. 5E, 2. 5F, 2. 10E, 2. 13A
DV2799	<i>ral-1(gk628801)</i> III; <i>let-60(n1046gf)</i> IV	2. 3A
DV2672	<i>exoc-8(ok2523)</i> I; <i>let-60(n1046gf)</i> IV	2. 3B
DV2698	<i>sec-5(pk2357) / mln1[mls14 dpy-10(e128)]</i> II; <i>let-60(n1046gf)</i> IV	2. 3C
DV2711	<i>exoc-7(ok2006)</i> I; <i>let-60(n1046gf)</i> IV	2. 4B
DV2682	<i>rlbp-1(tm3665)</i> I; <i>let-60(n1046gf)</i> IV	2. 3D
DV2443	<i>lin-12(n379d)</i> III; <i>him-8(e1489)</i> IV	2. 4C, 2. 4D, 2. 5G, 2. 6C, 2. 6D, 2. 6E, 2. 7A, 2. 7B, 2. 7C, 2. 7F, 2. 8B
DV3460	<i>ral-1(gk628801)</i> <i>lin-12(n379d)</i> III; <i>him-8(e1489)</i> IV	2. 4C
DV3298	<i>exoc-8(ok2523)</i> I; <i>lin-12(n379d)</i> III; <i>him-8(e1489)</i> IV	2. 4D
DV2657	<i>let-60(n1046gf)</i> IV; <i>gck-2(ok2867)</i> V	2. 5D, 2. 5E, 2. 10E
DV2710	<i>lin-12(n379d)</i> III; <i>him-8(e1489)</i> IV; <i>gck-2(ok2867)</i> V	2. 6C
DV2727	<i>lin-12(n379d)</i> III; <i>gck-2(tm2537)</i> V	2. 6D, 2. 8C
DV2965	<i>lin-12(n379d)</i> III; <i>mig-15(rh80)</i> X	2. 5G
DV2964	<i>lin-12(n379d)</i> III; <i>mig-15(rh148)</i> X	2. 5G
NJ490	<i>mig-15(rh148)</i> X	2. 6A
DV3498	<i>let-60(n1046gf)</i> IV; <i>mig-15(rh148)</i> X	2. 6B
MT378	<i>lin-3(n378rf)</i> IV	2. 6F
DV2833	<i>lin-3(n378rf)</i> IV; <i>gck-2(ok2867)</i> V	2. 6F
DV3326	<i>ral-1(re160gf[mKate2^3xFlag::ral-1(G26V)])</i> <i>lin-12 (n379d)</i> III; <i>him-8(e1489)</i> IV	2. 7B, 2. 7D
DV2712	<i>rels10[P_{lin-31}::ral-1(Q75L), P_{myo-2}::gfp]</i> I; <i>lin-12 (n379d)</i> III; <i>him-8(e1489)</i> IV	2. 7A, 2. 9A, 2. 9B, 2. 13B
DV3440	<i>lin-12(n379d)</i> III; <i>him-8(e1489)</i> IV; <i>gck-2(re113re222[mNG^3xFlag::gck-2(mid-Δ)])</i> V	2. 7F

Table 2. 1 Continued

Strain	Genotype	Used in Figures
DV3441	<i>lin-12(n379d)</i> III; <i>gck-2(re113re223[mNG^{3xFlag::gck-2(mid-Δ)}])</i> V	2. 7F
DV3228	<i>gck-2(re113[mNG^{3xFlag::gck-2}])</i> V	2. 7E, 2. 11A, 2. 11B, 2. 12B, 2. 12C, 2. 12D, 2. 12E, 2. 12F, 2. 12G, 2. 12H
DV3410	<i>gck-2(re113re222[mNG^{3xFlag::gck-2(mid-Δ)}])</i> V	2. 7E
DV3411	<i>gck-2(re113re223[mNG^{3xFlag::gck-2(mid-Δ)}])</i> V	2. 7E
DV3040	<i>lin-12(n379d)</i> III; <i>him-8(e1489)</i> IV; <i>reEx143[P_{lin-31::gck-2(mid-Δ)}, P_{myo-2::gfp}]</i> I;	2. 8B
DV3125	<i>lin-12(n379d)</i> III; <i>gck-2(tm2537)</i> V; <i>reEx161[P_{lin-31::gck-2(mid-Δ)}, P_{myo-2::gfp}]</i>	2. 8C
DV2725	<i>rels10[P_{lin-31::ral-1(Q75L)}, P_{myo-2::gfp}]</i> I; <i>lin-12(n379d)</i> III; <i>gck-2(ok2867)</i> V	2. 9A, 2. 10B
DV2726	<i>rels10[P_{lin-31::ral-1(Q75L)}, P_{myo-2::gfp}]</i> I; <i>lin-12(n379d)</i> III; <i>gck-2(tm2537)</i> V	2. 9A, 2. 9E, 2. 9F, 2. 10C, 2. 10D
DV2734	<i>rels10[P_{lin-31::ral-1(Q75L)}, P_{myo-2::gfp}]</i> I; <i>exoc-8(ok2523)</i> I; <i>lin-12(n379d)</i> III; <i>him-8(e1489)</i> IV	2. 9B
DV2449	<i>lin-12(n379d)</i> III; <i>lin-15(n765ts)</i> X	2. 9C, 2. 9D, 2. 10A
DV3499	<i>ral-1(gk628801)</i> <i>lin-12(n379d)</i> III; <i>him-8(e1489)</i> IV; <i>lin-15(n765ts)</i> X	2. 9C
DV3403	<i>lin-12(n379d)</i> III; <i>him-8(e1489)</i> IV; <i>gck-2(ok2867)</i> V; <i>lin-15(n765ts)</i> X	2. 9D
DV3194	<i>rels10[P_{lin-31::ral-1(Q75L)}, P_{myo-2::gfp}]</i> I; <i>lin-12(n379d)</i> III; <i>gck-2(tm2537)</i> V; <i>reEx176[P_{lin-31::gck-2(+)}, P_{myo-3::gfp}]</i>	2. 9E
DV3244	<i>rels10[P_{lin-31::ral-1(Q75L)}, P_{myo-2::gfp}]</i> I; <i>lin-12(n379d)</i> III; <i>gck-2(tm2537)</i> V; <i>reEx181[P_{lin-31::gck-2(K44E)}, P_{myo-3::gfp}]</i>	2. 9F
DV3138	<i>rels10[P_{lin-31::ral-1(Q75L)}, P_{myo-2::gfp}]</i> I; <i>lin-12(n379d)</i> III; <i>him-8(e1489)</i> IV; <i>gck-2(ok2867)</i> V; <i>reEx167[P_{lin-31::gck-2(+)}, P_{myo-3::gfp}]</i>	2. 10B
DV3195	<i>rels10[P_{lin-31::ral-1(Q75L)}, P_{myo-2::gfp}]</i> I; <i>lin-12(n379d)</i> III; <i>gck-2(tm2537)</i> V; <i>reEx177[P_{lin-31::gck-2(+)}, P_{myo-3::gfp}]</i>	2. 10C

Table 2. 1 Continued

Strain	Genotype	Used in Figures
DV3243	<i>rels10[P_{lin-31}::ral-1(Q75L), P_{myo-2}::gfp] I</i> ; <i>lin-12(n379d) III</i> ; <i>gck-2(tm2537) V</i> ; <i>reEx180[P_{lin-31}::gck-2(K44E), P_{myo-3}::gfp]</i>	2. 10D
DV2742	<i>let-60(n1046gf) IV</i> ; <i>reEx113[P_{lin-31}::gck-2(+), P_{myo-2}::gfp]</i>	2. 10E
DV2754	<i>let-60(n1046gf) IV</i> ; <i>gck-2(ok2867) V</i> ; <i>reEx112[P_{lin-31}::gck-2(+), P_{myo-2}::gfp]</i>	2. 10E
DV3238	<i>ral-1(re160gf[mKate2^{3xFlag}::ral-1(G26V)]) III</i>	2. 11C, 2. 11D, 2. 12J, 2. 12K, 2. 12L, 2. 12M, 2. 12N, 2. 12O, 2. 12P
DV3402	<i>ral-1(re218[mKate2^{3xFlag}::ral-1]) III</i>	2. 12R, 2. 12S, 2. 12T, 2. 12U, 2. 12V, 2. 12W, 2. 12X, 2. 12Y, 2. 12Z
DV3303	<i>ral-1(re160gf[mKate2^{3xFlag}::ral-1(G26V)]) III</i> ; <i>gck-2(re113[mNG^{3xFlag}::gck-2]) V</i>	2. 11E, 2. 11F, 2. 12AA, 2. 12AB
DV3163	<i>gck-2(re112[mNG^{SEC}^{3xFlag}::gck-2]) V</i>	2. 12B
DV3237	<i>ral-1(re159[mKate2^{SEC}^{3xFlag}::ral-1(G26V)]) III</i>	2. 12J
DV3401	<i>ral-1(re217[mKate2^{SEC}^{3xFlag}::ral-1]) III</i>	2. 12R
DV2706	<i>pmk-1(km25) let-60(n1046gf) IV</i>	2. 13A
DV2769	<i>rels10[P_{lin-31}::ral-1(Q75L), P_{myo-2}::gfp] I</i> ; <i>lin-12(n379d) III</i> ; <i>pmk-1(km25) IV</i>	2. 13B
DV3268	<i>pmk-1(re170[pmk-1::mNG^{3xFlag}]) IV</i>	2. 13C, 2. 13D, 2. 14B, 2. 14C, 2. 14D, 2. 14E, 2. 14F
AU0328	<i>P_{pmk-1}::pmk-1(+):gfp, rol-6 (su1006)</i>	2. 14G, 2. 14H, 2. 14I, 2. 14J
DV3256	<i>pmk-1(re169[pmk-1::mNG^{SEC}^{3xFlag}]) IV</i>	2. 14B
DV3496	<i>reSi6[P_{lin-31}::mKate2::linker::pmk-1::unc-54 3'UTR]</i>	2. 14K, 2. 14L, 2. 14M, 2. 14N

Reprinted with permission from Shin et. al, 2018

Table 2. 2 Primers for GCK-2 study

Name	Sequence	Use
REW1	5' -TTTTTTAAGCTTCATAAAGAAAGGCC CGGCGC- 3'	<i>luciferase</i> RNAi subcloning to generate pREW2
REW2	5' -GTTATTTATCGGAGTTGCAGTTGCG CCTCGAGAAAAA- 3'	<i>luciferase</i> RNAi subcloning to generate pREW2
REW94	5' -TTGGTTAGATCTGGGGTAATGAGTG CCGATGTAATCAAACG- 3'	<i>gck-2(+)</i> or <i>gck-2</i> (K44E) subcloning into pB255
REW126	5' -GACATACGGATACTCCAATCGCTG GATAAGCGGCCGCGAGGGGA- 3'	<i>gck-2(+)</i> or <i>gck-2</i> (K44E) subcloning into pB255
REW131	5' -ATGGGAGCATGTTTCTCAAAAGTTAT GG- 3'	<i>gck-2</i> mid-deletion in pREW24
REW132	5' -GAATCGAGGATATCATTCTGAAAGA ACACTT- 3'	<i>gck-2</i> mid-deletion in pREW24
DJR778	5' -TAGACAATTTAGGCCCAAACCCCC G- 3'	<i>ral-1(gk628801)</i> genotyping
DJR779	5' -CCAAATTTTCAGCCTAAAATCTCTT CCCAATACC- 3'	<i>ral-1(gk628801)</i> genotyping
REW85	5' -AAACATTTAATCGGTTCAAATTGCCG C- 3'	<i>pmk-1(km25)</i> genotyping
REW86	5' -CTTGA CTCCAATTGGTACCGGAG- 3'	<i>pmk-1(km25)</i> genotyping
REW87	5' -GTGGTCATCGTTGAGTCGCTG- 3'	<i>pmk-1(km25)</i> genotyping
REW88	5' -CCGTATTGGATGGCTCCGGAAG- 3'	<i>gck-2(ok2867)</i> , <i>gck-2(tm2537)</i> genotyping
REW89	5' -CATCCGGCATGCAGTTCGTATCG- 3'	<i>gck-2(ok2867)</i> , <i>gck-2(tm2537)</i> genotyping
REW90	5' -GCTCCTTCACTTCTCACACCGG- 3'	<i>gck-2(ok2867)</i> , <i>gck-2(tm2537)</i> genotyping
REW109	5' -CTCGTGAGACAGGCAACTATTCGAG G- 3'	<i>exoc-8(ok2523)</i> genotyping
REW110	5' -CACGAATGGAAACAGTGCCCGAC- 3'	<i>exoc-8(ok2523)</i> genotyping

Table 2. 2 Continued

Name	Sequence	Use
REW111	5' -CATCGTCGCTGAGCAGTTGGAC- 3'	<i>exoc-8(ok2523)</i> genotyping
TD185	5' -GCCGGAAGAGTGATGAACCC- 3'	<i>ral-1(re160)</i> , <i>ral-1</i> (<i>re218</i>) genotyping
TD186	5' -TAATGAGCTCGGAGACCATGGC- 3'	<i>ral-1(re160)</i> , <i>ral-1</i> (<i>re218</i>) genotyping
TD187	5' -CGCACCTCATCATACATGAACTGC- 3'	<i>ral-1(re160)</i> , <i>ral-1</i> (<i>re218</i>) genotyping
HS126	5' -TTGTCCTCCTCTCCCTTGG- 3'	<i>gck-2(re113)</i> , <i>pmk-1</i> (<i>re170</i>) genotyping
HS136	5' -GAGAAAACAACGGTCCTTCTATACAA C- 3'	<i>gck-2(re113)</i> genotyping
HS138	5' -CGTGAGGCACTGACGAAC- 3'	<i>gck-2(re113)</i> genotyping
HS278	5' -ATGCTCCTTCACTTCTCACACC- 3'	<i>gck-2(re113re222)</i> , <i>gck-2(re113re223)</i> genotyping
HS279	5' -TCAATGGCATACCGAAGAATGTCG- 3'	<i>gck-2(re113re222)</i> , <i>gck-2(re113re223)</i> genotyping
HS280	5' -CATCCGGCATGCAGTTCG- 3'	<i>gck-2(re113re222)</i> , <i>gck-2(re113re223)</i> genotyping
HS185	5' -CGCATTTGTAGTCGCGGTG- 3'	<i>pmk-1(re170)</i> genotyping
HS186	5' -CTCACTGATCTACTCATCGTTTGTCT AAG- 3'	<i>pmk-1(re170)</i> genotyping
DJR769	5' -CACCTCCTATTGCGAGATGTCTTG- 3'	Universal Mutagenesis PCR primer for sgRNA plasmid
HS130	5' -ACTGATGAGTGGGTGGTCGGGTTTA AGAGCTATGCTGGAAACAG- 3'	Mutagenesis PCR primer for mNG:: 3xFlag::GCK-2 CRISPR sgRNA #1 plasmid

Table 2. 2 Continued

Name	Sequence	Use
HS131	5' -ATTGTTATGGAGTACTGCGGGTTTA AGAGCTATGCTGGAAACAG- 3'	Mutagenesis PCR primer for mNG:: 3xFlag::GCK-2 CRISPR sgRNA #2 plasmid
TD143	5' -TTCAGAATGGAGGGTTACGGGTTT AAGAGCTATGCTGGAAACAG- 3'	Mutagenesis PCR primer for mKate2:: 3xFlag::RAL-1(+ or G26V) CRISPR sgRNA #1 plasmid
HS166	5' -GTTATTATGGTCGGAACCGGGTTT AAGAGCTATGCTGGAAACAG- 3'	Mutagenesis PCR primer for mKate2:: 3xFlag::RAL-1(+ or G26V) CRISPR sgRNA #2 plasmid
HS177	5' -TAAGGATGATTCAGTGCGGGGTT TAAGAGCTATGCTGGAAACAG- 3'	Mutagenesis PCR primer for PMK-1:: mNG::3xFlag CRISPR sgRNA #1 plasmid
HS178	5' -TGAGACATCTTACAATCCCAGTTT AAGAGCTATGCTGGAAACAG- 3'	Mutagenesis PCR primer for PMK-1:: mNG::3xFlag CRISPR sgRNA #2 plasmid
REW105	5' -GATTCAGTGGCAGCTGTCTGAAGTA GTCAAACCTCGAGGCGG- 3'	Mutagenesis PCR primer for generating GCK-2 (K44E) in pREW18
REW106	5' -GATTCAGTGGCAGCTGTCTGAAGTA GTCAAACCTCGAGGCGG- 3'	Mutagenesis PCR primer for generating GCK-2 (K44E) in pREW18
HS139	5' -TCCCAGTCACGACGTTGTAAAACG ACGGCCAGTCGCCGGCATAAATTCCC GCGTTCAGT- 3'	Primer for amplifying upstream homology arm to generate repair template (mNG::3xFlag::GCK- 2 CRISPR)

Table 2. 2 Continued

Name	Sequence	Use
HS133	5' -GCATGTTCTCCTTGATGAGCTCCTCT CCCTTGAGACCATTACCCCTGAAATTT TGAATATTTTTGTG- 3'	Primer for amplifying upstream homology arm to generate repair template (mNG::3xFlag::GCK- 2 CRISPR)
HS134	5' -CGACGACAAGCGTGATTACAAGGAT GACGATGACAAGAGAGGATCTGGAATG AGTGCCGATGTAATCAAAC- 3'	Primer for amplifying downstream homology arm to generate repair template (mNG::3xFlag::GCK- 2 CRISPR)
HS140	5' -TAACAATTTACACAGGAAACAGCTA TGACCATGTTATCGAGATAGAGAACCT GCATTGGG- 3'	Primer for amplifying downstream homology arm to generate repair template (mNG::3xFlag::GCK- 2 CRISPR)
TD173	5' -CCCAGTCACGACGTTGTAAACGA CGGCCAGTCGCCGGCACCGAGTTTTAT GATCCGGAA- 3'	Primer for amplifying upstream homology arm to generate repair template (mKate2::3xFlag::RA L-1(+ or G26V) CRISPR)
TD174	5' -TTCATATGCATGTTTTCTTTAATGAG CTCGGAGACCATGGCTGAAAATTGAG TTTTAGG- 3'	Primer for amplifying upstream homology arm to generate repair template (mKate2::3xFlag::RA L-1(+ or G26V) CRISPR)

Table 2. 2 Continued

Name	Sequence	Use
TD175	5' -CAAGCGTGATTACAAGGATGACGAT GACAAGAGATCAGCCGGAGGTAGCGC CGGCGGAAGTGCTGGTGGGAATGGCAT CGAAAAAAGCAAG- 3'	Primer for amplifying downstream homology arm to generate repair template (mKate2::3xFlag::RA L-1(+ or G26V) CRISPR)
TD177	5' -AACAATTTACACAGGAAACAGCTAT GACCATGTTATGGGTTTTTTGACATAAA ACTCGC- 3'	Primer for amplifying downstream homology arm to generate repair template (mKate2::3xFlag::RA L-1(+ or G26V) CRISPR)
HS181	5' -CCCAGTCACGACGTTGTAAAACGAC GGCCAGTCGCCGGCACATGTCAGTAAC TGGAACACCAG- 3'	Primer for amplifying upstream homology arm to generate repair template (PMK-1:: mNG::3xFlag)
HS182	5' -GGAGGGAGGCCATGTTGTCCTCCTC TCCCTTGGAGACCATTCACCAGCACT TCCGCCGGCGCTACCTCCGGCTGACG ATTCCATTTTCTCCTCATCTTCC- 3'	Primer for amplifying upstream homology arm to generate repair template (PMK-1:: mNG::3xFlag)
HS183	5' -CGACGACAAGCGTGATTACAAGGAT GACGATGACAAGAGATAGCATTGCTTT CTTTTTTGTATATCAGTTTTTC- 3'	Primer for amplifying downstream homology arm to generate repair template (PMK-1:: mNG::3xFlag)
HS184	5' -TAACAATTTACACAGGAAACAGCTA TGACCATGTTATCGCATCGTGCGTGTTA TCTACTGC- 3'	Primer for amplifying downstream homology arm to generate repair template (PMK-1:: mNG::3xFlag)

Table 2. 2 Continued

Name	Sequence	Use
HS264	5' -CTTCGTCAGAATCAGATCGGGTTTA AGAGCTATGCTGGAAACAG- 3'	Mutagenesis PCR primer for GCK-2 mid-Δ CRISPR sgRNA #1 plasmid
HS265	5' -ATTGATTCCAAAGGTTCCGAGTTTAA GAGCTATGCTGGAAACAG- 3'	Mutagenesis PCR primer for GCK-2 mid-Δ CRISPR sgRNA #2 plasmid
HS281	5' -AGAACATTTTCAGGAGGACCCTTGG CTAGCGTCGACGCCAATGGTCTCCGAG CTCATTAAGAAAAC- 3'	Primer for amplifying mKate2 to generate miniMos-based plasmid ($P_{lin-31}::$ <i>mKate2::linker::pmk-</i> <i>1</i>)
HS282	5' -TATGATCCATTGTTGTCTGTGGAAAC ATACCTCCGGCTGAACGGTGTCCGAGC TTGG- 3'	Primer for amplifying mKate2 to generate miniMos-based plasmid ($P_{lin-31}::$ <i>mKate2::linker::pmk-</i> <i>1</i>)
HS283	5' -TCCCATCCAAGCTCGGACACCGTTC AGCCGGAGGTATGTTTCCACAGACAAC AATGGATC- 3'	Primer for amplifying <i>pmk-1</i> to generate miniMos-based plasmid ($P_{lin-31}::$ <i>mKate2::linker::pmk-</i> <i>1</i>)
HS284	5' -GAGATGGCGATCTGATGACAGCGGC CGATGCGGAGCTGGCCTACGATTCCAT TTTCTCCTCATCTTC- 3'	Primer for amplifying <i>pmk-1</i> to generate miniMos-based plasmid ($P_{lin-31}::$ <i>mKate2::linker::pmk-</i> <i>1</i>)

Reprinted with permission from Shin et. al, 2018

Table 2. 3 Plasmids for GCK-2 study

Name	Description	Used for
pREW2	RNAi of <i>luciferase</i> was subcloned into L4440	Negative control for RNAi experiments
pREW18	<i>P_{lin-31}::gck-2(+):let-858 3'UTR</i>	Rescue experiment in <i>let-60(n1046gf); gck-2(ok2867)</i>
pREW24	<i>P_{lin-31}::gck-2(+):unc-54 3'UTR</i>	Rescue experiment in <i>rels10[ral-1(gf)]; lin-12(n379d); gck-2(ok2867)</i>
pREW25	<i>P_{lin-31}::gck-2(mid-deletion):unc-54 3'UTR</i>	2° induction experiment in <i>lin-12(n379d)</i> and <i>lin-12(n379d); gck-2(tm2537)</i>
pREW32	<i>P_{lin-31}::gck-2(K44E):unc-54 3'UTR</i>	Kinase dead negative control rescue experiment in <i>rels10[ral-1(gf)]; lin-12(n379d); gck-2(ok2867)</i>
pHS21	Homology arms (534 bp upstream and 875 bp downstream) was subcloned into pDD268	mNG ³ xFlag::GCK-2 CRISPR knock-in (repair template)
pHS13	Mutagenized pJW1236 using primers, DJR769 and HS130	mNG ³ xFlag::GCK-2 CRISPR knock-in (sgRNA-Cas9 plasmid) (sgRNA #1)
pHS14	Mutagenized pJW1236 using primers, DJR769 and HS131	mNG ³ xFlag::GCK-2 CRISPR knock-in (sgRNA-Cas9 plasmid) (sgRNA #2)
pTD36	Homology arms (869 bp upstream and 754 bp downstream) was subcloned into pDD285	mKate2 ³ xFlag::RAL-1(+) CRISPR knock-in (repair template)
pTD40	Homology arms (869 bp upstream and 754 bp downstream) was subcloned into pDD285	mKate2 ³ xFlag::RAL-1(G26V) CRISPR knock-in (repair template)
pTD38	Mutagenized pJW1236 using primers, DJR769 and TD143	mKate2 ³ xFlag::RAL-1(+) and mKate2 ³ xFlag::RAL-1(G26V) CRISPR knock-in (sgRNA-Cas9 plasmid) (sgRNA #1)
pHS23	Mutagenized pJW1236 using primers, DJR769 and HS166	mKate2 ³ xFlag::RAL-1(+) and mKate2 ³ xFlag::RAL-1(G26V) CRISPR knock-in (sgRNA-Cas9 plasmid) (sgRNA #2)

Table 2. 3 Continued

Name	Description	Used for
pHS40	Homology arms (785 bp upstream and 875 bp downstream) was subcloned into pDD268	PMK-1::mNG ³ xFlag CRISPR knock-in (repair template)
pHS26	Mutagenized pJW1236 using primers, DJR769 and HS177	PMK-1::mNG ³ xFlag CRISPR knock-in (sgRNA-Cas9 plasmid) (sgRNA #1)
pHS25	Mutagenized pJW1236 using primers, DJR769 and HS178	PMK-1::mNG ³ xFlag CRISPR knock-in (sgRNA-Cas9 plasmid) (sgRNA #2)
pHS38	Mutagenized pJW1236 using primers, DJR769 and HS264	GCK-2 mid-deletion CRISPR knock-in (sgRNA-Cas9 plasmid) (sgRNA #1)
pHS39	Mutagenized pJW1236 using primers, DJR769 and HS265	GCK-2 mid-deletion CRISPR knock-in (sgRNA-Cas9 plasmid) (sgRNA #2)
pHS41	Sequence of <i>mKate2::linker::pmk-1</i> was subcloned into pCC249 (<i>P_{lin-31}::unc-54</i> 3'UTR)	PMK-1 miniMos for generating <i>reSi6</i> [<i>P_{lin-31}::mKate2::linker::pmk-1::unc-54</i> 3'UTR]

Reprinted with permission form Shin et. al, 2018

Table 2. 4 sgRNA sequences and PAMs

sgRNA sequence and <u>PAM</u>	Used for
5' -ACTGATGAGTGGGTGGTCGG <u>AGG</u> - 3'	mNG ^{3xFlag} ::GCK-2 CRISPR knock-in sgRNA #1. Inserted in pHS13.
5' -ATTGTTATGGAGTACTGCGG <u>CGG</u> - 3'	mNG ^{3xFlag} ::GCK-2 CRISPR knock-in sgRNA #2. Inserted in pHS14.
5' -TTCAGAATGGAGGGTTACGGT <u>TGG</u> - 3'	mKate2 ^{3xFlag} ::RAL-1(+) and mKate2 ^{3xFlag} ::RAL-1(G26V) CRSIPR knock-in sgRNA #1. Inserted in pTD38.
5' -GCTTCATAAAAAACAAGGGG <u>CGG</u> - 3'	mKate2 ^{3xFlag} ::RAL-1(+) and mKate2 ^{3xFlag} ::RAL-1(G26V) CRSIPR knock-in sgRNA #2. Inserted in pHS23.
5' -TAAGGATGATTCAGTGCGG <u>GGG</u> - 3'	PMK-1::mNG ^{3xFlag} CRISPR knock-in sgRNA #1. Inserted in pHS26.
5' -GCTTCATAAAAAACAAGGGG <u>CGG</u> - 3'	PMK-1::mNG ^{3xFlag} CRISPR knock-in sgRNA #2. Inserted in pHS25.
5' -CTTCGTCAGAATCAGATCGG <u>AGG</u> - 3'	GCK-2 mid-deletion CRISPR knock-in sgRNA #1. Inserted in pHS38.
5' -ATTGATTCCAAAGGTTCCGAT <u>TGG</u> - 3'	GCK-2 mid-deletion CRISPR knock-in sgRNA #2. Inserted in pHS39.

Reprinted with permission form Shin et. al, 2018

Table 2. 5 Repair ssODN

ssODN sequence	Description
5' -TATCCTCATCGCCGAACACTTCGTCAGAATCAGATCCGATGGGAGCATGTTTCTCAAAGTTATGGATAGA-3'	Repair ssODN for GCK-2 (mid-Δ) (71 bp)
5' -CACTTGAACCTCAATACGGCAAGATGAGAATGACTGGAAACCGTACCGCATGCGGTGCCTATGGTAGCGGAGCTTCACATGGCTTCAGACCAACAGCCTAT- 3'	Repair ssODN for <i>dpy-10 (cn64gf)</i> (101 bp)

Reprinted with permission form Shin et. al, 2018

CHAPTER III

DEVELOPMENTAL FIDELITY IS IMPOSED BY GENETICALLY SEPARABLE RALGEF ACTIVITIES THAT MEDIATE OPPOSING SIGNALS

Introduction

Developmental patterning of the *C. elegans* vulva precursor cell (VPC) fates is a textbook system for analysis of cell-cell signaling. The vulva develops from six roughly equipotent VPCs – P3.p through P8.p – that are induced to assume a 3°-3°-2°-1°-2°-3° pattern of cell fates. The anchor cell (AC) in the somatic gonad produces the LIN-3/EGF inductive signal (Fig. 3. 1A). Historically, two models for VPC fate patterning have been advanced. The Morphogen Gradient Model posits that it is the distance of each VPC from the AC, and hence EGF-EGFR dose, that dictates its fate. (Katz et al., 1995; Katz et al., 1996; Sternberg and Horvitz, 1986, 1989).

In contrast, identification and molecular genetic analysis of genes that are necessary and sufficient for the 1°- and 2°-promoting VPC fate patterning signals led to the Sequential Induction Model. LIN-3 signals via the LET-23/EGFR-LET-60/Ras-LIN-45/Raf-MEK-2/MEK-MPK-1/ERK canonical MAP kinase cascade to induce 1° fate (Fig. 3. 1B; Sundaram, 2013). In turn, redundant DSL ligands produced by presumptive 1° cells induce neighboring VPCs via LIN-12/Notch to become 2° (Chen and Greenwald, 2004; Zhang and Greenwald, 2011); LIN-12 is

necessary and sufficient for 2° fate (Greenwald et al., 1983) and controls 2°-specific transcriptional targets (Fig. 3. 1B; Berset et al., 2001; Yoo et al., 2004; Yoo and Greenwald, 2005). LET-23 is necessary for 1° but not 2° fate (Koga and Ohshima, 1995; Simske and Kim, 1995), but these mosaic analyses did not address whether LET-23/EGFR might transduce a lower dose contribution to 2° fate induction, consistent with the Morphogen Gradient Model.

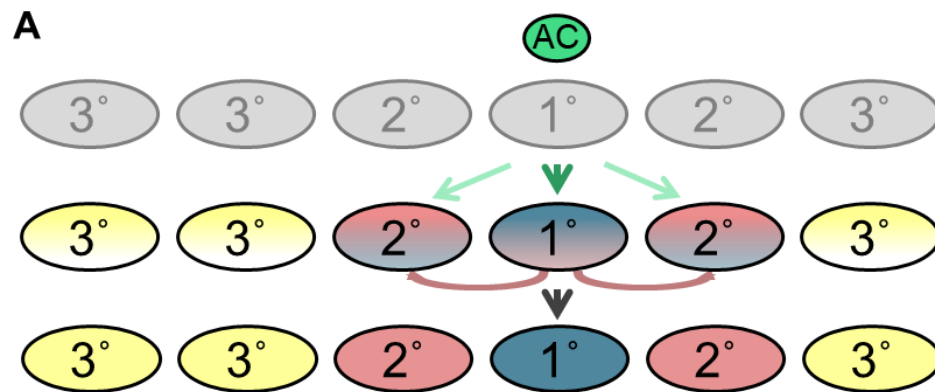


Figure 3. 1 Schematics of VPC fate patterning and its signaling network. A. Initially equipotent VPCs are induced by the Anchor Cell (AC) to assume the 3°-3°-2°-1°-2°-3° pattern of fates (anterior-to-posterior), based on their position relative to the AC. Over time, induced VPCs progress from naïve to initially specified to terminally committed to their fates, represented by equipotent and uninduced (gray) progressing through initially specified (hybrid colors with one color dominant) to terminally committed to 1° (blue), 2° (rose) or 3° (yellow) fates. Yet the precise time course, molecular steps and network re-wiring events required for this progression are still unclear.

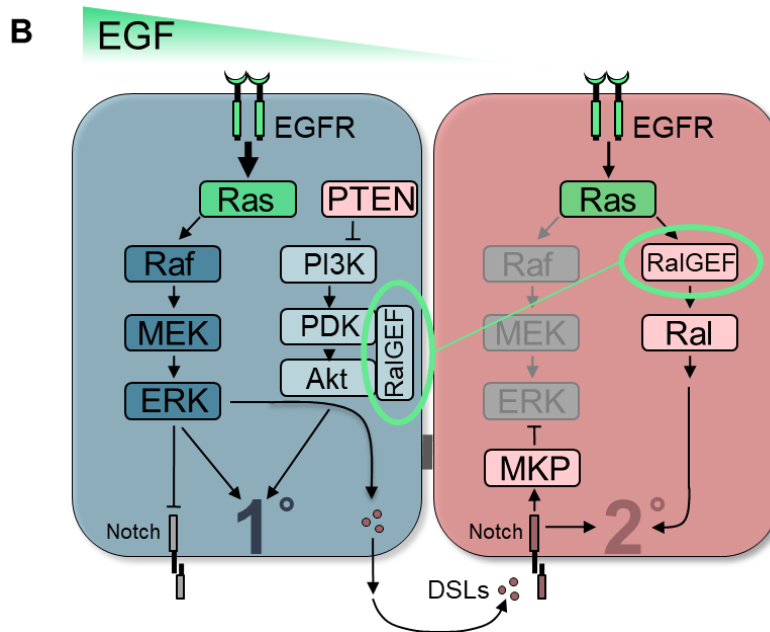


Figure 3. 1 Continued. B. The synthesis of the Sequential Induction, Morphogen Gradient, and Mutual Antagonism models of the VPC patterning signal transduction network, with the hypothesized RGL-1/RalGEF Balanced Switching mechanism superimposed. Necessary and sufficient cascades are in dark colors (dark blue for 1°-promoting LET-23/EGFR-LET-60/Ras-LIN-45/Raf-MEK-2/MEK-MPK-1/ERK; dark rose for LIN-12/Notch and the CSL transcriptional complex, CSL not pictured). Modulatory cascades are shown in lighter colors (light blue for 1°-promoting AGE-1/PI3K-PDK-1/PDK-AKT-1/Akt, with light rose for inhibitory DAF-18/PTEN lipid phosphatase; light rose for 2°-promoting RGL-1/RalGEF-RAL-1/Ral). Green represents proteins capable of promoting 1° or 2° fate, like LIN-3/EGF, LET-23/EGFR and LET-60/Ras, depending on signal dose and as yet unknown factors. Mutual antagonism operates by excluding potentially contradictory signals from initially specified VPCs: in presumptive 1° cells, LIN-12/Notch is internalized and degraded (gray), while in presumptive 2° cells MPK-1/ERK activation is repressed by transcriptional activation of LIP-1/MKP/DUSP/Erk phosphatase. The putative RGL-1/RALGEF Balanced Switch is circled in green both in presumptive 1° and presumptive 2° cells, and connected by a thin green line to represent the hypothetical switch in signaling activity.

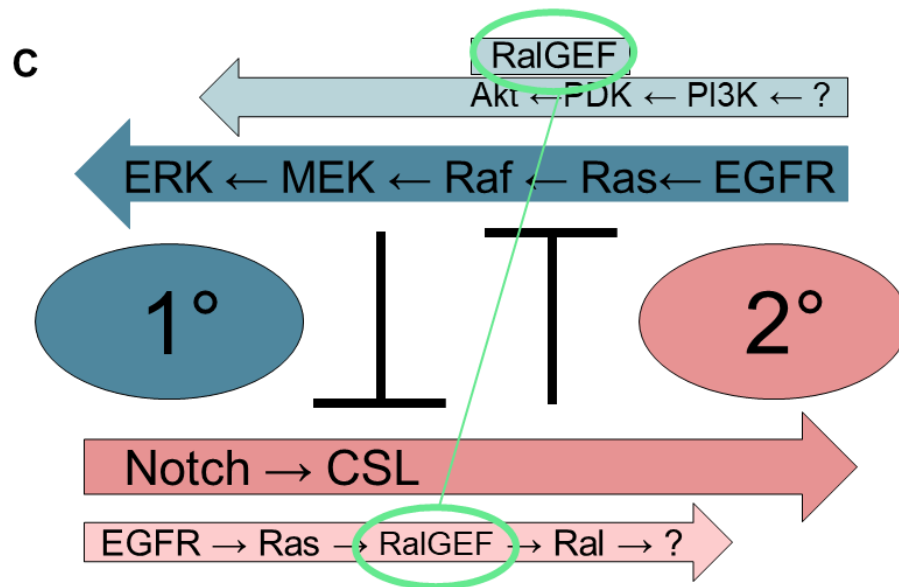


Figure 3. 1 Continued. C. A wiring diagram of the naive 1°/2° VPC patterning signaling network, illustrating parallel and anti-parallel signals, with essential signals in dark blue and rose, and modulatory signals in light blue and rose. Data support RGL-1/RalGEF functioning in antagonistic 1°-promoting (non-canonical) and 2°-promoting (canonical) cascades. Deletion of *rgl-1* would perturb both modulatory cascades but not alter the balance of 1°- and 2°-promoting signals, even in sensitized backgrounds.

Vulval induction is a stepwise progression: VPC fates are initially specified and later become committed (Fig. 3. 1A; Sternberg, 2005). Initial specification is accompanied by alterations of expression of certain signaling genes. Some of these transcriptional changes contribute to Mutual Antagonism, whereby contradictory signals are excluded from cells committing to cell fate. For example, the LIP-1/ERK phosphatase, a LIN-12 transcriptional client gene, is expressed in initially specified 2° cells to restrict inappropriate ERK activation (Berset et al.,

2001; Yoo et al., 2004). Conversely, LIN-12, via mechanisms not entirely understood, is targeted for internalization and degradation in initially specified 1° cells to restrict inappropriate 2°-promoting signal (Deng and Greenwald, 2016b; Shaye and Greenwald, 2002, 2005).

We reconciled these potentially contradictory models by identifying the mechanism by which the 2°-promoting activity of the EGF gradient was transduced. Initial sequential induction establishes the specification of the VPC pattern, and overlaid on this pattern is a spatial EGF gradient that reinforces the initial pattern. To interpret different doses of EGF signal, LET-60/Ras dynamically switches effectors during VPC fate patterning, from LIN-45/Raf signaling through the canonical MEK-2/MEK-MPK-1/ERK MAP kinase cascade to promote 1° fate, to RGL-1/RalGEF-RAL-1/Ral signaling to promote 2° fate (Reiner, 2011; Zand et al., 2011). Additionally, VPCs may undergo Notch autocrine signaling that reinforces graded EGF signaling (Hoyos et al., 2011).

We have further found that RAL-1 promotes 2° fate through EXOC-8/Exo84, a subunit of the heterooctameric exocyst complex, a known downstream oncogenic Ral signaling intermediary in mammalian cells. The GCK-2 MAP4 kinase and a downstream PMK-1/p38 MAP kinase cascade is necessary and sufficient for Ral-dependent induction of 2° cells, in support of the necessary and sufficient LIN-12 (Shin et al., 2018).

More recently, VPC fate patterning has been used to compare mechanisms of induction across nematode species both closely and distantly related to *C.*

C. elegans (Felix and Barkoulas, 2012; Grimbirt and Braendle, 2014; Mahalak et al., 2017; Sommer and Bumbarger, 2012). Additionally, the vulva has been used to assess heterogeneity in polymorphic wild *C. elegans* isolates (Grimbert and Braendle, 2014; Sterken et al., 2017), and also developmental robustness in the face of environmental insult: the VPCs are patterned with 99.8% accuracy (Braendle and Felix, 2008). But this accuracy is modulated by weak mutations or natural genetic variation affecting the delicate balance of 1° and 2° inductive signals (Barkoulas et al., 2013; Braendle et al., 2010; Duvéau and Felix, 2012; Milloz et al., 2008). One conclusion from these studies is that there are heretofore unidentified properties of signaling networks that increase fidelity and/or robustness.

Ras is the most mutated mammalian oncoprotein: more than a quarter of all tumors harbor activating mutations in Ras (Hobbs et al., 2016). Three main oncogenic Ras effector cascades have been identified (Fig. 3. 2). Two of these, the Raf-MEK-ERK MAP kinase and the PI3-Kinase-PDK-Akt cascades, have been extensively studied and pharmacologically targeted (Fruman et al., 2017; Papke and Der, 2017; Wong et al., 2010). The RalGEF-Ral effector signal is poorly characterized, though it may be as important for oncogenesis as the Raf and PI3K cascades (Feig, 2003; Hamad et al., 2002; Lim et al., 2005; Lim et al., 2006; Urano et al., 1996; White et al., 1996). Ras binds and activates RalGEF, an exchange factor that stimulates GTP loading on the Ral small GTPase. Ral is a Ras-like small GTPase subfamily, in the Ras family of the Ras superfamily, and

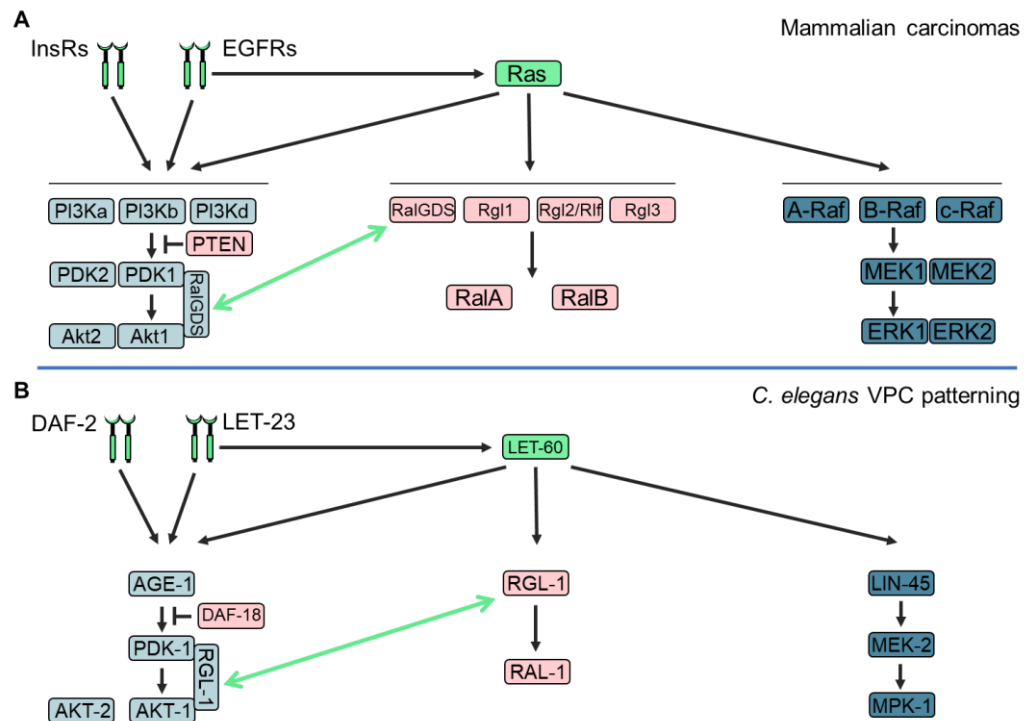


Figure 3. 2 Signaling network comparisons between humans and *C. elegans*.

A-B. Signaling relationships in (A) Mammalian carcinomas and (B) *C. elegans* VPC fate patterning. Historically, mammalian interactions have been shown directly, while *C. elegans* interactions were deduced from a combination of phenotypes, genetic epistasis, and inferences from biochemical relationships among mammalian orthologs. Color coding is the same as in other figures: blue = 1°-promoting, rose = 2°-promoter, dark = necessary and sufficient signal, light = modulatory signal. Green = both 1°- and 2°-promoting (rather than green, RGL-1 is shown in two places, with a green two-headed arrow denoting possible dual function in both non-canonical 1°-promoting and canonical 2°-promoting roles). Activation of *C. elegans* AGE-1/PI3K by a receptor other than DAF-2, or by LET-60/Ras, has not been suggested in the literature. The interactions between RGL-1, PDK-1 and AKT-1 are inferred from genetic relationships in this study, and have not been shown directly. JIP-1, a potential intermediary between Akt and RalGDS/RalGEFs inferred from mammalian biochemical analyses in the Feig lab, is not shown.

is conserved throughout Metazoa (Reiner and Lundquist, 2016). For most Ras family members, including Ral, this GDP/GTP cycle is controlled by activating GEFs and inactivating GAPs. Despite their structural and primary sequence similarities, Ral interacts with a very different set of effectors than does Ras (Gentry et al., 2014).

Mammals encode three Ras proteins (K-, N-, H-Ras), four GEFs with RA domains (RalGDS, RGL, RGL1, RGL2), two Rals (A, B), three Rafs (A-, B-, C-Raf) and three PI3Ks (α , β , δ). *C. elegans* and *Drosophila* each harbor single Ras-encoding genes, as well as single RalGEF-, Ral-, Raf-, and PI3K-encoding genes (Fig. 3. 2B). All three oncogenic Ras effectors are involved as essential or modulatory cascades promoting 1° or 2° VPC fate. The essential LET-60/Ras-LIN-45-MEK-ERK MAP kinase cascade promotes 1° fate with support of the modulatory AGE-1-PDK-1-AKT-1 cascade, while the essential LIN-12/Notch cascade promotes 2° fate with support of the modulatory LET-60/Ras-RGL-1-RAL-1 cascade.

Here we pursue the unexpected findings that RGL-1/RalGEF is functionally non-equivalent to RAL-1 in two distinct ways. First, while RAL-1 is essential for viability and fertility (Armenti et al., 2014; Zand et al., 2011), RGL-1 is inessential. Second, RGL-1 and RAL-1 are non-equivalent in VPC fate patterning. While RAL-1 functions as a simple intermediary to propagate the 2°-promoting LET-60-RGL-1-RAL-1 signal, RGL-1 additionally performs an opposing, putative 1°-promoting function that offsets its canonical 2°-promoting function. As a consequence,

deletion of RGL-1 has no net effect on the delicate balance of 1° - and 2° -promoting signals in sensitized mutant backgrounds. Using GEF-specific mutations and genetic bypass experiments, we show that the opposing functions of RGL-1 in VPC fate patterning are genetically separable, and that both RGL-1 activities function cell autonomously in VPCs. In the context of mammalian studies that argue that RalGEF physically interacts with PDK and Akt as a scaffold (Hao et al., 2008; Tian et al., 2002), our genetic epistasis results are consistent with RGL-1 functioning as a scaffold for PDK-1 and AKT-1 in the modulatory 1°-promoting AGE-1/PI3K cascade. Our analysis raises the question of how activity in two apparently opposing cascades contribute to VPC fate patterning. Comparing VPC fate patterning in different environments, we found that the error rate in patterning was 15-fold higher in the *rgl-1* deletion mutants than in the wild type. We hypothesize that the two opposing activities of RGL-1, which tie together the two opposing 1° and 2°-promoting modulatory cascades, are orchestrated to reduce the level of noise in the signaling network, and hence reduce the rate of ambiguous fates or mis-patterning events. We propose that these properties of RGL-1 identify a novel “balanced switch” to coordinate modulatory signaling activities in the reinforcement stage of VPC fate patterning that leads to fate commitment, and hence increases fidelity of the developmental process.

Results

The C. elegans RalGEF ortholog, RGL-1, is non-essential.

We previously described that *ral-1(tm2760)* mutant animals are sterile but otherwise wild type. Efforts to feed or inject dsRNA in the RNAi hypersensitive *rrf-3* background failed to phenocopy this sterility. Yet consistent with our depletion by bacterially mediated RNAi and injected dsRNA, *tm2760* abrogated the 2°-promoting activity of RAL-1 (Zand et al., 2011).

Subsequent analysis of the *ral-1(tm5205)* deletion allele led to the conclusion that RAL-1 function is maternally rescued and necessary for various facets of embryonic, post-embryonic, and germline development that require function of the PAR complex in cell polarity (Armenti et al., 2014). This function is ascribed to a central role of RAL-1 in the exocyst complex, as described for mammals (Brymora et al., 2001; Chien et al., 2006; Issaq et al., 2010; Jin et al., 2005; Moskalenko et al., 2002; Moskalenko et al., 2003; Sugihara et al., 2002). We observed that *ral-1(tm5205)* mutants become sickly in the fourth larval stage and become sterile adults, but VPCs are patterned normally (N = 52).

Mammalian studies suggest that Ral associates with the exocyst in an activity-dependent manner to promote complex assembly (Brymora et al., 2001; Chien et al., 2006; Issaq et al., 2010; Jin et al., 2005; Moskalenko et al., 2002; Moskalenko et al., 2003; Sugihara et al., 2002). Thus, abrogation of GTP-loading,

either through blockade of total RalGEF activity or Ral GTP-loading activity, should phenocopy loss of Ral and result in defective exocyst function. *C. elegans*, which encodes only a single RalGEF ortholog (Zand et al., 2011), provides a system to test this relationship between RalGEF and Ral *in vivo*.

rgl-1(RNAi) revealed a role in promoting 2° fate (Zand et al., 2011). We reproduced RNAi depletion of *rgl-1* with bacterially mediated and injected dsRNA in wild-type and *rrf-3* mutant backgrounds and observed no overall impact on development or fertility. Strikingly, four different deletion mutants of RGL-1 are superficially wild type, develop normally, are fertile, and can be grown indefinitely in culture (Table 3. 1). One of these mutations, *fax-1(gm27)*, deletes several neighboring genes on the X chromosome, including *rgl-1* (Much et al., 2000). Using robust primer sets (see Materials and Methods), we failed to amplify *rgl-1* sequences from the *gm27* mutant animal. No role for LET-60/Ras has been found in exocyst and PAR complex function (Yochem et al., 1997).

We also previously published that nonsense mutants for the alpha or beta subunits of the heterodimeric RalGAP, HGAP-1 and HGAP-2, respectively, are also viable and fecund (Martin et al., 2014). The G26V putative activating mutation in RAL-1 also fails to confer developmental defects in an otherwise wild-type background (Shin et al., 2018). The observation that deletion of RGL-1/RalGEF or HGAP-1/2/RalGAP does not result in the same phenotype as deletion of RAL-1 raises the interesting possibility that Ral and RalGEF are functionally non-

equivalent, contrary to the model derived from biochemical experiments in mammalian cell culture.

Sensitized genetic backgrounds reveal nuances in signaling.

Four signaling cascades – two central and two modulatory – control 1° and 2° fate induction. We present a schematic of the signaling cascades discussed in this study (Figs. 3. 1B-C; Fig. 3. 2). Core 1°- and 2°-promoting signals are detectable by direct mutation: since they are necessary and sufficient to induce their respective fates, mutational perturbation of them causes loss or gain of vulval cell types. In contrast, the role of the two modulatory cascades is not revealed through single mutant analysis, but rather requires sensitized genetic backgrounds.

To detect such signals, we use *let-60(n1046gf)*, a moderately activating G13E mutation analogous to mutations found in a subset of mammalian cancers (Golden, 2017). In this background, gain and loss of the RAL-1 2°-promoting signal resulted in decrease and increase of ectopic 1° cells, respectively. We have similarly used the *let-23(sa62gf)* activating mutation in the LET-23/EGFR. For an under-induced background, we used *lin-45(n2506)* (Zand et al., 2011). Through combined use of genetic principles of parallelism and epistasis, we are able to dissect the modulatory signals. We present these principles as a network circuitry diagram (Fig. 3. 1C). We have exploited such techniques to delineate a 2°-

promoting signaling cascade downstream of RAL-1 (Shin et al., 2018). Here we use these techniques to similarly dissect the two roles of RGL-1/RalGEF in 2°- and 1°-promoting activities.

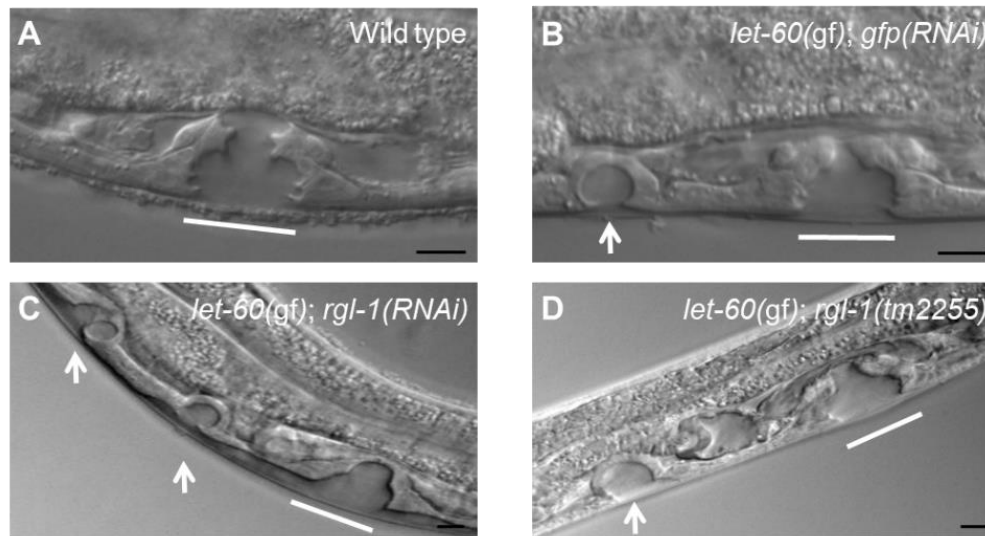


Figure 3. 3 RGL-1 and RAL-1 are functionally non-equivalent in VPC patterning. A-D. 1000x photomicrographs of late L4 (A) wild-type, (B) *let-60(n1046gf); gfp(RNAi)* compared to 600x photomicrographs of (C) *let-60(n1046gf); rgl-1(RNAi)*, and (D) *let-60(n1046gf); rgl-1(tm2255)* animals. White lines = normal 2°-1°-2° L4 vulvae, white arrows = L4 ectopic 1° pseudovulvae. Black scale bars = 5 μ m. Anterior is left and ventral down.

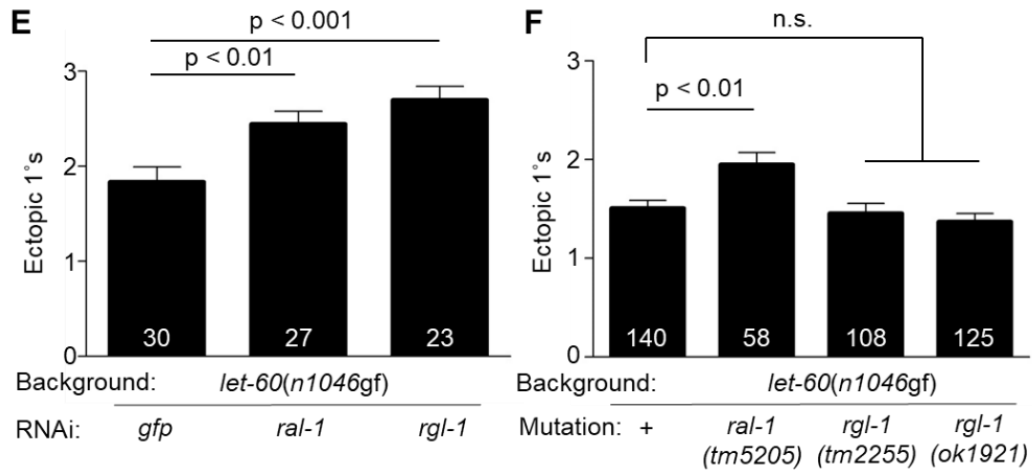


Figure 3.3 Continued. E. RNAi depletion of *rgl-1* and *ral-1* enhance 1° induction relative to *gfp*(RNAi) control. Data are the mean ± standard error of the mean (SEM). For statistical reasons single, non-pooled assays are shown, and white numbers represent animals scored therein. Significance was calculated by Kruskal-Wallis, Dunn test. Data shown were scored concurrently and are representative of 4 independent assays (this study) and 6 prior independent assays (Zand et al., 2011). The *let-60(n1046gf)* 1° induction baseline is consistently higher when grown on HT115 bacterially-mediated RNAi food compared to the standard OP50 (Shin et al., 2018; Zand et al., 2011). **F.** Deletion of *ral-1* but not *rgl-1* enhances ectopic 1° induction by *let-60(n1046gf)*. Data shown are representative of 4 assays, each scored concurrently.

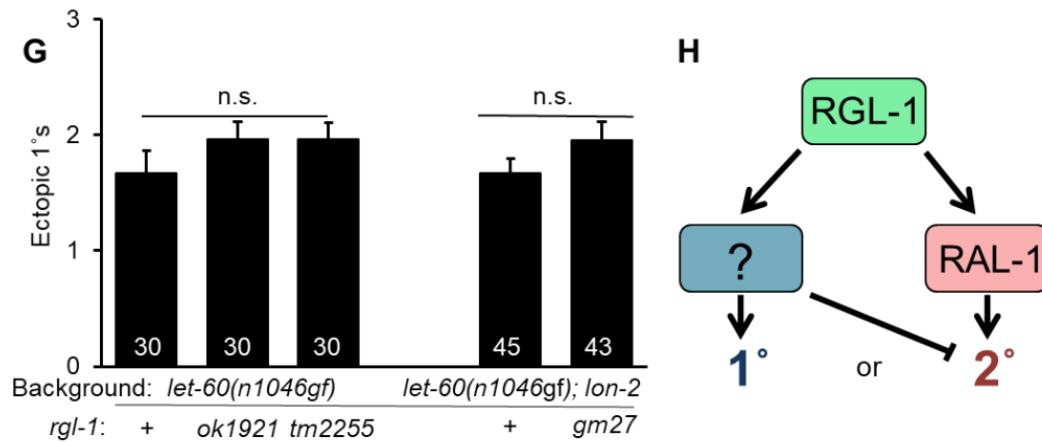


Figure 3.3 Continued. G. Re-constructed strains show the same result: *ok1921*, *tm2255* and *gm27* deletions fail to significantly enhance ectopic 1° induction by *let-60(n1046gf)*. Left: Three *n1046*-containing isolates, with and without *rgl-1* mutations and scored concurrently. The concurrently scored MT2124 1° induction baseline was not significantly different from outcrossed lines DV2214 and DV2215 (see Table 3. 1), N = 30 for each, and from assays that showed the most deviation of double mutants from the single mutant, but are still not significantly different. Right: DV2251 *let-60(n1046gf); lon-2(e678)* vs. DV2252 *let-60(n1046gf); lon-2(e678) gm27* animals scored concurrently but separate from the left group, representative of two assays. **H.** A general model for opposing RGL-1 GEF/RAL-1-dependent and -independent functions (green = bifunctional, blue = 1°-promoting, rose = 2°-promoting; see Fig. 3. 1).

RGL-1 performs a function in VPC cell fate patterning that opposes its canonical 2°-promoting function.

We previously showed that depletion of *rgl-1* by RNAi revealed a role of RGL-1 in promoting 2° fate consistent with the established Ras-RalGEF-Ral signal in

mammals (Zand et al., 2011). We reproduce these RNAi-based experiments here (Figs. 3. 3A-C, 3. 3E). We also found that *ral-1(tm5205)* confers enhancement of 1° induction in the *let-60(n1046gf)* background (Fig. 3. 3F), validating our previous results with RAL-1.

To our surprise, analysis of various strong loss or putative null *rgl-1* mutations in the *let-60(n1046gf)* background caused no net effect compared to the *let-60(n1046gf)* single mutant (Figs. 3. 3D, F, G; see Table 3. 1 and Fig. 3. 7A for *rgl-1* alleles). Using a 1° fate reporter that indicates adjacent 1° cells in the *let-60(gf)*

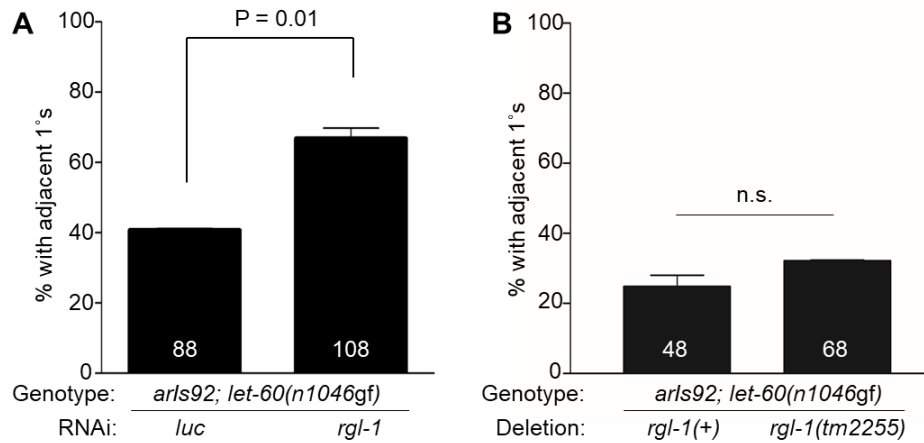


Figure 3. 4 RGL-1 controls cell fate decision. A. Percent Pn.px-staged *let-60(gf)* L3 larvae with CFP-positive lineages neighboring the P6.p lineage (P5.p or P7.p derived) with *luc(RNAi)* vs. *rgl-1(RNAi)*. Shown are average percentages of animals with adjacent 1° cell fate. **B.** Percent Pn.px-staged *let-60(gf)* L3 larvae with CFP-positive lineages neighboring the P6.p lineage (P5.p or P7.p derived) with *rgl-1(+)* or *rgl-1(tm2255Δ)*. Y axis is percent adjacent 1°s, white numbers in bars are number of animals scored per genotype.

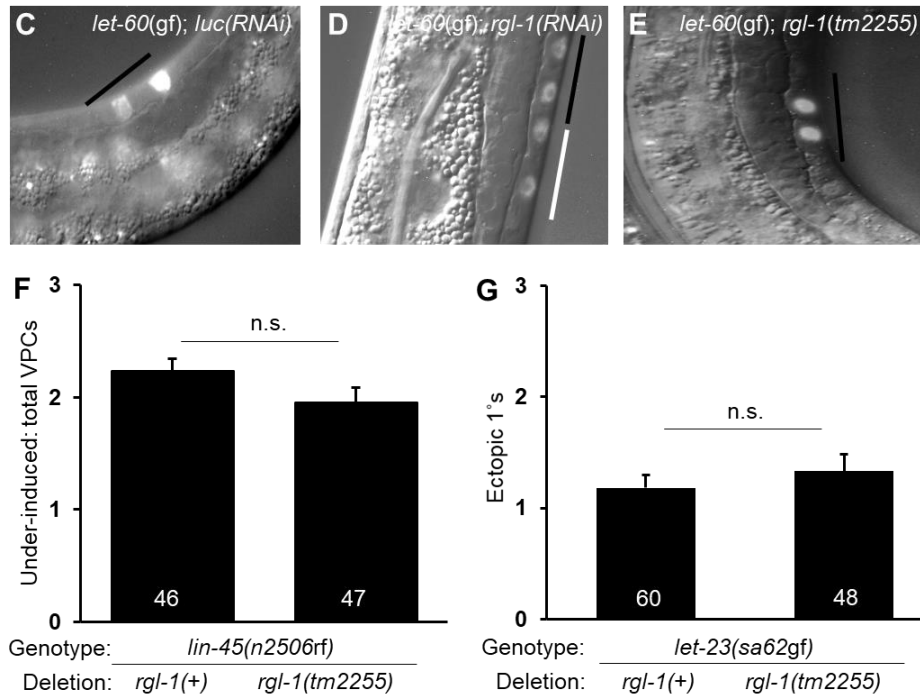


Figure 3.4 Continued. C-E. Expression of the 1° fate reporter *arls92 P_{egl-17::cfp-lacZ}* in VPC daughters. Overlaid DIC and CFP fluorescence images of (C) *let-60(n1046gf); luc(RNAi)*, (D) *let-60(n1046gf); rgl-1(RNAi)* and (E) *let-60(n1046gf); rgl-1(tm2255)* at the Pn.px stage. The black bar indicates P6.px and white bar indicates P7.px cells. **F.** Hypo-induced *lin-45(n2506)* background with and without *tm2255*. Y axis is total induced VPCs (0 = vulvaless, 3 = normal wild-type vulva.) White numbers are number of animals assayed. **G.** *let-23(sa62gf)* with and without *tm2255*. Y axis is mean ectopic 1° induction. Error bars show S.E.M. P value calculated via Mann-Whitney test.

background (Yoo et al., 2004; Zand et al., 2011), we found that *rgl-1(RNAi)* but not *rgl-1(tm2255)* significantly increases the occurrence of adjacent 1°s (Figs. 3.4A-E). To test that these results are not specific to the *let-60(n1046gf)* sensitized

background or a 1° over-inducing background, we also assessed the role of deleted *rgl-1* in under-induced background *lin-45(n2506)* and over- induced background *let-23(sa62gf)* (Katz et al., 1996; Zand et al., 2011), finding no effect of *rgl-1(tm2255)* (Figs. 3. 4F-G).

Our results are consistent with the working model that RGL-1 performs an additional, Ral-independent function that antagonizes its canonical function, perhaps by promoting 1° fate. The discrepancy between RNAi- and mutational-based analyses is consistent with RGL-1 having different functional thresholds in level of gene product for the two opposing activities, which we have been unable to further investigate.

The rgl-1 transcriptional fusion is expressed in both 1° and 2° lineages.

We previously described a transgenic *ral-1* transcriptional fusion that expressed GFP dynamically over the time course of VPC fate induction (Zand et al., 2011). To summarize published results, early in the 3rd larval stage (L3), GFP was expressed consistently in all six VPCs. Later in L3, after induction, GFP expression was excluded from presumptive 1° cells while persisting in presumptive 2° cells. These observations provided a potentially critical mechanistic insight: by reducing inferred RAL-1 expression in presumptive 1° cells while retaining expression in presumptive 2° cells, the signaling network attenuates inappropriate RAL-1 activation in presumptive 1° cells, thereby

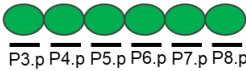
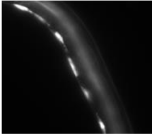
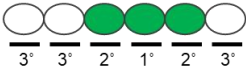
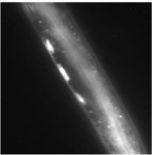
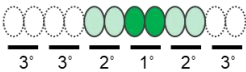
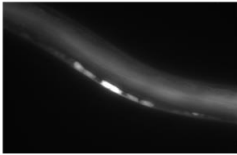
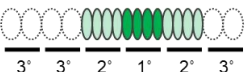
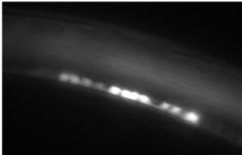
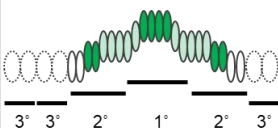
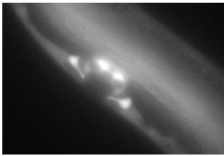
Stage/VPC and gonad status	Schematic	Images	Expression
L3: Pn.p. Before gonad extension. Before VPC induction.			All 6 VPCs
L3: Pn.p. Gonad tips extended halfway to anterior/posterior-most VPCs. VPC induction occurs.			P5.p, P6.p, P7.p
L3: Pn.px. Gonad tips not yet turned dorsally. Fate reinforcement completed, 3° cells fuse with Hyp7.			1° and 2° lineages, brighter in 1°
L3: Pn.pxx. Gonad tips reflexed, migrating. Further VPC Proliferation.			1° and 2° lineages, brighter in 1°
Late L3 through L4: Pn.pxxx. Gonad finishes migration, final vulval division and morphogenesis.			Vulval lineages

Figure 3. 5 VPC expression pattern of the *rgl-1* transcriptional GFP fusion over time. We used a combination of DIC analysis of VPCs and migration of the gonadal distal cells for staging to characterize the dynamic pattern of GFP expression from *sEx14985* (McKay et al., 2003) over time. Initial expression in naïve VPCs is uniform. Around the time of induction, expression is restricted to presumptive vulval lineages. Later expression, after the first cell division, remains higher in 1° than 2° lineages. Later stages show low levels of expression in surrounding non-vulval hypodermal cells.

preventing potentially contradictory LET-60 signaling through RGL-1-RAL-1 in presumptive 1° cells.

We similarly tested the expression pattern of a transgene harboring the *rgl-1* promoter transcriptional fusion to GFP, *sEx14985* (McKay et al., 2003). As with the *ral-1* promoter transcriptional fusion, the transgenic *rgl-1* reporter was expressed in all VPCs early in L3 (Fig. 3. 5). But, unlike the *ral-1* transcriptional fusion, GFP from the *rgl-1* transcriptional fusion persisted in presumptive 1° cells throughout vulval patterning, proliferation and morphogenesis. After the first VPC cell division GFP expression was consistently higher in 1° relative to 2° cells. The significance of this change is unclear, since many transcriptional fusions of vulval signaling genes change expression patterns around this time (Berset et al., 2001; Berset et al., 2005; Yoo et al., 2004; Yoo and Greenwald, 2005; Zand et al., 2011; Rasmussen *et al.*, re-submitted). Yet one interpretation is that increased expression of RGL-1 in presumptive 1° cells accounts for resistance to *rgl-1(RNAi)* of this putative 1°-promoting activity of RGL-1.

Tagged endogenous RGL-1 is expressed uniformly throughout VPC development.

To validate the RGL-1 transcriptional fusion, we used the self-excising cassette (SEC) approach (Dickinson et al., 2015) to tag the endogenous 5' end of the endogenous *rgl-1* locus with sequences encoding mNeonGreen fluorescent protein (mNG, FP) and a 3xFlag epitope tag (Fig. 3. 6). We observed mNG

throughout vulval lineages, consistent with that observed with the *rgl-1* promoter::gfp transcriptional fusion transgene.

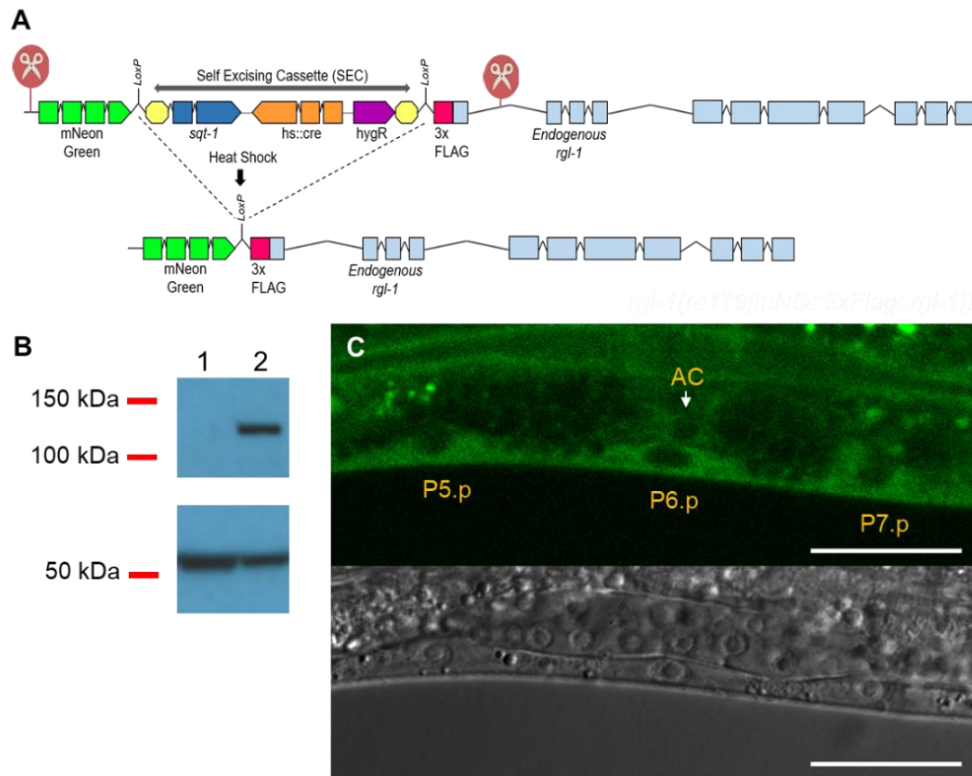


Figure 3. 6 N-terminal CRISPR tagging of endogenously expressed RGL-1 protein. **A.** Strategy for N-terminal tagging of the endogenous RGL-1 protein, using the SEC approach (Dickinson et al., 2015). See Methods. **B.** Western blot validation of RGL-1 N-terminal tag prior to (lane 1) and after SEC excision (lane 2). Below: alpha-tubulin loading control. **C.** Tagged endogenous mNG::RGL-1 is expressed in all VPCs. Scale bar = 20 μ m.

RGL-1 performs opposing GEF-dependent and GEF-independent functions in VPC fate patterning.

A list of *rgl-1* mutations and other genetic tools is shown (Figs. 3. 7A-B; Table 3. 1). The Million Mutation Project (MMP) described random sequence identification of a large collection of mutagenized *C. elegans* lines, demanding only that mutant animals be viable and fertile over many generations (Thompson et al., 2013). We analyzed the sole non-synonymous mutation in *ral-1*, *gk628801*, which caused an R139H mutation. Arg-139 is conserved in all Ras family members in metazoans. Outcrossed *ral-1(gk628801)* single mutant vulvae were superficially wild type (N = 83). In the *let-60(n1046gf)* background, *ral-1(gk628801)* increased 1° induction (Fig. 3. 7C), consistent with our previously published analysis using *ral-1(RNAi)* and deletion mutations (Fig. 3. 3; Zand et al., 2011). Thus, *ral-1(gk628801)* perturbs RAL-1 2°-promoting signaling but does not disrupt RAL-1 sufficiently to confer PAR- and exocyst-associated phenotypes.

Of 30 total non-synonymous mutations in *rgl-1*, two are likely to perturb function. *rgl-1(gk275304)* causes an R361Q change. Arg-361 is conserved in all CDC25/RasGEF domains. *rgl-1(gk275304)* conferred significant increase in ectopic 1° induction in the *n1046gf* background (Fig. 3. 7D), consistent with disrupting GEF domain function and hence abrogating activation of RAL-1. *rgl-1(gk275305)* causes a W163* change, which did not alter ectopic 1° induction in the *let-60(n1046gf)* background. Both outcrossed single mutant strains were

superficially wild type (N = 48 and 61, respectively). We therefore hypothesized that *rgl-1* encodes GEF-dependent and GEF-independent activities.

Using the VPC-specific *lin-31* promoter (Tan et al., 1998) in the *let-60(n1046gf); rgl-1(tm2255)* double mutant background we generated transgenic extrachromosomal arrays expressing VPC-specific RGL-1(+) or RGL-1(R324E), a mutation deficient in GEF catalytic activity in mammalian RalGDS (RalGEF; Wolthuis et al., 1997). Animals bearing the R324E transgenes showed significant increase in ectopic 1° induction compared to non-array-bearing siblings. Animals

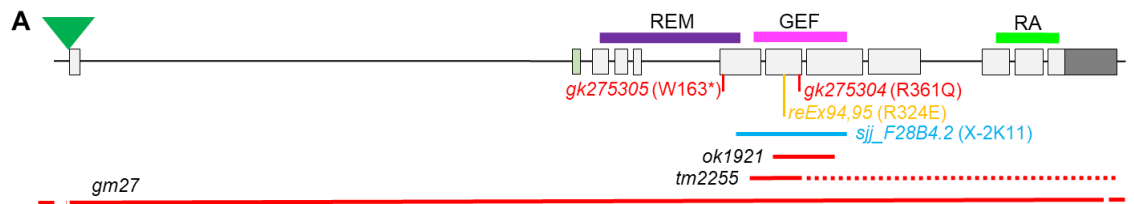


Figure 3. 7 RGL-1 encodes genetically separable functions. A. A schematic of the *rgl-1* gene and genetic reagents for this analysis. Green triangle = mNeonGreen::3xFlag tag by CRISPR (Fig. 3. 6). Light green exon 2: by RNAseq this is a rare mRNA species, and the 20 residues coded for by Exon 2 are not conserved among *Drosophila* and mammalian RalGEFs. Purple, pink and bright green lines: REM, GEF and RA (Ras Association) domains (The REM domain is a structural component of some but not all Ras family GEFs). Red *gk* alleles: W163* and R361Q mutations from the million mutation project. Orange: canonical R324E GEF-deficient mutation in transgenes *reEx94* and *reEx95*. Light blue: coverage of bacterially mediated RNAi clone (library location; Kamath et al., 2001). Red lines: sequences deleted by *ok921*, *tm2255* and *gm27* deletions (dotted line indicates that deletion ends out of frame).

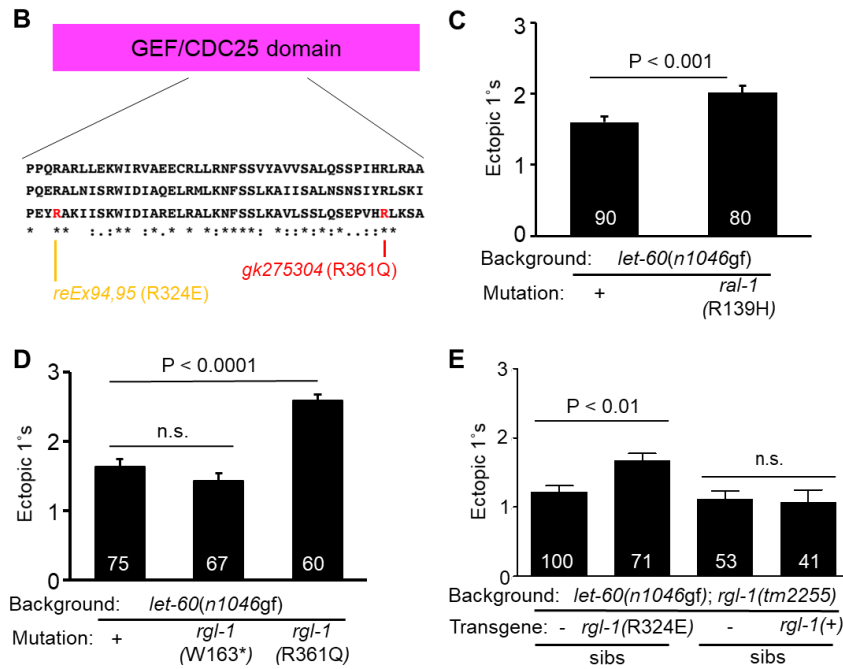


Figure 3. 7 Continued. B. An alignment of a portion of the RalGEF domain containing the canonical GEF-deficient R324E and *gk275304* R361Q mutations (top to bottom: Human RGL2, in which the GEF-deficient mutation was validated, fly RalGEF, *C. elegans* RGL-1). **C.** The *ral-1(gk628801)* R139H missense mutation enhances 1° induction in the *let-60(n1046gf)* background. **D.** *rgl-1* mutation *gk275304* (R361Q) but not *gk275305* (W163*) enhances 1° induction in the *let-60(n1046gf)* background. **E.** Transgenic rescue of *rgl-1(tm2255)* in the *let-60(n1046gf)* background. Transgenic array-bearing animals harboring *P_{lin-31}::rgl-1* cDNA with *P_{myo-2}::gfp* co-injection marker and their non-array-bearing siblings were scored. The *reEx94* (shown) and *reEx95* (not shown) R324E mutant transgenes enhanced 1° induction relative to their non-transgenic siblings, as scored in separate concurrent assays for each array, suggesting that a GEF-independent 1°-promoting activity of RGL-1 functions cell autonomously in the VPCs. The *reEx109* (shown) and *reEx110* (not shown) wild-type transgenes failed to alter 1° induction relative to their non-array-bearing siblings, as scored in separate concurrent assays for each array, suggesting that the GEF-dependent 2°-promoting activity of RGL-1 also functions cell autonomously in the VPCs.

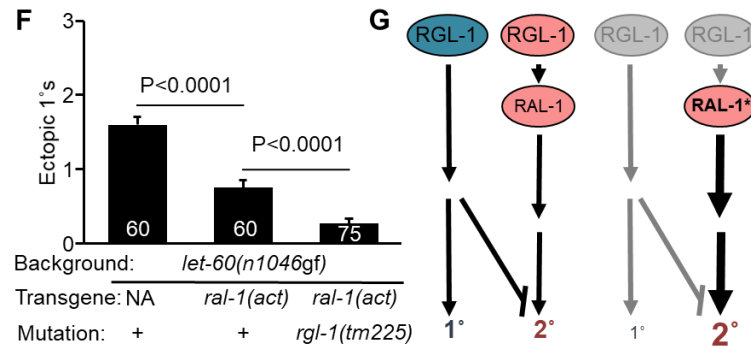


Figure 3. 7 Continued. F. *rels10*[*P_{lin-31}::ral-1A(Q75L)*, *P_{myo-2}::gfp*] (“*ral-1(act)*”) suppressed ectopic 1° induction in the *let-60(n1046gf)* background; in a single concurrent assay, 1° induction was further suppressed by *rgl-1(tm225)*, revealing an opposing RGL-1 signal that may be 1°-promoting. Data are the mean ± standard error of the mean (SEM). For statistical reasons single, non-pooled assays are shown, and white numbers represent animals scored therein. Significance was calculated by Kruskal-Wallis, Dunn test. **G.** A schematic of the bypass experiment in (F). Left: canonical and non-canonical RGL-1 activities are opposed and roughly equivalent (in the backgrounds assayed). Right: constitutive, VPC-specific activation of RAL-1 bypasses the GEF activity while also revealing a GEF-independent function of RGL-1, resulting in increased 2°-promoting signal and concomitant loss of 1°-promoting signal, with a net decrease of ectopic 1° cells.

bearing the wild-type transgenes were not different than their non-array-bearing siblings (Fig. 3. 7E). Consequently, we propose that RGL-1 performs GEF-dependent and GEF-independent functions that are genetically separable by mutating the GEF domain. We also conclude that the GEF-independent RGL-1 activity functions cell autonomously in the VPCs.

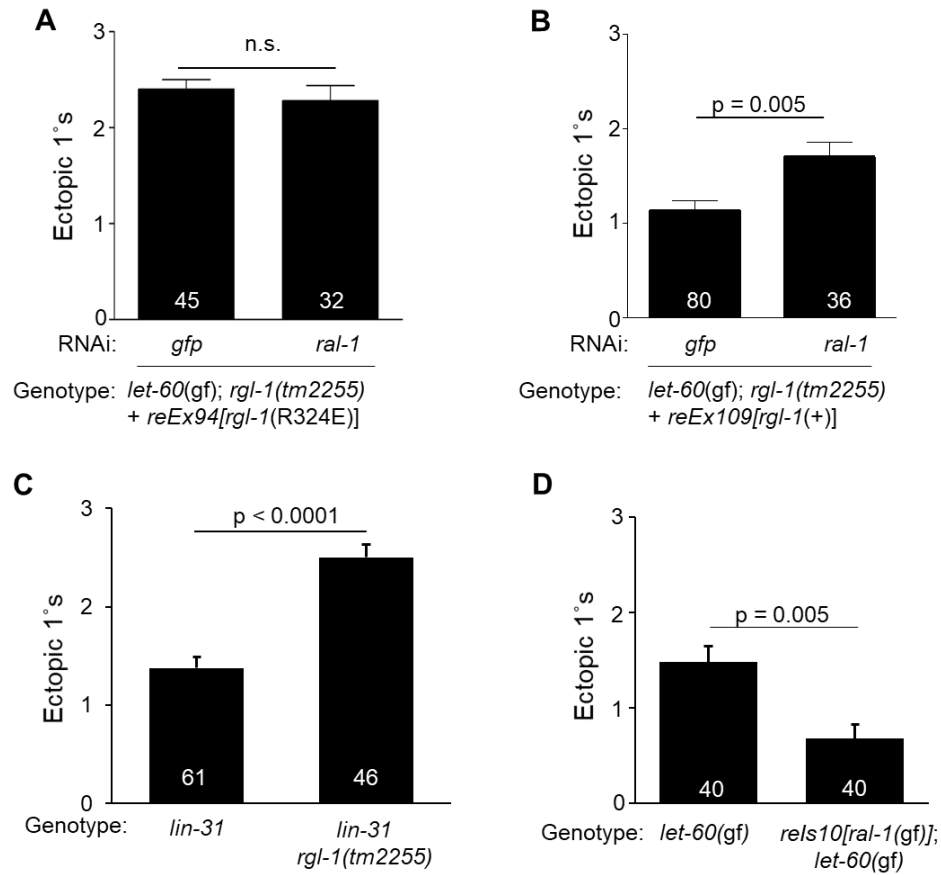


Figure 3.8 Genetically separable functions of RGL-1. **A.** *let-60(n1046gf); rgl-1(tm2255)* animals rescued by VPC-specific expression of GEF dead (R326E) RGL-1 fail to respond to *ral-1*-directed vs. control GFP RNAi. **B.** *let-60(n1046gf); rgl-1(tm2255)* animals rescued by VPC-specific expression of wild-type RGL-1 rescue responsiveness to *ral-1*-directed but not control GFP RNAi. **C.** *lin-31(n301)* bypassed the putative 1°-promoting but not the putative 2°-promoting activity of *rgl-1*, revealed by the *tm2255* mutation enhancing ectopic 1° induction. **D.** *rels10[P_{lin-31}::ral-1(Q75L) + P_{myo-2}::gfp]* suppressed the level of ectopic 1° induction in *let-60(n1046gf)*, as previously described for *reEx24* (Zand et al., 2011). Y axis represents mean ectopic 1° cells, white labels number of animals counted, error bars show S.E.M. P value calculated via Mann-Whitney test.

Transgenic animals expressing VPC-specific RGL-1(+) but not RGL-1(R324E) should restore responsiveness to *ral-1(RNAi)*. We evaluated responsiveness of the *let-60(n1046gf); rgl-1(tm2255)* background harboring each transgene. *reEx94/95* transgenic RGL-1(R324E) animals failed to respond to *ral-1(RNAi)* compared to control *gfp(RNAi)* (Fig. 3. 8A; the 1° induction baseline is elevated due to rescue of the putative GEF- independent function shown in Fig. 3. 7E). In contrast, *reEx109/110* transgenic RGL-1(+) animals restored responsiveness to *ral-1(RNAi)*, resulting in increased 1° induction, consistent with VPC-specific rescue of GEF activity and thus cell autonomy of the GEF-dependent function of RGL-1 (Fig. 3. 8B).

Genetic bypass further reveals a GEF-independent activity of RGL-1.

We previously showed that the ectopic vulva induction caused by mutation of *lin-31*, which confers ectopic 1° induction, was insensitive to perturbation of LET-60-LIN-45-MEK-2-MPK-1 1°-promoting signaling but sensitive to perturbation of LET-60-RGL-1- RAL-1 2°-promoting signaling. These results were consistent with the model of LIN-31 functioning downstream of ERK/MAPK-1 but in parallel to LET-60-RGL-1-RAL-1. In that assay, *rgl-1* function was assessed by RNAi, which resulted in increased 1° induction, as did depletion of *let-60* and *ral-1* (and *lin-12* positive control; Zand et al., 2011). Here, *rgl-1(tm2255)* similarly increased ectopic 1° induction of *lin-31(n301)* animals (Fig. 3. 8C). This result is consistent with

genetically separable functions of RGL-1, with the LIN-31/FoxB transcription factor functioning downstream of the putative non-canonical, GEF-independent signal, but in parallel to the canonical LET-60-RGL-1-RAL-1 signal (Zand et al., 2011).

We bypassed the requirement for RGL-1 GEF activity by generating the *rels10*[*P_{lin-31}::ral-1A(Q75L)*, *P_{myo-2}::gfp*] integrated transgene expressing mutationally activated RAL-1 specifically in the VPCs (Zand et al., 2011). *rels10* decreased ectopic 1° induction in the *let-60(n1046gf)* background (Fig. 3. 8D). Into this background we crossed the *rgl-1(tm2255)* out-of-frame deletion mutation and scored the three strains concurrently. *rgl-1(tm2255)* mutation significantly decreased ectopic 1° induction below the level observed with *rels10* alone, nearly to wild-type levels (Fig. 3. 7F). This result is consistent with further deletion of a 1°-promoting activity when RGL-1 GEF activity is bypassed by activated RAL-1. Taken together, these experiments suggest that *rgl-1* encodes two antagonistic signals, the GEF- and Ral-dependent 2°-promoting signal, and an unknown antagonistic signal, schematized in Fig. 3. 7G.

RGL-1 may function in the 1°-promoting PI3K-PDK-Akt cascade.

Mammalian RalGDS binds to PDK and Akt1 in cultured cells, possibly functioning as a scaffold for PDK and Akt (Hao et al., 2008; Tian et al., 2002). The AGE-1/PI3K-PDK-1 signal has been described as promoting 1° fate in VPC fate

patterning (Nakdimon et al., 2012), but AKT-1 was not implicated downstream of this process, potentially because of redundancy of AKT-1 and AKT-2 in *C. elegans* (Paradis et al., 1999; Paradis and Ruvkun, 1998). Previously, a gain-of-function mutation in AKT-1 was tested in a genetic background with reduced 1° induction:

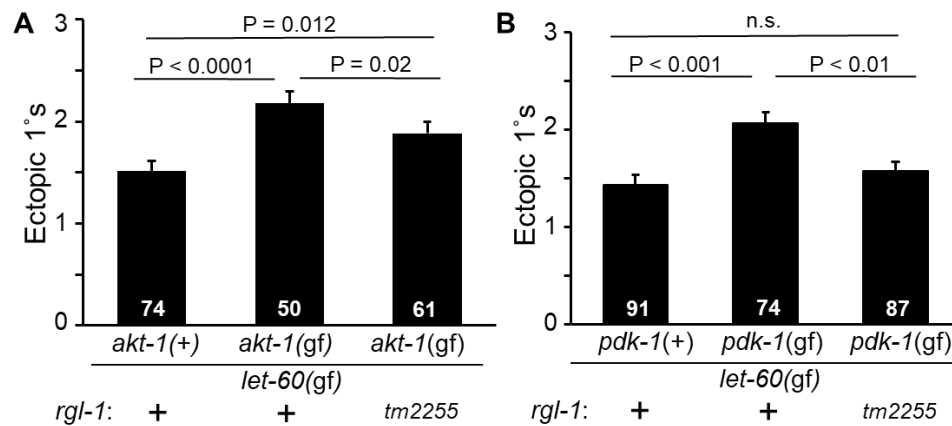


Figure 3. 9 RGL-1 may function in the 1°-promoting PI3K-PDK-Akt cascade.

A. The constitutively activating *akt-1(mg144gf)* mutation increased promotion of 1° fate in the *let-60(n1046gf)* background, and this effect was partially blocked by *rgl-1(tm2255)*, though the triple mutant was not suppressed to the double mutant baseline level. Animals were scored concurrently. These results were replicated with a re-built strain (Fig. 3. 10A) and the strain with *rgl-1(ok1921)* (Fig. 3. 10B). Data are the mean \pm standard error of the mean (SEM). For statistical reasons single, non-pooled assays are shown, and white numbers represent animals scored therein. Significance was calculated by Kruskal-Wallis, Dunn test. **B.** The constitutively activating *pdk-1(mg142gf)* mutation increased promotion of 1° fate in the *let-60(n1046gf)* background, and was completely suppressed to baseline level by *rgl-1(tm2255)*. Animals were scored concurrently and are representative of two assays.

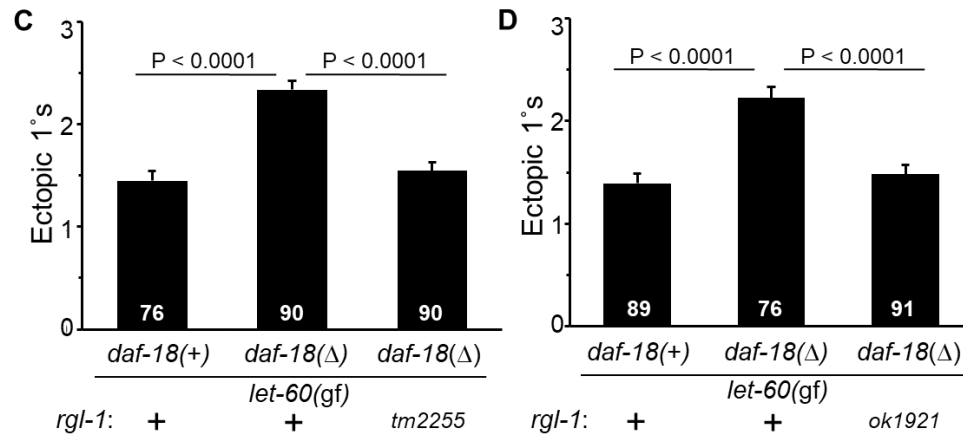


Figure 3. 9 Continued. C-D. Mutation of the negative regulatory PTEN ortholog by *daf-18(ok480)* similarly increased 1° induction, and was completely suppressed to baseline level by *rgl-1(tm2255)* (C) and *rgl-1(ok1921)* (D). Animals for each were scored concurrently and scoring was repeated once, with the same general results. *rgl-1(gk275305)* (nonsense; Fig. 3. 10C) but not *rgl-1(gk265304)* (GEF; Fig. 3. 10D) suppressed this *ok480* enhancement, suggesting that the pertinent RGL-1 activity is GEF-independent/non-canonical.

no effect was found, leading to the model that AKT-1 did not contribute to vulval induction (Nakdimon et al., 2012). We re-evaluated the *akt-1(mg144gf)* mutation in the *let-60(n1046gf)* background and observed significant increase in ectopic 1° induction (Fig. 3. 9A). To corroborate previously published results, we assessed the impact of both activated AKT-1 and PDK-1 in the hypo-induced *lin-45(n2506rf)* background: *akt-1(mg144gf)* did not alter the hypo-induced *lin-45(n2506rf)* phenotype, but *pdk-1(mg142gf)* did suppress the 1°-induction defect (Figs. 3. 10C-D). This result, coupled with earlier analysis (Nakdimon et al., 2012),

suggests that the canonical AGE-1/PI3K-PDK-1/PDK-AKT-1/Akt cascade functions to promote 1° vulval fate.

Including the *rgl-1(tm2255)* mutation in the *let-60(n1046gf); akt-1(mg144gf)* background significantly suppressed ectopic 1° induction, but not to the baseline of the *n1046gf* single mutant (Fig. 3. 9A). Since we observed intermediate suppression, we constructed this strain twice and observed a similar result (Fig. 3. 10A). We also reproduced this result with *rgl-1(ok1921)* and observed similar intermediate strength suppression that remained significantly above the baseline of the *let-60(n1046gf)* single mutant (Fig. 3. 10B).

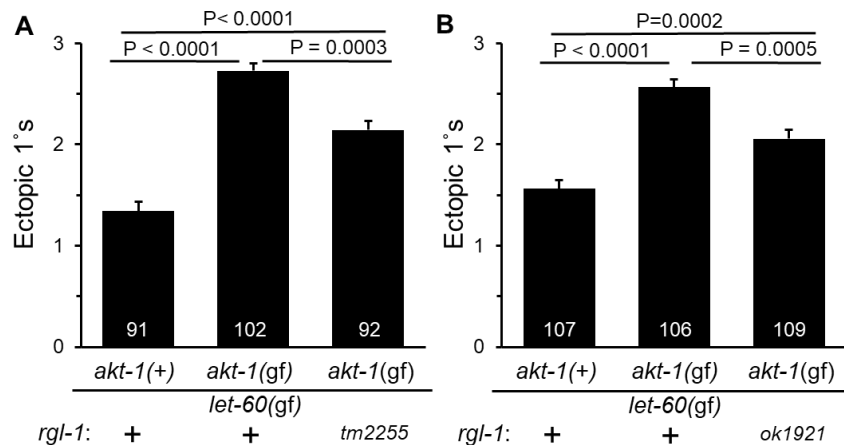


Figure 3. 10 RGL-1 interacts genetically with the 1°-promoting AGE-1/PI3K-PDK-1-AKT-1 cascade. A-B. *akt-1(mg144gf)* enhances 1° induction in *let-60(n1046gf)* animals, and this enhancement is blocked by (A) *rgl-1(tm2255)* and (B) *rgl-1(ok1921)*, though not to the original baseline.

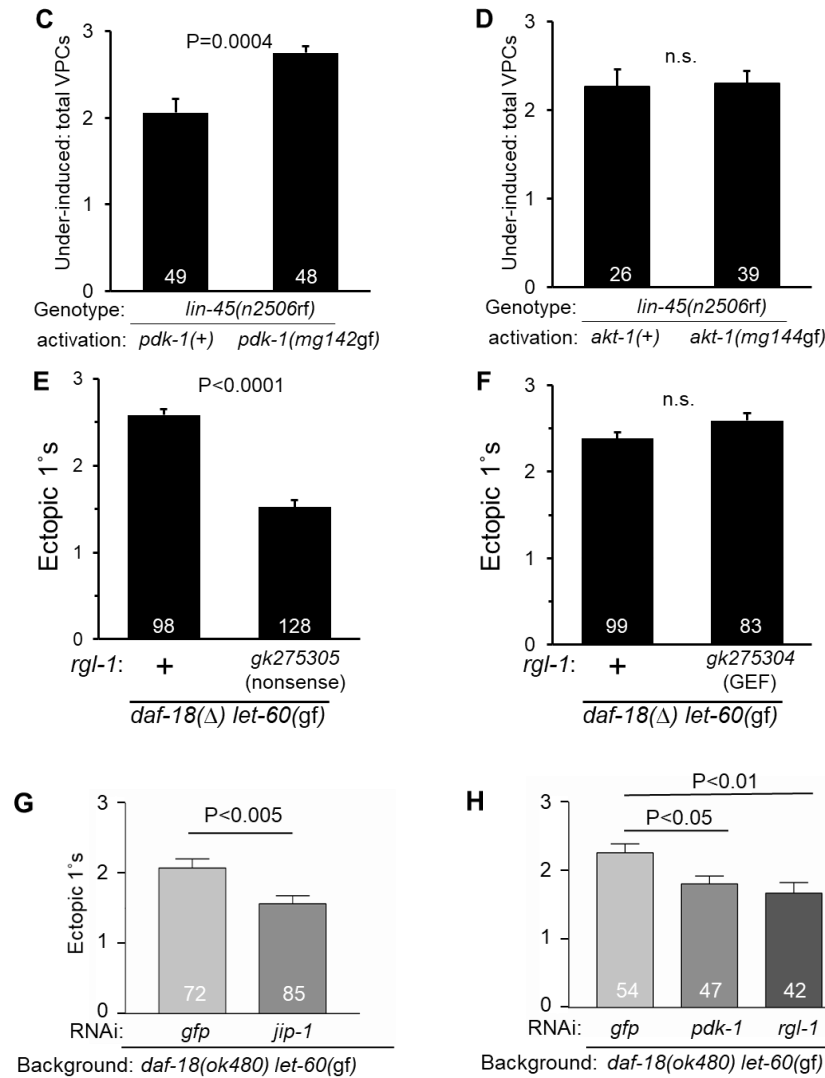


Figure 3.10 Continued. C-D. The *lin-45(n2506)* under-induced mutant is partially suppressed by (C) *pdk-1(mg142gf)* not (D) *akt-1(mg144gf)*. **E-F.** Unlike other assays, data shown are total induced VPCs, not ectopic 1°s. *daf-18(ok480)* enhances 1° induction in *let-60(n1046gf)* animals, and this enhancement is blocked by the (E) *rgl-1(gk275305)* nonsense mutation but not the (F) *rgl-1(gk275304)* R361Q putative GEF dead mutation. **G.** *jip-1*-directed RNAi suppressed the increase in ectopic 1° induction in the *let-60(n1046gf)* background conferred by *daf-18(ok480)*, compared to *gfp(RNAi)*. **H.** *pdk-1*- and *rgl-1*-directed RNAi similarly suppress *daf-18(ok480) let-60(n1046gf)* ectopic 1° induction.

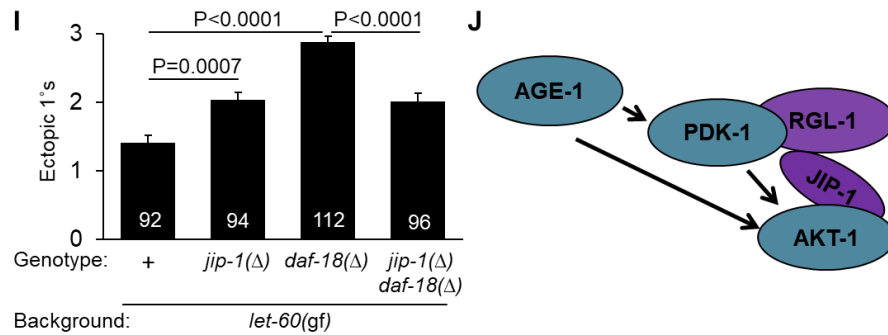


Figure 3. 10 Continued. I. The *jip-1* deletion mutation, *jip-1(tm6137)*, enhances *let-60(n1046gf)* alone but suppresses *daf-18(ok480) let-60(n1046gf)*, consistent with JIP-1 performing two functions. **J.** The observed genetic interactions are consistent with RGL-1 and JIP-1 functioning in the AGE-1-PDK-1-AKT-1 1° promoting cascade, as described for mammalian orthologs (Hao et al., 2008; Tian et al., 2002). Except for *lin-45(rf)*, Y axis represents mean ectopic 1° cells, white labels number of animals counted, error bars show S.E.M. P value calculated via Mann-Whitney test or ANOVA.

We further tested the relationship of RGL-1 with the rest of the PI3K cascade. Mutational activation of PDK-1 via the *pdk-1(mg142gf)* mutation also increased ectopic 1° induction in the *let-60(n1046gf)* background. This effect was completely suppressed by *rgl-1(tm2255)* (Fig. 3. 9B), suggesting a quantitatively detectable difference between the epistatic relationships of PDK-1 and AKT-1 with RGL-1. Genetic disruption of DAF-18/PTEN, a negative regulator of this cascade in *C. elegans* in general (Gil et al., 1999; Ogg and Ruvkun, 1998) and VPC fate patterning in particular (Nakdimon et al., 2012), increases ectopic 1° induction in the *n1046gf* background. We found that *rgl-1(tm2255)* completely blocked this

effect (Fig. 3. 9B). The nonsense *rgl-1(gk275305)* but not the putative GEF-deficient *rgl-1(gk275305)* mutation similarly suppressed (Figs. 3. 10E-F), suggesting that the putative RGL-1 1°-promoting is GEF-independent.

While mammalian RalGDS bound directly to PDK, RalGDS bound indirectly to Akt through the intermediary scaffold, JIP (JNK Interacting Protein; Hao et al., 2008; Tian et al., 2002). Deletion the sole *C. elegans* JIP ortholog, JIP-1 (Fig. 3. 10I) or RNAi depletion of JIP-1 (Fig. 3. 10G) suppressed the ectopic 1° phenotype of the *daf-18(ok480) let-60(n1046gf)* double mutant, consistent with JIP-1 collaborating with RGL-1 to scaffold PDK-1 and AKT-1 1°-promoting signaling. RNAi depletion of both *pdk-1* and *rgl-1* similarly suppressed the enhanced 1° induction of *daf-18(ok480) let-60(n1046gf)* (Fig. 3. 10H). However, the *jip-1* deletion allele enhanced *n1046gf* alone while suppressing *daf-18(ok480) let-60(n1046gf)* (Fig. 3. 10I). We speculate that JIP-1 functions in the PI3K cascade, but may also function elsewhere in VPC fate patterning, perhaps in its canonical role as a scaffold for JKK and JNK MAP kinases. Further investigation of the role of JIP-1 is beyond the scope of this study.

A common target of the *C. elegans* PI3K-Akt cascade is inhibition of the DAF-16/FoxO transcription factor (Lin et al., 1997; Ogg et al., 1997). We tested the role of *daf-16* alleles *mu26*, *mu86* and *mgDf47* in different backgrounds, with inconclusive results. Consequently, we were unable to determine the role, if any, of DAF-16/FoxO in VPC fate patterning.

Taken together, these genetic epistasis experiments, using an assay of parallelism with *let-60(n1046gf)*, suggest that RGL-1 contributes to the AGE-1/PI3K-PDK-1/PDK-AKT-1/Akt cascade, including the negative regulator lipid phosphatase, DAF-18/PTEN, in VPC fate patterning. Alone among the genetic tools used, the gain-of-function mutation in the downstream AKT-1 was only partially suppressed by *rgl-1(tm2255)*, while the effect of other Akt cascade activators was completely suppressed by *rgl-1(tm2255)*. We propose that RGL-1 is essential for the PDK-1 1°-promoting signal (and AGE-/PI3K, through inference from our DAF-18/PTEN deletion experiments), but only partially required for the AKT-1 1° promoting signal. We note that mammalian Akt is activated via parallel mechanisms: phosphorylation by upstream PDK and binding of PIP₃, resulting in recruitment to the plasma membrane and activation (Vanhaesebroeck and Alessi, 2000). If RGL-1 functions as a scaffold for PDK-1 and AKT-1, its deletion would be expected to result in reduction of the PDK-1 phosphorylation of AKT-1 but not PIP₃-dependent recruitment of AKT-1 to the plasma membrane. Thus, a parsimonious interpretation of our data is that RGL-1 functions as a scaffold for PDK-1-AKT-1 signaling in 1° fate induction, and that this activity is independent of the GEF-dependent role of RGL-1 in promoting 2° fate through RAL-1 activation. However, we cannot rule out the possibility of parallelism between a GEF-independent RGL-1 activity and the AKT-1 cascade, or RGL-1 functioning in a bifurcated cascade downstream of AKT-1 that is not revealed by the mechanism of constitutively activated PDK-1 or DAF-18/PTEN upstream.

Deletion of RGL-1 decreases fidelity of VPC patterning.

Based on a relatively small sample size, RGL-1 deletions cause no gross VPC patterning defects, consistent with both cascades being modulatory, not central. We hypothesized that RGL-1 orchestrates activation of these two potentially opposing cascades – Akt output to presumptive 1° cells and Ral output to presumptive 2° cells – to improve robustness of the VPC developmental system in response to environmental stressors. A previous study investigated the impact on VPC fate patterning of environmental stressors: the N2 baseline error rate under laboratory conditions was 0.2% (Braendle and Felix, 2008). We similarly investigated the impact of environmental stressors of starvation, heat, and osmotic stress, compared to non-stressful conditions, on wild-type, *rgl-1(ok1921)*, and *rgl-1(tm2255)* animals.

We evaluated 300 animals per genotype under each condition, totaling 1,200 animals per genotype and 3,600 animals overall (Fig. 3. 11A). Similar to previous results (Braendle and Felix, 2008), wild type animals exhibited very low error rates (0.0 – 0.3%), not only in control but also in stressful conditions. In contrast, the error rate in VPC patterning of both *rgl-1* mutants was substantially increased across all experimental environments (1.0 – 3.7%), including control environments, in which patterning error rates were increased more than 15-fold relative to the wild type. These results suggest an environmentally-insensitive increase in error rate in the absence of functional RGL-1. Consequently, we propose that RGL-1

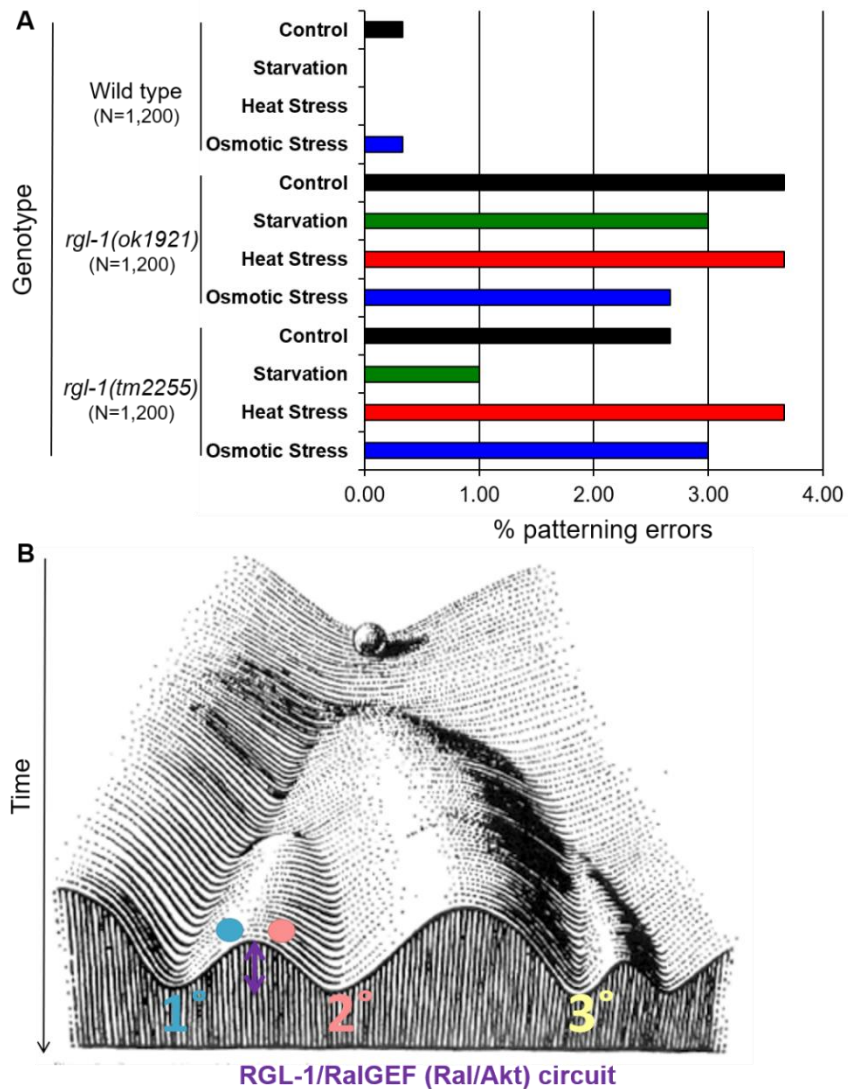


Figure 3. 11 Deletion of RGL-1 increases patterning errors but not susceptibility to environmental stress. **A.** *rgl-1* deletions *ok1921* and *tm2255*, introgressed to the wild type for eight generations (DV2696, DV2697), caused 15-fold increased patterning defects compared to the wild type. (N = 1,200 per genotype, pooled from 300 for each condition.) **B.** A model for the role of Balanced Switches in VPC fate patterning, in the context of “developmental topology” (e.g. “canalization”; Waddington, 1957). We hypothesize that through decreasing error rate, the RGL-1 signaling circuit effectively increases the “barrier” between 1° and 2° fates, thus decreasing error rate.

impacts robustness selectively, and not in response to environmental stressors. Rather, we hypothesize that RGL-1 mitigates stochasticity within the complex signaling network that regulates VPC fate patterning. This observation represents intriguing and unprecedented insight into the role of signaling networks in developmental fidelity.

Discussion

The impetus for this analysis was two enigmatic genetic observations. First, deletion of RAL-1 but not RGL-1 confers developmental defects. Second, deletion of RAL-1 but not RGL-1 confers a net effect on 1° vs. 2° induction. Thus, despite the linear Ras-RalGEF-Ral signaling module defined in mammals and validated in *C. elegans* VPC fate patterning, in two different ways RGL-1 is non-equivalent to RAL-1. By pursuing these two genetic observations, we arrived at important models regarding the multiple roles of RalGEF and Ral in signal transduction and development.

RAL-1 but not RGL-1 is essential for development.

RAL-1 was previously implicated in essential developmental events. Yet despite the ostensible linearity of Ras-RalGEF-Ral signaling, we unexpectedly found that RGL-1 is not essential. Given that deletion of neither the GEF nor the

GAP disrupts exocyst-dependent developmental events but deletion of RAL-1 does so, we hypothesize that the RAL-1 role as a membrane tether for the exocyst is independent of nucleotide-bound state. This hypothesis does not imply that there is no activation-dependent alteration of exocyst function by RAL-1, merely that such is not essential for the described developmental events.

An alternative hypothesis is that other GEFs or GAPs function redundantly with RGL-1 and HGAP-1/2 to regulate the GDP/GTP cycle of RAL-1 (and by extension, with LET-60/Ras). We find that RGL-1 and RAL-1 are required for the 2°-promoting signal. But this other GEF would need to be specific for RAL-1 association with the exocyst and their functions in development, but not signaling to promote 2° fate. While we cannot exclude this possibility, no GEFs fitting that role have been described in any system: RalGPS, a mammalian Ral-selective GEF that contains SH3 and PH domains, is not encoded in the *C. elegans* genome; (Zand et al., 2011), nor is TD-60/RCC2, similar to the Ran GEF RCC1 that controls nuclear import/export, which has been proposed to be an atypical GEF for RalA (Papini et al., 2015).

RGL-1 performs genetically separable and opposing functions in VPC fate patterning.

To our surprise, we found that deletion alleles of *rgl-1* caused no net alteration of the balance of 1° and 2° VPCs in the *let-60(gf)* background. By genetic analysis,

RGL-1 performs its canonical role in promoting 2° fate as a signaling intermediary between LET-60/Ras and RAL-1 (Zand et al., 2011; this study), a role that mirrors extensive biochemical and cell biological evidence from mammalian cell culture (reviewed in Feig, 2003; Gentry et al., 2014; Kashatus, 2013). Here, further genetic analysis reveals an additional, unexpected role for RGL-1, that of a non-canonical signaling participant opposing the canonical role as an activator of RAL-1. This non-canonical role apparently counteracts or “cancels out” the canonical role. In sensitized backgrounds, putative null mutations have no net effect on the sensitive balance between 1° and 2° VPC fates. We do not intend to imply that opposing functions are “equal”, only that in our assays they appear to counter-balance each other with approximate equivalency. The observation that deletion of RGL-1 increased the basal error rate of patterning 15-fold supports the idea that RGL-1 serves an important function, that of fidelity.

In mammalian cell culture RalGEF-Ral and PDK-Akt cascades worked in concert (Hao et al., 2008). Yet mammalian RalGEF-Ral signaling has also been found to oppose canonical Ras effectors in cell culture (Goi et al., 1999). We speculate that the relationship between these cascades may depend on cell context, and in the case of vertebrates, which paralog of RalGEF is expressed.

RGL-1 is not the first protein in the VPC fate patterning network found to be bifunctional and promote both 1° and 2° fates. Depending on signaling dose and via mechanisms we do not understand, LIN-3/EGF-LET-23/EGFR signaling was found to promote both 1° and 2° fates, resulting in the original Morphogen Gradient

Model (Katz et al., 1995; Katz et al., 1996; Sternberg and Horvitz, 1989). We found that LET-60/Ras can promote 1° or 2° fate depending on its use of effector, LIN-45/Raf or RGL-1/RalGEF (Reiner, 2011; Zand et al., 2011). Yet the situations are not equivalent. LIN-3, LET-23, and LET-60 are essential for vulval induction: strong loss results in complete absence of 1° fate induction and hence a vulvaless phenotype (Aroian et al., 1990; Beitel et al., 1990; Han and Sternberg, 1990; Hill and Sternberg, 1992), and thus their roles in 2° fate induction were teased out only in sensitized backgrounds or special assays (Katz et al., 1995; Katz et al., 1996; Zand et al., 2011). In contrast, RGL-1 is dispensable for 1° and 2° fate induction, permitting dissection of its balanced and opposing functions. Furthermore, deletion of RGL-1 does not alter any other known developmental events.

These observations positioned us to discover an unexpected aspect of RGL-1 function: it contributes to two modulatory cascades, neither of which is essential for VPC induction. And since the two cascades promote opposing outcomes, loss of both together has no net effect on the delicate balance between 1° and 2° fates. Consequently, this unusual feature of RGL-1 function in vulval signaling, in the anatomically simple nematode that mostly lacks paralog redundancy, provided the opportunity to discover what may be a heretofore unknown property of signaling networks. We speculate that we have identified a signaling switch that is dispensable for development, and that precise regulation of this switch increases the fidelity of signaling networks and hence development. Specifically, in this case

RGL-1 may orchestrate the opposing outputs of AKT-1, which promotes 1° fate through unknown downstream targets (this study), and RAL-1, which promotes 2° fate through EXOC-8/Exo84 of the exocyst, the GCK-2/MAP4 kinase, MLK-1/MAP3K, and PMK-1/p38 MAP kinase (Shin et al., 2018).

Linking opposed signaling cascades and mitigating development noise.

To occur with high fidelity, the VPC fate patterning system must strictly define developmental fields in response to an initial point source of LIN-3/EGF ligand. In other words, it must generate the precise 3°-3°-2°-1°-2°-3° pattern with 99.8% accuracy without mis-specified or ambiguous fates that might block mating and egg laying, which would negatively impact reproductive fitness. A critical question, then, is how the programming of signal transduction networks decreases the potential for errors (developmental stochasticity or “noise”). Previously, the fidelity of VPC fate patterning was thought to be a property that emerges from the combination of three mechanisms: 1) Sequential Induction sets up the basic pattern, 2) the Morphogen Gradient collaborates with Sequential Induction to more precisely sculpt the initial pattern, and 3) Mutual Antagonism serves to exclude potentially conflicting signals from cells that are initially specified, thus preventing assumption of wrong or ambiguous fates. We speculate that the roles we describe here for RGL-1 define a fourth method that is woven into the other three: orchestration of two modulatory cascades to more sharply demarcate fates

as a function of the VPC's spatial relationship to the AC and other VPCs. We name this property "Balanced Switches".

Yet is the participation of RGL-1 in two opposing cascades necessarily a novel mechanism that promotes fidelity? Perhaps not. Perhaps RGL-1 as a point of intersection between two conserved but opposing cascades is coincidental. In this alternative model, the loss of fidelity observed in deletion mutants of *rgl-1* may be merely the consequence of losing two independent modulatory cascades, with AKT-1 and RAL-1 outputs, that each reinforces their respective fates. In this model, the loss of fidelity observed in *rgl-1* deletion mutants is happenstance, a side effect of losing roughly equal and opposite modulatory cascades.

Yet the wiring of these two cascades together in opposition could be of mechanistic significance. How such a mechanism would function is unclear. One possibility is that the RGL-1 "Balanced Switch" functions as an "Insulated Switch". The simplest way to envision this model is through mechanisms of subcellular recruitment and sequestration: RGL-1 engagement in one signal could physically exclude its engagement in the opposing signal, perhaps because the RGL-1 protein has been re-localized to a portion of the cell insufficient to participate in both signals, or is concomitantly modified to prevent interaction in its complementary function. For example, binding of Ras to the RA domain presumably recruits RGL-1 to the plasma membrane, consistent with Ras interactions with other effectors in mammalian cells. This recruitment could sequester RGL-1 away from the subcellular compartment in which PDK-1 and

AKT-1 signal. Conversely, RGL-1 bound as a scaffold to PDK-1 and AKT-1 could be sequestered away from the subcellular compartment in which Ras interacts with RGL-1, preventing participation in the canonical LET-60-RGL-1-RAL-1 2°-promoting cascade. A metaphor for such a switch is the two-headed Pushmi-Pullyu from Dr. Doolittle: when one head pulls forward, the other is by necessity pulled back, and vice-versa. An inessential signaling protein with this property – like RGL-1 – could function to reinforce two different cell fates to improve developmental fidelity. And the mutually exclusive bi-directionality of such a switch would ensure that inappropriate signaling is minimized.

The mechanism by which RGL-1 contributes to different fates remains to be determined. We do not yet have fluorescent biomarkers for RAL-1 or AKT-1 output in the VPCs. And because of the brief developmental window of VPC patterning and the tiny volume of VPC lineages relative to the entire animal, biochemical approaches are inadequate. The concept of the “Balanced Switch” being woven into signaling networks is a fascinating one, and one difficult to test with the typical manifold gene redundancy present in mammalian systems, or the essential nature of many signaling genes in the developmentally more complex *Drosophila*. Perhaps developmental patterning of the *C. elegans* vulva is the right place to test this idea, but more tools are needed to do so. Yet, in the dawn of the CRISPR era, we remain confident about our ability to do so in the future, including the possibility of generating two *rgl-1* genes, each of which governs one but not the other function, *i.e.* uncoupling the two halves of the “switch”.

Robustness to stochastic variation vs. environmental variation.

Increasing noise could result from three sources: stochasticity, environmental insult, or genetic variability. Developmental fidelity depends on mitigating noise from all three sources. In the mostly isogenic lines containing two different introgressed *rgl-1* mutations, genetic variability is unlikely. Thus, we tested whether *rgl-1* mutants were more susceptible to environmental variability. To our surprise, deletion of RGL-1 increased robustness in response to stochastic variation but not environmental perturbation. Conversely, small changes in function, from weak mutation of certain cascades or introgression into different genetic backgrounds that might harbor mutations, caused increased sensitivity to environmental insult (Braendle and Felix, 2008; Milloz et al., 2008). A four-fold change in EGF dose did not appreciably alter VPC patterning (Barkoulas et al., 2013). We speculate that balanced change caused by deletion of RGL-1 does not decrease robustness. In other words, perhaps it is disruption of the delicate balance of 1°- and 2°-promoting signals that sensitizes the system to environmental insult.

Conclusions.

We define a putative regulatory system, which we term “Balanced Switching”, that potentially mitigates potential signaling noise and hence developmental error.

This system would likely not be discovered in experimental platforms with extensive paralog redundancy, or where the genes in question are essential for viability or the process being studied. Whether Balanced Switches are generalizable to other systems, and the molecular details by which they function, await further analysis.

In addition to divergent functions of RGL-1 in signaling, we also delineate mechanistic details of RAL-1 vs. RGL-1 function in essential functions performed by the exocyst and PAR complexes. Our results suggest that the role of RAL-1 in central machinery of cell biology is independent of GDP/GTP state, though we cannot rule out some switchable modulation of exocyst and PAR complex regulation by RAL-1.

Materials and Methods

C. elegans handling and genetics.

Nomenclature is as described (Dickinson et al., 2013; Horvitz et al., 1979). All strains were derived from the N2 wild type. Except where noted, animals were cultured on NGM agar plates with OP50 bacteria on at 20°C (Brenner, 1974). Strains used are shown in Table 3. 2. Data were analyzed with GraphPad Prism software (GraphPad Software Inc., La Jolla, CA).

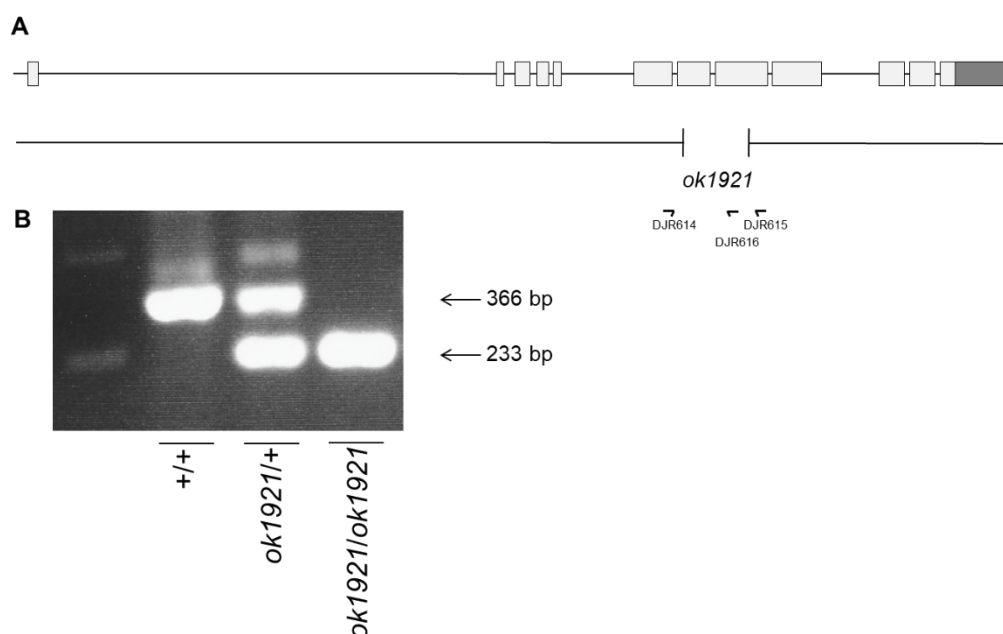


Figure 3. 12 PCR detection of *rgl-1(ok1921)*. **A.** A scale schematic of the *rgl-1* gene, the *ok1921* lesion, and detection primers. **B.** Agarose gel of *+/+*, *ok1921/+* and *ok1921/ok1921* single animal PCR reactions.

PCR primers are listed in Table 3. 3. For single animal genotyping PCR (Taq PCR Master Mix, Qiagen) reactions were run concurrently with *+/+*, *m/+* and *m/m* controls. Each PCR genotype was double-checked after completion of the strain construction. For newly analyzed mutations, PCR products were sequenced to confirm break points. *rgl-1(ok1921)* was detected by triplex PCR using primers DJR614/615/616 (Tm: 59°C, 35 cycles), resulting in 366 bp (wild type) and 233 bp (*ok1921*) bands (Fig. 3. 12). Point mutations in *rgl-1* were tracked in *trans* to *ok1921*. Early constructions detected *rgl-1(tm2255)* by triplex PCR using primers TZ20/DJR614/DJR615 (Tm: 58°, 35 cycles), resulting in 913 bp (wild-type) and

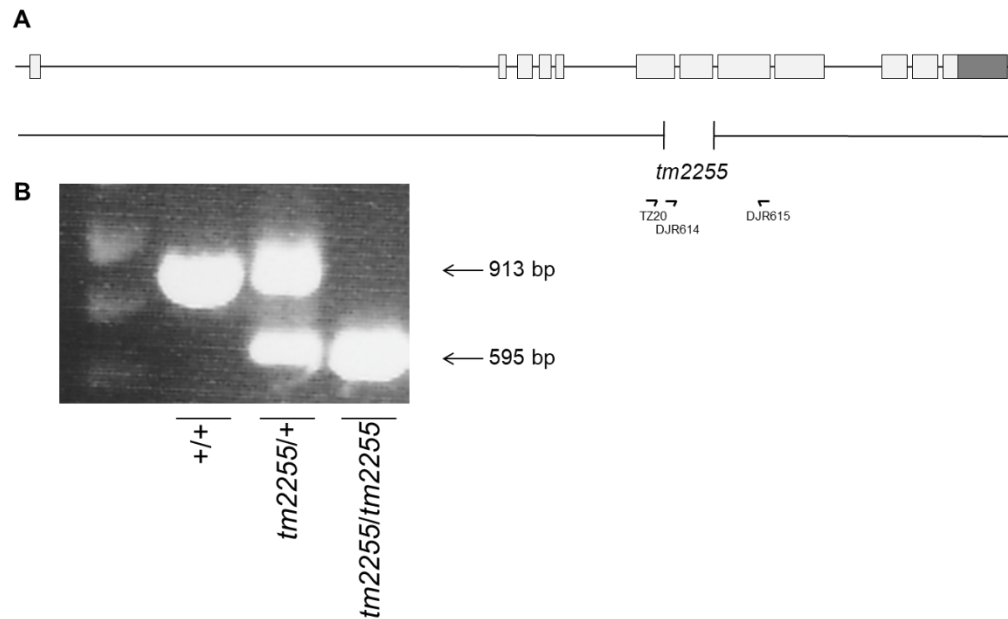


Figure 3. 13 PCR detection of *rgl-1(tm2255)*. **A.** A scale schematic of the *rgl-1* gene, the *tm2255* lesion, and detection primers. **B.** Agarose gel of *+/+*, *tm2255/+* and *tm2255/tm2255* single animal PCR reactions.

595 bp (*tm2255*) bands (Fig. 3. 13). Later constructions detected *rgl-1(tm2255)* by triplex PCR using primers FSM7/8/9 (Tm: 58°C, 35 cycles), resulting in 509 bp (wild-type) and 254 bp (*tm2255*) bands. *pdk-1(mg142gf)* was amplified by primers DRC1/2 (Tm: 60°C, 35 cycles) to generate a 426 bp band, then digested with Hpa II (NEB; 5 units added to total reaction a 426 bp band, then digested with Hpa II (NEB; 5 units added to total reaction volume doubled with water with NEB buffer #1 to 0.5x total, digested overnight at 37°C). The band from the wild-type allele was digested to yield 126 and 300 bp bands, while the *mg142* lesion abolishes the Hpa II site. *daf-18(ok480)* was detected by triplex PCR using primers

FSM4/5/6 (Tm: 54°C, 35 cycles), resulting in 388 bp (wild-type) and 216 bp (*ok480*) bands. For this study, *dpy-9(e14)* was used as a balancer for *daf-18(ok480)*, and the *ok480* genotype confirmed after construction. *akt-1(mg144gf)* was balanced during strain constructions by *dpy-11(e224) unc-76 (e905)*. *ral-1(gk628801)* was detected by amplification with primers DJR778/779 (Tm = 59.9°C, 35 cycles) to generate a 250 bp band and digested with HpyCH4 IV (NEB; 5 units added to total reaction volume doubled with water with NEB buffer #1 to 0.5x total, digested overnight at 37°C). The band from the wild-type allele was digested to yield 122 and 128 bp bands, while the *gk628801* lesion abolishes the HpyCH4 IV site.

Transgenic extrachromosomal array *reEx24[P_{lin-31}::ral-1(Q75L), P_{myo-2}::gfp]* (Zand et al., 2011) was integrated by irradiation of late L4 animals using a Stratalinker (Stratagene) at dose of 12 mJ/cm². 451 F2 progeny were screened for integration to obtain *rels10 [P_{lin-31}::ral-1(Q75L), P_{myo-2}::gfp]*. *rels10* was mapped to the region of Chromosome I +5.

VPC induction assays.

VPC induction was analyzed by DIC/Nomarski optics (Nikon eclipse Ni with images captured using NIS-Elements AR 4.20.00 software) in late L4 animals on an agar pad (molten 3% NG agar with 5 mM sodium azide) in a 5 µl drop of M9 buffer. Ectopic pseudovulvae were scored as invaginations at 600x or 1000x. Ectopic 1° vulval induction index, from 0 to 3 ectopic 1°s, is described elsewhere

(Shin et al., 2018; Zand et al., 2011). Under-induced backgrounds were scored as total VPCs induced, typically 0-3 (in under-induced backgrounds the entire vulva is frequently uninduced). To summarize, we scored the wild-type vulval induction based on the stereotypical 2°-1°-2° lineages centered on the AC at the A-P midpoint of the gonadal primordium (forming the “Christmas Tree” or “Stanley Cup” shape). In the *let-60(n1046gf)* and *let-23(sa62gf)* backgrounds, the morphology of ectopic 1° cells generally conformed with the described “cap” structure where the entire 1° lineage has pulled away from the cuticle (Katz et al., 1996). We did not observe ectopic pseudovulvae with the characteristic asymmetrical “beret” lineage of 2° lineages, where one side remains attached to the cuticle.

As described previously (Shin et al., 2018; Zand et al., 2011), we occasionally observed drift of the severity of the *let-60(n1046gf)* but not *let-23(sa62gf)* Muv phenotype. Consequently, we employed a stringent protocol for all VPC induction scoring experiments. We analyzed parental MT2124 and outcrossed strains harboring the *n1046gf* single mutant, and established that the baseline of undrifted strains averaged 1.2-1.5 ectopic 1°s. (When grown on bacterially mediated RNAi food source HT115, induction was consistently higher: 1.5-1.8; (Shin et al., 2018; Zand et al., 2011). We additionally always worked with freshly thawed or chunked strains; our animals were always freshly derived from a cross or thaw. For all strains harboring the *n1046gf* mutation we always employed stringent scoring criteria: the *n1046gf* single mutant was scored first, and experiments deviating from the aforementioned expected range of induction were

discarded. Additionally, we only compared genotypes that were scored concurrently, thus minimizing variation from assay to assay.

DIC, epifluorescence and confocal microscopy.

For epifluorescent imaging, animals were mounted in 2 mg/ml tetramisole/M9 buffer and visualized using a Nikon Eclipse TE2000U microscope equipped with a DVC-1412 CCD camera (Digital Video Camera Company), with Hamamatsu SimplePCI acquisition software. Confocal images were captured by A1si Confocal Laser Microscope (Nikon) using NIS Elements Advanced Research, Version 4.40 software (Nikon).

Bacterially mediated RNA interference.

RNAi was performed as described previously (Shin et al., 2018; Zand et al., 2011) with HT115 bacterial host (Timmons and Fire, 1998). RNAi plasmids used were: pREW2 (*luciferase/luc*; Shin et al., 2018), X-2K11 (*rgl-1*), III-7M13 (*ral-1*), I-1K04 (*pop-1*), and *gfp* (Zand et al., 2011). Each RNAi clone was sequence verified. Bacteria were grown on NGM plates supplemented with 50 µg/ml carbenicillin and 1 mM IPTG. Bacteria were grown (but not overgrown) overnight, without antibiotic selection. 80 µl of fresh culture was seeded on plates on day 1, grown overnight,

L4 animals were added on day 2, transferred to a fresh plate on day 3, and scored on day 5.

Plasmid subcloning and transgene generation.

Using primers RGL-1F and RGL-1R, the *rgl-1a* cDNA was amplified from clone yk643d11, and digested with Bgl II and Not I. This isoform lacks exon 2, which by RNAseq data is rare (Wormbase WS263), yet still rescues, arguing that exon-2 is not required for vulval signaling. Plasmid vector pB255, which contains the *lin-31* promoter and additional regulatory sequences and drives expression in VPCs (Tan et al., 1998), was digested with Bgl II and Not I to receive the *rgl-1* insert. The putative R324E GEF-deficient mutation was introduced by PCR with Pfu Turbo using primers KM1 and KM2. The resulting plasmids, *P_{lin-31}::rgl-1(+)* and *P_{lin-31}::rgl-1(R324E)*, were injected at 5 ng/μl along with co-injection marker pPD118.33(*P_{myo-2}::gfp*) at 5 ng/μl into strain DV2190 *let-60(n1046gf); rgl-1(tm2255)* to generate arrays *reEx109* and *reEx110 (rgl-1(+))* and *reEx94* and *reEx95 (rgl-1(R324E))*, which express wild-type and GEF-deficient RGL-1, respectively, specifically in VPCs.

CRISPR/Cas9-dependent genome editing.

rgl-1(re179[mNeonGreen::3xFlag::rgl-1]) was generated using the positive-negative selection self-excising cassette method (Dickinson et al., 2015). The repair template for *rgl-1* 5' tagging was generated by Gibson Assembly (NEB) with digested target SEC vector pDD268, and ~500 bp of homology arms amplified from genomic DNA by Q5 polymerase (NEB). We used two sgRNA sequences: (#1) 5'-ACACCTTCGTATCCTTGTGGCGG-3' and (#2) 5'-GGTCTGAGTTCTTCTGACGATTGG-3' (PAMs underlined), and hence generated two targeting vectors and one repair template. Repair template (20 ng/μl), sgRNA-Cas9 #1 (25 ng/μl), sgRNA-Cas9 #2 (25 ng/μl) and injection marker *P_{myo-2}::mCherry* (2.5 ng/μl) were microinjected into wild-type animals. Genotyping and sequencing of *rgl-1* 5' CRISPR tagging was performed with HS125/126/127 (Tm: 54°C). Validation was performed by western blotting using monoclonal anti-Flag antibody (Sigma-Aldrich F1804; 1:2000), monoclonal anti-α-tubulin antibody (Sigma-Aldrich T6199; 1:2000) and goat anti-mouse secondary antibody (MilliporeSigma 12-349; 1:5000).

For reasons unknown, all seven *rgl-1* CRISPR alleles generated harbored mutations. Repair templates were re-checked by sequencing to confirm that sequences were wild type. DV3225 *rgl-1(re179[mNeonGreen::3xFlag::rgl-1])* harbored only promoter mutations (C insertion at -614, C deleted at -375, C to T at -395) and so was selected for further analysis. Analysis of the ModEncode

database showed no peaks of promoter occupancy at these sites. *rgl-1(re179[mNeonGreen::3xFlag::rgl-1])* had no effect on 1° induction in the *let-60(n1046gf)* background ($P = 0.57$ between strains with and without the *re179* insertion, $N = 86$ and 78 , respectively).

Assessment of patterning error rate with environmental insults.

The vulval cell lineages and Pn.p fates (and errors) were described in early to mid L4 individuals as previously described (Braendle and Felix, 2008; Sternberg and Horvitz, 1986). Nematode populations of N2 wild type and the two *rgl-1* mutations were kept in identical environmental conditions for at least three generations prior to experiments. Animals were age-synchronized by hypochlorite treatment and liquid arrest for ~24 hours, then randomly allocated to the four experimental environments: control (20°C), heat stress (29°C), osmotic stress (250 mM NaCl NGM plates, 20°C; Lamitina et al., 2004), and starvation (20°C; Grimbirt et al., 2018). In starvation conditions, L1 larvae were cultivated on standard NGM plates until they reached the mid L2 stage, at which point they were transferred to unseeded NGM plates containing 1mg/ml of ampicillin to prevent bacterial growth. After 48 hours, starved animals were transferred to regular NGM plates seeded with *E. coli* OP50 and the vulval phenotype was scored when animals had reached the early or mid L4 stage (Grimbert et al., 2018).

Table 3. 1 *rgl-1* and *ral-1* alleles and mutant phenotypes

Allele	Lesion	Superficial Phenotype	Net VPC alteration ^a
<i>rgl-1(ok1921)</i>	In-frame deletion, GEF domain	Wild type	none
<i>rgl-1(tm2255)</i>	Out-of-frame deletion, GEF domain	Wild type	none
<i>fax-1(gm27)^b</i>	<i>rgl-1</i> and 8 other genes deleted	Unc ^c	none
<i>rgl-1(gk275305)</i>	nonsense	Wild type	none
<i>rgl-1(gk275304)</i>	Missense, R361Q, GEF domain	Wild type	Decreased 2°
<i>ral-1(tm2760)</i>	Intron 3 deletion	Sterile ^d	Decreased 2° ^d
<i>ral-1(tm5205)</i>	Exons 2 and 3 deletion	Variable, Sterile ^e	Decreased 2° ^e
<i>ral-1(gk628801)</i>	Missense, R139H	Wild type	Decreased 2°
<i>ral-1(re179)</i>	mNeonGreen::3xFlag::rgl-1	Wild type	none ^f

^a Alteration in network signaling determined from phenotype in *let-60(n1046gf)*.

^b Documented in (Much et al., 2000).

^c Deletion of *fax-1* causes an Uncoordinated phenotype (Much et al., 2000).

^d Intron 2 deletion breaks in the middle of the splice donor site, conferring sterility, reduced 2° induction, and disruption of polarity (Zand et al., 2011).

^e Exons 2 and 3 deletion removes GTPase domain sequences, confers sterility, delayed growth and reduced 2° induction (Armenti et al., 2014), this study.

^f No effect in *let-60(n1046gf)* background

Table 3. 2 Strains for RGL-1 study

Strain	Genotype	Application
DV3311	<i>ral-1(tm2760) / qC1 [dpy-19(e1259ts) glp-1(q339) nls189[P_{myo-2}::gfp]] III</i>	Inspecting mutant VPCs
DV2924	<i>ral-1(tm5205) / qC1 [dpy-19(e1259ts) glp-1(q339) nls189[P_{myo-2}::gfp]] III</i>	Inspecting mutant VPCs
MT2124	<i>let-60(n1046gf) IV</i>	Fig. 3. 3B, 3. 3C, 3. 3E, baselines throughout
DV2214	<i>let-60(n1046gf) IV (2x outcrossed)</i>	Results
DV2215	<i>let-60(n1046gf) IV (2x outcrossed)</i>	Results
RB1576	<i>rgl-1(ok1921) X</i>	Starting reagent
DV2194	<i>rgl-1(ok1921) X (4x outcrossed)</i>	throughout
FX2255	<i>rgl-1(tm2255) X</i>	Starting reagent
DV2175	<i>rgl-1(tm2255) X (4x outcrossed)</i>	throughout
DV2937	<i>ral-1(tm5205) / qC1 [dpy-19(e1259ts) glp-1(q339) nls189[P_{myo-2}::gfp]] III; let-60(n1046gf) IV</i>	Fig. 3. 3F
DV2190	<i>let-60(n1046gf) IV; rgl-1(tm2255) X</i>	Fig. 3. 3D, 3. 3F, 3. 3G
DV2248	<i>let-60(n1046gf) IV; rgl-1(ok1921) X</i>	Fig. 3. 3F, 3. 3G
DV2251	<i>let-60(n1046gf) IV; lon-2(e678) X</i>	Fig. 3. 3G
DV2252	<i>let-60(n1046gf) IV; fax-1(gm27) lon-2(e678) X</i>	Fig. 3. 3G
DV2191	<i>let-60(n1046gf) IV; arls92[P_{egl-17}::NLS-cfp::LacZ + P_{ttx-3}::gfp] V</i>	Fig. 3. 4A, 3. 4C, 3. 4D
DV2750	<i>let-60(n1046gf) IV; arls92[P_{egl-17}::NLS-cfp::LacZ + P_{ttx-3}::gfp] V; rgl-1(tm2255) X</i>	Fig. 3. 4B, 3. 4E
WU49	<i>lin-45(n2506rf) unc-24(e138) IV</i>	Fig. 3. 4F, 3. 10E, 3. 10F
DV2783	<i>lin-45(n2506rf) unc-24(e138) IV; rgl-1(tm2255) X</i>	Fig. 3. 4F
PS1524	<i>unc-4(e120) let-23(sa62gf) II</i>	Fig. 3. 4G
DV2958	<i>unc-4(e120) let-23(sa62gf) II; rgl-1(tm2255) X</i>	Fig. 3. 4G
BC14985	<i>dpy-5(e907) I; sEx14985[rCesF28B4.2::gfp + pCeh361(dpy-5(+))]</i>	Fig. 3. 5
DV3312	<i>rgl-1(re179[mNeonGreen^3xFlag::rgl-1]) X</i>	Fig. 3. 6
VC40420	<i>ral-1(gk628801rf) III (unoutcrossed)</i>	Results

Table 3. 2 Continued

Strain	Genotype	Application
DV2942	<i>ral-1(gk628801rf)</i> III (6x outcrossed)	Results
DV2799	<i>ral-1(gk628801rf)</i> III; <i>let-60(n1046gf)</i> IV	Fig. 3. 7C
VC20011	<i>rgl-1(gk275304)</i> X (unoutcrossed)	Results
DV2883	<i>rgl-1(gk275304)</i> X (4x outcrossed)	Results
VC40052	<i>rgl-1(gk275305)</i> X (unoutcrossed)	Results
DV2884	<i>rgl-1(gk275305)</i> X (4x outcrossed)	Results
DV2764	<i>let-60(n1046gf)</i> IV; <i>rgl-1(gk275304)</i> X	Fig. 3. 7D
DV2765	<i>let-60(n1046gf)</i> IV; <i>rgl-1(gk275305)</i> X	Fig. 3. 7D
DV2537	<i>let-60(n1046gf)</i> IV; <i>rgl-1(tm2255)</i> X; <i>reEx94[P_{lin-31}::rgl-1(R324E) + P_{myo-2}::gfp]</i>	Fig. 3. 7E, 3. 8A
DV2538	<i>let-60(n1046gf)</i> IV; <i>rgl-1(tm2255)</i> X; <i>reEx95[P_{lin-31}::rgl-1(R324E) + P_{myo-2}::gfp]</i>	Fig. 3. 7E, 3. 8A
DV2736	<i>let-60(n1046gf)</i> IV; <i>rgl-1(tm2255)</i> X; <i>reEx109[P_{lin-31}::rgl-1(+) + P_{myo-2}::gfp]</i>	Fig. 3. 7E, 3. 8B
DV2737	<i>let-60(n1046gf)</i> IV; <i>rgl-1(tm2255)</i> X; <i>reEx110[P_{lin-31}::rgl-1(+) + P_{myo-2}::gfp]</i>	Fig. 3. 7E, 3. 8B
MT301	<i>lin-31(n301)</i> II	Fig. 3. 8C
DV2763	<i>lin-31(n301)</i> II; <i>rgl-1(tm2255)</i> X	Fig. 3. 8C
DV2140	<i>let-60(n1046gf)</i> IV; <i>reEx24[P_{lin-31}::ral-1(Q75L), P_{myo-2}::gfp]</i>	Zand et al., 2011 derived <i>rels10</i>
DV2335	<i>rels10[P_{lin-31}::ral-1(Q75L) + P_{myo-2}::gfp]</i> I	Results
DV2699	<i>rels10[P_{lin-31}::ral-1(Q75L) + P_{myo-2}::gfp]</i> I; <i>let-60(n1046gf)</i> IV	Fig. 3. 7F, 3. 8D
DV2700	<i>rels10[P_{lin-31}::ral-1(Q75L) + P_{myo-2}::gfp]</i> I; <i>let-60(n1046gf)</i> IV; <i>rgl-1(tm2255)</i> X	Fig. 3. 7F
CB2065	<i>dpy-11(e224) unc-76(e905)</i> V	<i>akt-1</i> balancer
GR1310	<i>akt-1(mg144gf)</i> V	Fig. 3. 9
DV2746	<i>let-60(n1046gf)</i> IV; <i>akt-1(mg144gf)</i> V	Fig. 3. 9A, 3. 10A
DV2747	<i>let-60(n1046gf)</i> IV; <i>akt-1(mg144gf)</i> V; <i>rgl-1(tm2255)</i> X	Fig. 3. 9A, 3. 10A
GR1318	<i>pdk-1(mg142gf)</i> X	Fig. 3. 9
DV2773	<i>let-60(n1046gf)</i> IV; <i>pdk-1(mg142gf)</i> X	Fig. 3. 9B, 3. 10B
DV2782	<i>let-60(n1046gf)</i> IV; <i>pdk-1(mg142gf)</i> X	Fig. 3. 9B
DV2844	<i>let-60(n1046gf)</i> IV; <i>pdk-1(mg142gf)</i> X	Fig. 3. 9B

Table 3. 2 Continued

Strain	Genotype	Application
SP934	<i>unc-1(e538) dpy-3(e27) X</i>	Fig. 3. 9B
DV2774	<i>unc-1(e538) dpy-3(e27) rgl-1(tm2255) X</i>	Fig. 3. 9B
DV2819	<i>pdk-1(mg142gf) rgl-1(tm2255) X</i>	Fig. 3. 9B
DV2822	<i>let-60(n1046gf) IV; pdk-1(mg142gf) rgl-1(tm2255) X</i>	Fig. 3. 9B
DV2791	<i>lin-45(n2506rf) unc-24(e138) IV; akt-1(mg144gf) V</i>	Fig. 3. 10F
DV2795	<i>lin-45(n2506rf) unc-24(e138) IV; pdk-1(mg142gf) X</i>	Fig. 3. 10E
RB712	<i>daf-18(ok480) IV</i>	Starting reagent
DV2855	<i>daf-18(ok480) IV (2x outcrossed)</i>	Fig. 3. 9
DV2510	<i>daf-18(ok480) let-60(n1046gf) IV</i>	Fig. 3. 9C, 3. 9D, 3. 10C, 3. 10D, 3. 10G, 3. 10H
DV2535	<i>daf-18(ok480) let-60(n1046gf) IV; rgl-1(tm2255) X</i>	Fig. 3. 9C
DV2509	<i>daf-18(ok480) let-60(n1046gf) IV; rgl-1(tm2255) X</i>	Fig. 3. 9D
DV2679	<i>jip-1(km18) II</i>	Fig. 3. 10I
DV3013	<i>jip-1(km18) II; let-60(n1046gf) IV</i>	Fig. 3. 10I
DV3358	<i>jip-1(tm6137) II (4x outcrossed)</i>	Fig. 3. 10I
DV3505	<i>jip-1(tm6137) II; let-60(n1046gf) IV</i>	Fig. 3. 10I
DV3506	<i>jip-1(tm6137) II; daf-18(ok480) let-60(n1046gf) IV</i>	Fig. 3. 10I
DV2696	<i>rgl-1(ok1921) X (8x outcrossed)</i>	Fig. 3. 11
DV2697	<i>rgl-1(tm2255) X (8x outcrossed)</i>	Fig. 3. 11

Table 3. 3 Primers for RGL-1 study

Name	Sequence	Use
DJR614	5'-GAGCAACTGACGTTTTGGGATGC-3'	<i>rgl-1(ok1921)</i> genotyping
DJR615	5'-GATCTGGAGTGGAGTGCATTGG-3'	<i>rgl-1(ok1921)</i> genotyping
DJR616	5'-CGAAAAGCTCCCCACTTCGACG-3'	<i>rgl-1(ok1921)</i> genotyping
DJR778	5'-TAGACAATTTAGGCCCAAACCCCCG-3'	<i>ral-1(gk628801)</i> genotyping
DJR779	5'-CCAAATTTTCAGCCTAAAATCTCTTCCCA ATACC-3'	<i>ral-1(gk628801)</i> genotyping
RGL-1F	5'-GCGGGATCCGAAAAAATGGCTACGCGTT ACTGGGGTGACG-3'	Cloning <i>rgl-1a</i> cDNA
RGL-1R	5'-ATAAGAATGCGGCCGCTTTACAAGTAGC CACTGCTCCATG-3'	Cloning <i>rgl-1a</i> cDNA
DRC1	5'-AGATGCTAGCTGACGGAGATGTGGG-3'	<i>pdk-1(mg142gf)</i> genotyping
DRC2	5'-AAATGTGGCTGGAATGTAGGCGTGC-3'	<i>pdk-1(mg142gf)</i> genotyping
FSM4	5'-ATATTCGAGGAGTCGGTGGTCC-3'	<i>daf-18(ok480)</i> genotyping
FSM5	5'-GAGGCTACCGGATAATGTGC-3'	<i>daf-18(ok480)</i> genotyping
FSM6	5'-GGCAACGAATGAATACGCAGG-3'	<i>daf-18(ok480)</i> genotyping
FSM7	5'-GAAGTCAAGCCGCTCTTCC-3'	<i>rgl-1(tm2255)</i> genotyping
FSM8	5'-GGAGAACTGCTGGAGAACG-3'	<i>rgl-1(tm2255)</i> genotyping
FSM9	5'-CCGTTCCCTGACATTCGG-3'	<i>rgl-1(tm2255)</i> genotyping
HS160	5'-ACACCTTCGTATCCTTGTGGGTTTAAGAG CTATGCTGGAAACAG-3'	RGL-1 CRISPR sgRNA Cas-9 plasmid #1
HS161	5'-GGTCTGAGTTCTTCTGACGAGTTTAAGA GCTATGCTGGAAACAG-3'	RGL-1 CRISPR sgRNA Cas-9 plasmid #2
DJR769	5'-CACCTCCTATTGCGAGATGTCTTG-3'	Universal sgRNA plasmid Mutagenesis

Table 3. 3 Continued

Name	Sequence	Use
HS120	5'-CCAGTCACGACGTTGTAAAACGACGGCC AGTCGCCGGCACCGCATCCATTCACAGTG TAC-3'	Left homology arm for RGL-1 CRISPR repair template
HS159	5'-AGGGAGGCCATGTTGTCCTCCTCTCCCT TGGAGACCATACGCGTAGCCATTTAAGATT GGTCTGAGTTCTTCTGACG-3'	Left homology arm for RGL-1 CRISPR repair template
HS122	5'-CGACGACAAGCGTGATTACAAGGATGAC GATGACAAGAGAGGATCTGGAATGGCTAC GCGTTACTGGG-3'	Right homology arm for RGL-1 CRISPR repair template
HS123	5'-TAACAATTTACACAGGAAACAGCTATGA CCATGTTATCGAAGTGGCACTCAGCTTCAT C-3'	Right homology arm for RGL-1 CRISPR repair template
HS125	5'-CTTGTCAGTGTAAAGGGAAGATTTCC-3'	RGL-1 CRISPR genotyping
HS126	5'-TTGTCCTCCTCTCCCTTGG-3'	RGL-1 CRISPR genotyping
HS127	5'-ACGTAGAATGTTCCAGAGTTCCAG-3'	RGL-1 CRISPR genotyping
KM1	5'-GCCGGCCCGAATACGAAGCGAAGATAAT CAGCAAGTGGATCG-3'	R324E mutagenesis
KM2	5'-GATCCACTTGCTGATTATCTTCGCTTCGT ATTCGGGCCGG-3'	R324E mutagenesis

CHAPTER IV

RAS EFFECTOR SWITCHING MECHANISM

Introduction

Ras is the most mutated oncoprotein across all cancers (Bos, 1989) and is the founding member of the Ras superfamily of small GTPases (Wennerberg et al., 2005). Ras paralogs are encoded by three distinct genes, and each Ras protein binds to GDP/GTP with picomolar affinity, thus preventing direct pharmacological inhibition. Ras uses many effectors, with three main effectors associated with cancer: Raf S/T kinase, PI3K lipid kinase, and RalGEF exchange factor for the Ras-like small GTPase, Ral. Like most small GTPases, Ras is lipid-modified at its C-terminus to regulate membrane-targeting. Yet blockade of Ras lipid modification fails due to alternative lipid modification (Cox et al., 2014). Therefore, Ras is thought to be mostly undruggable, with certain exceptions (Downward, 2014; Papke and Der, 2017). Historically, canonical Ras-Raf and Ras-PI3K have been shown to cause cancer transformation of mouse primary fibroblasts (Khosravi-Far et al., 1996; Kyriakis et al., 1992; Shields et al., 2000; White et al., 1995). Subsequent studies supported the idea that Ras-RalGEF-Ral mediates the transformation of immortalized human epithelial cells (Hamad et al., 2002); most malignant human cancers are derived from epithelial cells (Hanahan and Weinberg, 2011). Furthermore, loss of the heterodimeric RalGAP, a putative

tumor suppressor, promotes tumorigenesis independently of Ras (Oeckinghaus et al., 2014; Saito et al., 2013). Therefore, Ras-RalGEF-Ral is an oncogenic signal perhaps as canonical Ras effectors Raf and PI3K.

RalGEF was identified as a Ras effector by yeast two hybrid screens in early 1990s (Albright et al., 1993; Hofer et al., 1994; Spaargaren and Bischoff, 1994; Wolthuis et al., 1996). RalGEF is a guanine nucleotide exchange factor for small GTPase Ral. The RalGEF has a REM (Ras Exchanger Motif) domain, a CDC25 homology domain (RasGEF), and a RA (Ras Association) domain (Ferro and Trabalzini, 2010). Humans have four RalGEFs: RalGDS (Ral Guanine nucleotide Dissociation Stimulator), Rgl1, 2, and 3 (Isomura et al., 1996; Kikuchi et al., 1994; Shao and Andres, 2000; Wolthuis et al., 1996). *C. elegans* encodes a single RalGEF, RGL-1, while *Drosophila* encodes two RalGEF proteins from a single gene (RGL and RGL2; Gentry et al., 2014).

Ras uses different effectors, or combinations of effectors, in different cancers (Martin et al., 2011). This phenomenon raises the question of combinatorial effector inhibitors as a strategy to treat Ras-dependent tumors. It also raises the interesting question of how Ras decides between effectors: currently we have no idea how this switching is regulated. RalGEF has been shown to enhance Ras-mediated-transformation and -tumorigenic growth in human cells (Lim et al., 2005). The activated RalGEF, Rgl2, promotes anchorage-independent growth and invasion in human pancreatic adenocarcinoma cell lines and immortalized rodent melanocytic cells (Mishra et al., 2010; Vigil et al., 2010).

In the response of LIN-3/EGF, LET-23/EGFR signals through LET-60/Ras-LIN-45/Raf-MEK-2/MEK-MPK-1/ERK to promote 1° fate in *C. elegans* vulva precursor cell (VPC) fate patterning. The LET-23-mediated 1°-promoting signal in turn induces DSL Notch ligands expression in the presumptive 1° cell, P6.p. DSL Notch ligands are secreted from the P6.p to signal laterally to the adjacent P5.p and P7.p. The spatially graded LIN-3 promotes LET-23/EGFR-LET-60/Ras-RGL-1/RalGEF-RAL-1/Ral to induce P5.p and P7.p become 2° cells in support of LIN-12/Notch activation (Zand et al., 2011).

There are additional complications of LET-60 signaling and outcomes in *C. elegans*. Different LET-60 gain-of-function mutants showed different phenotypes. For examples, *let-60(n1046gf)* has the canonical G13E mutation and shows Multivulva (Muv) phenotype with mild fertility defect (Beitel et al., 1990; Han and Sternberg, 1991), but no obvious effect on fluid homeostasis. Another LET-60 gf mutant, *ay75ts*, has G60R mutation, which promotes mammalian Ras transforming activity (Lowy et al., 1991). The *let-60(ay75ts)* shows strong fluid homeostasis defect (Schutzman et al., 2001). On the other hand, *let-60(ga89ts)*, which has a L19F mutation, confers strong sterility (Eisenmann and Kim, 1997). The LET-60 signals through LIN-45/Raf to function in all three tissues, so these differences are difficult to explain. One possibility is that LET-60 orchestrates multiple effectors in each tissue. The functions of LET-60-RGL-1 have not been investigated except its role as a 2°-promoting signal in VPC fate patterning. The different effectors, LIN-45 and RGL-1, may shape different LET-60 activity to be

able to regulate multiple functions in different tissues, or even other effectors could be involved. However, we do not know how LET-60 switches its effectors or whether LET-60 uses multiple or one effector for the specific functions. We will investigate LET-60 effector switching mechanism using *C. elegans*.

Patterning of *C. elegans* VPC fates is an ideal system to study this question, since this developmental decision is dispensable for viability. Additionally, *C. elegans* lacks the paralog redundancy of mammals (e.g. three Ras-, three Raf- and four RalGEF-encoding genes). The developmental simplicity of *C. elegans* is also an advantage: mutation of many of the relevant genes in *C. elegans* are lethal or at least yield some live animals, while most are essential in *Drosophila*. The relative ease of CRISPR manipulation (Dickinson et al., 2015; Dickinson et al., 2013) and the optical clarity of the third larval stage animal positions us to observe effector recruitment in real time.

Plasma membrane-localized Ras in its GTP-bound state recruits Raf to the plasma membrane by binding to the Ras binding domain (RBD) of Raf (Leevers et al., 1994; Pritchard and McMahon, 1997; Stokoe et al., 1994; Tamada et al., 1997). The activation of Raf also requires phosphorylation/dephosphorylation (Dhillon et al., 2002; Fabian et al., 1993). In *C. elegans*, SOC-2/SUR-8 has been shown to function as a scaffold protein between LET-60 and LIN-45 genetically (Selfors et al., 1998; Sieburth et al., 1998) and was later shown to bind to both (Li et al., 2000; Matsunaga-Udagawa et al., 2010).

Our preliminary data showed that upon VPC induction, LIN-45/Raf and RGL-1/RalGEF are differently recruited to the basolateral plasma membrane of the presumptive 1° cell and the apical plasma membrane in presumptive 2° cells, respectively. We conclude we are witnessing two distinct regulatory axes. First, we observed clear segregation of signals along the apical-basolateral axis, with no evidence of either effector being mislocalized. Second, we observed clear segregation between presumptive 1° and 2° VPCs, though in this case low level and sporadic recruitment of RGL-1 to the apical plasma membrane of presumptive 1° cells was also observed. Thus, we will follow multiple avenues of investigation to determine mechanisms for both of these segregations. We plan to thus determine the mechanism of Ras effector switching.

Going forward we will test multiple hypotheses. First, we hypothesize the different localization of LET-60 effectors in different cells is controlled by restriction of specific scaffold proteins to either apical membrane or basolateral membrane in VPCs. The LIN-45 recruitment to the basolateral membrane in 1° cell could be restricted by SOC-2, a well-known scaffold protein between LET-60 and LIN-45. Alternatively, SOC-2 could function as an insulator, excluding RGL-1 from the basolateral cell compartment. Or a similar scaffold could function to spatially regulate the LET-60-RGL-1 interaction.

Another hypothesis is that the PAR system, which generally sets of polarity in polarized epithelial cells across metazoans (Thompson et al., 2013) sets up apical-basal polarity of LET-60 effector usage. Ample PAR tools are available in

C. elegans, the animal in which the PAR system was discovered (Kemphues, 2000).

A hypothesis addressing 1° vs. 2° segregation of RGL-1 is that phosphorylation of RGL-1 regulates the interaction between it and LET-60. The RGL-1 has a potential phosphorylation site neighboring the RA domain (Bodenmiller and Aebersold, 2011). This putative phosphosite is similar to consensus sequence for phosphorylation by MAP kinases or CDKs, Cyclin-Dependent Kinases. The LET-60/Ras-LIN-45/Raf-MEK-2/MEK-MPK-1/ERK signaling cascade promotes 1° fate. We hypothesize that phosphorylation of this putative phosphosite by MPK-1/ERK in the presumptive 1° cell could abolish LET-60/Ras binding to RGL-1. Conversely, since MPK-1/ERK activity is quenched by 2°-specific expression of the LIP-1/ERK phosphatase, RGL-1 may remain unphosphorylated and permit binding to LET-60.

We will additionally prepare tools for pairwise immunoprecipitation and mass spectrometry to discover shared LET-60-RGL-1 and LET-60-LIN-45 binding partners. This unbiased approach will complement our mechanistically specific approaches. I expect this extension of my thesis work to uncover important mechanistic features of Ras effector switching.

Results

LIN-45/Raf was recruited to the basolateral membrane in presumptive 1° cell, but not in presumptive 2° cells.

The Ras effector, Raf, showed recruitment to the plasma membrane in mammalian cell culture system (Block et al., 1996; Chiu et al., 2002). The LET-60/Ras-LIN-45/Raf is a well-known 1°-promoting signal in *C. elegans* VPC fate patterning. Since LET-60 and LIN-45 are necessary and sufficient for 1° fate induction, we hypothesized that LIN-45 should be recruited to the plasma membrane of presumptive 1° VPCs during induction. Therefore, using CRISPR/Cas9-mediated genome editing (Dickinson et al., 2013) we tagged endogenous LIN-45 with mNeonGreen (mNG; Shaner et al., 2013) fluorescent protein (FP) and the 3xFlag epitope tag (generously provided by N. Rasmussen).

mNG::LIN-45 appears to be ubiquitously expressed in the animal. Specifically, mNG::LIN-45 is localized in the cytoplasm of VPCs at early Pn.p stage, 1-cell stage (Figs. 4. 1A-B). During VPC induction LIN-45::mNG is recruited to the basolateral plasma membrane in presumptive 1° but not 2° cells (Figs. 4. 1A-B). The basolateral surface of presumptive 1° cell, P6.p, is juxtaposed with the ventral surface of the AC, and so is close to the source of LIN-3/EGF. P6.p, the presumptive 1° cell, is at least twice the width of the AC (Sherwood and Sternberg, 2003). The basolateral LIN-45::mNG spans the P6.p cell, and is greater than twice

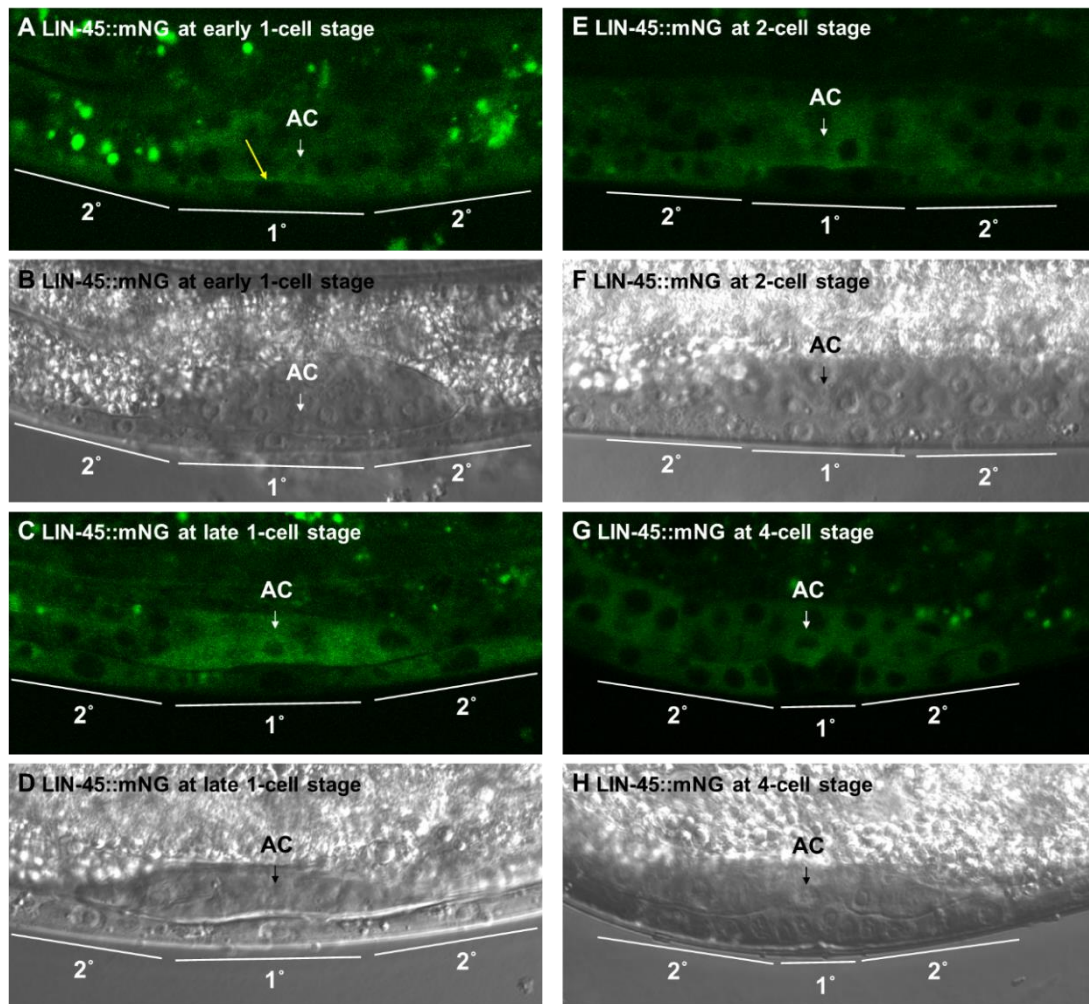


Figure 4. 1 Subcellular localization of LIN-45::mNG in VPCs at different stages. **A.** LIN-45::mNG is localized to the cytoplasm of VPCs and the AC at early Pn.p, 1-cell, stage. LIN-45::mNG is recruited to basolateral membrane in 1° cell, but not in 2° cells at early 1-cell stage. **B.** DIC image of early 1-cell stage. **C.** The LIN-45::mNG starts to be degraded in 1° cell at late 1-cell stage. However, the signal of LIN-45::mNG is maintained in 2° cells at late 1-cell stage. **D.** DIC image of late 1-cell stage. **E.** The LIN-45::mNG is degraded in the daughters of 1° cell while expressing in the daughters of 2° cells at 2-cell stage. **F.** DIC image of 2-cell stage. **G.** The LIN-45::mNG is not expressed in the daughters of 1° cell at 4-cell stage. However, the LIN-45::mNG is still expressed in the daughters of 2° cells at 4-cell stage. **H.** DIC image of 4-cell stage.

the size of the AC (Figs. 4.1A-B). Thus, the observed LIN-45::mNG signal is likely to be in the VPC, and not the nearby AC. This issue can be resolved in the future with conditional and VPC-specific degradation of LET-60, and perhaps the use of super-resolution confocal microscopy.

LIN-45::mNG started to disappear from the 1° cell at late Pn.p stage, 1-cell stage (Figs. 4. 1C-D). At the 2-cell and 4-cell stage when VPC fate patterning is completed, LIN-45::mNG is degraded in the daughters of P6.p, 1° cell (Figs. 4. 1E-H). This observation validates the published expression pattern of LIN-45 reporter, $P_{lin-31}::YFP::LIN-45$, which described targeted degradation of LIN-45 after initial induction (de la Cova and Greenwald, 2012). There, YFP::LIN-45 was not expressed in the daughters of presumptive 1° cell at 2-cell stage. It has been proposed that SEL-10/FBW7 negatively regulates LIN-45 in P6.p, 1° cell, through ubiquitination and degradation (de la Cova and Greenwald, 2012). Yet in this study, exogenously expressed YFP::LIN-45 was not observed to be recruited to the basolateral plasma membrane. We speculate that over-expression of signaling proteins can drown out the signal of sub-populations of protein that might be relocalized to specific subcellular compartments. Consequently, we will continue to use CRISPR-dependent tagging of endogenous proteins to track recruitment of putative LET-60 effectors

RGL-1/RalGEF was recruited apically in 2° cells, but not in 1° cell at late 1-cell stage.

Mammalian RalGEF is also shown to be recruited to the plasma membrane in cell culture system (Matsubara et al., 1999). And, activated RalGEF can be generated by adding the C-terminal membrane-targeting HVR+CAAX (hyper-variable region, Cys-Aliphatic-Aliphatic-any amino acid) from Ras to the C-terminus of RalGEF (Linnemann et al., 2002; Matsubara et al., 1999; Wolthuis et al., 1997). The membrane localization of RalGEF, like other Ras effectors, is important for its functional activity in mammalian cells. In *C. elegans*, LET-60/Ras-RGL-1/RalGEF-RAL-1/Ral is a modulatory signaling cascade for inducing 2° fate in VPC fate patterning (Zand et al., 2011). We tagged the endogenous RGL-1 with mNG and 3xFlag by CRISPR-Cas9 knock-in to examine potential subcellular localization of RGL-1 in the VPCs (Shin et al., 2018 submitted). mNG::RGL-1 is expressed in the cytoplasm in all cells of the animal, including vulval lineages (Figs. 4. 2A-B). We observed mNG::RGL-1 to be recruited to the apical plasma membrane in presumptive 2° cells, but not in 1° cells, at the late Pn.p stage prior to cell division (Figs. 4. 2C-D). mNG::RGL-1 is also localized to the apical plasma membrane in both 1° and 2° lineages at 2-cell and 4-cell stages (Figs. 4. 2E-H).

Based on the observation of mNG::RGL-1 localization in early vs. late Pn.p stage, we did blind tests with ~60 randomly captured images. Since there are no measurement tools for the time when LIN-3/EGF starts to secret to the VPCs from

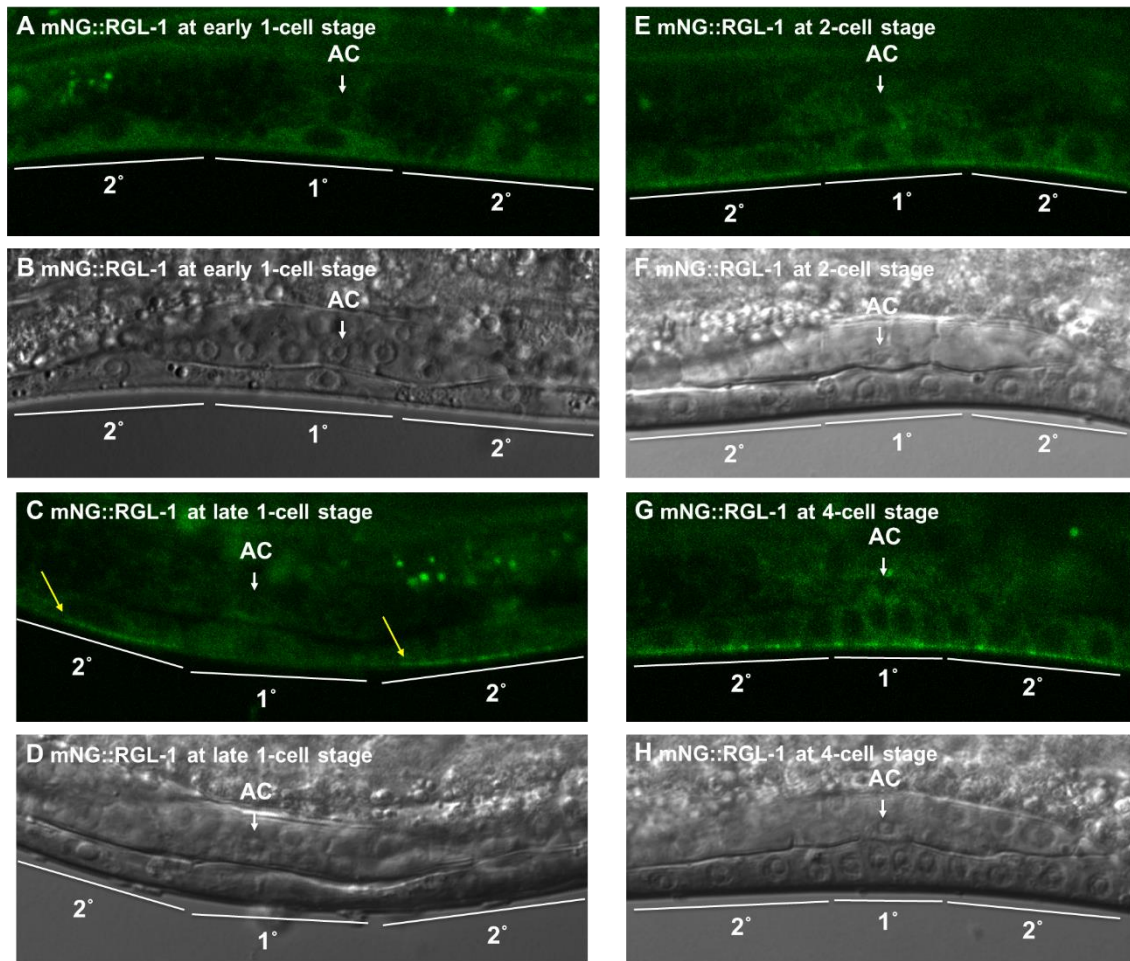


Figure 4. 2 Subcellular localization of mNG::RGL-1 in VPCs at different stages. **A.** mNG::RGL-1 is expressed in the cytoplasm of VPCs and the AC at early Pn.p,1-cell, stage. **B.** DIC image of early 1-cell stage. **C.** The mNG::RGL-1 is expressed in cytoplasm of 1° and 2° cells with enrichment at the apical membrane in 2° cells, but not in 1° cell. **D.** DIC image of late 1-cell stage showing that 1° cell is dividing. **E.** mNG::RGL-1 is expressed in the cytoplasm with apical enrichment in the daughters of 1° and 2° cells. **F.** DIC image of 2-cell stage. **G.** mNG::RGL-1 is expressed in cytoplasm and localized at the apical membrane and junctions in the daughters of 1° and 2° cells at 4-cell stage. **H.** DIC image of 4-cell stage.

the AC, we correlated before/after induction based on the length of gonad by DIC-based examination of the migration of distal tip cells (DTCs), at the leading point of each gonad arm, relative to VPC nuclei. If the DTCs were positioned between P3.p and P8.p, we inferred this to be early Pn.p stage, and before induction. If the DTCs had migrated further, we inferred this to be late Pn.p stage, and hence after induction. VPCs that had divided to yield two Pn.px cells were known to be post-induction. We divided the images into “no apical”, “apical”, and “uncertain” groups without knowing the stage of animals as assessed by DTC position, which is not visible in these confocal fluorescence images.

From the blind test, we found that most of the animals have no apical signal in the 1° and 2° cells, P5.p-P7.p, at early Pn.p stage, before induction (Figs. 4. 3A-C). However, at the late Pn.p stage, after induction, the apical localization of RGL-1 significantly increased in 2° cells, P5.p and P7.p, from ~10% to ~60%, but not in the 1° cell, P6.p (Figs. 4. 3D-F). We concluded that RGL-1 is apically localized in the 2° cells after LIN-3/EGF induction.

The RGL-1 apical localization is LET-60/Ras-dependent.

To validate the observed phenomenon of spatially and temporally dependent mNG::RGL-1 apical localization, tested whether this localization depended on functional LET-60/Ras. Since RaGEF binds to Ras through RA domain, we tested the RGL-1 apical localization is abolished by the LET-60 null mutant. *let-60(dx16)*

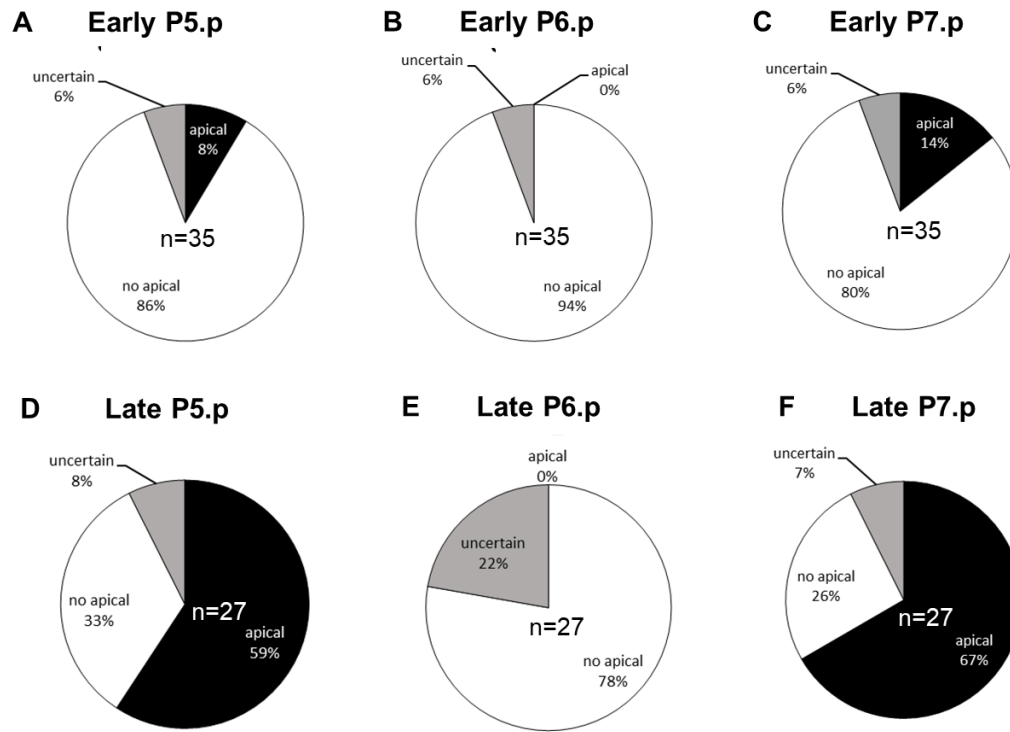


Figure 4. 3 mNG::RGL-1 is localized to the apical membrane in presumptive 2° but not 1° cells, and in late but not early VPCs. Each pie graph shows percentage of apical vs. no apical signal of mNG::RGL-1 in each VPCs. We divided the images into three groups, apical, no apical, and uncertain. The “uncertain” group means the image is not clear to say it is apical or no apical. **A-C.** mNG::RGL-1 in P5.p, P6.p, and P7.p at early L3 stage. Around 10% of animal show apical localization of mNG::RGL-1 in the presumptive 2° cells, P5.p and P7.p while the mNG::RGL-1 is in the cytoplasm with no apical localization in the presumptive 1° cell, P6.p. **D-F.** The apical localization of mNG::RGL-1 is increased in the 2° cells, P5.p and P7.p. Around 60% of animal show apical localization of mNG::RGL-1 in the 2° cells at late L3 stage while the mNG::RGL-1 is not localized to the apical membrane in 1° cell at late L3 stage.

let-60(dx16) confers severe sterility and lethality defects with a subset of homozygous larvae escaping lethality. Consequently, we had difficulty obtaining properly staged L3 animals from heterozygous *let-60(dx16)/nT1g* mothers (the balancing chromosome is GFP-tagged). Therefore, we used Pn.px (2-cell) stage animals, when mNG::RGL-1 was uniformly recruited to the apical plasma membrane (Figs. 4. 4A-B), to assess dependency of recruitment on LET-60 function. We observed that apical localization of mNG::RGL-1 was abolished in the *let-60(dx16)* background at 2-cell stage (Figs. 4. 4C-D). This result is

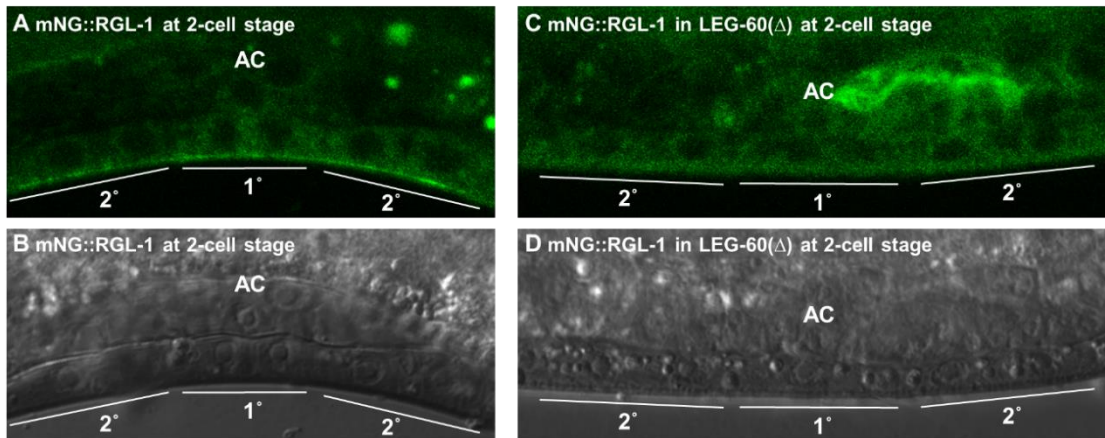


Figure 4. 4 The validation of mNG::RGL-1 apical localization system by using LET-60 null mutant. A. mNG::RGL-1 is in the cytoplasm with localization to the apical membrane in the daughters of 1° and 2° cells at 2-cell stage. **B.** DIC image of the mNG::RGL-1 at 2-cell stage. **C.** The apical localization of mNG::RGL-1 is abolished by LET-60 null mutant, *let-60(dx16)*, at 2-cell stage. **D.** DIC image of mNG::RGL-1 in *let-60(dx16)* at 2-cell stage.

consistent with mNG::RGL-1 localization being dependent on LET-60. Thus, we hypothesize that the apical and 2°-specific recruitment of endogenous mNG::RGL-1 to reflect activation of RAL-1 by LET-60 in response to graded signal.

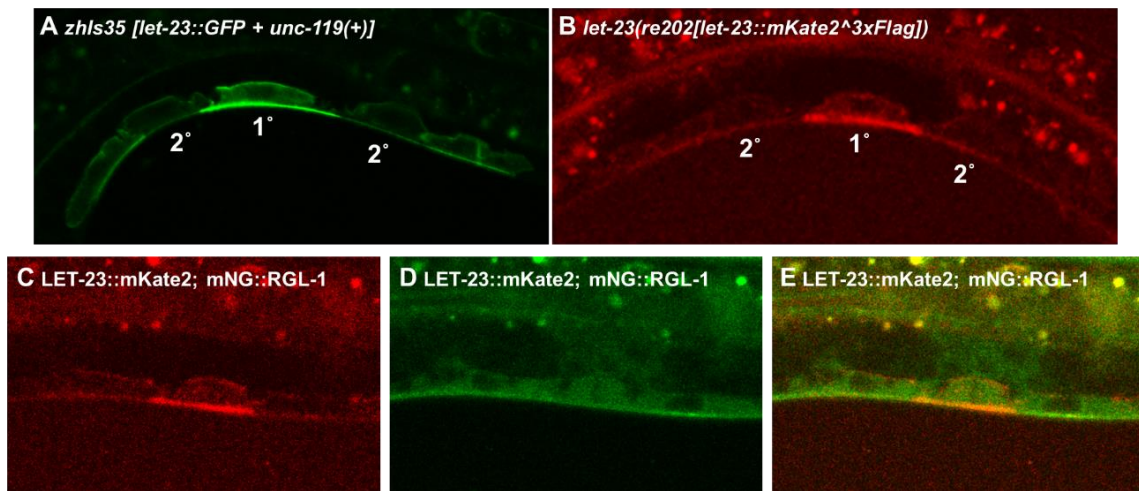


Figure 4.5 mNG::RGL-1 co-localizes with LET-23::mK2 at the plasma membrane.

A. *zhls35* [*let-23::GFP* + *unc-119(+)*] from Dr. Hajnal lab. LET-23::GFP is expressed at the plasma membrane in 1° and 2° cells at 1-cell, Pn.p, stage. The expression of LET-23::GFP is highly elevated in the 1° cell. **B.** *let-23(re202[let-23::mKate2^{3xFlag}])* generated by Dr. Tam Duong. The expression pattern is similar to the *zhls35*. LET-23::mKate2 is mostly at the plasma membrane in 1° and 2° cells with stronger expression in 1° cell at L3 stage. **C-E.** Images of *let-23(re202[let-23::mKate2^{3xFlag}]); rgl-1(re179[mNG^{3xFlag}::rgl-1])* at 1-cell stage. **C.** LET-23::mKate2 is localized at the plasma membrane in VPCs with elevated expression level in the 1° cell. **D.** mNG::RGL-1 is expressed in the cytoplasm with apical membrane localization in 2° cells, not in 1° cell. **E.** merged image of LET-23::mKate2 and mNG::RGL-1.

mNG::RGL-1 co-localizes with LET-23::mK2 at the plasma membrane.

LET-23/EGFR is localized at the plasma membrane in VPCs. *zhls35 [let-23::GFP + unc-119(+)]*, low copy number of LET-23::GFP, was expressed at the plasma membrane with higher expression in 1° cell (Haag et al., 2014; Fig. 4. 5A; image captured by Hanna Shin). Our lab generated endogenous tagged LET-23 with mKate2 and 3xFlag, *let-23(re202[let-23::mKate2^3xFlag])*, by CRISPR knock-in using Self-Excising Cassette (SEC) (Dickinson et al., 2015; kindly provided by T. Duong). We found that the expression pattern of endogenous tagged LET-23 is similar to LET-23::GFP. The LET-23 is mostly at the plasma membrane with high level of expression in 1° cell (Fig. 4. 5B). We generated double of LET-23::mKate2 and mNG::RGL-1 to see whether they are co-localized at the plasma membrane in VPCs. The LET-23::mKate2 and mNG::RGL-1 is at the plasma membrane in the 2° cells at 1-cell stage (Figs. 4. 5C-E).

mNG::RGL-1 apical localization may be functional.

The positioning of LET-23 to the basolateral membrane in 1° cell is an important mechanism of LET-23 functional activity to induce 1° fate (Kaeck et al., 1998; Simske et al., 1996; Whitfield et al., 1999). Basolateral localization of LET-23 is regulated by LIN-2/-7/-10 protein complex (Kaeck et al., 1998; Simske et al., 1996; Whitfield et al., 1999). Consequently, in the mutants of LIN-2/-7/-10, LET-

23 is mislocalized only at the apical membrane in all VPCs (Kaeche et al., 1998). *let-23(sy1)*, which deletes the last six amino acids, shows LET-23 localized only at the apical membrane in VPCs, suggesting that the C-terminus of LET-23 is important for interaction with LIN-2/-7/-10 protein complex, probably via the PDZ domain of LIN-7 recognizing the PDZ recognition sequence at the C-terminus of LET-23 (Kaeche et al., 1998). Both LIN-2/-7/-10 mutant and *let-23(sy1)* has vulvaless phenotype because of failing to 1° fate induction (Kaeche et al., 1998; Simske et al., 1996; Whitfield et al., 1999).

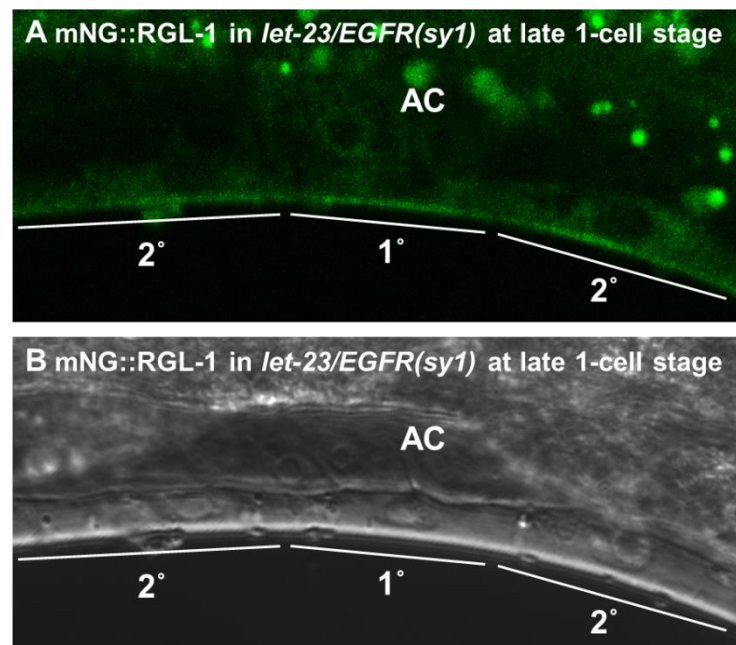


Figure 4.6 mNG::RGL-1 is localized to the apical membrane in VPCs in *let-23(sy1)* background. **A.** mNG::RGL-1 is expressed in the cytoplasm with enrichment at the apical membrane in VPCs in the *let-23(sy1)* background at late 1-cell, Pn.p, stage. **B.** DIC image of mNG::RGL-1 in *let-23(sy1)* at late 1-cell stage.

We evaluated mNG::RGL-1 localization in the *let-23(sy1)* mutant. We observed that mNG::RGL-1 was localized to the apical plasma membrane in P5.p-P7.p, consistent with the apical mis-localization of LET-23 in VPCs as a consequence of the *sy1* mutation (Figs. 4. 6A-B). In a wild-type background, these VPCs typically assume the 2°-1°-2° pattern. But in the absence of successful induction of 1° fate in the *let-23(sy1)* background, P6.p, presumptive 1° cell, permits the recruitment of a putative 2°-promoting signal. These results suggest that *let-23(sy1)* mutant receptor retains the ability to recruit RGL-1 to the apical plasma membrane, despite *let-23(sy1)* being insufficient to promote 1° fate. These results also suggest that an induced 1° cell enacts some mechanism to block the theorized 2°-promoting recruitment of RGL-1 to the apical plasma membrane. These observations raise testable hypotheses that I will discuss in the Discussion section.

Discussion

We found that LET-60/Ras effectors that function to promote different VPC fates are recruited to different subcellular locations in VPCs. LIN-45/Raf is localized to the basolateral membrane in 1° VPCs at the Pn.p (1-cell) stage, while RGL-1/RalGEF is recruited to the apical membrane in 2° VPCs at the Pn.p stage. Preliminary results suggest that recruitment of the two different effectors is temporally distinct, with LIN-45 recruited earlier than RGL-1. This asynchrony of

recruitment may represent a spatial representation of the morphogen gradient, but more data analysis will be needed to confirm this observation. Here, we discuss about validation and functional activity of RGL-1 recruitment to the membrane, improvement of our tools/systems technically, and potential mechanisms.

LIN-45 localization at the basolateral membrane in 1° cell and LIN-45 expression pattern in VPCs.

LIN-45::mNG is present in the cytoplasm of presumptive 1° and 2° cells with enrichment at the basolateral membrane only in 1° cell, but not in 2° cells. LIN-45::mNG started to disappear in the presumptive 1° VPC after basolateral recruitment, and was mostly absent by the Pn.px (2-cell) stage. This putative post-induction degradation of LIN-45 from 1° cell is governed by SEL-10/FBW7-mediated ubiquitination and degradation (de la Cova and Greenwald, 2012). The degradation of LIN-45 was hypothesized to be a negative feedback loop of 1°-promoting signal in VPC fate patterning.

Fluorescent signal from mNG::RGL-1 and LIN-45::mNG I was relatively weak even when using a confocal microscope. Therefore, we will attempt to improve our tools with two strategies to improve signal-to-noise ratio. First, we will tag endogenous LIN-45 and RGL-1 with mNG::mNG double tag to get stronger signal of these effectors. Second, we will tag downstream signaling partners in case the

signal is amplified downstream. Downstream of LIN-45 is the MEK-2/MAPK2 and the Raf-MEK scaffold protein KSR-1 (Kornfeld et al., 1995b; Sundaram and Han, 1995), either of which might both be recruited and provided a stronger signal. For LIN-45::mNG, via CRISPR we will introduce the L429A/L431A mutations of the Cdc4 Phosphodegron (CPD) target of SEL-10/FBW7, which in ectopically expressed protein stabilized LIN-45 (de la Cova and Greenwald, 2012). As an alternative, we will work in a *sel-10* mutant background, with the caveat that SEL-10 also represses LIN-12/Notch signaling, and thus could disrupt the signaling network (Deng and Greenwald, 2016a; Hubbard et al., 1997). Downstream of RGL-1 we will tag RLBP-1 (RalBP1; reviewed in Gentry et al., 2014), a conventional target of RAL-1 that may provide a stronger and less variable reporter for spatial activation of LET-60-RGL-1 activation. Each new tag will be subjected to validation. For example, localization of tagged RLBP-1 should be abrogated by a mutation in *ral-1*.

mNG::RGL-1 is localized to the apical membrane in 2° cells, not in 1° cell, at late 1-cell stage, and daughters of 1° and 2° cells at 2-cell stage.

We did not expect to see that plasma membrane recruitment of RGL-1 is polarized to the apical surface of presumptive 2° VPCs. We propose that the spatial regulation of LIN-45 vs. RGL-1 recruitment represents a major mechanism of Ras effector switching. We hypothesize that the regulators or scaffold proteins

between LET-60 and RGL-1 are polarized so that the RGL-1 is recruited to the membrane-bound LET-60 at the apical surface of 2° cells. We will further discuss hypothesis below in Discussion.

We also observed that RGL-1 is apically localized in daughters of both 1° and 2° cells at the Pn.px (2-cell) and Pn.pxx (4-cell) stage. The VPC fate patterning occurs during the second half of the Pn.p (1-cell) stage, though even after the first cell division ectopic EGF/LIN-3 induction can reverse cell fate induction. The reason why we see the apical localization of RGL-1 at the Pn.px (2-cell) stage may be that RGL-1 functions in defining sub-lineages and morphogenesis later in vulva development. Another explanation would be RGL-1 maintains 2°-promoting signal in the daughters of 2° cells after VPC fate patterning for fidelity of fate decision. The apical localization of RGL-1 in the daughters of 1° cell may not function as a 2°-promoting signal because of the negative regulators of LET-60-RGL-1-RAL-1-GCK-2-PMK-1 signaling cascade, such as RalGAP or PMK-1/p38 phosphatase, so this activity may be quenched or signal through another, non-2°-promoting effector of RAL-1.

Validation of the RGL-1 recruitment system.

RGL-1 is also apically localized in the daughters of 1° and 2° cells at 2-cell stage. As we expected, this apical localization of RGL-1 is abrogated by LET-60 null mutant, *let-60(dx16)*. Because few *dx16* mutant animals survive to the L3

stage and the time window of 2°-specific mNG::RGL-1 recruitment is short, we were not be able to validate RGL-1 localization system at 1-cell stage. Therefore, we will generate conditional LET-60 knock-out by using Auxin-Inducible Degradation (AID) system to validate RGL-1 recruitment system (Zhang et al., 2015). By using AID system, degron tagged target protein can be degraded by a TIR1 protein, which is modified from *Arabidopsis* protein, in the presence of auxin (Zhang et al., 2015). We are tagging endogenous LET-60 with degron by CRISPR knock-in in the TIR1-expressing animals. Since LET-60 is critical for development prior to the L1 stage, we will delete LET-60 conditionally post-embryonically by treating auxin at L1 or L2 stage. We will use this tool to conclusively validate RGL-1 recruitment to the membrane in VPCs.

In addition, RGL-1 recruitment to the plasma membrane will be validated by RA dead mutation in RGL-1. RalGEF was identified by screening of Ras interacting proteins (Hofer et al., 1994; Kikuchi et al., 1994; Spaargaren and Bischoff, 1994), and RalGEF interacts with Ras through the RA (Ras Association) domain (Kishida et al., 1997; Matsubara et al., 1999; reviewed in Feig et al., 1996). Missense RA mutations have been shown to abrogate mammalian Ras interaction with RalGEF (Huang et al., 1998; Linnemann et al., 2002; Vetter et al., 1999). Therefore, the RA dead mutation is expected to disrupt RGL-1 recruitment to the plasma membrane in VPCs. We will generate RA dead mutation in the mNG::RGL-1 by CRISPR knock-in.

Does RGL-1 apical localization mean it is functionally active?

In *let-23(sy1)* mutant and LIN-2/-7/-10 mutants, LET-23 is mislocalized to the apical membrane in VPCs, and no longer can be found at the basolateral surface (Kaech et al., 1998). The LET-23 and LIN-2/-7/-10 mutants have a vulvaless phenotype, suggesting that basolateral localization of LET-23 is important for 1° fate induction and that *let-23(sy1)* is non-functional (Kaech et al., 1998; Simske et al., 1996; Whitfield et al., 1999). We observed RGL-1 is localized to the apical membrane of VPCs in *let-23(sy1)* mutant background, but now in P5-7.p, suggesting the 1° fate is necessary to prevent RGL-1 recruitment in P6.p. We will use *let-23(sy1)* to test whether apical localization of RGL-1 results in a functional 2°-promoting signal. We will test whether *let-23(sy1)* has 2°-promoting activity in the genetically sensitized background. We previously used *lin-12(n379d)*; *lin-15(n765ts)* as a sensitized background to control EGF-dependent 2°-promoting signal (Shin et al., 2018; Zand et al., 2011). We will test whether the *let-23(sy1)* abolishes induction of ectopic 2°s in the *lin-12(n379d)*; *lin-15(n765ts)* background. If not, we will test in the *lin-12(n379d)*; *let-23(sy1)*; *lin-15(n765ts)* triple mutant whether increased ectopic secondaries are RGL-1-dependent by using RNAi of *rgl-1* or RGL-1 deletion mutants. We hypothesize that apical localization of RGL-1 functions to promote 2° fate, which also argues that *let-23(sy1)* still transduces the 2°-promoting signal but just fails to transduce the 1°-promoting signal for 1° fate induction. We will further test whether LIN-2/-7/-10 mutation shows RGL-1

apical localization and is functional in the same genetically sensitized background, *lin-12(n379d); lin-15(n765ts)*.

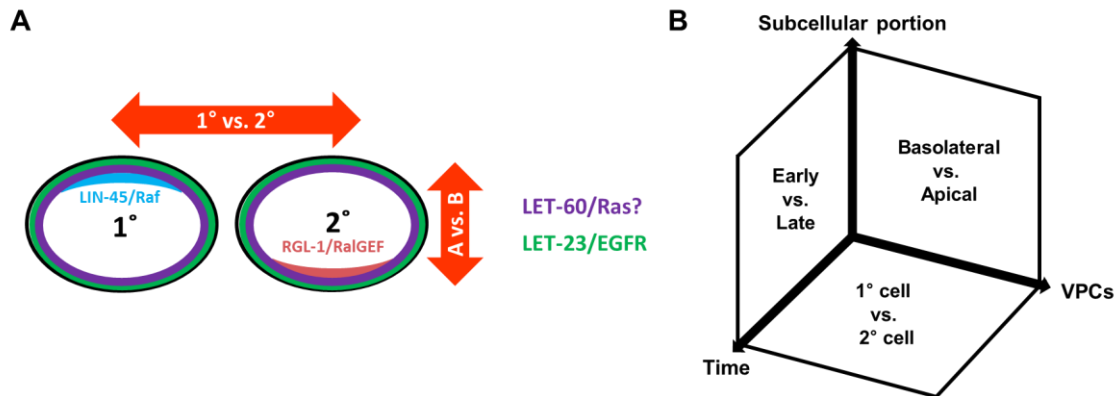


Figure 4.7 Three axes of Ras effectors recruitment to the membrane. A. LET-60/Ras effectors are segregated in VPCs. LET-60/Ras (purple) is probably at the plasma membrane in 1° and 2° cells. LET-23/EGFR (green) is also at the plasma membrane in VPCs. LIN-45/Raf (light blue) recruitment has been shown to be at the apical membrane in 1° cell while RGL-1/RalGEF (pink) is recruited to the apical membrane in 2° cells. **B.** Three dimensional axes of LET-60/Ras effector recruitment. Three axes show differential factors that affect LET-60/Ras effector recruitment to the membrane. LIN-45/Raf and RGL-1/RalGEF are segregated based on subcellular portion (basolateral membrane vs. apical membrane), time (early 1-cell stage vs. late 1-cell stage), and different VPCs (1° cell vs. 2° cell).

Potential mechanisms of effector segregation.

Here we discuss potential mechanisms of LET-60/Ras effector switching. There are three axes that make different LET-60 effectors to be recruited to the membrane differently (Figs. 4. 7A-B). First axis is different cells, 1° cell versus 2° cell (Fig. 4. 7B). LIN-45/Raf is recruited to the plasma membrane in the 1° cell while RGL-1/RalGEF is recruited to the plasma membrane in the 2° cells. LET-60-LIN-45 is a 1°-promoting signal while LET-60-RGL-1 is a 2°-promoting signal in VPC fate patterning. We hypothesize that phosphorylation of RGL-1 regulates recruitment to the plasma membrane. RalGEF has REM domain, CDC25 domain, and RA domain, which protein sequences are conserved between species. The RA domain is highly conserved between mammals, *Drosophila*, and *C. elegans* (Fig. 4. 8). There is a potential phosphorylation site, Serine-Proline (SP), right after the RA domain in the *C. elegans* RGL-1 protein sequence (Fig. 4. 8) in the “phosphopep” database (<http://www.unipep.org/phosphopep/index.php>). And, the potential phosphorylation site “SP” is conserved between human RGL3 and *C. elegans* RGL-1. The Serine-Proline sequence has been shown as a consensus phosphorylation site for CDKs or MAPKs (Scansite 3). The LET-60/Ras-LIN-45/Raf-MEK-2/MEK-MPK-1/ERK is activated in presumptive 1° cell to promote 1° fate. However, the 1°-promoting MPK-1/ERK is inhibited by ERK phosphatase LIP-1/MKP in the presumptive 2° cells to prevent the presumptive 2° cells from adopting 1° fate. We hypothesize that MPK-1 regulates phosphorylation of RGL-

		RA domain
D_RGL	SHNGTTNGGSPHINAQLVQPSSGTPHSAP	DFYIIIRVTYETDNIELDGIVLYKSIMLGNN
D_RGL-Isoform E	SHNGTTNGGSPHINAQLVQPSSGTPHSAP	DFYIIIRVTYETDNIELDGIVLYKSIMLGNN
H_RGL1	VSVTSITSTVLPPVYNQ-----	NEDTCIIRISVED-----NNGNMYKSIMLTSQ
H_RalGDS	VSGLCNSSSALP-LYNQQ-----	VGDCCIIRVSLDV-----DNGNMYKSILVTSQ
H_RGL2	ASCGSPLSGGAEASGGTGYGEGSGPGAS	DCRIIRVOMELG-----EDGSVYKSILVTSQ
H_RGL3	LDLPSRPFALPLGSPRIPLPA	QCS-----SEARVIRVSIDN-----DHGNLYRSILLTSQ
C_RGL-1	VFSHQKKGSDASSCSSSSSLANGNSQAQN	SFYLARVGLDDDLQN-----TDGANYKCIKIENG
		. : * : : * : .
D_RGL	ERTPQVIRNAMIKLGLEDD-PDRFTLAQVLP-DKELVMPKNANVYYAVN---	TNYNLNFI
D_RGL-Isoform E	ERTPQVIRNAMIKLGLEDD-PDRFTLAQVLP-DKELVMPKNANVYYAVN---	TNYNLNFI
H_RGL1	DKTPAVICRAMIKHNLDSDPAEYELVQVISEDKELVIPDSANVFYAMN---	SCVNFDFI
H_RalGDS	DKAPAVIRKAMIKHNLEEEEPEDYELLQILSDDRKLKIPENANVFYAMN---	STANYDFV
H_RGL2	DKAPSVISRVLKNNRDSAVASEHELVQLLPGERELTIPASANVFYAMD---	GASHDFLL
H_RGL3	DKAPSVVRRALCKHNVPQFWACDYQLFQVLPGDRVLLIPDNANVFYAMS---	PVAPRDFM
C_RGL-1	DRMPQLVARALEKHLIEDD-KNTYLLVQLLPRGGEFVLPDNCNPFYAMAPDPTSPMLNLI	
		:: * :: . : * . * * : . : : * . * : * : : :
D_RGL	LRPRKEEGVAGS-----	
D_RGL-Isoform E	LRPRKEEGVAGSSTAVPLS-----QLWC LGYE GEE-----	
H_RGL1	LRKKNSMEEQVKLRRTSLT-----LPRTAKRGCSNRHSKITL	
H_RalGDS	LKKR-TETKGVKVKHGASST-----LPRMKQKGLKIAKGIF---	
H_RGL2	RQRRSSSTATPGVTSGPSASGTPPSEGGGGSFPRIKATGRKRIARLF---	
H_RGL3	LRRKEGTRNTLSV-SPS-----	
C_RGL-1	LRKRDGNGTIEGGASPLQGP-----SAKKLNRMKRTNLLRWSSGYL---	
		: :

Figure 4. 8 RGL-1/RalGEF RA domain is conserved between species. The identity of RA domain sequences of four human RalGEF, RalGDS, RGL1, RGL2, and RGL3, two *Drosophila* RalGEFs, RGL and RGL2 (Isoform E), and single *C. elegans* RalGEF, RGL1, are determined by CLUSTALW multiple sequence alignment. Green box shows RA domain. The lysine (K) residue in read box is identical between species. The serine-proline (SP) residues are a potential phosphorylation site for CDKs and MAPKs and conserved between human RGL3 and *C. elegans* RGL-1.

1 in the 1° cell. The phosphorylated RGL-1 may not be able to bind to membrane-bound LET-60 in the 1° cell. However, the phosphorylation event on RGL-1 may be abolished by 1°-antagonizing LIP-1, MPK-1/ERK phosphatase, function in the 2° cells. Therefore, the un-phosphorylated RGL-1 could be recruited to the plasma

membrane in 2° cells. We will test whether phospho-mimetic or phospho-defective mutation in RGL-1 by CRISPR knock-in affects the localization of RGL-1 at the apical membrane in VPCs. We will also test whether the potential kinase, MPK-1, or phosphatase, LIP-1, regulates localization of RGL-1 in VPCs cell biologically.

Second, LET-60/Ras effectors are recruited to different subcellular location in presumptive 1° vs. presumptive 2° VPCs (Fig. 4. 7B). Ras is known to have variable interactions with effectors in cancer (Yuan et al., 2018). Ras interacts with effectors through Ras Binding or Ras Association domain (RBD or RA domain) (McCormick and Wittinghofer, 1996). The scaffold protein between Ras and Ras effectors may spatially regulate the interaction between Ras and Ras effectors. *C. elegans* SOC-2/SUR-8 functions downstream of or parallel to LET-60/Ras genetically (Li et al., 2000; Sieburth et al., 1998). Mammalian Shoc2, an ortholog of *C. elegans* SOC-2/SUR-8, functions as a scaffold protein between Ras and Raf (Li et al., 2000; Sieburth et al., 1998). Thus, recruitment of LIN-45 to the basolateral membrane in 1° cell could be mediated by the scaffold protein SOC-2/SUR-8, or that SOC-2/SUR-8 excludes RGL-1 recruitment to the basolateral compartment.

We hypothesize that RGL-1 2°-specific apical recruitment by LET-60 is regulated by LET-413, an ortholog of mammalian Erbin and *Drosophila* Scribble. Erbin/Scribble shares remarkable sequence identity with Shoc2/SOC-2/SUR-8 through their LRR (Leucine-rich repeats) domains, which in human shoc2 forms the binding interface with Ras and Raf (Jang and Galperin, 2016). Erbin down-

regulates ERK activation by Ras-Raf (Huang et al., 2003). Erbin has been shown to be a negative regulator of Shoc2 scaffolding of Ras and Raf in mammalian cells, interacting with GTP-bound Ras to sequester interaction of Ras with Raf through Shoc2 (Dai et al., 2006). However, RalGEF interaction with Erbin has not been tested in any system. An interesting model is that these two antagonistic LRR-domain proteins, SOC-2/SUR-8/Shoc2 vs. LET-413/Scribble/Erbin, function to restrict LET-60/Ras interactions with its two antagonistic effectors, LIN-45 and RGL-1. We will test whether the apical recruitment of RGL-1 and basolateral recruitment of LIN-45 is mediated by LET-413. We will use VPC-specific RNAi depletion of LET-413 to assess disruption of apical vs. basolateral recruitment events. We will additionally use VPC-specific RNAi to determine whether LET-413 has 2°-promoting activity in genetically sensitized background. We will use CRISPR to tag endogenous LET-413 with Auxin-inducible degron, fluorescent protein, and an epitope tag, combined with VPC-specific expression of the TIR1 co-factor, to degrade LET-413 specifically in VPCs just prior to induction.

Other scaffold proteins or regulators may control segregation of LET-60 effectors. Therefore, we will use co-immunoprecipitation followed by mass spectrometry (IP-mass spec) to proteins that come down with both tagged LET-60 and tagged RGL-1. Though IP-mass spec is notoriously promiscuous, we propose that the set of proteins lped as coincident partners of both LET-60 and RGL-1 is very small. We will genetically test whether the candidates show 2°-promoting activity in genetically sensitized background and whether the mutant or

RNAi of candidates abolishes apical localization of RGL-1 in VPCs cell biologically.

Yet identification of partners that impose polarity on effector usage, while important, probably still leaves open the question of what system imposes polarity on those partners. The obvious candidates would be the PAR genes, which control cell polarity throughout metazoans, but were discovered in *C. elegans* (Kemphues, 2000; Thompson, 2013). Yet little is known of VPC polarity. Depletion of PAR-1 results in disrupted vulval morphogenesis, and PAR-1 is localized to the adherens junctions of VPCs prior to induction (Hurd and Kemphues, 2003). PAR-1 is also thought to repress 1° induction at the level of LIN-45/Raf and KSR-1 (Yoder et al., 2004). Yet the role of establishment and maintenance of polarity in VPCs has not been determined, nor has the PAR complex been visualized. We will consider whether the PAR complex plays an important role in establishing polarity of effector usage. By comparison to other epithelial systems, we would expect PAR-3, PAR-6 and aPKC to function apically, while PAR-1 could function basolaterally (Thompson, 2013). Interestingly, Scribble (LET-413 and Erbin) has been associated with PAR-1 and the basolateral cellular compartment in *Drosophila* (Bilder and Perrimon, 2000), counter to our model that LET-413/Scribble would scaffold LET-60 and RGL-1 apical recruitment. In light of this connection, perhaps LET-413 functions to exclude RGL-1 from the basolateral compartment. Yet we will need to examine the consequences of RNAi depletion and localization of PAR components, including LET-413/Scribble, to inform further hypotheses and tests.

Third axis of polarized effector segregation is time (Fig. 4. 7B). Different LET-60 effectors are recruited to the plasma membrane at different time points. Based on preliminary data, we think LIN-45 is recruited to the basolateral membrane at early 1-cell stage while RGL-1 is recruited to the apical membrane at late 1-cell stage. We hypothesize that LET-60 effector segregation at different times is regulated by the time at which inductive signal starts to signal through LET-60-LIN-45 for 1° fate or LET-60-RGL-1 for 2° fate. In other words, the different times of LIN-45 vs. RGL-1 effector recruitment reflect the sequential induction model, suggesting that some consequence of LIN-12/Notch lateral signal is necessary to permit recruitment of RGL-1 to the apical compartment in presumptive 2° cells. We will test this idea by observing RGL-1 recruitment in the LIN-12 null mutant background.

Materials and Methods

C. elegans handling and genetics.

All strains used are shown in Table 4. 1. The strains were derived from the N2 wild type. Nomenclature was used as described (Horvitz et al., 1979). Animals were cultured at 20°C using standard conditions on OP50 bacteria on NGM agar plates (Brenner, 1974).

CRISPR/Cas9-mediated genome engineering.

The RGL-1 CRISPR knock-in to tag endogenous RGL-1 with mNG and 3xFlag was described in the Chapter 3 (Shin et al., 2018, submitted). To tag endogenous LIN-45 with mNG and 3xFlag and endogenous LET-23 with mKate2 and 3xFlag, Self Excising Cassette (SEC) strategy was used (Dickinson et al., 2015). The sgRNA targeting sites were selected by using MIT-CRISPR web-site (<http://crispr.mit.edu/>) based on the sgRNA score and off target effect. Two sgRNA sites were used for both LIN-45 and LET-23 CRISPR (LIN-45 sgRNA targeting sequences: #1 GTATGCCTTCTTGTTAGCAGCGG, #2 TATCGGGATGGGTGATGAGGGGG and LET-23 sgRNA targeting sequences: #1 TGGTTCATTGTAATATCCAGAGG, #2 TGTATGAGATGAATGGCAACGGG). The sgRNA sequences were inserted into the Cas9-sgRNA plasmid, pJW1236, by Q5 site-Directed Mutagenesis (NEB) (Ward, 2015). And, the repair template plasmid was generated by amplifying ~500 bp of homology arms from N2 genomic DNA (NEB Q5 polymerase), digesting of the target SEC vector, pDD268, and Gibson Assembly (NEB) directed by homologous ends. The primers used for amplification of homology arms in the repair template are listed in Table 4. 2. The mNG^{3xFlag}::LIN-45 was generated by microinjection of sgRNA-Cas9 #1 (50 ng/μl), sgRNA-Cas9 #2 (50 ng/μl), repair template (10 ng/μl), and injection marker *P_{myo-3}::gfp* (10 ng/μl) into N2 animals. And, the LET-23::mKate2^{3xFlag} was generated by microinjection of sgRNA-Cas9 #1 (43.5 ng/μl), sgRNA-Cas9 #2

(11.8 ng/μl), repair template (10 ng/μl), and injection marker $P_{myo-2}::gfp$ (10 ng/μl) into N2 animals. Animals were picked, treated with 5 mg/ml hygromycin, and heat-shocked followed by the protocol from Dickinson et al., 2015. The CRISPR knock-in results were confirmed by genotyping PCR using Taq PCR Master Mix (QIAGEN). The *lin-45(re208[mNG^{3xFlag}::lin-45])* and *let-23(re202[let-23::mKate2^{3xFlag}])* sequences were confirmed by sanger sequencing (Genewiz).

Imaging with fluorescent microscope.

Early L2 to late L3 stage animals were mounted in 5 mM sodium azide/M9 buffer on slides with 3% agar pad. The images were captured by A1si Confocal Laser Microscope (Nikon) using NIS Elements Advanced Research, Version 4.40 software (Nikon).

Table 4. 1 Strains for effector switching mechanism study

Strain	Genotype	Used in Figures
DV3312	<i>rgl-1(re179[mNG^{3xFlag}::rgl-1])</i> X	Fig. 4. 2A-H, 4. 4A-B
DV3386	<i>lin-45(re208[mNG^{3xFlag}::lin-45])</i> IV	Fig. 4. 1A-H
DV3352	<i>let-60(dx16)/nT1g</i> IV; <i>rgl-1(re179[mNG^{3xFlag}::rgl-1])</i> X	Fig. 4. 4C-D
AH1747	<i>unc-119(ed3)</i> III; <i>zhls35</i> [<i>P_{let-23}::LET-23::GFP</i> ; <i>unc-119(+)</i>]	Fig. 4. 5A
DV3366	<i>let-23(re202[let-23::mKate2^{3xFlag}])</i> II	Fig. 4. 5B
DV3396	<i>let-23(re202[let-23::mKate2^{3xFlag}])</i> II; <i>rgl-1(re179[mNG^{3xFlag}::rgl-1])</i> X	Fig. 4. 5C-E
DV3343	<i>let-23(sy1)</i> II; <i>rgl-1(re179[mNG^{3xFlag}::rgl-1])</i> X	Fig. 4. 6A-B

Table 4. 2 Primers for effector switching mechanism study

Name	Sequence	Use
DJR769	5' -CACCTCCTATTGCGAGATGTCTTG-3'	Universal Mutagenesis PCR primer for sgRNA plasmid
NR140	5' -GTATGCCTTCTTGTTAGCAGGTTTAA GAGCTATGCTGGAAACAG- 3'	Mutagenesis PCR primer for mNG::3xFlag::LIN-45 CRISPR sgRNA #1 plasmid
NR141	5' -TATCGGGATGGGTGATGAGGGTTTA AGAGCTATGCTGGAAACAG- 3'	Mutagenesis PCR primer for mNG::3xFlag::LIN-45 CRISPR sgRNA #2 plasmid
NR136	5' -ACGTTGTAAAACGACGGCCAGTCGC CGGCAAGATCAGATATTGTTTATGGTT GGAAGAGG- 3'	Primer for amplifying upstream homology arm to generate repair template (mNG::3xFlag::LIN-45 CRISPR)

Table 4. 2 Continued

Name	Sequence	Use
NR137	5' -CATCGATGCTCCTGAGGCTCCCGAT GCTCCAATGAGACCATAGACATTGTAG TATGCC- 3'	Primer for amplifying upstream homology arm to generate repair template (mNG::3xFlag::LIN-45 CRISPR)
NR138	5' -TTACAAGGATGACGATGACAAGAGA TAGTTTTATTTTGTGTTTTTTTTTTGAAAA TCAAGG- 3'	Primer for amplifying downstream homology arm to generate repair template (mNG::3xFlag::LIN-45 CRISPR)
NR139	5' -GGAAACAGCTATGACCATGTTATCG ATTTCTAAAATAAATGGAAGTTTCAAAA TGTGTTC- 3'	Primer for amplifying downstream homology arm to generate repair template (mNG::3xFlag::LIN-45 CRISPR)
NR145	5' -TGAGAAGCCAAATGCTTTCC- 3'	<i>lin-45(re208)</i> genotyping
NR146	5' -GAAGTCGACTCCGTTGATGG- 3'	<i>lin-45(re208)</i> genotyping
NR147	5' -TACATATTCGGGGAGAGACG- 3'	<i>lin-45(re208)</i> genotyping
TD241	5' -TGGTTCATTGTAATATCCAGGTTTAA GAGCTATGCTGGAAACAG- 3'	Mutagenesis PCR primer for LET-23::mKate2 ^{3xFlag} CRISPR sgRNA #1 plasmid
TD242	5' -TGTATGAGATGAATGGCAACGTTTA AGAGCTATGCTGGAAACAG- 3'	Mutagenesis PCR primer for LET-23::mKate2 ^{3xFlag} CRISPR sgRNA #2 plasmid
TD237	5' -CCCAGTCACGACGTTGTAAAACGAC GGCCAGTCGCCGGCACGGAGCCTTTT GATTGTAAG- 3'	Primer for amplifying upstream homology arm to generate repair template (LET-23::mKate2 ^{3xFlag} CRISPR)

Table 4. 2 Continued

Name	Sequence	Use
TD238	5' -GGAGACCATCGATGCTCCTGAGGC TCCCGATGCTCCAGGTTTTTTAGTTTTG AGATGTGG- 3'	Primer for amplifying upstream homology arm to generate repair template (LET-23::mKate2 ^{3xFlag} CRISPR)
TD239	5' -GCGTGATTACAAGGATGACGATGAC AAGAGAGGAAGCGGAGAAACATCAGA AGAGGCTGA- 3'	Primer for amplifying downstream homology arm to generate repair template (LET-23::mKate2 ^{3xFlag} CRISPR)
TD240	5' -TTCACACAGGAAACAGCTATGACCA TGTTATCGATTTTCGTCTTGAAAGCAACA GAAGAAG- 3'	Primer for amplifying downstream homology arm to generate repair template (LET-23::mKate2 ^{3xFlag} CRISPR)
TD243	5' -GATCTGATGAATCGAATGCAATCAG- 3'	<i>let-23(re202)</i> genotyping
TD244	5' -CCTCCATGTAGAGCTTCATATGC- 3'	<i>let-23(re202)</i> genotyping
TD245	5' -GTACAAGACAACGAAGACCCG- 3'	<i>let-23(re202)</i> genotyping

CHAPTER V

CONCLUSIONS AND REMARKS

The LET-60/Ras-RGL-1/RalGEF-RAL-1/Ral modulatory signaling cascade induces 2° fate in support of LIN-12/Notch in *C. elegans* VPC fate patterning (Zand et al., 2011). The mechanism how LIN-3/EGF morphogen gradient induces 2° fate in support of LIN-12 was an interesting question for a long time (Kenyon, 1995). This system provides a framework for studying downstream Ral signal transduction, mechanisms of effector switching, and principles of network orchestration in a live animal (Reiner, 2011).

We explored the cascade downstream of 2°-promoting RAL-1 signaling. EXOC-8/Exo84, an inessential component of the exocyst complex, mediates the RAL-1 2°-promoting signal in VPC fate patterning. GCK-2, a CNH-containing MAP4 kinase, functioned downstream of RAL-1-EXOC-8 to signal through PMK-1/p38 MAP kinase to promote 2° fate in support of LIN-12. Constitutively activated RAL-1 was sufficient to induce ectopic 2° cells in a genetically sensitized background. Genetic perturbation of GCK-2, EXOC-8, and PMK-1 phenocopied the loss of RAL-1 function and blocked the phenotype of mutationally activated RAL-1. Endogenous GCK-2 and PMK-1 tagging with fluorescent protein revealed expression in the VPCs. RAL-1 and GCK-2 function cell autonomously in the VPCs. EXOC-8 and GCK-2 function as atypical effectors of RAL-1: unlike most effectors, GCK-2 is not recruited to the membrane-bound RAL-1 in VPCs. We

hypothesize that RAL-1, along with potentially hundreds of other proteins, interacts with EXOC-8 in the cell. Consequently, RAL-1 downstream signaling partners, like GCK-2, may be activated via coincident localization and/or co-activating kinases.

Our discovery of a RAL-1 downstream signaling cascade is useful in three ways. First, we have extended the RAL-1 2°-promoting signal through a p38 MAP kinase cascade, thus providing interesting perspective on how the EGF gradient signal is transduced. Of equal interest is extending our knowledge of this cascade to its mechanistic output. Second, Identification of a p38 cascade downstream of Ral, which has not been done in any other system, provides potential phosphorylated biomarkers that could be screened in Ral-positive human tumors, starting with Ras-positive tumors. We draw a comparison with phospho-Akt and Phospho-ERK, which are routinely surveyed for activated effector status in Ras-positive tumors. Third, if this p38 cascade was validated in tumors, it would provide a four-kinase cascade of potential druggable targets downstream of Ral. Additionally, our development of the constitutively active endogenous RAL-1 has identified other RAL-1-mediated functions outside of VPCs that appear to be independent of GCK-2 (data not shown). We propose that we identified an area of signaling richness that has not previously suspected.

Mutational analysis of RGL-1 reveals two unexpected pictures of RalGEF. First, RGL-1 is not essential, while RAL-1 is essential. RAL-1 appears to be a key component of the exocyst complex: deletion of RAL-1 reveals function in cell

polarity, embryonic development and germline activity (Armenti et al., 2014). In contrast, multiple deletions of RGL-1 are superficially wild type. Given the exclusive relationship between RalGEF and Ral in other systems (Camonis and White, 2005), RAL-1 activation is expected to depend solely on RGL-1. Therefore, we hypothesize that the proposed function of RAL-1 as a core component of the exocyst complex is independent of its GDP/GTP bound state. This observation is supported by previous analysis from our lab that shows that perturbation of the heterodimeric RalGAP also results in healthy animals. However, we cannot rule out the possibility that there exist other Ral-specific GAPs in the genome.

We additionally found that RGL-1 performs RAL-1-dependent and RAL-1-independent functions in VPC fate patterning. These two functions are genetically separable. RAL-1 and RGL-1 also showed non-equivalence in VPC fate patterning. RAL-1 performs a single known function downstream of LET-60-RGL-1 to promote 2° fate, and thus deletion, RNAi depletion, or a hypomorphic point mutation in *ral-1* all confer the same phenotype: reduced 2°-promoting signal. In contrast, null mutations in RGL-1 show no phenotypic changes in the balance between 1° and 2° signals. We showed both 1°-promoting and 2°-promoting signaling activities of RGL-1 can be separated genetically by using GEF-specific mutations and genetic bypass experiments. Mammalian RalGEF physically interacts with PDK and Akt as a scaffold protein. *C. elegans* PDK-1 was previously shown to promote 1° fate (Nakdimon et al., 2012). Our genetic analysis is consistent with RGL-1 also functioning as a scaffold protein for PDK-1/PDK and

AKT-1/Akt to promote 1° fate in the AGE-1/PI3K mediated 1°-promoting modulatory cascade. RGL-1 mutants showed 15-fold higher error rate in VPC fate patterning than the wild type. This observation indicates that the opposing activities of RGL-1 for 1°- and 2°-promoting modulatory signaling cascade in AGE-1-PDK-1-AKT-1 and LET-60-RGL-1-RAL-1, respectively, are controlled in order to decrease signaling noise and mis-patterning of VPC fate. From our study of opposing RGL-1 activities, we hypothesize that RGL-1 functions as a “balanced switch” to reinforce precise VPC fate patterning and hence contribute to fidelity of vulva development.

While we showed that LET-60/Ras switches effectors during VPC fate patterning, we know nothing in any system about how different effector use is regulated. We find that LET-60/Ras effectors are segregated within a VPC and between VPCs at different time points. The 1°-promoting LIN-45/Raf is recruited to the basolateral membrane in 1° cell, but not in 2° cells, at early Pn.p (1-cell) stage. In contrast, 2°-promoting RGL-1/RalGEF is localized to the apical membrane in 2° cells, but not in 1° cell, at late Pn.p (1-cell) stage. The Ras effector recruitment to the plasma membrane has been shown in mammalian cell culture system. However, interestingly LET-60/Ras effectors are polarized in the *C. elegans*, *in vivo* system. We validated RGL-1 recruitment to the plasma membrane in VPCs by LET-60/Ras null mutant. The RGL-1 recruitment to the apical membrane is also shown in the LET-23 mutant, which expression of LET-23 is only at the apical membrane in all VPCs. We will test the functional activity

of apically localized RGL-1 by using the LET-23 mutant in the genetically sensitized background. We will further study mechanism of LET-60 effector segregation using *in vivo* model system. We hypothesize that phosphorylation of RGL-1 regulates segregation of RGL-1 between 1° and 2° cells and the polarization of LET-60 effectors are mediated through regulators and scaffold proteins between LET-60 and its effectors. We observed that LIN-45 is recruited to the plasma membrane earlier than RGL-1 is. The “Sequential Induction Model” and “Morphogen Gradient Model” have not been reconciled for decades (Kenyon, 1995). However, the two competing models were reconciled by LET-60 effector switching study done by Zand et al., 2011 genetically showing that the graded LIN-3/EGF mediates the activation of LET-60-RGL-1-RAL-1 signaling cascade in support of LIN-12/Notch. The observation of LET-60 effector segregation at different time supports the genetic study for reconciling the two models cell biologically. The study of Ras effector switching and segregation mechanism is critical for understanding Ras in cancer biology and developmental biology.

REFERENCES

- Albright, C.F., Giddings, B.W., Liu, J., Vito, M., and Weinberg, R.A. (1993). Characterization of a guanine nucleotide dissociation stimulator for a ras-related GTPase. *EMBO J* 12, 339-347.
- Allen, B.L., and Taatjes, D.J. (2015). The Mediator complex: a central integrator of transcription. *Nat Rev Mol Cell Biol* 16, 155-166.
- Andersen, E.C., and Horvitz, H.R. (2007). Two *C. elegans* histone methyltransferases repress *lin-3* EGF transcription to inhibit vulval development. *Development* 134, 2991-2999.
- Andersen, E.C., Saffer, A.M., and Horvitz, H.R. (2008). Multiple levels of redundant processes inhibit *Caenorhabditis elegans* vulval cell fates. *Genetics* 179, 2001-2012.
- Armenti, S.T., Chan, E., and Nance, J. (2014). Polarized exocyst-mediated vesicle fusion directs intracellular lumenogenesis within the *C. elegans* excretory cell. *Dev Biol* 394, 110-121.
- Aroian, R.V., Koga, M., Mendel, J.E., Ohshima, Y., and Sternberg, P.W. (1990). The *let-23* gene necessary for *Caenorhabditis elegans* vulval induction encodes a tyrosine kinase of the EGF receptor subfamily. *Nature* 348, 693-699.
- Aroian, R.V., and Sternberg, P.W. (1991). Multiple functions of *let-23*, a *Caenorhabditis elegans* receptor tyrosine kinase gene required for vulval induction. *Genetics* 128, 251-267.

Arribere, J.A., Bell, R.T., Fu, B.X., Artiles, K.L., Hartman, P.S., and Fire, A.Z. (2014). Efficient marker-free recovery of custom genetic modifications with CRISPR/Cas9 in *Caenorhabditis elegans*. *Genetics* 198, 837-846.

Avery, L., and Shtonda, B.B. (2003). Food transport in the *C. elegans* pharynx. *J Exp Biol* 206, 2441-2457.

Balakireva, M., Rosse, C., Langevin, J., Chien, Y.C., Gho, M., Gonzy-Treboul, G., Voegelinge-Lemaire, S., Aresta, S., Lepesant, J.A., Bellaiche, Y., *et al.* (2006). The Ral/exocyst effector complex counters c-Jun N-terminal kinase-dependent apoptosis in *Drosophila melanogaster*. *Mol Cell Biol* 26, 8953-8963.

Barbieri, M.A., Roberts, R.L., Gumusboga, A., Highfield, H., Alvarez-Dominguez, C., Wells, A., and Stahl, P.D. (2000). Epidermal growth factor and membrane trafficking. EGF receptor activation of endocytosis requires Rab5a. *J Cell Biol* 151, 539-550.

Barkoulas, M., van Zon, J.S., Milloz, J., van Oudenaarden, A., and Felix, M.A. (2013). Robustness and epistasis in the *C. elegans* vulval signaling network revealed by pathway dosage modulation. *Dev Cell* 24, 64-75.

Beitel, G.J., Clark, S.G., and Horvitz, H.R. (1990). *Caenorhabditis elegans* ras gene *let-60* acts as a switch in the pathway of vulval induction. *Nature* 348, 503-509.

Beitel, G.J., Tuck, S., Greenwald, I., and Horvitz, H.R. (1995). The *Caenorhabditis elegans* gene *lin-1* encodes an ETS-domain protein and defines a branch of the vulval induction pathway. *Genes Dev* 9, 3149-3162.

Ben-Levy, R., Hooper, S., Wilson, R., Paterson, H.F., and Marshall, C.J. (1998). Nuclear export of the stress-activated protein kinase p38 mediated by its substrate MAPKAP kinase-2. *Curr Biol* 8, 1049-1057.

Berset, T., Hoier, E.F., Battu, G., Canevascini, S., and Hajnal, A. (2001). Notch inhibition of RAS signaling through MAP kinase phosphatase LIP-1 during *C. elegans* vulval development. *Science* 291, 1055-1058.

Berset, T.A., Hoier, E.F., and Hajnal, A. (2005). The *C. elegans* homolog of the mammalian tumor suppressor Dep-1/Scc1 inhibits EGFR signaling to regulate binary cell fate decisions. *Genes Dev* 19, 1328-1340.

Bilder, D., and Perrimon, N. (2000). Localization of apical epithelial determinants by the basolateral PDZ protein Scribble. *Nature* 403, 676-680.

Block, C., Janknecht, R., Herrmann, C., Nassar, N., and Wittinghofer, A. (1996). Quantitative structure-activity analysis correlating Ras/Raf interaction in vitro to Raf activation in vivo. *Nat Struct Biol* 3, 244-251.

Bodemann, B.O., Orvedahl, A., Cheng, T., Ram, R.R., Ou, Y.H., Formstecher, E., Maiti, M., Hazelett, C.C., Wauson, E.M., Balakireva, M., *et al.* (2011). RalB and the exocyst mediate the cellular starvation response by direct activation of autophagosome assembly. *Cell* 144, 253-267.

Bodenmiller, B., and Aebersold, R. (2011). Phosphoproteome resource for systems biology research. *Methods Mol Biol* 694, 307-322.

Bos, J.L. (1989). ras oncogenes in human cancer: a review. *Cancer Res* 49, 4682-4689.

Braendle, C., Baer, C.F., and Felix, M.A. (2010). Bias and evolution of the mutationally accessible phenotypic space in a developmental system. *PLoS Genet* 6, e1000877.

Braendle, C., and Felix, M.A. (2008). Plasticity and errors of a robust developmental system in different environments. *Dev Cell* 15, 714-724.

Brenner, S. (1974). The genetics of *Caenorhabditis elegans*. *Genetics* 77, 71-94.

Brymora, A., Valova, V.A., Larsen, M.R., Roufogalis, B.D., and Robinson, P.J. (2001). The brain exocyst complex interacts with RalA in a GTP-dependent manner: identification of a novel mammalian Sec3 gene and a second Sec15 gene. *J Biol Chem* 276, 29792-29797.

Burdine, R.D., Branda, C.S., and Stern, M.J. (1998). EGL-17(FGF) expression coordinates the attraction of the migrating sex myoblasts with vulval induction in *C. elegans*. *Development* 125, 1083-1093.

Burdine, R.D., Chen, E.B., Kwok, S.F., and Stern, M.J. (1997). egl-17 encodes an invertebrate fibroblast growth factor family member required specifically for sex myoblast migration in *Caenorhabditis elegans*. *Proc Natl Acad Sci U S A* 94, 2433-2437.

Bustelo, X.R., Crespo, P., Fernandez-Pisonero, I., and Rodriguez-Fdez, S. (2018). RAS GTPase-dependent pathways in developmental diseases: old guys, new lads, and current challenges. *Curr Opin Cell Biol* 55, 42-51.

Camonis, J.H., and White, M.A. (2005). Ral GTPases: corrupting the exocyst in cancer cells. *Trends Cell Biol* 15, 327-332.

Casanova, J.E. (2007). Regulation of Arf activation: the Sec7 family of guanine nucleotide exchange factors. *Traffic* 8, 1476-1485.

Ceol, C.J., and Horvitz, H.R. (2001). dpl-1 DP and efl-1 E2F act with lin-35 Rb to antagonize Ras signaling in *C. elegans* vulval development. *Mol Cell* 7, 461-473.

Ceol, C.J., and Horvitz, H.R. (2004). A new class of *C. elegans* synMuv genes implicates a Tip60/NuA4-like HAT complex as a negative regulator of Ras signaling. *Dev Cell* 6, 563-576.

Ceol, C.J., Stegmeier, F., Harrison, M.M., and Horvitz, H.R. (2006). Identification and classification of genes that act antagonistically to let-60 Ras signaling in *Caenorhabditis elegans* vulval development. *Genetics* 173, 709-726.

Ceresa, B.P. (2006). Regulation of EGFR endocytic trafficking by rab proteins. *Histol Histopathol* 21, 987-993.

Chang, C., Hopper, N.A., and Sternberg, P.W. (2000). *Caenorhabditis elegans* SOS-1 is necessary for multiple RAS-mediated developmental signals. *EMBO J* 19, 3283-3294.

Chapman, J.O., Li, H., and Lundquist, E.A. (2008). The MIG-15 NIK kinase acts cell-autonomously in neuroblast polarization and migration in *C. elegans*. *Dev Biol* 324, 245-257.

Chen, N., and Greenwald, I. (2004). The lateral signal for LIN-12/Notch in *C. elegans* vulval development comprises redundant secreted and transmembrane DSL proteins. *Dev Cell* 6, 183-192.

Chien, Y., Kim, S., Bumeister, R., Loo, Y.M., Kwon, S.W., Johnson, C.L., Balakireva, M.G., Romeo, Y., Kopelovich, L., Gale, M., Jr., *et al.* (2006). RalB GTPase-mediated activation of the I κ B family kinase TBK1 couples innate immune signaling to tumor cell survival. *Cell* 127, 157-170.

Chisholm, A.D., and Hardin, J. (2005). Epidermal morphogenesis. *WormBook*, 1-22.

Chiu, V.K., Bivona, T., Hach, A., Sajous, J.B., Silletti, J., Wiener, H., Johnson, R.L., 2nd, Cox, A.D., and Philips, M.R. (2002). Ras signalling on the endoplasmic reticulum and the Golgi. *Nat Cell Biol* 4, 343-350.

Christensen, S., Kodoyianni, V., Bosenberg, M., Friedman, L., and Kimble, J. (1996). lag-1, a gene required for lin-12 and glp-1 signaling in *Caenorhabditis elegans*, is homologous to human CBF1 and *Drosophila* Su(H). *Development* 122, 1373-1383.

Clark, S.G., Lu, X., and Horvitz, H.R. (1994). The *Caenorhabditis elegans* locus lin-15, a negative regulator of a tyrosine kinase signaling pathway, encodes two different proteins. *Genetics* 137, 987-997.

Clark, S.G., Stern, M.J., and Horvitz, H.R. (1992). *C. elegans* cell-signalling gene sem-5 encodes a protein with SH2 and SH3 domains. *Nature* 356, 340-344.

Corl, A.B., Berger, K.H., Ophir-Shohat, G., Gesch, J., Simms, J.A., Bartlett, S.E., and Heberlein, U. (2009). Happyhour, a Ste20 family kinase, implicates EGFR signaling in ethanol-induced behaviors. *Cell* 137, 949-960.

Couteau, F., Guerry, F., Muller, F., and Palladino, F. (2002). A heterochromatin protein 1 homologue in *Caenorhabditis elegans* acts in germline and vulval development. *EMBO Rep* 3, 235-241.

Cox, A.D., Fesik, S.W., Kimmelman, A.C., Luo, J., and Der, C.J. (2014). Drugging the undruggable RAS: Mission possible? *Nat Rev Drug Discov* 13, 828-851.

Cui, M., Chen, J., Myers, T.R., Hwang, B.J., Sternberg, P.W., Greenwald, I., and Han, M. (2006). SynMuv genes redundantly inhibit lin-3/EGF expression to prevent inappropriate vulval induction in *C. elegans*. *Dev Cell* 10, 667-672.

Dai, P., Xiong, W.C., and Mei, L. (2006). Erbin inhibits RAF activation by disrupting the sur-8-Ras-Raf complex. *J Biol Chem* 281, 927-933.

Dan, I., Watanabe, N.M., and Kusumi, A. (2001). The Ste20 group kinases as regulators of MAP kinase cascades. *Trends Cell Biol* 11, 220-230.

Davison, E.M., Saffer, A.M., Huang, L.S., DeModena, J., Sternberg, P.W., and Horvitz, H.R. (2011). The LIN-15A and LIN-56 transcriptional regulators interact to negatively regulate EGF/Ras signaling in *Caenorhabditis elegans* vulval cell-fate determination. *Genetics* 187, 803-815.

de la Cova, C., and Greenwald, I. (2012). SEL-10/Fbw7-dependent negative feedback regulation of LIN-45/Braf signaling in *C. elegans* via a conserved phosphodegron. *Genes Dev* 26, 2524-2535.

de la Cova, C., Townley, R., Regot, S., and Greenwald, I. (2017). A Real-Time Biosensor for ERK Activity Reveals Signaling Dynamics during *C. elegans* Cell Fate Specification. *Dev Cell* 42, 542-553 e544.

de Souza, N., Vallier, L.G., Fares, H., and Greenwald, I. (2007). SEL-2, the *C. elegans* neurobeachin/LRBA homolog, is a negative regulator of lin-12/Notch activity and affects endosomal traffic in polarized epithelial cells. *Development* 134, 691-702.

Delpire, E. (2009). The mammalian family of sterile 20p-like protein kinases. *Pflugers Arch* 458, 953-967.

Deng, Y., and Greenwald, I. (2016a). Determinants in the LIN-12/Notch Intracellular Domain That Govern Its Activity and Stability During *Caenorhabditis elegans* Vulval Development. *G3 (Bethesda)* 6, 3663-3670.

Deng, Y., and Greenwald, I. (2016b). Determinants in the LIN-12/Notch Intracellular Domain That Govern Its Activity and Stability During *Caenorhabditis elegans* Vulval Development. *G3 (Bethesda)*.

Dhillon, A.S., Meikle, S., Yazici, Z., Eulitz, M., and Kolch, W. (2002). Regulation of Raf-1 activation and signalling by dephosphorylation. *EMBO J* 21, 64-71.

Dickinson, D.J., Pani, A.M., Heppert, J.K., Higgins, C.D., and Goldstein, B. (2015). Streamlined Genome Engineering with a Self-Excising Drug Selection Cassette. *Genetics* 200, 1035-1049.

Dickinson, D.J., Ward, J.D., Reiner, D.J., and Goldstein, B. (2013). Engineering the *Caenorhabditis elegans* genome using Cas9-triggered homologous recombination. *Nat Methods* 10, 1028-1034.

Dinneen, J.L., and Ceresa, B.P. (2004). Continual expression of Rab5(Q79L) causes a ligand-independent EGFR internalization and diminishes EGFR activity. *Traffic* 5, 606-615.

Downward, J. (2014). RAS's cloak of invincibility slips at last? *Cancer Cell* 25, 5-6.

Doyle, T.G., Wen, C., and Greenwald, I. (2000). SEL-8, a nuclear protein required for LIN-12 and GLP-1 signaling in *Caenorhabditis elegans*. *Proc Natl Acad Sci U S A* 97, 7877-7881.

Dutt, A., Canevascini, S., Froehli-Hoier, E., and Hajnal, A. (2004). EGF signal propagation during *C. elegans* vulval development mediated by ROM-1 rhomboid. *PLoS Biol* 2, e334.

Duveau, F., and Felix, M.A. (2012). Role of pleiotropy in the evolution of a cryptic developmental variation in *Caenorhabditis elegans*. *PLoS Biol* 10, e1001230.

Egan, S.E., Giddings, B.W., Brooks, M.W., Buday, L., Sizeland, A.M., and Weinberg, R.A. (1993). Association of Sos Ras exchange protein with Grb2 is implicated in tyrosine kinase signal transduction and transformation. *Nature* 363, 45-51.

Eisenmann, D.M., and Kim, S.K. (1997). Mechanism of activation of the *Caenorhabditis elegans* ras homologue let-60 by a novel, temperature-sensitive, gain-of-function mutation. *Genetics* 146, 553-565.

- Euling, S., and Ambros, V. (1996). Heterochronic genes control cell cycle progress and developmental competence of *C. elegans* vulva precursor cells. *Cell* 84, 667-676.
- Fabian, J.R., Daar, I.O., and Morrison, D.K. (1993). Critical tyrosine residues regulate the enzymatic and biological activity of Raf-1 kinase. *Mol Cell Biol* 13, 7170-7179.
- Fantz, D.A., Jacobs, D., Glossip, D., and Kornfeld, K. (2001). Docking sites on substrate proteins direct extracellular signal-regulated kinase to phosphorylate specific residues. *J Biol Chem* 276, 27256-27265.
- Farooqui, S., Pellegrino, M.W., Rimann, I., Morf, M.K., Muller, L., Frohli, E., and Hajnal, A. (2012). Coordinated lumen contraction and expansion during vulval tube morphogenesis in *Caenorhabditis elegans*. *Dev Cell* 23, 494-506.
- Fay, D.S., and Yochem, J. (2007). The SynMuv genes of *Caenorhabditis elegans* in vulval development and beyond. *Dev Biol* 306, 1-9.
- Feig, L.A. (2003). Ral-GTPases: approaching their 15 minutes of fame. *Trends Cell Biol* 13, 419-425.
- Feig, L.A., Urano, T., and Cantor, S. (1996). Evidence for a Ras/Ral signaling cascade. *Trends Biochem Sci* 21, 438-441.
- Felix, M.A., and Barkoulas, M. (2012). Robustness and flexibility in nematode vulva development. *Trends Genet* 28, 185-195.

Ferguson, E.L., and Horvitz, H.R. (1985). Identification and characterization of 22 genes that affect the vulval cell lineages of the nematode *Caenorhabditis elegans*. *Genetics* 110, 17-72.

Ferguson, E.L., and Horvitz, H.R. (1989). The multivulva phenotype of certain *Caenorhabditis elegans* mutants results from defects in two functionally redundant pathways. *Genetics* 123, 109-121.

Ferguson, E.L., Sternberg, P.W., and Horvitz, H.R. (1987). A genetic pathway for the specification of the vulval cell lineages of *Caenorhabditis elegans*. *Nature* 326, 259-267.

Ferro, E., and Trabalzini, L. (2010). RalGDS family members couple Ras to Ral signalling and that's not all. *Cell Signal* 22, 1804-1810.

Frische, E.W., Pellis-van Berkel, W., van Haaften, G., Cuppen, E., Plasterk, R.H., Tijsterman, M., Bos, J.L., and Zwartkruis, F.J. (2007). RAP-1 and the RAL-1/exocyst pathway coordinate hypodermal cell organization in *Caenorhabditis elegans*. *EMBO J* 26, 5083-5092.

Frokjaer-Jensen, C., Davis, M.W., Sarov, M., Taylor, J., Flibotte, S., LaBella, M., Pozniakovsky, A., Moerman, D.G., and Jorgensen, E.M. (2014). Random and targeted transgene insertion in *Caenorhabditis elegans* using a modified Mos1 transposon. *Nat Methods* 11, 529-534.

Fruman, D.A., Chiu, H., Hopkins, B.D., Bagrodia, S., Cantley, L.C., and Abraham, R.T. (2017). The PI3K Pathway in Human Disease. *Cell* 170, 605-635.

Fukai, S., Matern, H.T., Jagath, J.R., Scheller, R.H., and Brunger, A.T. (2003). Structural basis of the interaction between RalA and Sec5, a subunit of the sec6/8 complex. *EMBO J* 22, 3267-3278.

Gentry, L.R., Martin, T.D., Reiner, D.J., and Der, C.J. (2014). Ral small GTPase signaling and oncogenesis: More than just 15minutes of fame. *Biochim Biophys Acta* 1843, 2976-2988.

Gil, E.B., Malone Link, E., Liu, L.X., Johnson, C.D., and Lees, J.A. (1999). Regulation of the insulin-like developmental pathway of *Caenorhabditis elegans* by a homolog of the PTEN tumor suppressor gene. *Proc Natl Acad Sci U S A* 96, 2925-2930.

Goi, T., Rusanescu, G., Urano, T., and Feig, L.A. (1999). Ral-specific guanine nucleotide exchange factor activity opposes other Ras effectors in PC12 cells by inhibiting neurite outgrowth. *Mol Cell Biol* 19, 1731-1741.

Golden, A. (2017). From phenologs to silent suppressors: Identifying potential therapeutic targets for human disease. *Mol Reprod Dev* 84, 1118-1132.

Gonzalez-Serricchio, A.S., and Sternberg, P.W. (2006). Visualization of *C. elegans* transgenic arrays by GFP. *BMC Genet* 7, 36.

Gonzalez, F.A., Seth, A., Raden, D.L., Bowman, D.S., Fay, F.S., and Davis, R.J. (1993). Serum-induced translocation of mitogen-activated protein kinase to the cell surface ruffling membrane and the nucleus. *J Cell Biol* 122, 1089-1101.

Grants, J.M., Ying, L.T., Yoda, A., You, C.C., Okano, H., Sawa, H., and Taubert, S. (2016). The Mediator Kinase Module Restrains Epidermal Growth Factor

Receptor Signaling and Represses Vulval Cell Fate Specification in *Caenorhabditis elegans*. *Genetics* 202, 583-599.

Green, J.L., Inoue, T., and Sternberg, P.W. (2008). Opposing Wnt pathways orient cell polarity during organogenesis. *Cell* 134, 646-656.

Greenwald, I. (2005). LIN-12/Notch signaling in *C. elegans*. *WormBook*, 1-16.

Greenwald, I., and Kovall, R. (2013). Notch signaling: genetics and structure. *WormBook*, 1-28.

Greenwald, I., and Rubin, G.M. (1992). Making a difference: the role of cell-cell interactions in establishing separate identities for equivalent cells. *Cell* 68, 271-281.

Greenwald, I.S., Sternberg, P.W., and Horvitz, H.R. (1983). The *lin-12* locus specifies cell fates in *Caenorhabditis elegans*. *Cell* 34, 435-444.

Grimbert, S., and Braendle, C. (2014). Cryptic genetic variation uncovers evolution of environmentally sensitive parameters in *Caenorhabditis* vulval development. *Evol Dev* 16, 278-291.

Grimbert, S., Tietze, K., Barkoulas, M., Sternberg, P.W., Felix, M.A., and Braendle, C. (2016). Anchor cell signaling and vulval precursor cell positioning establish a reproducible spatial context during *C. elegans* vulval induction. *Dev Biol* 416, 123-135.

Grimbert, S., Vargas Velazquez, A.M., and Braendle, C. (2018). Physiological Starvation Promotes *Caenorhabditis elegans* Vulval Induction. *G3 (Bethesda)*.

Guerry, F., Marti, C.O., Zhang, Y., Moroni, P.S., Jaquier, E., and Muller, F. (2007). The Mi-2 nucleosome-remodeling protein LET-418 is targeted via LIN-1/ETS to the promoter of *lin-39/Hox* during vulval development in *C. elegans*. *Dev Biol* 306, 469-479.

Haag, A., Gutierrez, P., Buhler, A., Walser, M., Yang, Q., Langouet, M., Kradolfer, D., Frohli, E., Herrmann, C.J., Hajnal, A., *et al.* (2014). An in vivo EGF receptor localization screen in *C. elegans* identifies the Ezrin homolog ERM-1 as a temporal regulator of signaling. *PLoS Genet* 10, e1004341.

Hamad, N.M., Elconin, J.H., Karnoub, A.E., Bai, W., Rich, J.N., Abraham, R.T., Der, C.J., and Counter, C.M. (2002). Distinct requirements for Ras oncogenesis in human versus mouse cells. *Genes Dev* 16, 2045-2057.

Han, M., Aroian, R.V., and Sternberg, P.W. (1990). The *let-60* locus controls the switch between vulval and nonvulval cell fates in *Caenorhabditis elegans*. *Genetics* 126, 899-913.

Han, M., Golden, A., Han, Y., and Sternberg, P.W. (1993). *C. elegans* *lin-45 raf* gene participates in *let-60 ras*-stimulated vulval differentiation. *Nature* 363, 133-140.

Han, M., and Sternberg, P.W. (1990). *let-60*, a gene that specifies cell fates during *C. elegans* vulval induction, encodes a ras protein. *Cell* 63, 921-931.

Han, M., and Sternberg, P.W. (1991). Analysis of dominant-negative mutations of the *Caenorhabditis elegans let-60 ras* gene. *Genes Dev* 5, 2188-2198.

Hanahan, D., and Weinberg, R.A. (2011). Hallmarks of cancer: the next generation. *Cell* 144, 646-674.

Hao, Y., Wong, R., and Feig, L.A. (2008). RalGDS couples growth factor signaling to Akt activation. *Mol Cell Biol* 28, 2851-2859.

Hart, A.H., Reventar, R., and Bernstein, A. (2000). Genetic analysis of ETS genes in *C. elegans*. *Oncogene* 19, 6400-6408.

Herman, R.K., and Hedgecock, E.M. (1990). Limitation of the size of the vulval primordium of *Caenorhabditis elegans* by *lin-15* expression in surrounding hypodermis. *Nature* 348, 169-171.

Hill, R.J., and Sternberg, P.W. (1992). The gene *lin-3* encodes an inductive signal for vulval development in *C. elegans*. *Nature* 358, 470-476.

Hobbs, G.A., Der, C.J., and Rossman, K.L. (2016). RAS isoforms and mutations in cancer at a glance. *Journal of cell science* 129, 1287-1292.

Hofer, F., Fields, S., Schneider, C., and Martin, G.S. (1994). Activated Ras interacts with the Ral guanine nucleotide dissociation stimulator. *Proc Natl Acad Sci U S A* 91, 11089-11093.

Hopper, N.A., Lee, J., and Sternberg, P.W. (2000). ARK-1 inhibits EGFR signaling in *C. elegans*. *Mol Cell* 6, 65-75.

Horvitz, H.R., Brenner, S., Hodgkin, J., and Herman, R.K. (1979). A uniform genetic nomenclature for the nematode *Caenorhabditis elegans*. *Mol Gen Genet* 175, 129-133.

Horvitz, H.R., and Sulston, J.E. (1980). Isolation and genetic characterization of cell-lineage mutants of the nematode *Caenorhabditis elegans*. *Genetics* 96, 435-454.

Hoskins, R., Hajnal, A.F., Harp, S.A., and Kim, S.K. (1996). The *C. elegans* vulval induction gene *lin-2* encodes a member of the MAGUK family of cell junction proteins. *Development* 122, 97-111.

Howard, R.M., and Sundaram, M.V. (2002). *C. elegans* EOR-1/PLZF and EOR-2 positively regulate Ras and Wnt signaling and function redundantly with LIN-25 and the SUR-2 Mediator component. *Genes Dev* 16, 1815-1827.

Howell, K., Arur, S., Schedl, T., and Sundaram, M.V. (2010). EOR-2 is an obligate binding partner of the BTB-zinc finger protein EOR-1 in *Caenorhabditis elegans*. *Genetics* 184, 899-913.

Hoyos, E., Kim, K., Milloz, J., Barkoulas, M., Penigault, J.B., Munro, E., and Felix, M.A. (2011). Quantitative variation in autocrine signaling and pathway crosstalk in the *Caenorhabditis* vulval network. *Curr Biol* 21, 527-538.

Huang, L., Hofer, F., Martin, G.S., and Kim, S.H. (1998). Structural basis for the interaction of Ras with RalGDS. *Nat Struct Biol* 5, 422-426.

Huang, L.S., Tzou, P., and Sternberg, P.W. (1994). The *lin-15* locus encodes two negative regulators of *Caenorhabditis elegans* vulval development. *Mol Biol Cell* 5, 395-411.

Huang, Y.Z., Zang, M., Xiong, W.C., Luo, Z., and Mei, L. (2003). Erbin suppresses the MAP kinase pathway. *J Biol Chem* 278, 1108-1114.

Hubbard, E.J., Wu, G., Kitajewski, J., and Greenwald, I. (1997). *sel-10*, a negative regulator of *lin-12* activity in *Caenorhabditis elegans*, encodes a member of the CDC4 family of proteins. *Genes Dev* 11, 3182-3193.

Hunt-Newbury, R., Viveiros, R., Johnsen, R., Mah, A., Anastas, D., Fang, L., Halfnight, E., Lee, D., Lin, J., Lorch, A., *et al.* (2007). High-throughput in vivo analysis of gene expression in *Caenorhabditis elegans*. *PLoS Biol* 5, e237.

Hurd, D.D., and Kemphues, K.J. (2003). PAR-1 is required for morphogenesis of the *Caenorhabditis elegans* vulva. *Dev Biol* 253, 54-65.

Inoue, T., Oz, H.S., Wiland, D., Gharib, S., Deshpande, R., Hill, R.J., Katz, W.S., and Sternberg, P.W. (2004). *C. elegans* LIN-18 is a Ryk ortholog and functions in parallel to LIN-17/Frizzled in Wnt signaling. *Cell* 118, 795-806.

Inoue, T., Sherwood, D.R., Aspöck, G., Butler, J.A., Gupta, B.P., Kirouac, M., Wang, M., Lee, P.Y., Kramer, J.M., Hope, I., *et al.* (2002). Gene expression markers for *Caenorhabditis elegans* vulval cells. *Mech Dev* 119 Suppl 1, S203-209.

Inoue, T., Wang, M., Ririe, T.O., Fernandes, J.S., and Sternberg, P.W. (2005). Transcriptional network underlying *Caenorhabditis elegans* vulval development. *Proc Natl Acad Sci U S A* 102, 4972-4977.

Ishizaki, R., Shin, H.W., Mitsuhashi, H., and Nakayama, K. (2008). Redundant roles of BIG2 and BIG1, guanine-nucleotide exchange factors for ADP-ribosylation factors in membrane traffic between the trans-Golgi network and endosomes. *Mol Biol Cell* 19, 2650-2660.

Isomura, M., Okui, K., Fujiwara, T., Shin, S., and Nakamura, Y. (1996). Isolation and mapping of RAB2L, a human cDNA that encodes a protein homologous to RalGDS. *Cytogenet Cell Genet* 74, 263-265.

Issaq, S.H., Lim, K.H., and Counter, C.M. (2010). Sec5 and Exo84 foster oncogenic ras-mediated tumorigenesis. *Mol Cancer Res* 8, 223-231.

Jacobs, D., Beitel, G.J., Clark, S.G., Horvitz, H.R., and Kornfeld, K. (1998). Gain-of-function mutations in the *Caenorhabditis elegans* lin-1 ETS gene identify a C-terminal regulatory domain phosphorylated by ERK MAP kinase. *Genetics* 149, 1809-1822.

Jang, E.R., and Galperin, E. (2016). The function of Shoc2: A scaffold and beyond. *Commun Integr Biol* 9, e1188241.

Jin, R., Junutula, J.R., Matern, H.T., Ervin, K.E., Scheller, R.H., and Brunger, A.T. (2005). Exo84 and Sec5 are competitive regulatory Sec6/8 effectors to the RalA GTPase. *The EMBO journal* 24, 2064-2074.

Joazeiro, C.A., Wing, S.S., Huang, H., Leverson, J.D., Hunter, T., and Liu, Y.C. (1999). The tyrosine kinase negative regulator c-Cbl as a RING-type, E2-dependent ubiquitin-protein ligase. *Science* 286, 309-312.

Jongeward, G.D., Clandinin, T.R., and Sternberg, P.W. (1995). sli-1, a negative regulator of let-23-mediated signaling in *C. elegans*. *Genetics* 139, 1553-1566.

Kaech, S.M., Whitfield, C.W., and Kim, S.K. (1998). The LIN-2/LIN-7/LIN-10 complex mediates basolateral membrane localization of the *C. elegans* EGF receptor LET-23 in vulval epithelial cells. *Cell* 94, 761-771.

Kamath, R.S., Fraser, A.G., Dong, Y., Poulin, G., Durbin, R., Gotta, M., Kanapin, A., Le Bot, N., Moreno, S., Sohrmann, M., *et al.* (2003). Systematic functional analysis of the *Caenorhabditis elegans* genome using RNAi. *Nature* 421, 231-237.

Kamath, R.S., Martinez-Campos, M., Zipperlen, P., Fraser, A.G., and Ahringer, J. (2001). Effectiveness of specific RNA-mediated interference through ingested double-stranded RNA in *Caenorhabditis elegans*. *Genome biology* 2, Research0002.

Kashatus, D.F. (2013). Ral GTPases in tumorigenesis: emerging from the shadows. *Exp Cell Res* 319, 2337-2342.

Katz, W.S., Hill, R.J., Clandinin, T.R., and Sternberg, P.W. (1995). Different levels of the *C. elegans* growth factor LIN-3 promote distinct vulval precursor fates. *Cell* 82, 297-307.

Katz, W.S., Lesa, G.M., Yannoukakos, D., Clandinin, T.R., Schlessinger, J., and Sternberg, P.W. (1996). A point mutation in the extracellular domain activates LET-23, the *Caenorhabditis elegans* epidermal growth factor receptor homolog. *Mol Cell Biol* 16, 529-537.

Kemphues, K. (2000). PARsing embryonic polarity. *Cell* 101, 345-348.

Kenyon, C. (1995). A perfect vulva every time: gradients and signaling cascades in *C. elegans*. *Cell* 82, 171-174.

Khan, M.H., Hart, M.J., and Rea, S.L. (2012). The role of MAP4K3 in lifespan regulation of *Caenorhabditis elegans*. *Biochem Biophys Res Commun* 425, 413-418.

Khosravi-Far, R., White, M.A., Westwick, J.K., Soltski, P.A., Chrzanowska-Wodnicka, M., Van Aelst, L., Wigler, M.H., and Der, C.J. (1996). Oncogenic Ras activation of Raf/mitogen-activated protein kinase-independent pathways is sufficient to cause tumorigenic transformation. *Mol Cell Biol* 16, 3923-3933.

Kidd, A.R., 3rd, Muniz-Medina, V., Der, C.J., Cox, A.D., and Reiner, D.J. (2015). The *C. elegans* Chp/Wrch Ortholog CHW-1 Contributes to LIN-18/Ryk and LIN-17/Frizzled Signaling in Cell Polarity. *PLoS One* 10, e0133226.

Kiefer, F., Tibbles, L.A., Anafi, M., Janssen, A., Zanke, B.W., Lassam, N., Pawson, T., Woodgett, J.R., and Iscove, N.N. (1996). HPK1, a hematopoietic protein kinase activating the SAPK/JNK pathway. *EMBO J* 15, 7013-7025.

Kikuchi, A., Demo, S.D., Ye, Z.H., Chen, Y.W., and Williams, L.T. (1994). ralGDS family members interact with the effector loop of ras p21. *Mol Cell Biol* 14, 7483-7491.

Kim, S.K. (1997). Polarized signaling: basolateral receptor localization in epithelial cells by PDZ-containing proteins. *Curr Opin Cell Biol* 9, 853-859.

Kimble, J. (1981). Alterations in cell lineage following laser ablation of cells in the somatic gonad of *Caenorhabditis elegans*. *Dev Biol* 87, 286-300.

Kishida, S., Koyama, S., Matsubara, K., Kishida, M., Matsuura, Y., and Kikuchi, A. (1997). Colocalization of Ras and Ral on the membrane is required for Ras-dependent Ral activation through Ral GDP dissociation stimulator. *Oncogene* 15, 2899-2907.

Koga, M., and Ohshima, Y. (1995). Mosaic analysis of the *let-23* gene function in vulval induction of *Caenorhabditis elegans*. *Development* 121, 2655-2666.

Komatsu, N., Aoki, K., Yamada, M., Yukinaga, H., Fujita, Y., Kamioka, Y., and Matsuda, M. (2011). Development of an optimized backbone of FRET biosensors for kinases and GTPases. *Mol Biol Cell* 22, 4647-4656.

Kornfeld, K., Guan, K.L., and Horvitz, H.R. (1995a). The *Caenorhabditis elegans* gene *mek-2* is required for vulval induction and encodes a protein similar to the protein kinase MEK. *Genes Dev* 9, 756-768.

Kornfeld, K., Hom, D.B., and Horvitz, H.R. (1995b). The *ksr-1* gene encodes a novel protein kinase involved in Ras-mediated signaling in *C. elegans*. *Cell* 83, 903-913.

Kyriakis, J.M., App, H., Zhang, X.F., Banerjee, P., Brautigan, D.L., Rapp, U.R., and Avruch, J. (1992). Raf-1 activates MAP kinase-kinase. *Nature* 358, 417-421.

Lackner, M.R., Kornfeld, K., Miller, L.M., Horvitz, H.R., and Kim, S.K. (1994). A MAP kinase homolog, *mpk-1*, is involved in ras-mediated induction of vulval cell fates in *Caenorhabditis elegans*. *Genes Dev* 8, 160-173.

Lambie, E.J., and Kimble, J. (1991). Two homologous regulatory genes, *lin-12* and *glp-1*, have overlapping functions. *Development* 112, 231-240.

Lamitina, S.T., Morrison, R., Moeckel, G.W., and Strange, K. (2004). Adaptation of the nematode *Caenorhabditis elegans* to extreme osmotic stress. *American journal of physiology Cell physiology* 286, C785-791.

Lanzetti, L., Rybin, V., Malabarba, M.G., Christoforidis, S., Scita, G., Zerial, M., and Di Fiore, P.P. (2000). The Eps8 protein coordinates EGF receptor signalling through Rac and trafficking through Rab5. *Nature* 408, 374-377.

Lee, J., Jongeward, G.D., and Sternberg, P.W. (1994). *unc-101*, a gene required for many aspects of *Caenorhabditis elegans* development and behavior, encodes a clathrin-associated protein. *Genes Dev* 8, 60-73.

Leevers, S.J., Paterson, H.F., and Marshall, C.J. (1994). Requirement for Ras in Raf activation is overcome by targeting Raf to the plasma membrane. *Nature* 369, 411-414.

Lenormand, P., Sardet, C., Pages, G., L'Allemain, G., Brunet, A., and Pouyssegur, J. (1993). Growth factors induce nuclear translocation of MAP kinases (p42mapk and p44mapk) but not of their activator MAP kinase kinase (p45mapkk) in fibroblasts. *J Cell Biol* 122, 1079-1088.

Lesa, G.M., and Sternberg, P.W. (1997). Positive and negative tissue-specific signaling by a nematode epidermal growth factor receptor. *Mol Biol Cell* 8, 779-793.

Letunic, I., Goodstadt, L., Dickens, N.J., Doerks, T., Schultz, J., Mott, R., Ciccarelli, F., Copley, R.R., Ponting, C.P., and Bork, P. (2002). Recent improvements to the SMART domain-based sequence annotation resource. *Nucleic Acids Res* 30, 242-244.

Levitan, D., and Greenwald, I. (1998). LIN-12 protein expression and localization during vulval development in *C. elegans*. *Development* 125, 3101-3109.

Levkowitz, G., Waterman, H., Ettenberg, S.A., Katz, M., Tsygankov, A.Y., Alroy, I., Lavi, S., Iwai, K., Reiss, Y., Ciechanover, A., *et al.* (1999). Ubiquitin ligase activity and tyrosine phosphorylation underlie suppression of growth factor signaling by c-Cbl/Sli-1. *Mol Cell* 4, 1029-1040.

Li, W., Han, M., and Guan, K.L. (2000). The leucine-rich repeat protein SUR-8 enhances MAP kinase activation and forms a complex with Ras and Raf. *Genes Dev* 14, 895-900.

Lim, K.H., Baines, A.T., Fiordalisi, J.J., Shipitsin, M., Feig, L.A., Cox, A.D., Der, C.J., and Counter, C.M. (2005). Activation of RalA is critical for Ras-induced tumorigenesis of human cells. *Cancer Cell* 7, 533-545.

Lim, K.H., O'Hayer, K., Adam, S.J., Kendall, S.D., Campbell, P.M., Der, C.J., and Counter, C.M. (2006). Divergent roles for RalA and RalB in malignant growth of human pancreatic carcinoma cells. *Curr Biol* 16, 2385-2394.

Lin, K., Dorman, J.B., Rodan, A., and Kenyon, C. (1997). daf-16: An HNF-3/forkhead family member that can function to double the life-span of *Caenorhabditis elegans*. *Science* 278, 1319-1322.

Linnemann, T., Kiel, C., Herter, P., and Herrmann, C. (2002). The activation of RalGDS can be achieved independently of its Ras binding domain. Implications of an activation mechanism in Ras effector specificity and signal distribution. *J Biol Chem* 277, 7831-7837.

Liu, J., Tzou, P., Hill, R.J., and Sternberg, P.W. (1999). Structural requirements for the tissue-specific and tissue-general functions of the *Caenorhabditis elegans* epidermal growth factor LIN-3. *Genetics* 153, 1257-1269.

Lowy, D.R., Zhang, K., DeClue, J.E., and Willumsen, B.M. (1991). Regulation of p21ras activity. *Trends Genet* 7, 346-351.

Lu, X., and Horvitz, H.R. (1998). lin-35 and lin-53, two genes that antagonize a *C. elegans* Ras pathway, encode proteins similar to Rb and its binding protein RbAp48. *Cell* 95, 981-991.

Mahalak, K.K., Jama, A.M., Billups, S.J., Dawes, A.T., and Chamberlin, H.M. (2017). Differing roles for sur-2/MED23 in *C. elegans* and *C. briggsae* vulval development. *Dev Genes Evol* 227, 213-218.

Maloof, J.N., and Kenyon, C. (1998). The Hox gene lin-39 is required during *C. elegans* vulval induction to select the outcome of Ras signaling. *Development* 125, 181-190.

Manolea, F., Claude, A., Chun, J., Rosas, J., and Melancon, P. (2008). Distinct functions for Arf guanine nucleotide exchange factors at the Golgi complex: GBF1 and BIGs are required for assembly and maintenance of the Golgi stack and trans-Golgi network, respectively. *Mol Biol Cell* 19, 523-535.

Martin, T.D., Chen, X.W., Kaplan, R.E., Saltiel, A.R., Walker, C.L., Reiner, D.J., and Der, C.J. (2014). Ral and Rheb GTPase activating proteins integrate mTOR and GTPase signaling in aging, autophagy, and tumor cell invasion. *Mol Cell* 53, 209-220.

Martin, T.D., Samuel, J.C., Routh, E.D., Der, C.J., and Yeh, J.J. (2011). Activation and involvement of Ral GTPases in colorectal cancer. *Cancer Res* 71, 206-215.

Martinu, L., Santiago-Walker, A., Qi, H., and Chou, M.M. (2002). Endocytosis of epidermal growth factor receptor regulated by Grb2-mediated recruitment of the Rab5 GTPase-activating protein RN-tre. *J Biol Chem* 277, 50996-51002.

Matsubara, K., Kishida, S., Matsuura, Y., Kitayama, H., Noda, M., and Kikuchi, A. (1999). Plasma membrane recruitment of RalGDS is critical for Ras-dependent Ral activation. *Oncogene* 18, 1303-1312.

Matsunaga-Udagawa, R., Fujita, Y., Yoshiki, S., Terai, K., Kamioka, Y., Kiyokawa, E., Yugi, K., Aoki, K., and Matsuda, M. (2010). The scaffold protein Shoc2/SUR-8 accelerates the interaction of Ras and Raf. *J Biol Chem* 285, 7818-7826.

McCormick, F., and Wittinghofer, A. (1996). Interactions between Ras proteins and their effectors. *Curr Opin Biotechnol* 7, 449-456.

McKay, S.J., Johnsen, R., Khattra, J., Asano, J., Baillie, D.L., Chan, S., Dube, N., Fang, L., Goszczynski, B., Ha, E., *et al.* (2003). Gene expression profiling of cells, tissues, and developmental stages of the nematode *C. elegans*. *Cold Spring Harb Symp Quant Biol* 68, 159-169.

Mertenskotter, A., Keshet, A., Gerke, P., and Paul, R.J. (2013). The p38 MAPK PMK-1 shows heat-induced nuclear translocation, supports chaperone expression, and affects the heat tolerance of *Caenorhabditis elegans*. *Cell Stress Chaperones* 18, 293-306.

Miller, L.M., Gallegos, M.E., Morisseau, B.A., and Kim, S.K. (1993). lin-31, a *Caenorhabditis elegans* HNF-3/fork head transcription factor homolog, specifies three alternative cell fates in vulval development. *Genes Dev* 7, 933-947.

Milloz, J., Duvéau, F., Nuez, I., and Felix, M.A. (2008). Intraspecific evolution of the intercellular signaling network underlying a robust developmental system. *Genes Dev* 22, 3064-3075.

Minor, P.J., He, T.F., Sohn, C.H., Asthagiri, A.R., and Sternberg, P.W. (2013). FGF signaling regulates Wnt ligand expression to control vulval cell lineage polarity in *C. elegans*. *Development* 140, 3882-3891.

Mishra, P.J., Ha, L., Rieker, J., Sviderskaya, E.V., Bennett, D.C., Oberst, M.D., Kelly, K., and Merlino, G. (2010). Dissection of RAS downstream pathways in melanomagenesis: a role for Ral in transformation. *Oncogene* 29, 2449-2456.

Mizuno, T., Hisamoto, N., Terada, T., Kondo, T., Adachi, M., Nishida, E., Kim, D.H., Ausubel, F.M., and Matsumoto, K. (2004). The *Caenorhabditis elegans* MAPK phosphatase VHP-1 mediates a novel JNK-like signaling pathway in stress response. *EMBO J* 23, 2226-2234.

Mohapatra, B., Ahmad, G., Nadeau, S., Zutshi, N., An, W., Scheffe, S., Dong, L., Feng, D., Goetz, B., Arya, P., *et al.* (2013). Protein tyrosine kinase regulation by ubiquitination: critical roles of Cbl-family ubiquitin ligases. *Biochim Biophys Acta* 1833, 122-139.

Mok, D.Z., Sternberg, P.W., and Inoue, T. (2015). Morphologically defined sub-stages of *C. elegans* vulval development in the fourth larval stage. *BMC Dev Biol* 15, 26.

Morinaga, N., Tsai, S.C., Moss, J., and Vaughan, M. (1996). Isolation of a brefeldin A-inhibited guanine nucleotide-exchange protein for ADP ribosylation factor (ARF) 1 and ARF3 that contains a Sec7-like domain. *Proc Natl Acad Sci U S A* 93, 12856-12860.

Moskalenko, S., Henry, D.O., Rosse, C., Mirey, G., Camonis, J.H., and White, M.A. (2002). The exocyst is a Ral effector complex. *Nat Cell Biol* 4, 66-72.

Moskalenko, S., Tong, C., Rosse, C., Mirey, G., Formstecher, E., Daviet, L., Camonis, J., and White, M.A. (2003). Ral GTPases regulate exocyst assembly through dual subunit interactions. *J Biol Chem* 278, 51743-51748.

Much, J.W., Slade, D.J., Klampert, K., Garriga, G., and Wightman, B. (2000). The *fax-1* nuclear hormone receptor regulates axon pathfinding and neurotransmitter expression. *Development* 127, 703-712.

Myers, T.R., and Greenwald, I. (2005). *lin-35* Rb acts in the major hypodermis to oppose ras-mediated vulval induction in *C. elegans*. *Dev Cell* 8, 117-123.

Nakdimon, I., Walser, M., Frohli, E., and Hajnal, A. (2012). PTEN negatively regulates MAPK signaling during *Caenorhabditis elegans* vulval development. *PLoS Genet* 8, e1002881.

Nilsson, L., Li, X., Tiensuu, T., Auty, R., Greenwald, I., and Tuck, S. (1998). *Caenorhabditis elegans* lin-25: cellular focus, protein expression and requirement for sur-2 during induction of vulval fates. *Development* 125, 4809-4819.

Nilsson, L., Tiensuu, T., and Tuck, S. (2000). *Caenorhabditis elegans* lin-25: a study of its role in multiple cell fate specification events involving Ras and the identification and characterization of evolutionarily conserved domains. *Genetics* 156, 1083-1096.

Oeckinghaus, A., Postler, T.S., Rao, P., Schmitt, H., Schmitt, V., Grinberg-Bleyer, Y., Kuhn, L.I., Gruber, C.W., Lienhard, G.E., and Ghosh, S. (2014). kappaB-Ras proteins regulate both NF-kappaB-dependent inflammation and Ral-dependent proliferation. *Cell Rep* 8, 1793-1807.

Ogg, S., Paradis, S., Gottlieb, S., Patterson, G.I., Lee, L., Tissenbaum, H.A., and Ruvkun, G. (1997). The Fork head transcription factor DAF-16 transduces insulin-like metabolic and longevity signals in *C. elegans*. *Nature* 389, 994-999.

Ogg, S., and Ruvkun, G. (1998). The *C. elegans* PTEN homolog, DAF-18, acts in the insulin receptor-like metabolic signaling pathway. *Molecular cell* 2, 887-893.

Pan, C.L., Baum, P.D., Gu, M., Jorgensen, E.M., Clark, S.G., and Garriga, G. (2008). *C. elegans* AP-2 and retromer control Wnt signaling by regulating mig-14/Wntless. *Dev Cell* 14, 132-139.

Papini, D., Langemeyer, L., Abad, M.A., Kerr, A., Samejima, I., Eysers, P.A., Jeyapragash, A.A., Higgins, J.M., Barr, F.A., and Earnshaw, W.C. (2015). TD-60 links RalA GTPase function to the CPC in mitosis. *Nat Commun* 6, 7678.

- Papke, B., and Der, C.J. (2017). Drugging RAS: Know the enemy. *Science* 355, 1158-1163.
- Paradis, S., Ailion, M., Toker, A., Thomas, J.H., and Ruvkun, G. (1999). A PDK1 homolog is necessary and sufficient to transduce AGE-1 PI3 kinase signals that regulate diapause in *Caenorhabditis elegans*. *Genes Dev* 13, 1438-1452.
- Paradis, S., and Ruvkun, G. (1998). *Caenorhabditis elegans* Akt/PKB transduces insulin receptor-like signals from AGE-1 PI3 kinase to the DAF-16 transcription factor. *Genes Dev* 12, 2488-2498.
- Pellegrino, M.W., Farooqui, S., Frohli, E., Rehrauer, H., Kaeser-Pebernard, S., Muller, F., Gasser, R.B., and Hajnal, A. (2011). LIN-39 and the EGFR/RAS/MAPK pathway regulate *C. elegans* vulval morphogenesis via the VAB-23 zinc finger protein. *Development* 138, 4649-4660.
- Petcherski, A.G., and Kimble, J. (2000). LAG-3 is a putative transcriptional activator in the *C. elegans* Notch pathway. *Nature* 405, 364-368.
- Poulin, G., Dong, Y., Fraser, A.G., Hopper, N.A., and Ahringer, J. (2005). Chromatin regulation and sumoylation in the inhibition of Ras-induced vulval development in *Caenorhabditis elegans*. *EMBO J* 24, 2613-2623.
- Pritchard, C., and McMahon, M. (1997). Raf revealed in life-or-death decisions. *Nat Genet* 16, 214-215.
- Pu, P., Stone, C.E., Burdick, J.T., Murray, J.I., and Sundaram, M.V. (2017). The Lipocalin LPR-1 Cooperates with LIN-3/EGF Signaling To Maintain Narrow Tube Integrity in *Caenorhabditis elegans*. *Genetics* 205, 1247-1260.

Rapoport, I., Miyazaki, M., Boll, W., Duckworth, B., Cantley, L.C., Shoelson, S., and Kirchhausen, T. (1997). Regulatory interactions in the recognition of endocytic sorting signals by AP-2 complexes. *EMBO J* 16, 2240-2250.

Reiner, D.J. (2011). Ras effector switching as a developmental strategy. *Small GTPases* 2, 109-112.

Reiner, D.J., and Lundquist, E.A. (2016). Small GTPases. *WormBook*, 1-99.

Ririe, T.O., Fernandes, J.S., and Sternberg, P.W. (2008). The *Caenorhabditis elegans* vulva: a post-embryonic gene regulatory network controlling organogenesis. *Proc Natl Acad Sci U S A* 105, 20095-20099.

Roehl, H., Bosenberg, M., Billewicz, R., and Kimble, J. (1996). Roles of the RAM and ANK domains in signaling by the *C. elegans* GLP-1 receptor. *EMBO J* 15, 7002-7012.

Ryan, M.B., Der, C.J., Wang-Gillam, A., and Cox, A.D. (2015). Targeting RAS-mutant cancers: is ERK the key? *Trends Cancer* 1, 183-198.

Saffer, A.M., Kim, D.H., van Oudenaarden, A., and Horvitz, H.R. (2011). The *Caenorhabditis elegans* synthetic multivulva genes prevent ras pathway activation by tightly repressing global ectopic expression of *lin-3* EGF. *PLoS Genet* 7, e1002418.

Saito, R., Shirakawa, R., Nishiyama, H., Kobayashi, T., Kawato, M., Kanno, T., Nishizawa, K., Matsui, Y., Ohbayashi, T., Horiguchi, M., *et al.* (2013). Downregulation of Ral GTPase-activating protein promotes tumor invasion and metastasis of bladder cancer. *Oncogene* 32, 894-902.

Sakaguchi, A., Matsumoto, K., and Hisamoto, N. (2004). Roles of MAP kinase cascades in *Caenorhabditis elegans*. *J Biochem* 136, 7-11.

Sawamoto, K., Winge, P., Koyama, S., Hirota, Y., Yamada, C., Miyao, S., Yoshikawa, S., Jin, M.H., Kikuchi, A., and Okano, H. (1999). The *Drosophila* Ral GTPase regulates developmental cell shape changes through the Jun NH(2)-terminal kinase pathway. *J Cell Biol* 146, 361-372.

Schutzman, J.L., Borland, C.Z., Newman, J.C., Robinson, M.K., Kokel, M., and Stern, M.J. (2001). The *Caenorhabditis elegans* EGL-15 signaling pathway implicates a DOS-like multisubstrate adaptor protein in fibroblast growth factor signal transduction. *Mol Cell Biol* 21, 8104-8116.

Selfors, L.M., Schutzman, J.L., Borland, C.Z., and Stern, M.J. (1998). soc-2 encodes a leucine-rich repeat protein implicated in fibroblast growth factor receptor signaling. *Proc Natl Acad Sci U S A* 95, 6903-6908.

Shaner, N.C., Lambert, G.G., Chammas, A., Ni, Y., Cranfill, P.J., Baird, M.A., Sell, B.R., Allen, J.R., Day, R.N., Israelsson, M., *et al.* (2013). A bright monomeric green fluorescent protein derived from *Branchiostoma lanceolatum*. *Nat Methods* 10, 407-409.

Shao, H., and Andres, D.A. (2000). A novel RalGEF-like protein, RGL3, as a candidate effector for rit and Ras. *J Biol Chem* 275, 26914-26924.

Shaye, D.D., and Greenwald, I. (2002). Endocytosis-mediated downregulation of LIN-12/Notch upon Ras activation in *Caenorhabditis elegans*. *Nature* 420, 686-690.

Shaye, D.D., and Greenwald, I. (2005). LIN-12/Notch trafficking and regulation of DSL ligand activity during vulval induction in *Caenorhabditis elegans*. *Development* 132, 5081-5092.

Shcherbo, D., Murphy, C.S., Ermakova, G.V., Solovieva, E.A., Chepurnykh, T.V., Shcheglov, A.S., Verkhusha, V.V., Pletnev, V.Z., Hazelwood, K.L., Roche, P.M., *et al.* (2009). Far-red fluorescent tags for protein imaging in living tissues. *Biochem J* 418, 567-574.

Sherwood, D.R., and Sternberg, P.W. (2003). Anchor cell invasion into the vulval epithelium in *C. elegans*. *Dev Cell* 5, 21-31.

Shields, J.M., Pruitt, K., McFall, A., Shaub, A., and Der, C.J. (2000). Understanding Ras: 'it ain't over 'til it's over'. *Trends Cell Biol* 10, 147-154.

Shin, H., Kaplan, R.E.W., Duong, T., Fakieh, R., and Reiner, D.J. (2018). Ral Signals through a MAP4 Kinase-p38 MAP Kinase Cascade in *C. elegans* Cell Fate Patterning. *Cell Rep* 24, 2669-2681 e2665.

Sieburth, D.S., Sun, Q., and Han, M. (1998). SUR-8, a conserved Ras-binding protein with leucine-rich repeats, positively regulates Ras-mediated signaling in *C. elegans*. *Cell* 94, 119-130.

Simske, J.S., Kaech, S.M., Harp, S.A., and Kim, S.K. (1996). LET-23 receptor localization by the cell junction protein LIN-7 during *C. elegans* vulval induction. *Cell* 85, 195-204.

Simske, J.S., and Kim, S.K. (1995). Sequential signalling during *Caenorhabditis elegans* vulval induction. *Nature* 375, 142-146.

Singh, N., and Han, M. (1995). *sur-2*, a novel gene, functions late in the *let-60* ras-mediated signaling pathway during *Caenorhabditis elegans* vulval induction. *Genes Dev* 9, 2251-2265.

Skorobogata, O., Escobar-Restrepo, J.M., and Rocheleau, C.E. (2014). An AGEF-1/Arf GTPase/AP-1 ensemble antagonizes LET-23 EGFR basolateral localization and signaling during *C. elegans* vulva induction. *PLoS Genet* 10, e1004728.

Skorobogata, O., and Rocheleau, C.E. (2012). RAB-7 antagonizes LET-23 EGFR signaling during vulva development in *Caenorhabditis elegans*. *PLoS One* 7, e36489.

Solari, F., and Ahringer, J. (2000). NURD-complex genes antagonise Ras-induced vulval development in *Caenorhabditis elegans*. *Curr Biol* 10, 223-226.

Sommer, R.J., and Bumbarger, D.J. (2012). Nematode model systems in evolution and development. *Wiley Interdiscip Rev Dev Biol* 1, 389-400.

Spaargaren, M., and Bischoff, J.R. (1994). Identification of the guanine nucleotide dissociation stimulator for Ral as a putative effector molecule of R-ras, H-ras, K-ras, and Rap. *Proc Natl Acad Sci U S A* 91, 12609-12613.

Sterken, M.G., van Bemmelen van der Plaat, L., Riksen, J.A.G., Rodriguez, M., Schmid, T., Hajnal, A., Kammenga, J.E., and Snoek, B.L. (2017). Ras/MAPK Modifier Loci Revealed by eQTL in *Caenorhabditis elegans*. *G3 (Bethesda)* 7, 3185-3193.

Sternberg, P.W. (1988). Lateral inhibition during vulval induction in *Caenorhabditis elegans*. *Nature* 335, 551-554.

Sternberg, P.W. (2005). Vulval development. *WormBook*, 1-28.

Sternberg, P.W., and Horvitz, H.R. (1986). Pattern formation during vulval development in *C. elegans*. *Cell* 44, 761-772.

Sternberg, P.W., and Horvitz, H.R. (1989). The combined action of two intercellular signaling pathways specifies three cell fates during vulval induction in *C. elegans*. *Cell* 58, 679-693.

Stevens, J.L., Cantin, G.T., Wang, G., Shevchenko, A., Shevchenko, A., and Berk, A.J. (2002). Transcription control by E1A and MAP kinase pathway via Sur2 mediator subunit. *Science* 296, 755-758.

Stokoe, D., Macdonald, S.G., Cadwallader, K., Symons, M., and Hancock, J.F. (1994). Activation of Raf as a result of recruitment to the plasma membrane. *Science* 264, 1463-1467.

Struhl, G., Fitzgerald, K., and Greenwald, I. (1993). Intrinsic activity of the Lin-12 and Notch intracellular domains in vivo. *Cell* 74, 331-345.

Su, Y.C., Maurel-Zaffran, C., Treisman, J.E., and Skolnik, E.Y. (2000). The Ste20 kinase misshapen regulates both photoreceptor axon targeting and dorsal closure, acting downstream of distinct signals. *Mol Cell Biol* 20, 4736-4744.

Su, Y.C., Treisman, J.E., and Skolnik, E.Y. (1998). The *Drosophila* Ste20-related kinase misshapen is required for embryonic dorsal closure and acts through a

JNK MAPK module on an evolutionarily conserved signaling pathway. *Genes Dev* 12, 2371-2380.

Sugihara, K., Asano, S., Tanaka, K., Iwamatsu, A., Okawa, K., and Ohta, Y. (2002). The exocyst complex binds the small GTPase RalA to mediate filopodia formation. *Nature cell biology* 4, 73-78.

Sulston, J.E., and Horvitz, H.R. (1977). Post-embryonic cell lineages of the nematode, *Caenorhabditis elegans*. *Dev Biol* 56, 110-156.

Sulston, J.E., and Horvitz, H.R. (1981). Abnormal cell lineages in mutants of the nematode *Caenorhabditis elegans*. *Dev Biol* 82, 41-55.

Sulston, J.E., and White, J.G. (1980). Regulation and cell autonomy during postembryonic development of *Caenorhabditis elegans*. *Dev Biol* 78, 577-597.

Sun, C., Wang, L., Huang, S., Heynen, G.J., Prahallad, A., Robert, C., Haanen, J., Blank, C., Wesseling, J., Willems, S.M., *et al.* (2014). Reversible and adaptive resistance to BRAF(V600E) inhibition in melanoma. *Nature* 508, 118-122.

Sundaram, M., and Han, M. (1995). The *C. elegans* *ksr-1* gene encodes a novel Raf-related kinase involved in Ras-mediated signal transduction. *Cell* 83, 889-901.

Sundaram, M.V. (2005). The love-hate relationship between Ras and Notch. *Genes Dev* 19, 1825-1839.

Sundaram, M.V. (2013). Canonical RTK-Ras-ERK signaling and related alternative pathways. *WormBook*, 1-38.

Tall, G.G., Barbieri, M.A., Stahl, P.D., and Horazdovsky, B.F. (2001). Ras-activated endocytosis is mediated by the Rab5 guanine nucleotide exchange activity of RIN1. *Dev Cell* 1, 73-82.

Tamada, M., Hu, C.D., Kariya, K., Okada, T., and Kataoka, T. (1997). Membrane recruitment of Raf-1 is not the only function of Ras in Raf-1 activation. *Oncogene* 15, 2959-2964.

Tan, P.B., Lackner, M.R., and Kim, S.K. (1998). MAP kinase signaling specificity mediated by the LIN-1 Ets/LIN-31 WH transcription factor complex during *C. elegans* vulval induction. *Cell* 93, 569-580.

Tanaka-Hino, M., Sagasti, A., Hisamoto, N., Kawasaki, M., Nakano, S., Ninomiya-Tsuji, J., Bargmann, C.I., and Matsumoto, K. (2002). SEK-1 MAPKK mediates Ca²⁺ signaling to determine neuronal asymmetric development in *Caenorhabditis elegans*. *EMBO Rep* 3, 56-62.

Tanaka, T., Goto, K., and Iino, M. (2017). Diverse Functions and Signal Transduction of the Exocyst Complex in Tumor Cells. *J Cell Physiol* 232, 939-957.

Tax, F.E., Thomas, J.H., Ferguson, E.L., and Horvitz, H.R. (1997). Identification and characterization of genes that interact with lin-12 in *Caenorhabditis elegans*. *Genetics* 147, 1675-1695.

Thien, C.B., and Langdon, W.Y. (2001). Cbl: many adaptations to regulate protein tyrosine kinases. *Nat Rev Mol Cell Biol* 2, 294-307.

Thompson, B.J. (2013). Cell polarity: models and mechanisms from yeast, worms and flies. *Development* 140, 13-21.

Thompson, O., Edgley, M., Strasbourger, P., Flibotte, S., Ewing, B., Adair, R., Au, V., Chaudhry, I., Fernando, L., Hutter, H., *et al.* (2013). The million mutation project: a new approach to genetics in *Caenorhabditis elegans*. *Genome Res* 23, 1749-1762.

Tian, X., Rusanescu, G., Hou, W., Schaffhausen, B., and Feig, L.A. (2002). PDK1 mediates growth factor-induced Ral-GEF activation by a kinase-independent mechanism. *EMBO J* 21, 1327-1338.

Tiensuu, T., Larsen, M.K., Vernersson, E., and Tuck, S. (2005). *lin-1* has both positive and negative functions in specifying multiple cell fates induced by Ras/MAP kinase signaling in *C. elegans*. *Dev Biol* 286, 338-351.

Timmons, L., and Fire, A. (1998). Specific interference by ingested dsRNA. *Nature* 395, 854.

Tuck, S., and Greenwald, I. (1995). *lin-25*, a gene required for vulval induction in *Caenorhabditis elegans*. *Genes Dev* 9, 341-357.

Underwood, R.S., Deng, Y., and Greenwald, I. (2017). Integration of EGFR and LIN-12/Notch Signaling by LIN-1/Elk1, the Cdk8 Kinase Module, and SUR-2/Med23 in Vulval Precursor Cell Fate Patterning in *Caenorhabditis elegans*. *Genetics* 207, 1473-1488.

Unhavaithaya, Y., Shin, T.H., Miliaras, N., Lee, J., Oyama, T., and Mello, C.C. (2002). MEP-1 and a homolog of the NURD complex component Mi-2 act together to maintain germline-soma distinctions in *C. elegans*. *Cell* 111, 991-1002.

Urano, T., Emkey, R., and Feig, L.A. (1996). Ral-GTPases mediate a distinct downstream signaling pathway from Ras that facilitates cellular transformation. *EMBO J* 15, 810-816.

Van Buskirk, C., and Sternberg, P.W. (2007). Epidermal growth factor signaling induces behavioral quiescence in *Caenorhabditis elegans*. *Nat Neurosci* 10, 1300-1307.

Vanhaesebroeck, B., and Alessi, D.R. (2000). The PI3K-PDK1 connection: more than just a road to PKB. *Biochem J* 346 Pt 3, 561-576.

Vetter, I.R., Linnemann, T., Wohlgemuth, S., Geyer, M., Kalbitzer, H.R., Herrmann, C., and Wittinghofer, A. (1999). Structural and biochemical analysis of Ras-effector signaling via RalGDS. *FEBS Lett* 451, 175-180.

Vigil, D., Martin, T.D., Williams, F., Yeh, J.J., Campbell, S.L., and Der, C.J. (2010). Aberrant overexpression of the Rgl2 Ral small GTPase-specific guanine nucleotide exchange factor promotes pancreatic cancer growth through Ral-dependent and Ral-independent mechanisms. *J Biol Chem* 285, 34729-34740.

Waddington, C.H. (1957). *The Strategy Of The Genes* (London: Allen and Unwin).

Wagmaister, J.A., Gleason, J.E., and Eisenmann, D.M. (2006). Transcriptional upregulation of the *C. elegans* Hox gene *lin-39* during vulval cell fate specification. *Mech Dev* 123, 135-150.

Ward, J.D. (2015). Rendering the Intractable More Tractable: Tools from *Caenorhabditis elegans* Ripe for Import into Parasitic Nematodes. *Genetics* 201, 1279-1294.

Wennerberg, K., Rossman, K.L., and Der, C.J. (2005). The Ras superfamily at a glance. *J Cell Sci* 118, 843-846.

White, M.A., Nicolette, C., Minden, A., Polverino, A., Van Aelst, L., Karin, M., and Wigler, M.H. (1995). Multiple Ras functions can contribute to mammalian cell transformation. *Cell* 80, 533-541.

White, M.A., Vale, T., Camonis, J.H., Schaefer, E., and Wigler, M.H. (1996). A role for the Ral guanine nucleotide dissociation stimulator in mediating Ras-induced transformation. *J Biol Chem* 271, 16439-16442.

Whitfield, C.W., Benard, C., Barnes, T., Hekimi, S., and Kim, S.K. (1999). Basolateral localization of the *Caenorhabditis elegans* epidermal growth factor receptor in epithelial cells by the PDZ protein LIN-10. *Mol Biol Cell* 10, 2087-2100.

Wilkinson, H.A., and Greenwald, I. (1995). Spatial and temporal patterns of *lin-12* expression during *C. elegans* hermaphrodite development. *Genetics* 141, 513-526.

Wolthuis, R.M., Bauer, B., van 't Veer, L.J., de Vries-Smits, A.M., Cool, R.H., Spaargaren, M., Wittinghofer, A., Burgering, B.M., and Bos, J.L. (1996). RalGDS-like factor (Rlf) is a novel Ras and Rap 1A-associating protein. *Oncogene* 13, 353-362.

Wolthuis, R.M., de Ruiter, N.D., Cool, R.H., and Bos, J.L. (1997). Stimulation of gene induction and cell growth by the Ras effector Rlf. *EMBO J* 16, 6748-6761.

Wong, K.K., Engelman, J.A., and Cantley, L.C. (2010). Targeting the PI3K signaling pathway in cancer. *Curr Opin Genet Dev* 20, 87-90.

Wu, B., and Guo, W. (2015). The Exocyst at a Glance. *J Cell Sci* 128, 2957-2964.

Wu, Y., Han, M., and Guan, K.L. (1995). MEK-2, a *Caenorhabditis elegans* MAP kinase kinase, functions in Ras-mediated vulval induction and other developmental events. *Genes Dev* 9, 742-755.

Yan, L., Mieulet, V., Burgess, D., Findlay, G.M., Sully, K., Procter, J., Goris, J., Janssens, V., Morrice, N.A., and Lamb, R.F. (2010). PP2A T61 epsilon is an inhibitor of MAP4K3 in nutrient signaling to mTOR. *Mol Cell* 37, 633-642.

Yochem, J., Sundaram, M., and Han, M. (1997). Ras is required for a limited number of cell fates and not for general proliferation in *Caenorhabditis elegans*. *Mol Cell Biol* 17, 2716-2722.

Yoder, J.H., Chong, H., Guan, K.L., and Han, M. (2004). Modulation of KSR activity in *Caenorhabditis elegans* by Zn ions, PAR-1 kinase and PP2A phosphatase. *EMBO J* 23, 111-119.

Yoo, A.S., Bais, C., and Greenwald, I. (2004). Crosstalk between the EGFR and LIN-12/Notch pathways in *C. elegans* vulval development. *Science* 303, 663-666.

Yoo, A.S., and Greenwald, I. (2005). LIN-12/Notch activation leads to microRNA-mediated down-regulation of Vav in *C. elegans*. *Science* 310, 1330-1333.

Yoon, C.H., Chang, C., Hopper, N.A., Lesa, G.M., and Sternberg, P.W. (2000). Requirements of multiple domains of SLI-1, a *Caenorhabditis elegans* homologue of c-Cbl, and an inhibitory tyrosine in LET-23 in regulating vulval differentiation. *Mol Biol Cell* 11, 4019-4031.

Yoon, C.H., Lee, J., Jongeward, G.D., and Sternberg, P.W. (1995). Similarity of *sli-1*, a regulator of vulval development in *C. elegans*, to the mammalian proto-oncogene *c-cbl*. *Science* 269, 1102-1105.

Yuan, T.L., Amzallag, A., Bagni, R., Yi, M., Afghani, S., Burgan, W., Fer, N., Strathern, L.A., Powell, K., Smith, B., *et al.* (2018). Differential Effector Engagement by Oncogenic KRAS. *Cell Rep* 22, 1889-1902.

Zand, T.P., Reiner, D.J., and Der, C.J. (2011). Ras effector switching promotes divergent cell fates in *C. elegans* vulval patterning. *Dev Cell* 20, 84-96.

Zhang, L., Ward, J.D., Cheng, Z., and Dernburg, A.F. (2015). The auxin-inducible degradation (AID) system enables versatile conditional protein depletion in *C. elegans*. *Development* 142, 4374-4384.

Zhang, X., and Greenwald, I. (2011). Spatial regulation of *lag-2* transcription during vulval precursor cell fate patterning in *Caenorhabditis elegans*. *Genetics* 188, 847-858.